

molecules of NDMR may attach to the receptor, in which case the receptor is not available to agonists; no current flow is recorded. In the presence of moderate concentrations of NDMR, the amount of current flowing through the entire end plate at any instant is reduced from normal, which results in a smaller end-plate potential and, if carried far enough, a block in neurotransmission or the production of neuromuscular paralysis.

Normally, acetylcholinesterase destroys acetylcholine and removes it from competition for a receptor; therefore, an NDMR has a better chance of inhibiting transmission. If, however, an inhibitor of acetylcholinesterase such as neostigmine is added, then the cholinesterase cannot destroy acetylcholine. The concentration of agonist in the cleft remains high, and this high concentration shifts the competition between acetylcholine and a NDMR in favor of the former, thereby improving the chance of two acetylcholine molecules binding to a receptor even though NDMR is still in the environment. This mechanism causes the cholinesterase inhibitors to overcome the neuromuscular paralysis produced by NDMRs. The channel opens only when acetylcholine attaches to both recognition sites. A single molecule of antagonist, however, is adequate to prevent depolarization of that receptor. This modifies the competition by strongly biasing it in favor of the antagonist (relaxant). Mathematically, if the concentration of a NDMR is doubled, then the concentration of acetylcholine must be increased four-fold if acetylcholine is to remain competitive. Paralysis produced by high concentrations of muscle relaxants (antagonist) is more difficult to reverse with cholinesterase inhibitors than that produced by low concentrations. After large doses of NDMRs, cholinesterase inhibitors may be ineffective until the concentration of relaxant in the perijunctional area decreases to a lower level by the redistribution or elimination of the drug. This is the molecular basis for the recommendation to not administer anticholinesterases too early (i.e., at a deep block). In contrast to reversal with a cholinesterase inhibitor, cyclodextrin encapsulation takes place at any concentration of a steroid-based compound, such as vecuronium or rocuronium, and reversal by this novel mechanism can therefore be achieved at any level of neuromuscular block provided the amount of cyclodextrin (sugammadex) is large enough.

CLASSIC ACTIONS OF DEPOLARIZING MUSCLE RELAXANTS

Depolarizing relaxants (e.g., succinylcholine, decamethonium) initially simulate the effect of acetylcholine and can be considered agonists, despite the fact that they block neurotransmission after the initial stimulation. Structurally, succinylcholine is very similar to the natural ligand acetylcholine and consists of two molecules of acetylcholine bound together through their backbones. It is thus not surprising that succinylcholine can mimic the effects of acetylcholine.

Succinylcholine or decamethonium can bind to the receptor, open the channel, pass current, and depolarize the end plate. These agonists, similar to acetylcholine, attach only briefly; each opening of a channel is very short

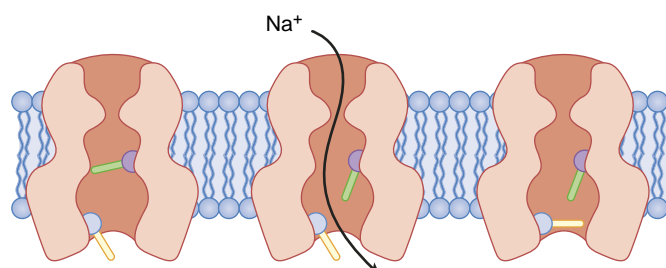


Fig. 12.6 Illustration of a sodium (Na^+) channel. The bars represent parts of the molecule that act as gates. The upper bar is voltage dependent; the lower bar is time dependent. The left side of the drawing represents the resting state. Once activated by a change in voltage, the molecule and its gates progress as illustrated (left to right). See text for details.

in duration—1 ms or less. The response to acetylcholine, however, is over in milliseconds because of its rapid degradation by acetylcholinesterase, and the end plate resets to its resting state long before another nerve impulse arrives. In contrast, the depolarizing relaxants characteristically have a biphasic action on muscle—an initial contraction, followed by relaxation lasting from minutes to hours. Because they are not susceptible to hydrolysis by acetylcholinesterase, the depolarizing relaxants are not eliminated from the junctional cleft until after they are eliminated from plasma. The time required to clear the drug from the body is the principal determinant of how long the drug effect lasts. Whole-body clearance of the relaxant is very slow in comparison to acetylcholine, particularly when plasma (pseudo) cholinesterase is abnormal. Because the relaxant molecules are not quickly cleared from the cleft, compared with acetylcholine, they repeatedly react with receptors even with normal levels of plasma cholinesterase, almost immediately attaching to a receptor after separating from another, thereby repeatedly depolarizing the end plate and opening channels. For details on the effect of succinylcholine in patients with cholinesterase deficiency, also see [Chapter 27](#).

The quick shift from excitation of muscle contraction to block of transmission by depolarizing relaxants occurs because the end plate is continuously depolarized. This comes about as a result of the juxtaposition of the edge of the end plate with a different kind of ion channel, the sodium channel that does not respond to chemicals but opens when exposed to a transmembrane voltage change. Just as the AChR, the sodium channel is also a cylindrical transmembrane protein through which sodium ions can flow. Two parts of its structure act as gates that allow or stop the flow of sodium ions.⁵⁸ Both gates must be open if sodium is to flow through the channel; closing of either cuts off the flow. Because these two gates act sequentially, a sodium channel has three functional conformational states and can progressively move from one state to another (Fig. 12.6). This whole process is short lived when depolarization occurs with acetylcholine.⁵⁸ The initial response of a depolarizing muscle relaxant resembles that of acetylcholine, but because the muscle relaxant is not rapidly hydrolyzed, depolarization of the end plate is not brief.

Depolarization of the end plate by the depolarizing relaxant initially causes the voltage gate in adjacent sodium channels to open, thereby producing a wave of

depolarization that sweeps along the muscle and generates a muscle contraction. Shortly after the voltage-dependent gate opens, the time-dependent inactivation gate closes. Because the relaxant is not removed from the cleft, the end plate continues to be depolarized. Because the sodium channels immediately adjacent to the end plate are influenced by depolarization of the end plate, their voltage-dependent gates stay open and their inactivation gates stay closed. Since sodium cannot flow through a channel that has a closed inactivation gate, the perijunctional muscle membrane does not depolarize. When the flow of ions through sodium channels in the perijunctional zone stops because of a closure of the inactivation gates, the channels downstream (beyond the perijunctional zone) are freed of depolarizing influence. In effect, the perijunctional zone becomes a buffer that shields the rest of the muscle from events at the end plate. Consequently, the muscle membrane is separated into three zones: (1) the end plate, which is depolarized by succinylcholine; (2) the perijunctional muscle membrane, in which the sodium channels are frozen in an inactivated state; and (3) the rest of the muscle membrane, in which the sodium channels are in the resting state. Because a burst of acetylcholine from the nerve cannot overcome the inactivated sodium channels in the perijunctional zone, neuromuscular transmission is blocked. This phenomenon is also called *accommodation*. During accommodation, when the synapse is inexcitable through the nerve (transmitter), direct electrical stimulation of muscle causes muscle contraction because the sodium channels beyond the junctional area are in the resting excitable state.

The extraocular muscles are tonic muscles, which are multiply innervated and chemically excitable along most of their surfaces.²⁰⁻²³ Despite their innervated state, the ocular muscles express both mature and immature receptors.^{20,22} Accommodation does not occur, and these muscles can undergo a sustained contracture in the presence of succinylcholine. The tension that develops forces the eye against the orbit and accounts for part of the increase in intraocular pressure produced by depolarizing relaxants. The extraocular muscles contain a special type of receptor that does not become desensitized (see later discussion) during the continued presence of acetylcholine or other agonists.^{21,23} A single dose of succinylcholine can cause contracture lasting several minutes.²³ Whether it is the immature γ -subunit AChR or the $\alpha 7$ AChR subunit that plays a role in this resistance to desensitization in the ocular muscles is unknown.

NONCLASSIC AND NONCOMPETITIVE ACTIONS OF NEUROMUSCULAR DRUGS

Several drugs can interfere with the receptor, directly or through its lipid environment, and can change transmission (Box 12.1). These drugs react with the neuromuscular receptor to change its function and impair transmission, but they do not act through the acetylcholine binding site. These reactions cause drug-induced changes in the dynamics of the receptor; instead of sharply opening and closing, the modified channels are sluggish. They open more slowly and stay open longer, or they close slowly and in several steps, or both. These effects on channels cause corresponding changes in the flow of ions and distortions of the end-plate potential. The clinical effect depends on the molecular

BOX 12.1 Drugs That Can Cause or Promote Desensitization of Muscle Nicotinic Receptors

Volatile anesthetics

Halothane
Sevoflurane
Isoflurane

Antibiotics

Polymyxin B

Cocaine

Alcohols

Ethanol
Butanol
Propanol
Octanol

Barbiturates

Thiopental
Pentobarbital

Agonists

Acetylcholine
Decamethonium
Carbachol
Succinylcholine

Acetylcholinesterase inhibitors

Neostigmine
Pyridostigmine
Di-isopropyl-fluorophosphate
Edrophonium

Local anesthetics

Dibucaine
Lidocaine
Prilocaine
Etidocaine

Phenothiazines

Chlorpromazine
Trifluoperazine
Prochlorperazine

Phencyclidine

Calcium channel blockers

Verapamil

events. For example, procaine, ketamine, inhaled anesthetics, or other drugs that dissolve in the membrane lipid may change the opening or closing characteristics of the channel.^{57,59} If the channel is prevented from opening, then transmission is weakened. If, however, the channel is prevented from or slowed in closing, then transmission may be enhanced. These drugs do not fit the classic model, and the impaired neuromuscular function is not antagonized by increasing perijunctional acetylcholine concentrations with cholinesterase inhibitors. Such drugs can be involved in two clinically important reactions: receptor desensitization and channel block. The former occurs in the receptor molecule, whereas the latter occurs in the ion channel.

DESENSITIZATION BLOCK

The AChR, as a result of its flexibility and the fluidity of the lipid around it, is capable of existing in a number of conformational states.⁵⁷⁻⁶¹ Because the resting receptor is free of agonist, its channel is closed. The second state exists when two molecules of agonist are bound to the α -subunit of the receptor and the receptor has undergone the conformational

change that opens the channel and allows ions to flow. These reactions are the bases of normal neuromuscular transmission. Some receptors that bind to agonists, however, do not undergo the conformational change to open the channel. Receptors in these states are called desensitized (i.e., they are not sensitive to the channel-opening actions of agonists). They bind agonists with exceptional avidity, but the binding does not result in the opening of the channel. The mechanisms by which desensitization occurs are not known. The receptor macromolecule, 1000 times larger by weight than most drugs or gases, provides many places at which the smaller molecules may act. The interface between lipid and receptor protein provides additional potential sites of reaction. Several different conformations of the protein are known, and because acetylcholine cannot cause the ion channel to open in any of them, they all are included in the functional term *desensitization*. Desensitization is accompanied by phosphorylation of a tyrosine unit in the receptor protein.^{61,62}

Although agonists (e.g., succinylcholine) induce desensitization, the receptors are in a constant state of transition between resting and desensitized states, regardless of whether agonists are present. Agonists do promote transition to a desensitized state or, because they bind very tightly to desensitized receptors, trap a receptor in a desensitized state. NDMRs also tightly bind to desensitized receptors and can trap molecules in these states. This action of NDMRs is not competitive with that of acetylcholine; it may be augmented by acetylcholine if the latter promotes the change to a desensitized state. Desensitization can lead to significant misinterpretation of data. Superficially, the preparation seems to be normal, but its responsiveness to agonists or antagonists is altered. One variety occurs very rapidly, within a few milliseconds after application of an agonist, which may explain the increased sensitivity to nondepolarizing relaxant after the prior administration of succinylcholine. Desensitization may also be a part of the phenomenon known as *phase II block* (see section on “Phase II Block”), which is caused by a prolonged administration of depolarizing relaxants. Phase II block is frequently referred to as a desensitization block, but it should not be because desensitization of receptors is only one of many phenomena that contribute to the process.

Many other drugs used by anesthetists also promote the shift of receptors from a normal state to a desensitized state.⁵⁸⁻⁶⁰ These drugs, some of which are listed in *Box 12.1*, can weaken neuromuscular transmission by reducing the margin of safety that normally exists at the neuromuscular junction, or they can cause an apparent increase in the capacity of NDMRs to block transmission. These actions are independent of the classic effects, based on competitive inhibition of acetylcholine. The presence of desensitized receptors means that fewer receptor channels than usual are available to carry transmembrane current. The production of desensitized receptors decreases the efficacy of neuromuscular transmission. If many receptors are desensitized, then insufficient normal ones are left to depolarize the motor end plate, and neuromuscular transmission will not occur. Even if only some receptors are desensitized, neuromuscular transmission will be impaired, and the system will be more susceptible to block by conventional antagonists such as atracurium or rocuronium.

CHANNEL BLOCK

Local anesthetics and calcium entry blockers prevent the flow of sodium or calcium through their respective channels, thus explaining the term *channel-blocking drugs*. Similarly, block of the flow of ions can occur at the AChR with concentrations of drugs used clinically and may contribute to some of the phenomena and drug interactions observed at the receptor. Two major types, closed-channel and open-channel block, can occur.^{60,63,64} In a closed-channel block, certain drugs can occupy the mouth of the channel and prevent ions from passing through the channel to depolarize the end plate. The process can take place even when the channel is not open. In an open-channel block, a drug molecule enters a channel that has been opened by reaction with acetylcholine but does not necessarily penetrate all the way through. Open-channel block is a use-dependent block, which means that molecules can enter the channel only when it is open. In open- and closed-channel blocks, the normal flow of ions through the receptor is impaired, thereby resulting in the prevention of depolarization of the end plate and a weakened or blocked neuromuscular transmission. However, because the action is not at the acetylcholine recognition site, it is not a competitive antagonism of acetylcholine and is not relieved by anticholinesterases that increase concentrations of acetylcholine. Increasing the concentration of acetylcholine may cause the channels to open more often and, consequently, become more susceptible to block by use-dependent compounds. Evidence suggests that neostigmine and related cholinesterase inhibitors can act as channel-blocking drugs.^{17,63}

Channel block may account for the antibiotic-, cocaine-, quinidine-, piperocaine-, tricyclic antidepressant-, naltrexone-, naloxone-, and histrionicotoxin-induced alterations in neuromuscular function. Muscle relaxants, in contrast, can bind to the acetylcholine recognition site of the receptor and occupy the channel. Pancuronium preferentially binds to the recognition site. Gallamine (not used clinically anymore) seems to act equally at the two sites (channel-blocking and acetylcholine-blocking sites). (Gallamine was synthesized by Daniel Bovet, a Swiss-born Italian pharmacologist and received the Nobel Prize in Physiology or Medicine in 1957 for his work on cardiovascular and neuromuscular pharmacology.) Tubocurarine, the first NDMR used clinically, is in between; at small doses that clinically produce minimal blockage of transmission, the drug is essentially a pure antagonist at the recognition site; at larger doses, it also enters and blocks channels. Decamethonium and succinylcholine, as agonists, can open channels and, as slender molecules, also enter and block them. Decamethonium and some other long, thin molecules can penetrate all the way through the open channel and enter the cytoplasm of muscle cells. Whether prolonged administration of NDMRs, as used in an intensive care unit, can result in the NDMR occupation of the channel, and even entry of drug into the cytosol, is unknown.

PHASE II BLOCK

A phase II block is a complex phenomenon associated with a typical fade in muscle during continuous exposure to depolarizing drugs. This fade phenomenon is likely due to the

interaction of depolarizing action of succinylcholine on distinct neuronal (prejunctional) AChRs; these prejunctional receptors are blocked by higher-than-usual concentrations of succinylcholine. This fade after succinylcholine is at least partly dependent on a presynaptic interaction with cholinergic transmission of importance for neurotransmitter mobilization and release. However, fade in muscle during repetitive nerve stimulation can also be attributable to postjunctional AChR block.⁶⁵

Other factors may also be involved. The repeated opening of channels allows a continuous efflux of potassium and influx of sodium, and the resulting abnormal electrolyte balance distorts the function of the junctional membrane. Calcium entering the muscle through the opened channels can cause disruption of receptors and the sub-end-plate elements themselves. The activity of the sodium-potassium adenosine triphosphatase pump in the membrane increases with increasing intracellular sodium and, by pumping sodium out of the cell and potassium into it, works to restore the ionic balance and membrane potential toward normal. As long as the depolarizing drug is present, the receptor channels remain open and ion flux through them remains frequent.⁶⁶

Factors influencing the development of a phase II block include the duration of exposure to the drug, the particular drug used and its concentration, and even the type of muscle (i.e., fast or slow twitch). Interactions with anesthetics and other agents also affect the process. All these drugs may also have prejunctional effects on the rate and amount of transmitter released and mobilized. With so many variables involved in the interference with neuromuscular transmission, a phase II block is a complex and ever-changing phenomenon. The reversal response of a phase II block produced by a depolarizing muscle relaxant to the administration of cholinesterase inhibitors is difficult to predict. It is therefore best that reversal by cholinesterase inhibitors not be attempted, although the response to tetanus or train-of-four stimulation resembles that produced by NDMRs.

Biology of Prejunctional and Postjunctional Nicotinic Acetylcholine Receptors

POSTJUNCTIONAL CONVENTIONAL ACETYLCHOLINE RECEPTORS IN MUSCLE VERSUS NEURONAL ACETYLCHOLINE RECEPTORS IN MUSCLE

Currently, three variants of postjunctional AChRs have been identified. The AChR isoform present in the innervated, adult neuromuscular junction is referred to as the adult, mature, or junctional receptor. Another AChR isoform, also described more than 4 decades ago, is expressed when activity in muscle is decreased, as observed in the fetus before innervation or after chemically- or physically-induced immobilization; after lower or upper motor neuron injury, burns, or sepsis; or after other events that cause increased muscle protein catabolism, including sepsis or generalized inflammation.¹⁻³ In contrast with the mature or

junctional receptors, the other isoform is referred to as the immature, extrajunctional, or fetal form of AChR. Some evidence suggests that the immature isoform is not observed in the muscle protein catabolism and wasting that occur with malnutrition.⁶⁷ Qualitative differences in the mature isoform can occur as a result of gene mutations, which therefore alters the subunit protein structure. These qualitative changes in AChR can also cause abnormalities in neurotransmission (e.g., slow- or fast-channel syndrome)^{27,47} and therefore the response to muscle relaxants.

At the molecular level, the mature and immature receptors consist of five subunits (see Fig. 12.4).¹⁻³ The mature junctional receptor is a pentamer of two $\alpha 1$ -subunits and one each of the $\beta 1$ -, δ -, and ϵ -subunits. The immature receptor consists of two $\alpha 1$ -subunits and one each of the $\beta 1$ -, δ -, and γ -subunits; that is, in the immature receptor, the γ -subunit is present instead of the ϵ -subunit. The γ - and ϵ -subunits differ very little from each other in amino acid homology, but the differences are great enough to affect the physiologic function and pharmacologic characteristics of the receptor and its ion channel. Junctional receptors are always confined to the end-plate region of the muscle membrane. The immature, or extrajunctional, receptor may be expressed anywhere on the muscle membrane, although their junctional expression seems minimal.¹⁶ During development and in certain pathologic states, junctional and extrajunctional receptors can coexist in the perijunctional area of the muscle membrane (Fig. 12.7).

Quite in contrast to the conventional muscle AChRs consisting of $\alpha 1$ -, $\beta 1$ -, δ -, and ϵ/γ -subunits described earlier, receptors formed of $\alpha 7$ AChR subunits have recently been found in skeletal muscle during immobilization, sepsis, and denervation.^{68,69} Two recent studies have evidenced the increased expression of $\alpha 7$ AChR subunits in muscle by western blotting, ligand binding or genetic techniques after sepsis, and burn injury or immobilization, during which no overt denervation occurs.^{16,70} These $\alpha 7$ AChR subunits are homomeric (i.e., formed of the same subunits) channels arranged as pentameres (see Fig. 12.4). Ligand (drug)-binding pockets are thought to be formed at negative and positive faces of the $\alpha 7$ -subunit assembly interphases. As expected, the endogenous agonist, acetylcholine, binds to $\alpha 7$ AChR subunits, and each of the five subunits has the potential to bind acetylcholine or succinylcholine molecules.^{18,69} Other agonists, including nicotine and choline, and antagonists, including muscle relaxants, cobra toxin, and α -bungarotoxin, also bind to the $\alpha 7$ AChR.^{18,69-72}

The $\alpha 7$ AChRs in muscle display unusual functional and pharmacologic characteristics when compared with conventional muscle ($\alpha 1$, $\beta 1$, δ , ϵ/γ) AChRs or neuronal $\alpha 7$ AChRs in the brain. Choline, a precursor and metabolite of acetylcholine (and succinylcholine), is a weak agonist of conventional muscle AChRs but is a full agonist of muscle $\alpha 7$ AChRs; that is, concentrations of choline that do not open conventional AChR channels will open $\alpha 7$ AChR channels.⁶⁹ Furthermore, no desensitization of the $\alpha 7$ AChRs occurs even during the continued presence of choline,⁶⁹ thus allowing a greater chance for potassium to efflux (approximately 145 mEq/L) from within the cell to the extracellular space, including plasma (approximately 4.5 mEq/L), down its concentration gradient. The chemical

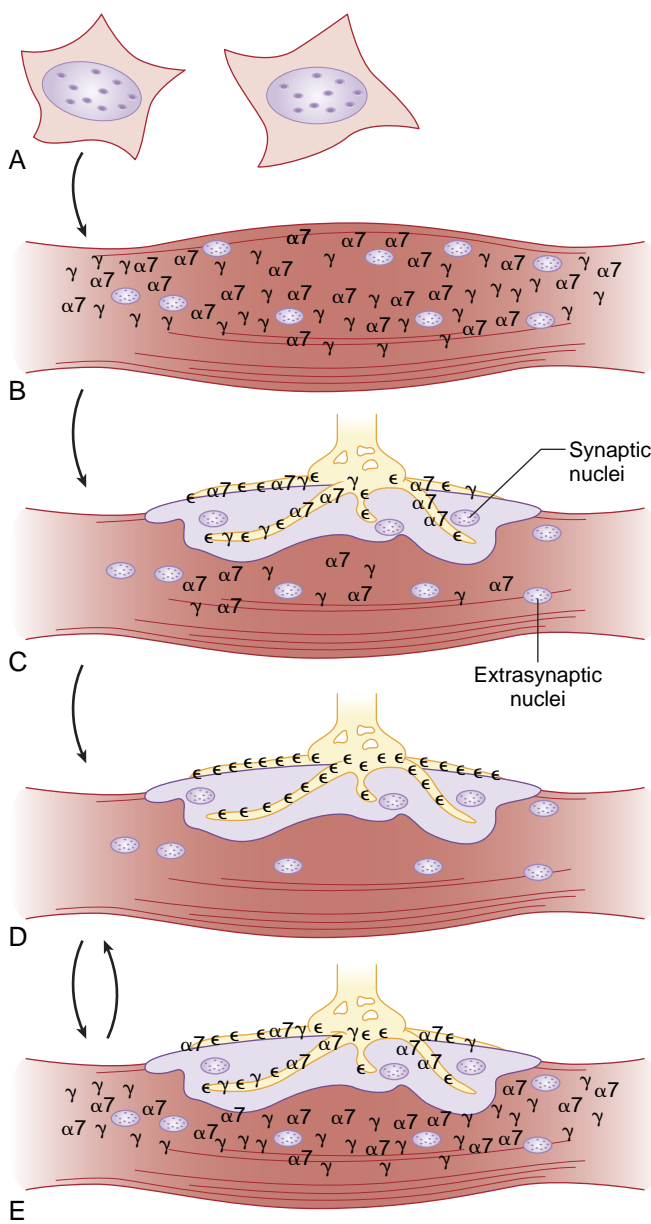


Fig. 12.7 Distribution of acetylcholine receptors in developing adult mature, denervated or immobilized muscle and in inflammation-induced catabolic muscle. (A and B) In the early fetal stage, mononucleated myoblasts, derived from the mesoderm, fuse with each other to form multinucleated myotubes. The γ -subunit-containing immature acetylcholine receptors (AChRs) and the neuronal α -7-subunit AChRs are scattered throughout the muscle membrane before innervation. (C) As the nerve makes contact with muscle, clustering of the receptors occurs at the synapse and is associated with some loss of extrasynaptic receptors. (D) Maturation of the junction is said to occur when ϵ -subunit-containing receptors replace γ -subunit- and α -7-subunit-containing AChRs at the neuromuscular junction. Even mature muscle is multinucleated, but it is devoid of extrasynaptic AChRs. (E) Denervation and some other pathologic states, even without anatomic denervation (e.g., burns, immobilization, chronic muscle relaxant therapy, stroke, sepsis), lead to the re-expression of the γ -subunit-containing AChRs mostly at the extrajunctional areas. The α -7-subunit AChRs are expressed in the junctional areas and are also most likely in the extrajunctional areas. These receptor changes are potentially reversible if muscle immobilization, catabolism, and inflammation are restored to normal.

α -conotoxin GI from the snail specifically inhibits the conventional (mature and immature) AChRs in muscle but does not inhibit α -7 AChRs. The important role of α -7 AChRs in resistance to NDMRs is evidenced by the presence of immobilization-induced resistance in wild-type mice and the absence of resistance in α -7 AChRs knockout mice.⁷³ The α -7 AChRs expressed in neuronal tissue are also readily desensitized with choline, a feature that contrasts with muscle α -7 AChRs, which do not desensitize with choline.⁶⁹ The α -7 AChRs in muscle also have lower affinity for its antagonists, including pancuronium, rocuronium, atracurium, or α -bungarotoxin; higher concentrations of these drugs are therefore required to block agonist-induced depolarization in α -7 AChRs in vitro or cause neuromuscular paralysis in vivo or ex vivo when α -7 AChRs are upregulated.⁶⁹⁻⁷² In the conventional muscle AChRs, binding of even one of the α -1-subunits by an antagonist results in inactivation of that receptor because acetylcholine needs both α -1-subunits of the AChR for its activation. In α -7 AChRs, however, even when three subunits are bound by an antagonist (e.g., muscle relaxant), two other subunits are still available for binding by agonist and cause depolarization. This feature may account for some of the resistance to muscle relaxants when α -7 AChRs are expressed in muscle and other tissues in pathologic states.⁶⁹⁻⁷³

The clinical pharmacologic characteristics of the muscle α -7 AChR have not yet been completely studied, but its basic composition also provides some insight into succinylcholine-related hyperkalemia. Chemical or physical denervation of muscle results in not only upregulation and qualitative (ϵ -subunit \rightarrow γ -subunit) changes in AChRs, but it also results in upregulation of α -7 AChRs in muscle. Succinylcholine, a synthetic analog of acetylcholine that consists of two molecules of acetylcholine joined together, is capable of depolarizing not only conventional AChRs but also α -7 AChRs in muscle.⁷² In addition, the metabolite of succinylcholine, choline, can depolarize α -7 AChRs with little desensitization. The depolarizing effects of succinylcholine and choline on upregulated α -7 AChRs can result in continued leakage of intracellular potassium and flooding of extracellular fluid, including plasma, thereby leading to hyperkalemia. Thus, differences in the subunit composition and increased numbers of the three isoforms junctionally and extrajunctionally expressed may account for aberrant responses to muscle relaxants clinically observed as resistant only to NDMRs and hyperkalemic response to succinylcholine.^{2,72,73}

MAINTENANCE OF MATURE NEUROMUSCULAR JUNCTIONS

Quite unlike other cells, muscle cells are unusual in that they have many, usually hundreds, of nuclei per cell. Each nucleus has the genes to make all three isoform receptors. Multiple factors, including electrical activity, growth factor signaling (e.g., insulin, agrin, neuregulins), and the presence or absence of innervation, control the expression of the three types of receptor isoforms.^{19,37} This control is most clearly observed in the developing embryo as the neuromuscular junction is formed. Before they are innervated, the muscle cells of a fetus synthesize only immature

and $\alpha 7$ AChRs—hence the term *fetal isoform* for the former receptor. Synthesis is directed by nearly all of the nuclei in the cell, and the AChRs are expressed throughout the membrane of the muscle cell (see Fig. 12.7). As the fetus develops and the muscles become innervated, muscle cells begin to synthesize the mature isoform of receptors, which are exclusively inserted into the developing (future) end-plate area.¹⁴⁻¹⁹ The nerve releases several growth factors that influence the synthetic apparatus of the nearby nuclei. First, nerve-supplied factors induce the subsynaptic nuclei to increase synthesis of AChRs. Next, the nerve-induced electrical activity results in the repression of receptors in the extrajunctional area (see Fig. 12.7B and C). Nerve-derived growth factors, including agrin and ARIA/neuregulin, cause the receptors to cluster in the subsynaptic area and prompt the expression of the mature isoform.^{19,37} Several lines of evidence indicate that clustering, expression, and stabilization of mature receptors are triggered by at least two growth factors: agrin, neuregulin/ARIA, and possibly calcitonin gene-related peptide.^{56,74,75} Neuregulin and agrin are also released from muscle, but muscle-derived agrin is not as important in clustering and maturation of the receptor. ARIA is made in the nerve and plays a role in the maturation of vesicular arrangement and conversion of the γ -to- ϵ switch.⁷⁵ All of these growth factors interact with distinct membrane and cytosolic receptor proteins to cause phosphorylation and activation of nuclear (gene) transcriptional systems. Agrin signals through MuSK and neuregulins through ErbB receptors (Fig. 12.8). These receptors control qualitative and quantitative changes at the junction. Once begun, the process is very stable, and nuclei in the junctional area continue to express mature receptors. In certain pathologic state-induced insulin resistance, a concomitant proliferation of AChRs seems to occur beyond the junctional area. Conditions in which this form of insulin resistance (i.e., decreased growth factor signaling) has been observed include immobilization, burn injury, sepsis, and denervation⁷⁵⁻⁷⁸; in these conditions, not only does upregulation of total AChRs occur, but *de novo* upregulation of the immature and $\alpha 7$ AChR isoforms are also observed (see Fig. 12.7D).¹⁻³ This upregulation may be related to the lack of growth factor effects of agrin and possibly neuregulin, which signal via some of the same downstream signaling proteins as insulin (e.g., phosphoinositide 3-kinase).^{56,76-79} Therefore, agrin and neuregulin signaling may be important for the suppression of $\alpha 7$ AChRs and immature AChRs in the normal neuromuscular junction.

Before innervation, as in the fetus, AChRs are present throughout the muscle membrane. After innervation, AChRs become more and more concentrated at the post-synaptic membrane and are virtually absent in the extra-synaptic area at birth. The innervation process progresses somewhat slowly during fetal life and matures during infancy and early childhood.¹⁴⁻¹⁹ With time, the immature receptors diminish in concentration and disappear from the peripheral part of the muscle. In the active, adult, and normal innervated muscle, just the nuclei under and very near the end plate direct the synthesis of the receptor; only the genes for expressing mature receptors are active. Nuclei beyond the junctional area are not active, and therefore no receptors are expressed anywhere in the muscle cells beyond the perijunctional area. Conversion of all the

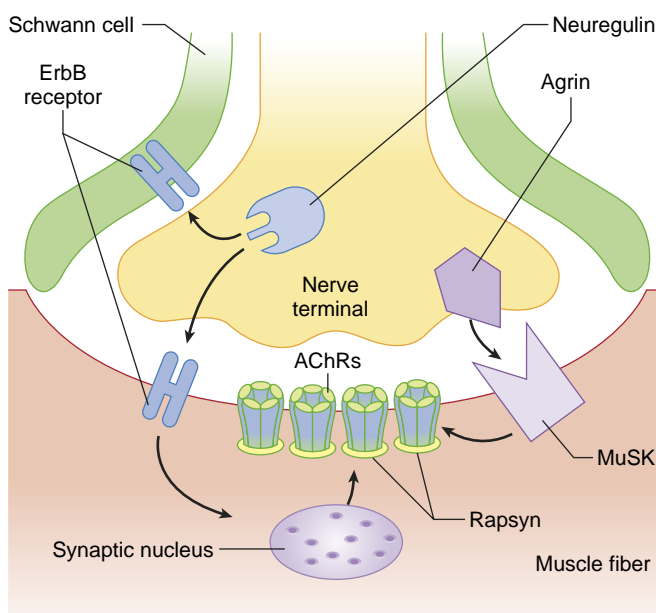


Fig. 12.8 Diagram of agrin- and acetylcholine receptor-inducing activity (ARIA)/neuregulin-dependent events during maturation of the neuromuscular junction. After the establishment of a nerve on the muscle, growth factors, including agrin and neuregulins, are released. Neuregulin signaling is essential for Schwann cell survival, and Schwann cells are essential for axonal maintenance. Agrin interacting with its receptor muscle-specific tyrosine kinase (*MuSK*) enhances the clustering of synaptic proteins, including acetylcholine receptors (*AChRs*), rapsyn, and ErbB receptors. ARIA/neuregulin is the best candidate for the involvement in the conversion of γ -subunit-containing immature receptor to ϵ -subunit-containing mature (innervated) receptor, which is synapse specific and therefore not inserted in the extrajunctional area.

γ -subunit- to ϵ -subunit-containing AChRs in the perijunctional area continues to take place after birth. In the rodent, conversion takes approximately 2 weeks.¹⁴⁻¹⁹ In humans, this process takes longer. The timeframe for the disappearance of $\alpha 7$ AChRs in the fetus or newborn is also unknown. Proteins implicated in the linking of mature receptors to the cytoskeleton include integrin, syntrophin, utrophin, α - and β -dystroglycan, and rapsyn, just to name a few.¹⁴⁻¹⁹

RE-EXPRESSION OF IMMATURE (FETAL) γ -SUBUNIT AND $\alpha 7$ -SUBUNIT ACETYLCHOLINE RECEPTORS IN ADULT LIFE

The extrajunctional immature receptors can reappear soon after upper and lower motor denervation and in certain pathologic states (e.g., burns, sepsis, immobilization, chronic muscle relaxant therapy or botulism, loss of muscle electrical activity). Stimulation of a denervated muscle with an external electrical stimulus can prevent the appearance of immature receptors. It has been suggested that the calcium that enters the muscle during activity is important in the suppression process.^{16,17} In the pathologic states previously enumerated, if the process is severe and prolonged, then extrajunctional receptors are inserted all over the surface of the muscle, including the perijunctional area (see Fig. 12.7D). The junctional nuclei also continue to make mature receptors. The synthesis of immature receptors is initiated within hours of inactivity, but it takes several

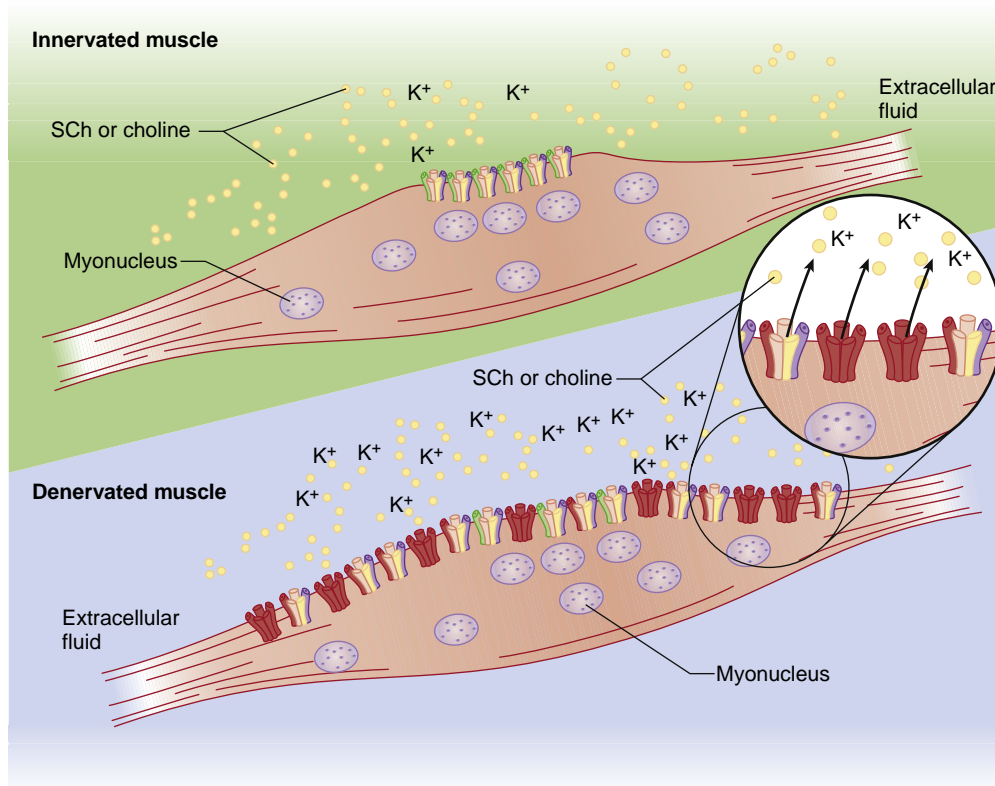


Fig. 12.9 Schematic of the succinylcholine (SCh)-induced potassium (K⁺) release in an innervated (top) and denervated muscle (bottom). In the innervated muscle, the systemically administered SCh reaches all the muscle membrane but depolarizes only the junctional ($\alpha 1, \beta 1, \delta/\epsilon$) receptors because acetylcholine receptors (AChRs) are located only in this area. With denervation, the muscle nuclei express not only extrajunctional ($\alpha 1, \beta 1, \delta/\gamma$) AChRs but also $\alpha 7$ -nicotinic AChRs throughout the muscle membrane. Systemic SCh, in contrast to acetylcholine released locally, can depolarize all the upregulated AChRs, which leads to massive efflux of intracellular K⁺ into the circulation, resulting in hyperkalemia. The metabolite of SCh, choline, and possibly succinylmonocholine, can maintain this depolarization via $\alpha 7$ -nicotinic AChRs, enhancing the K⁺ release and maintaining the hyperkalemia. (From Martyn JA, Richtsfeld M. Succinylcholine-induced hyperkalemia in acquired pathologic states: etiologic factors and molecular mechanisms. *Anesthesiology*. 2006;104:158–169, 2006.)

days for the whole muscle membrane to be fully covered with receptors. This upregulation of receptors has implications for the use of depolarizing and possibly NDMRs. The changes in $\alpha 7$ AChRs parallel the expression of immature receptors, although this has not been well studied.

The changes in subunit composition (γ vs. ϵ) in the receptor confer certain changes in electrophysiologic (functional), pharmacologic, and metabolic characteristics.^{16–18} Mature receptors are metabolically stable, with a half-life approximating 2 weeks, whereas immature receptors have a metabolic half-life of less than 24 hours. Immature receptors have a smaller single-channel conductance and a twofold to tenfold longer mean channel open time than do mature receptors (see Fig. 12.4). The changes in subunit composition may also alter the sensitivity or affinity, or both, of the receptor for specific ligands. Depolarizing or agonist drugs such as succinylcholine and acetylcholine more easily depolarize immature receptors, thereby resulting in cation fluxes; doses one tenth to one hundredth of those needed for mature receptors can effect depolarization.² The potency of NDMRs is also reduced, as demonstrated by the resistance to their neuromuscular effects documented in patients with burns, denervation, sepsis, and immobilization.^{1,3} In light of recent research, however, it seems that the resistance to nondepolarizers is more likely due to the junctional area expression of the $\alpha 7$ AChRs, which has a decreased affinity

to NDMRs.^{16,69–73} Some NDMRs may also cause a partial agonist response in immature receptors, thus explaining the decreased potency in conditions in which upregulation of AChRs occurs.⁸ The upregulation of immature AChRs in the perijunctional and extrajunctional areas may have a buffering effect for diffusion of relaxants, contributing to resistance to NDMRs.⁸⁰

The altered sensitivity to muscle relaxants may occur in only certain parts of the body or certain muscles if only some muscles are affected by the diminution in nerve activity (e.g., after a stroke). Sensitivity to relaxants can begin to change beyond 72 hours after an injury or hospitalization. The most serious side effect with the use of succinylcholine in the presence of upregulated AChRs in one or more muscles is hyperkalemia.^{1–3} In these subjects, the receptors can be scattered over a large surface of the muscle. The AChR channels opened by the agonist (succinylcholine) allow potassium to escape from the muscle and enter the blood (Fig. 12.9).^{2,3} If a large part of the muscle surface consists of upregulated (immature) receptor channels, each of which stays open for a longer time, then the amount of potassium that moves from muscle to blood can be considerable. The resulting hyperkalemia can cause dangerous disturbances in cardiac rhythm, including ventricular fibrillation. Moreover, hyperkalemia probably cannot be prevented by prior administration of NDMRs because large doses required to

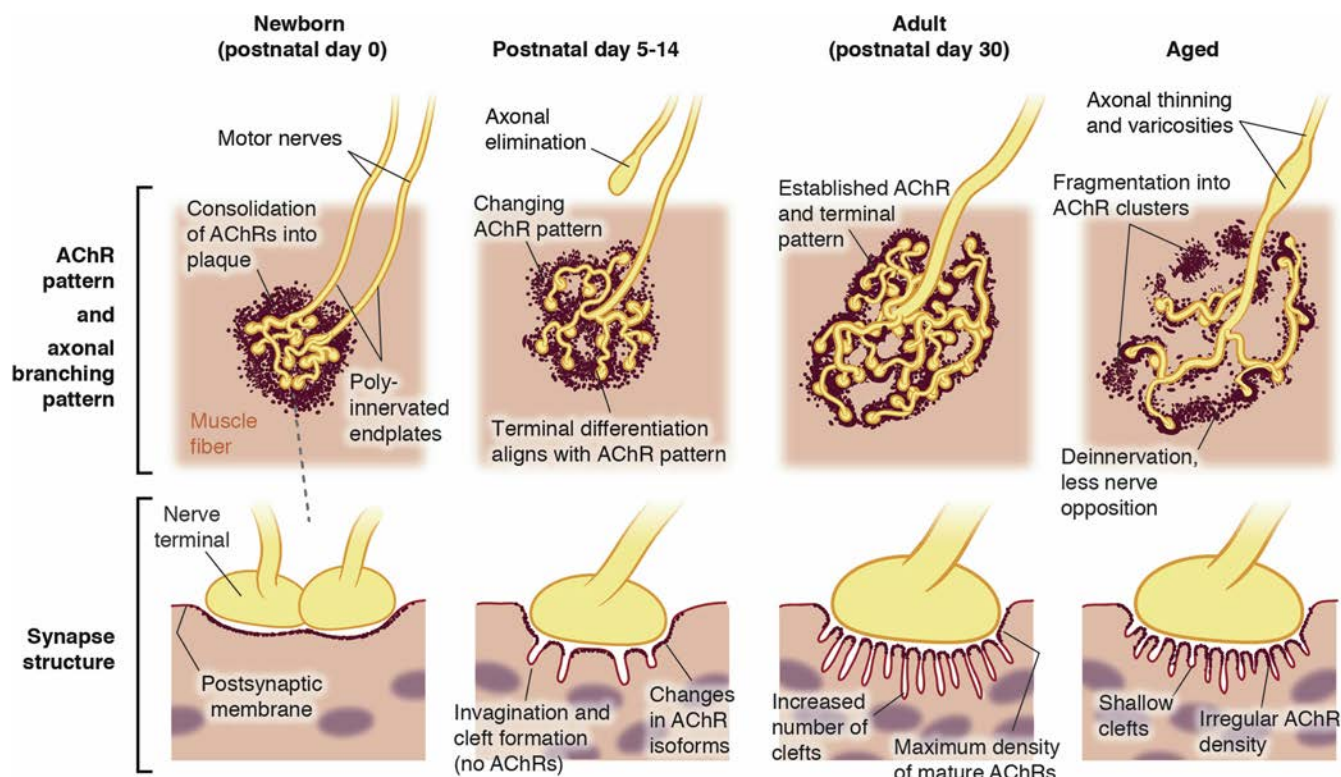


Fig. 12.10 Maturation of the postsynaptic apparatus. *Postnatal day 0 (Newborn)*: At the time of birth, the aggregates of acetylcholine receptors (AChRs) have consolidated to form an oval-like plaque with irregular borders. At this point, each junction may have more than one nerve terminal innervating it. *Postnatal day 5 to 14*: Approximately 5 to 14 days after birth, the postsynaptic membrane invaginates to form a gutter and small perforations develop on the plaque. These perforations reflect gaps due to the synaptic clefts (which do not have AChRs). During this time, the immature γ -subunit-containing AChRs are completely replaced by mature AChRs containing ϵ -subunit. The invaginations or clefts increase in numbers, resulting in more perforations in the synaptic AChRs giving it an almost pretzel-shaped junction. The perforations, as indicated, correspond to the synaptic clefts or folds. *Postnatal day 30*: The neuromuscular junction is completely developed (mature) at 30 days after birth with a larger pretzel-shaped appearance. The AChRs have maximal density. A distinct set of postsynaptic proteins and signaling molecules are selectively transcribed in the subsynaptic area, providing integrity to the neuromuscular junction and efficient neurotransmission. *Aged NMJ*: Examination of NMJ in the aged mice and humans reveal marked morphological changes. Some of the synapses undergo partial degeneration and synaptic staining becomes fainter. The synaptic folds are smaller in depth. The nerve terminals become thinner and appear swollen or bulbous with less apposition with the synapse. The Schwann cells seems to invade into the NMJ more (not shown). *NMJ*, neuromuscular junction.

block the AChRs, in and of itself, will cause paralysis, obviating the need for succinylcholine.³ Larger-than-normal doses of NDMRs may attenuate the increase in blood potassium concentrations but cannot completely prevent it. In other words, no hyperkalemic response to succinylcholine has been seen earlier than 4 days after perturbations described previously.⁵⁰ However, hyperkalemia and cardiac arrest can occur after the administration of succinylcholine, even in the absence of denervation states. These effects are observed in certain congenital muscle dystrophies in which the muscle membrane is prone to damage by the depolarization produced by succinylcholine, resulting in potassium release via the membrane damage.⁸¹

PREJUNCTIONAL ACETYLCHOLINE RECEPTORS

Nicotinic AChRs exist in a variety of forms apart from that observed in muscle.^{16,18} The classic muscle-type nicotinic AChR is postsynaptically present, whereas neuronal subtype receptors may be presynaptically and postsynaptically present. The neuronal subtype nicotinic AChRs expressed

prejunctionally are usually heteromeric and built up by only α - and β -subunits. This family of nicotinic AChRs is widely expressed in the peripheral and central nervous systems, on autonomous nerves and ganglia on oxygen-sensing cells within the carotid bodies. There are also $\alpha 7$ AChRs in immune-competent cells, such as macrophages, microglia lymphocytes and granulocytes, and fibroblasts and chondrocytes.^{16,18} Diverse genes encode the heterogeneous AChRs, and the ion channel is formed of multiple subunits (multimers). Seventeen AChR genes have been cloned from vertebrates. They include various combinations of α -subunits ($\alpha 1$ through $\alpha 10$) and β -subunits ($\beta 1$ through $\beta 4$) and one each of γ -, δ -, and ϵ -subunits. The γ -, δ -, and ϵ -subunits are found only in muscle.¹⁶⁻¹⁸

Prejunctional- or nerve terminal-associated cholinergic receptors have been demonstrated by morphologic pharmacologic and by molecular biologic techniques, but their form and functions are not as completely understood as those in the postjunctional area. Many drugs with an abundance of potential targets for drug action can affect the capacity of the nerve terminal to carry out its functions. The

trophic function to maintain nerve-muscle contact involves the release and replenishment of acetylcholine together with other trophic factors that require signaling through many receptors, of which the prejunctional nicotinic AChR is just one. Succinylcholine produces fasciculations that can be prevented by NDMRs. Because a fasciculation is, by definition, the simultaneous contraction of the multitude of muscle cells in a single motor unit and because only the nerve can synchronize all the muscles in its motor unit, it became apparent that succinylcholine must also act on nerve endings. Because NDMRs prevent fasciculation, it was concluded that they acted on the same prejunctional receptor. Very small doses of cholinergic agonists (e.g., succinylcholine) and antagonists (e.g., NDMRs) affect nicotinic receptors on the nerve ending; the former by depolarizing the ending and sometimes inducing repetitive firing of the nerve and the latter by preventing the action of agonists.⁵

By the use of specific monoclonal antibodies, the presence of nicotinic $\alpha 3$ -subunits has been demonstrated in the nerve terminal.⁸² Another clue to the differences between prejunctional and postjunctional AChRs was the finding that some drugs (e.g., dihydro- β -erythroidine) bind only to prejunctional AChRs, whereas other drugs (e.g., α -bungarotoxin) bind only to postjunctional receptors.⁶⁵ Additional clues were found in the many demonstrations of quantitative differences in the reaction of prejunctional and postjunctional nicotinic receptors to other cholinergic agonists and antagonists.^{65,82-84} For instance, it was known that tubocurarine, the first NDMR introduced to clinical practice in 1942 (not used in US or Europe), binds with lower affinity to the recognition sites of ganglionic nicotinic cholinoreceptors and is not a competitive antagonist of acetylcholine at this site. Decamethonium (i.e., a depolarizing muscle relaxant no longer clinically used) is a selective inhibitor of the muscle receptor, and hexamethonium is a selective inhibitor of nicotinic receptors in the autonomic ganglia.⁸⁰⁻⁸⁵ Instead, tubocurarine and hexamethonium can block the opened channels of these receptors and owe their ability to block ganglionic transmission to this property. The functional characteristics of prejunctional receptor channels may also be different. For example, the depolarization of motor nerve endings initiated by the administration of acetylcholine can be prevented by tetrodotoxin, a specific blocker of sodium flux with no effect on the end plate.

Specific information on the molecular organization of neuronal nicotinic receptors on the motor neuron terminal is still lacking. Some of the subunit composition is similar, but other subunits do not resemble those of the postjunctional receptor. Of the 16 different nicotinic AChR gene products identified, only 12 ($\alpha 2$ to $\alpha 10$ and $\beta 2$ to $\beta 4$) are thought to contribute nicotinic receptors expressed on neurons. Most strikingly, nervous tissue does not express γ -, δ -, or ϵ -receptor subunits; it contains genes only for the α - and β -subunits. The α - and β -subunit genes in nerve and muscle are not exactly the same; they are variants. To emphasize the distinction between neural and muscle nicotinic receptors, the former are sometimes designated Nn and the latter Nm . With so many different subunits available, possible combinations are many, and it is not known which combinations are found in motor nerves. Their physiologic roles have also not been completely characterized. Expression of neuronal nicotinic AChRs in *in vitro* systems has confirmed

that muscle relaxants and their metabolites can bind to some of these neuronal AChRs.^{53,83-85}

The nicotinic receptor on the junctional surface of the nerve (nerve terminal) senses transmitter in the cleft and, by means of a positive-feedback system, causes the release of more transmitter. In other parts of the nervous system, this positive feedback is complemented by a negative-feedback system that senses when the concentration of transmitter in the synaptic cleft has appropriately increased and shuts down the release system. It is believed that tetanic fade and train-of-four fade during neuromuscular block with NDMRs arise from presynaptic cholinergic autoreceptors at the motor nerve ending.^{5,52}

The neuronal AChR subtype that is critically involved in acetylcholine release and subsequent fade phenomenon (as observed in tetanic or train-of-four stimulus patterns) has been identified as the $\alpha 3\beta 2$ -subtype nicotinic AChR.^{10,84} When this prejunctional receptor is specifically blocked by a nondepolarizing relaxant such as tubocurarine, a reduction in neurotransmitter release occurs upon repeated stimulation with subsequent fade phenomenon. It should be noted, however, block of the prejunctional AChRs alone is not necessary and sufficient to induce fade; concomitant reduction in the safety of neurotransmission prejunctionally or postjunctionally must be present for it to be noticeable.⁶⁵ Although all clinically used nondepolarizing neuromuscular blocking drugs inhibit this prejunctional nicotinic AChR, as well as several other neuronal nicotinic AChRs, in the clinically relevant concentration range, succinylcholine neither activates nor inhibits the presynaptic $\alpha 3\beta 2$ autoreceptor at clinically relevant concentrations.^{53,85} However, the existence of the $\alpha 3\beta 2$ autoreceptor at the prejunctional area has never been demonstrated by western blot or mRNA techniques. Thus, this prejunctional receptor has not been completely characterized.

This observation may be the reason for the typical lack of fade during succinylcholine-induced neuromuscular block. Succinylcholine, however, does not interact with $\alpha 3\beta 4$ AChR found in autonomic ganglia.⁵³ It has also been shown that NDMRs reduce the hypoxic ventilatory response in partially paralyzed humans,⁸⁶ and the mechanism behind the depression might be related to inhibition of nicotine receptors on the carotid body.¹¹ Nicotinic $\alpha 3$, 7, and $\beta 2$ AChRs have recently been documented in the human carotid body.⁸⁷ Whether the inhibition of these receptors plays a role in attenuated response to hypoxia drive needs further investigation. The motor nerve terminal is also known to bear several other receptors, such as opioid, adrenergic, dopamine, purine, and adenosine receptors, as well as receptors for endogenous hormones, neuropeptides, and a variety of proteins.^{88,89} The physiologic roles of these receptors and the effects of anesthetics on them are unknown.

Neuromuscular Junction at Extremes of Age

NEWBORN

Just before birth, the AChRs are all clustered around the nerve in the junctional area, and minimal extrajunctional AChRs are present. The newborn postsynaptic membrane, itself, is not specialized, having almost no synaptic

folds, a widened synaptic space, and a reduced number of AChRs.^{14,19} The early postnatal AChR cluster appears as an oval plaque (Fig. 12.10). Within a few days, simplified folds appear. With continued maturation, the plaque is transformed to a multiperforated pretzel-like structure. The polyinnervated end plate is converted to a singly innervated junction because of a retraction of all but one terminal. In the adult, the terminals perfectly align with the AChR clusters. Morphologically, the postsynaptic membrane of the newborn and that from the patient with myasthenia gravis is not too different; the AChR number is decreased, and the postsynaptic folds are decreased. It is not surprising therefore that neurotransmission is not as efficient in the newborn and in patients with myasthenia gravis. For this reason, neonates and infants behave similar to patients with myasthenia gravis when NDMRs are administered to them.⁹⁰ In humans, maturation of the neuromuscular junction probably occurs at approximately 2 years of age.⁹⁰

OLD AGE

With increasing life expectancy, typical changes associated with aging is a gradual loss of lean body mass and strength referred to as sarcopenia (Greek: sarco-flesh, penia- poverty), which has received increased attention recently.⁹¹ These sarcopenic changes occur in association with denervation-like changes at the synapse and altered anabolic or growth factor signaling changes within muscle.⁹¹⁻⁹³ Old age-associated functional denervation, muscle wasting, and weakness is now well established.^{91,92} Age-related morphologic changes include increase in length and area of the post-synaptic AChR, degenerating synaptic folds, and more invasion of synaptic folds by Schwann cells. The nerve terminals are thinned out and show terminal swelling with less apposition of the nerve to the synapse (see Fig. 12.10). Coupled with the morphologic changes in the neuromuscular junction that occur with aging, the functional changes that occur with it can include increased quantal content of neurotransmitter release and more rapid rundown of end-plate potential during stimulation of the preterminal neuron.⁹¹⁻⁹³ Regardless of these enumerated structured and functioned changes with aging, it appears that because of the superb margin of safety of neurotransmission, disability is not easily demonstrable by simple methods such as grip strength in most instances.⁹³ Despite the structural and functional changes associated with aging, the overall margin of safety is better in the older individual than in the neonate.⁹⁴ Even with these denervation-like changes in the elderly, there is no evidence that these patients are more prone to succinylcholine-induced hyperkalemia. There are also no studies confirming increased or decreased sensitivity to nondepolarizing blockers due to the neuromuscular junction changes. Some nondepolarizing neuromuscular blockers have prolonged effect in old age (e.g., vecuronium) due to pharmacokinetic causes.

 Complete references available online at expertconsult.com.

References

- Martyn JA, et al. *Anaesthesia*. 2009;64(suppl 1):1.
- Martyn JA, Richtsfeld M. *Anesthesiology*. 2006;104:158.
- Fagerlund MJ, Eriksson LI. *Br J Anaesth*. 2009;103(1):108.
- Gilhus NE. *Curr Opin Neurol*. 2012;25:523.
- Bowman WC, et al. *Ann N Y Acad Sci*. 1990;604:69.
- Frick CG, et al. *Anesthesiology*. 2007;106:1139.
- Frick CG, et al. *Anesth Analg*. 2012;114:102.
- Lape R, et al. *Nature*. 2008;454:722.
- Paul M, et al. *Eur J Pharmacol*. 2002;438:35.
- Vizi ES, Lendvai B. *Pharmacol Ther*. 1997;73:75.
- Jonsson M, et al. *Eur J Pharmacol*. 2004;497:173.
- Sunaga H, et al. *Anesthesiology*. 2010;112:892.
- Fryer AD, Maclagan J. *Naunyn Schmiedebergs Arch Pharmacol*. 1987;335:367.
- Li L, et al. *Annu Rev Physiol*. 2018;80:159.
- Tintignac LA, et al. *Physiol Rev*. 2015;95:809.
- Lee S, et al. *Anesthesiology*. 2014;120(1):76-85.
- Sine SM. *Physiol Rev*. 2012;92:1189.
- Albuquerque EX, et al. *Physiol Rev*. 2009;89:73.
- Shi L, et al. *Trends Neurosci*. 2012;35:441.
- Fraterman S, et al. *Invest Ophthalmol Vis Sci*. 2006;47:3828.
- Büttner-Ennever JA, Horn AK. *Mov Disord*. 2002;17(suppl 2):S2.
- Kaminski HJ, et al. *Invest Ophthalmol Vis Sci*. 1996;37:345.
- Lennérstrand G, et al. *Acta Ophthalmol*. 2010;88:872.
- Vachon CA, et al. *Anesthesiology*. 2003;99:220.
- Catterall WA. *J Physiol*. 2012;590:2577.
- Catterall WA, et al. *J Biol Chem*. 2013;288:10742.
- Engel AG, et al. *Ann N Y Acad Sci*. 2012;1275:54.
- Heuser JE, Reese TS. *J Cell Biol*. 1981;88:564.
- Rash JE, et al. *J Electron Microsc Tech*. 1988;10(153).
- Sieburth D, et al. *Nature*. 2005;436:510.
- Littleton JT, Sheng M. *Nature*. 2003;423:931.
- Rich MM. *Neuroscientist*. 2006;12:134.
- Wang X, et al. *J Neurosci*. 2004;24:10687.
- Katz B, Miledi R. *Proc R Soc Lond B Biol Sci*. 1979;215:369.
- Uchitel OD, et al. *Proc Natl Acad Sci U S A*. 1992;89:3330.
- van Sonderen A, et al. *Curr Treat Options Neurol*. 2013;15:224-239.
- Naguib M, et al. *Anesthesiology*. 2002;96:202.
- Sudhof TC. *Neuron*. 2012;75:11.
- Jahn R, Fasshauer D. *Nature*. 2012;490:201.
- Heidelberger R. *Nature*. 2007;450:623.
- Turton K, et al. *Trends Biochem Sci*. 2002;27:552.
- Restani L, et al. *PLoS Pathog*. 2012;8:e1003087.
- Schurh B. *Drugs Today (Barc)*. 2004;40:205.
- Schiavo G. *Nature*. 2006;444:1019.
- Lange DJ, et al. *Muscle Nerve*. 1991;14:672.
- Heeroma JH, et al. *Neuroscience*. 2003;120:733.
- Engel AG, Sine SM. *Curr Opin Pharmacol*. 2005;5:308.
- Abraham RB, et al. *Anesthesiology*. 2002;97:989.
- Karwa M, et al. *Crit Care Med*. 2005;33:S75.
- Richtsfeld M, et al. *Anesthesiology*. 2013;119:412.
- Kopta C, Steinbach JH. *J Neurosci*. 1994;14:3922.
- Jonsson M, et al. *Anesthesiology*. 2006;105:521.
- Jonsson M, et al. *Anesthesiology*. 2006;104:724.
- Griesmann GE, et al. *J Neurochem*. 1990;54:1541.
- Gullberg D. *Nature*. 2003;424:138.
- Missias AC, et al. *Dev Biol*. 1996;179:223.
- McCarthy MP, Stroud RM. *Biochemistry*. 1989;28:40.
- Yamaoka K, et al. *Curr Pharm Des*. 2006;12:429.
- Raines DE. *Anesthesiology*. 1996;84:663.
- Gage PW. *Biophys Chem*. 1988;29:95.
- Swope SL, et al. *Ann N Y Acad Sci*. 1995;757:197.
- Plestis CP, et al. *Neurology*. 2002;59:1682.
- Albuquerque EX, et al. *J Pharmacol Exp Ther*. 1997;280:1117.
- Maelicke A, et al. *J Recept Signal Transduct Res*. 1997;17:11.
- Nagashima M, et al. *Anesth Analg*. 2013;116:994.
- Creese R, et al. *J Physiol*. 1987;384:377.
- Ibebungo C, Martyn JA. *Anesth Analg*. 2000;91:1243.
- Fischer U, et al. *Eur J Neurosci*. 1999;11:2856.
- Tsuneki H, et al. *J Physiol*. 2003;54(7):169.
- Liu L, et al. *Br J Anaesth*. 2014;112:159.
- Lindstrom JM. *Ann N Y Acad Sci*. 2003;998:41.
- Khan MA, et al. *Shock*. 2012;38:213.
- Lee S, et al. *Alpha7 AChRs play a pivotal role in the immobilization-induced resistance to atracurium in mice*. Abstract A1007; Presented at the ASA Annual Meeting, 2012.
- Placzek AN, et al. *Mol Pharmacol*. 2004;66:169.
- Tansey MG, et al. *J Cell Biol*. 1996;134:465.
- Hirose M, et al. *Am J Physiol*. 2000;279:E1235.

77. Sugita M, et al. *Metabolism*. 2012;61:127.
78. Hirose M, et al. *Metabolism*. 2001;50:216.
79. Samuel MA, et al. *PLoS One*. 2012;7:e456663.
80. Dilger JP. *Anesth Analg*. 2013;117:792.
81. Gronert GA. *Anesthesiology*. 2001;94:523.
82. Tsuneki H, et al. *Neurosci Lett*. 1995;196:13.
83. Chiodini F, et al. *Anesthesiology*. 2001;94:643.
84. Faria M, et al. *Synapse*. 2003;49:77.
85. Martyn J, Durieux ME. *Anesthesiology*. 2006;104:633.
86. Eriksson LI. *Acta Anaesthesiol Scand*. 1996;40:520.
87. Mkrtchian S, et al. *J Physiol*. 2012;590:3807.
88. Santafe MM, et al. *Eur J Neurosci*. 2003;17:119.
89. Wessler I. *Trends Pharmacol Sci*. 1989;10:110.
90. Goudsouzian NG, Standaert FG. *Anesth Analg*. 1986;65:1208.
91. Shafiee G, et al. *J Diabetes Metab Disord*. 2017;16:21.
92. Yang JC, Van Remmen H. *Exp Gerontol*. 2011;46(2-3):193.
93. Willadt, et al. *Ann NY Acad Sci*. 2018;1412:41–53.
94. Sanes JR, Lichtman JW. *Nat Rev Neurosci*. 2001;2:791.

References

- Martyn JA, Jonsson M, Fagerlund MJ, et al. Basic principles of neuromuscular transmission. *Anesthesia*. 2009;64(suppl 1):1–9.
- Martyn JA, Richtsfeld M. Succinylcholine-induced hyperkalemia in acquired pathologic states: etiologic factors and molecular mechanisms. *Anesthesiology*. 2006;104:158–169.
- Fagerlund MJ, Eriksson LI. Current concepts in neuromuscular transmission. *Br J Anaesth*. 2009;103(1):108–114.
- Gilhus NE. Myasthenia and the neuromuscular junction. *Curr Opin Neurol*. 2012;25:523–529.
- Bowman WC, Prior C, Marshall IG. Presynaptic receptors in the neuromuscular junction. *Ann N Y Acad Sci*. 1990;604:69–81.
- Frick CG, Richtsfeld M, Sahani ND, et al. Long-term effects of botulinum toxin on neuromuscular function. *Anesthesiology*. 2007;106:1139–1146.
- Frick CG, Fink H, Blobner M, Martyn JA. A single injection of botulinum toxin decreases the margin of safety of neurotransmission at local and distant sites. *Anesth Analg*. 2012;114:102–109.
- Lape R, Colquhoun D, Sivilotti LG. On the nature of partial agonism in the nicotinic receptor superfamily. *Nature*. 2008;454:722–727.
- Paul M, Kindler CH, Fokt RM, et al. Isobolographic analysis of non-depolarising muscle relaxant interactions at their receptor site. *Eur J Pharmacol*. 2002;438:35–43.
- Vizi ES, Lendvai B. Side effects of nondepolarizing muscle relaxants: relationship to their antinicotinic and antimuscarinic actions. *Pharmacol Ther*. 1997;73:75–89.
- Jonsson M, Wyon N, Lindahl SGE. Neuromuscular blocking agents block carotid body neuronal nicotinic acetylcholine receptors. *Eur J Pharmacol*. 2004;497:173–180.
- Sunaga H, Zhang Y, Savarese JJ, Emala CW. Gantacurium and CW002 do not potentiate muscarinic receptor-mediated airway smooth muscle constriction in guinea pigs. *Anesthesiology*. 2010;112:892–899.
- Fryer AD, Maclagan J. Pancuronium and gallamine are antagonists for pre- and post-junctional muscarinic receptors in the guinea-pig lung. *Naunyn Schmiedebergs Arch Pharmacol*. 1987;335:367–371.
- Li L, Xiong WC, Mei L. Neuromuscular junction formation, aging, and disorders. *Annu Rev Physiol*. 2018;80:159–188.
- Tintignac LA, Brenner HR, Rüegg MA. Mechanisms regulating neuromuscular junction development and function and causes of muscle wasting. *Physiol Rev*. 2015;95:809–852.
- Lee S, Yang HS, Sasakawa T, et al. Immobilization with atrophy induces de novo expression of neuronal nicotinic $\alpha 7$ acetylcholine receptors in muscle contributing to neurotransmission. *Anesthesiology*. 2014;120(1):76–85.
- Sine SM. End-plate acetylcholine receptor: structure, mechanism, pharmacology, and disease. *Physiol Rev*. 2012;92:1189–1234.
- Albuquerque EX, Pereira EF, Alkondon M, Rogers SW. Mammalian nicotinic acetylcholine receptors: from structure to function. *Physiol Rev*. 2009;89:73–120.
- Shi L, Fu AK, Ip NY. Molecular mechanisms underlying maturation and maintenance of the vertebrate neuromuscular junction. *Trends Neurosci*. 2012;35:441–453.
- Fraterman S, Khurana TS, Rubinstein NA. Identification of acetylcholine receptor subunits differentially expressed in singly and multiply innervated fibers of extraocular muscles. *Invest Ophthalmol Vis Sci*. 2006;47:3828–3834.
- Büttner-Ennever JA, Horn AK. Oculomotor system: a dual innervation of the eye muscles from the abducens, trochlear, and oculomotor nuclei. *Mov Disord*. 2002;17(suppl 2):S2.
- Kaminski HJ, Kusner LL, Block CH. Expression of acetylcholine receptor isoforms at extraocular muscle endplates. *Invest Ophthalmol Vis Sci*. 1996;37:345–351.
- Lenserstrand G, Bolzani R, Tian S, et al. Succinylcholine activation of human horizontal eye muscles. *Acta Ophthalmol*. 2010;88:872–876.
- Vachon CA, Warner DO, Bacon DR. Succinylcholine and the open globe. Tracing the teaching. *Anesthesiology*. 2003;99:220–223.
- Catterall WA. Voltage-gated sodium channels at 60: structure, function and pathophysiology. *J Physiol*. 2012;590:2577–2589.
- Catterall WA, Leal K, Nanou E. Calcium channels and short-term synaptic plasticity. *J Biol Chem*. 2013;288:10742–10749.
- Engel AG, Shen XM, Selcen D, Sine S. New horizons for congenital myasthenic syndromes. *Ann N Y Acad Sci*. 2012;1275:54–62.
- Heuser JE, Reese TS. Structural changes after transmitter release at the frog neuromuscular junction. *J Cell Biol*. 1981;88:564–580.
- Rash JE, Walrond JP, Morita M. Structural and functional correlates of synaptic transmission in the vertebrate neuromuscular junction. *J Electron Microsc Tech*. 1988;10:153–185.
- Sieburth D, Ch'ng Q, Dybbs M, et al. Systematic analysis of genes required for synapse structure and function. *Nature*. 2005;436:510–517.
- Littleton JT, Sheng M. Neurobiology: synapses unplugged. *Nature*. 2003;423:931–932.
- Rich MM. The control of neuromuscular transmission in health and disease. *Neuroscientist*. 2006;12:134–142.
- Wang X, Engisch KL, Li Y, et al. Decreased synaptic activity shifts the calcium dependence of release at the mammalian neuromuscular junction in vivo. *J Neurosci*. 2004;24:10687–10692.
- Katz B, Miledi R. Estimates of quantal content during “chemical potentiation” of transmitter release. *Proc R Soc Lond B Biol Sci*. 1979;205:369–378.
- Uchitel OD, Protti DA, Sanchez V, et al. P-type voltage dependent calcium channel mediates presynaptic calcium influx and transmitter release in mammalian synapses. *Proc Natl Acad Sci U S A*. 1992;89:3330–3333.
- van Sonderen A, Wirtz PW, Verschuur JJ, et al. Paraneoplastic syndromes of the neuromuscular junction: therapeutic options in myasthenia gravis, Lambert-Eaton myasthenic syndrome, and neuromyotonia. *Curr Treat Options Neurol*. 2013;15(2):224–239.
- Naguib M, Flood P, McArdle JJ, Brenner HR. Advances in neurobiology of the neuromuscular junction: implications for the anesthesiologist. *Anesthesiology*. 2002;96:202–231.
- Sudhof TC. The presynaptic active zone. *Neuron*. 2012;75:11–25.
- Jahn R, Fasshauer D. Molecular machines governing exocytosis of synaptic vesicles. *Nature*. 2012;490:201–207.
- Heidelberger R. Neuroscience: sensors and synchronicity. *Nature*. 2007;450:623–625.
- Turton K, Chaddock JA, Acharya KR. Botulinum and tetanus neurotoxins: structure, function and therapeutic utility. *Trends Biochem Sci*. 2002;27:552–558.
- Restani L, Giribaldi F, Manich M, et al. Botulinum neurotoxins A and E undergo retrograde axonal transport in primary motor neurons. *PLoS Pathog*. 2012;8:e1003087.
- Schucht B. The role of botulinum toxin in neurology. *Drugs Today (Barc)*. 2004;40:205–212.
- Schiavo G. Structural biology: dangerous liaisons on neurons. *Nature*. 2006;444:1019–1020.
- Lange DJ, Rubin M, Green PE, et al. Distant effects of locally injected botulinum toxin: a double-blind study of single fiber EMG changes. *Muscle Nerve*. 1991;14:672–675.
- Heeroma JH, Plomp JJ, Roubos EW, Verhage M. Development of the mouse neuromuscular junction in the absence of regulated secretion. *Neuroscience*. 2003;120:733–744.
- Engel AG, Sine SM. Current understanding of congenital myasthenic syndromes. *Curr Opin Pharmacol*. 2005;5:308–321.
- Abraham RB, Rudick V, Weinbroum AA. Practical guidelines for acute care of victims of bioterrorism: conventional injuries and concomitant nerve agent intoxication. *Anesthesiology*. 2002;97:989–1004.
- Karwa M, Currie B, Kvetan V. Bioterrorism: preparing for the impossible or the improbable. *Crit Care Med*. 2005;33:S75–95.
- Richtsfeld M, Yasuhara S, Fink H. Prolonged administration of pyridostigmine impairs neuromuscular function with down-regulation of acetylcholine receptors with and without down-regulation. *Anesthesiology*. 2013;119:412–421.
- Kopta C, Steinbach JH. Comparison of mammalian adult and fetal nicotinic acetylcholinic receptors stably expressed in fibroblasts. *J Neurosci*. 1994;14:3922–3933.
- Jonsson M, Gulrey D, Dabrowski M, et al. Distinct pharmacologic properties of neuromuscular blocking agents on human neuronal nicotinic acetylcholine receptors: a possible explanation for the train-of-four fade. *Anesthesiology*. 2006;105:521–533.
- Jonsson M, Dabrowski M, Gurley DA, et al. Activation and inhibition of human muscular and neuronal nicotinic acetylcholine receptors by succinylcholine. *Anesthesiology*. 2006;104:724–733.
- Griesmann GE, McCormick DJ, De Aizpuru HJ, et al. Alpha-bungarotoxin binds to human acetylcholine receptor alpha-subunit peptide 185–199 in solution and solid phase but not to peptides 125–147 and 389–409. *J Neurochem*. 1990;54:1541–1547.

55. Gullberg D. Cell biology: The molecules that make muscle. *Nature*. 2003;424:138–140.
56. Missias AC, Chu GC, Klocke BJ, et al. Maturation of the acetylcholine receptor in skeletal muscle: regulation of the AChR gamma-to-epsilon switch. *Dev Biol*. 1996;179:223–238.
57. McCarthy MP, Stroud RM. Conformational states of the nicotinic acetylcholine receptor from *Torpedo californica* induced by the binding of agonist, antagonists, and local anesthetics. Equilibrium measurements using tritium-hydrogen exchange. *Biochemistry*. 1989;28:40–48.
58. Yamaoka K, Vogel SM, Seyama I. Na⁺ channel pharmacology and molecular mechanisms of gating. *Curr Pharm Des*. 2006;12:429–442.
59. Raines DE. Anesthesia and nonanesthetic volatile compounds have dissimilar activities on nicotinic acetylcholine receptor desensitization kinetics. *Anesthesiology*. 1996;84:663–671.
60. Gage PW. Ion channels and postsynaptic potentials. *Biophys Chem*. 1988;29:95–101.
61. Swope SL, Qu Z, Huganir RL. Phosphorylation of nicotinic acetylcholine receptor by protein tyrosine kinases. *Ann N Y Acad Sci*. 1995;757:197–214.
62. Plested CP, Tang T, Spreadbury I, et al. AChR phosphorylation and indirect inhibition of AChR function in seronegative MG. *Neurology*. 2002;59:1682–1688.
63. Albuquerque EX, Alkondon M, Pereira EF, et al. Properties of neuronal nicotinic acetylcholine receptors: pharmacologic characterization and modulation of synaptic function. *J Pharmacol Exp Ther*. 1997;280:1117–1136.
64. Maelicke A, Coban T, Storch A, et al. Allosteric modulation of *Torpedo* nicotinic acetylcholine receptor ion channel activity by noncompetitive agonists. *J Recept Signal Transduct Res*. 1997;17:11–28.
65. Nagashima M, Yasuhara S, Martyn JA. Train-of-four and tetanic fade are not always a prejunctional phenomenon as evaluated by toxins having highly specific pre- and post-junctional actions. *Anesth Analg*. 2013;116:994–1000.
66. Creese R, Head SD, Jenkinson DF. The role of the sodium pump during prolonged end-plate currents in guinea-pig diaphragm. *J Physiol*. 1987;384:377–403.
67. Ibebunjo C, Martyn JA. Thermal injury induces greater resistance to d-tubocurarine in local than in distant muscles in the rat. *Anesth Analg*. 2000;91:1243–1249.
68. Fischer U, Reinhardt S, Albuquerque EX, Maelicke A. Expression of functional alpha 7 nicotinic acetylcholine receptor during mammalian muscle development and denervation. *Eur J Neurosci*. 1999;11:2856–2864.
69. Tsuneki H, Salas R, Dani JA. Mouse denervation increases expression of alpha 7 nicotinic receptor with unusual pharmacology. *J Physiol*. 2003;54(7):169–170.
70. Liu L, Min S, Li W, et al. Pharmacodynamic changes with vecuronium in sepsis are associated with expression of α7- and γ-nicotinic acetylcholine receptor in an experimental rat model of neuromyopathy. *Br J Anaesth*. 2014;112(1):159–168.
71. Lindstrom JM. Nicotinic acetylcholine receptors of muscles and nerves: comparison of their structures, functional roles, and vulnerability to pathology. *Ann N Y Acad Sci*. 2003;998:41–52.
72. Khan MA, Farkhondeh M, Crombie J, et al. Lipopolysaccharide upregulates α7 acetylcholine receptors: stimulation with GTS-21 mitigates growth arrest of macrophages and improves survival in burned mice. *Shock*. 2012;38:213–219.
73. Lee S, Yang HS, Sasakawa T, Martyn JA. *Alpha7 AChRs play a pivotal role in the immobilization-induced resistance to atracurium in mice*. Abstract A1007; Presented at the ASA Annual Meeting, 2012.
74. Placzek AN, Grassi F, Papke T, et al. A single point mutation confers properties of the muscle-type nicotinic acetylcholine receptor to homomeric alpha 7 receptors. *Mol Pharmacol*. 2004;66:169–177.
75. Tansey MG, Chu GC, Merlie JP. ARIA/HRG regulates AChR epsilon subunit gene expression at the neuromuscular synapse via activation of phosphatidylinositol 3-kinase and Ras/MAPK pathway. *J Cell Biol*. 1996;134:465–476.
76. Hirose M, Kaneki M, Martyn JA, et al. Immobilization depresses insulin signaling in skeletal muscle. *Am J Physiol*. 2000;279:E1235–1241.
77. Sugita M, Sugita H, Kim M, et al. Inducible nitric oxide synthase deficiency ameliorates skeletal muscle insulin resistance but does not alter unexpected lower blood glucose levels after burn injury in C57BL/6 mice. *Metabolism*. 2012;61:127–136.
78. Hirose M, Kaneki M, Martyn JA, et al. Long-term denervation impairs insulin receptor substrate (IRS)-1-mediated insulin signaling in skeletal muscle. *Metabolism*. 2001;50:216–222.
79. Samuel MA, Valdez G, Tapia JC, et al. Agrin and synaptic laminin are required to maintain adult neuromuscular junctions. *PLoS One*. 2012;7:e46663.
80. Dilger JP. Simulation of the kinetics of neuromuscular block: implications for speed of onset. *Anesth Analg*. 2013;117:792–802.
81. Gronert GA. Cardiac arrest after succinylcholine: mortality greater with rhabdomyolysis than receptor upregulation. *Anesthesiology*. 2001;94:523–529.
82. Tsuneki H, Kimura I, Dezaki K, et al. Immunohistochemical localization of neuronal nicotinic receptor subtypes at the pre- and postjunctional sites in mouse diaphragm muscle. *Neurosci Lett*. 1995;196:13–16.
83. Chioldi F, Charpentier E, Muller D, et al. Blockade and activation of the human neuronal nicotinic acetylcholine receptors by atracurium and laudanosine. *Anesthesiology*. 2001;94:643–651.
84. Faria M, Oliveira L, Timoteo MA, et al. Blockade of neuronal facilitatory nicotinic receptors containing alpha 3 beta 2 subunits contribute to tetanic fade in the rat isolated diaphragm. *Synapse*. 2003;49:77–88.
85. Martyn J, Durieux ME. Succinylcholine: new insights into mechanisms of action of an old drug. *Anesthesiology*. 2006;104:633–634.
86. Eriksson LI. Reduced hypoxic chemosensitivity in partially paralysed man. A new property of muscle relaxants? *Acta Anaesthesiol Scand*. 1996;40:520–523.
87. Mkrtchian S, Kahlin J, Ebberyd A, et al. The human carotid body transcriptome with focus on oxygen sensing and inflammation—a comparative analysis. *J Physiol*. 2012;590:3807–3819.
88. Santafe MM, Salom I, Garcia N, et al. Modulation of ACh release by presynaptic muscarinic autoreceptors in the neuromuscular junction of the newborn and adult rat. *Eur J Neurosci*. 2003;17:119–127.
89. Wessler I. Control of transmitter release from the motor nerve by presynaptic nicotinic and muscarinic autoreceptors. *Trends Pharmacol Sci*. 1989;10:110–114.
90. Goudsouzian NG, Standaert FG. The infant and the myoneural junction. *Anesth Analg*. 1986;65:1208–1217.
91. Shafiee G, Keshtkar A, Soltani A, et al. Prevalence of sarcopenia in the world: a systematic review and meta-analysis of general population studies. *J Diabetes Metab Disord*. 2017;16:21.
92. Yang JC, Van Remmen H. Age-associated alterations of the neuromuscular junction. *Exp Gerontol*. 2011;46(2-3):193–198.
93. Willadt S, Nash M, Slater C. Age-related changes in the structure and function of mammalian neuromuscular junctions. *Ann NY Acad Sci*. 2018;1412:41–53.
94. Sanes JR, Lichtman JW. Induction, assembly, maturation and maintenance of a postsynaptic apparatus. *Nat Rev Neurosci*. 2001;2:791–805.

KEY POINTS

- Removal of carbon dioxide (CO_2) is determined by alveolar ventilation, not by total (minute) ventilation.
- Dead space ventilation can be dramatically increased in patients with chronic obstructive pulmonary disease and pulmonary embolism to more than 80% of minute ventilation.
- Breathing at small lung volumes increases airway resistance and promotes closure of airways.
- Hypoxemia can be caused by alveolar hypoventilation, diffusion impairment, ventilation-perfusion mismatch, and right-to-left shunt.
- Almost all anesthetics reduce skeletal muscle tone, which decreases functional residual capacity (FRC) to levels close to the awake residual volume.
- Atelectasis during anesthesia is caused by decreased FRC and the use of high inspired oxygen concentrations (FiO_2), including breathing oxygen before induction of anesthesia.
- General anesthesia causes ventilation-perfusion mismatch (airway closure) and shunts (atelectasis).
- Venous admixture is due to \dot{V}_A/\dot{Q} mismatch (response to increased FiO_2) and shunts (unresponsive to increased FiO_2).
- Hypoxic pulmonary vasoconstriction is blunted by most anesthetics, and this results in increased ventilation-perfusion mismatching.
- Respiratory work is increased during anesthesia as a consequence of reduced respiratory compliance and increased airway resistance.

Respiratory Physiology Is Central to the Practice of Anesthesia

Respiratory function is inextricably linked to the practice of anesthesia. Adverse respiratory effects can occur during anesthesia,¹ and the most serious cases involve hypoxemia. These events range from intractable hypoxemia caused by loss of airway patency to postoperative respiratory depression from opioids or regional anesthesia.^{2,3} In the absence of adverse outcomes, general anesthesia still has significant effects on respiratory function and lung physiology, documented by observations made in the operating and recovery rooms. Improved appreciation of anesthesia-induced physiologic alterations (e.g., mechanisms of bronchospasm,⁴ impact of mechanical ventilation),⁵ as well as pioneering developments in monitoring (e.g., pulse oximetry and capnography),⁶ together are associated with the specialty of anesthesiology's emergence as a leader in patient safety.⁷ Finally, integrative measures of respiratory function, ranging from exercise capacity,⁸ spirometry to tissue oxygenation,⁹ to global O_2 consumption,⁸ may help predict outcomes following anesthesia and surgery.

Pulmonary Physiology in Health

The mechanisms by which anesthesia-associated respiratory dysfunction is caused can be determined with an

examination of normal functions and mechanisms of respiration in health. We briefly review cellular respiration, whereby O_2 is consumed and CO_2 is produced, the transport of O_2 and CO_2 in the blood, and the principles by which the lung oxygenates blood and eliminates CO_2 .

RESPIRATION IN THE CELL

The partial pressure of oxygen (PaO_2) in normal arterial blood is approximately 100 mm Hg, and decreases to 4 to 22 mm Hg in the mitochondrion, where it is consumed. Glucose ($\text{C}_6\text{H}_{12}\text{O}_6$) is converted into pyruvate ($\text{CH}_3\text{COCOO}^-$) and H^+ by glycolysis in the cytoplasm, and the pyruvate diffuses into the mitochondria and forms the initial substrate for Krebs cycle, which in turn produces nicotinamide adenine dinucleotide (NADH), as well as adenosine triphosphate (ATP), CO_2 , and H_2O . The NADH is a key electron (and H^+) donor in the process of oxidative phosphorylation, wherein O_2 and adenosine diphosphate are consumed and ATP and H_2O are produced. Thus the net effect is oxidation of glucose to produce energy (ultimately as ATP), H_2O , and CO_2 .¹⁰

TRANSPORT OF O_2 IN THE BLOOD

O_2 reaches the cells following transport by arterial blood, and the overall delivery of O_2 ($\dot{D}\text{O}_2$) is the product of the arterial blood O_2 content (CaO_2) and blood flow (cardiac output, \dot{Q}) as

[†]Deceased.

$$\dot{D}O_2 = CaO_2 \times \dot{Q}$$

Oxygen is carried in the blood in two forms: O₂ bound to hemoglobin (the vast bulk), and O₂ dissolved in the plasma, and the content is expressed as the sum of these components:

$$CaO_2 = \left[\begin{array}{l} (SaO_2 \times Hb \times O_2 \text{ combining capacity of Hb}) \\ + (O_2 \text{ solubility} \times PaO_2) \end{array} \right]$$

where CaO₂ (O₂ content) is the milliliters of O₂ per 100 mL of blood, SaO₂ is the fraction of hemoglobin (Hb) that is saturated with O₂, O₂-combining capacity of Hb is 1.34 mL of O₂ per gram of Hb, Hb is grams of Hb per 100 mL of blood, PaO₂ is the O₂ tension (i.e., dissolved O₂), and solubility of O₂ in plasma is 0.003 mL of O₂ per 100 mL plasma for each mm Hg PaO₂.

The binding of O₂ to hemoglobin is a complex, allosteric mechanism. Important insights can be gained by understanding how characteristic abnormalities of blood O₂ carriage (e.g., carbon monoxide [CO] poisoning, methemoglobinemia) affect O₂ tension, content, and delivery.

Methemoglobin (MetHb), formed by the oxidation to Fe³⁺ (ferric) instead of the usual Fe²⁺ (ferrous) iron, is less able to bind O₂, resulting in diminished O₂ content and less O₂ delivery. Here, the PaO₂ (in the absence of lung disease) will be normal: if the O₂ content is calculated from the PaO₂, it will appear normal, but if directly measured, it will be low. In contrast, MetHb level will be elevated. In severe cases, lactic acidosis develops because of impaired O₂ delivery. In addition, because MetHb has a blue-brown color, the patient will appear blue, even if the fraction of MetHb is modest; specialized oximetry can separately measure MetHb levels.^{11,12} The apparent cyanosis is not responsive to supplemental O₂, and therapy involves converting (i.e., reducing) the MetHb to Hb (e.g., by using methylene blue). Important medical causes of MetHb include benzocaine, dapsone, or in susceptible patients, inhaled nitric oxide (NO).

In CO poisoning, the CO binds to Hb, with far greater (over 200-fold) avidity than molecular O₂, tightly forming CO-Hb and resulting in two main effects.¹³ First, formation of CO-Hb results in fewer sites available for O₂ binding, and this reduces the blood O₂ content. Second, the formation of CO-Hb causes conformational changes in the Hb molecule such that the tendency to release bound O₂ is reduced. This effect corresponds to a leftward shift of the Hb-O₂ dissociation curve, and although this aspect of CO binding does not reduce the O₂ content or “global” delivery of O₂, it does reduce the release of O₂ and its local delivery to the cells. Because the color of CO-Hb closely resembles that of O₂-Hb, the color of the blood (and the patient) is bright red; however, as with MetHb, the PaO₂ will be normal (assuming no pulmonary disease) as will be the calculated CaO₂; however, the measured CaO₂ will be low and if severe, a lactic acidosis will be present. Modern pulse oximeters can distinguish between Hb-O₂ and CO-Hb.¹³

Finally, the *Bohr effect* refers to a shift of the Hb-O₂ dissociation curve caused by changes in CO₂ or pH.¹⁴ In the systemic capillaries, the PCO₂ is higher than in the arterial blood (and the pH correspondingly lower) because of local CO₂ production. These circumstances shift the Hb-O₂ dissociation curve to the right, which increases the offloading of O₂ to the tissues. The opposite occurs in the pulmonary

capillaries; here, the PCO₂ is lower (and the pH correspondingly higher) because of CO₂ elimination, and the dissociation curve is shifted to the left to facilitate O₂ binding to Hb.

TRANSPORT OF CO₂ IN THE BLOOD

CO₂ is produced by metabolism in the mitochondria, where the CO₂ levels are highest. The transport path (involving progressively decreasing pressure gradients) is from mitochondria through cytoplasm, into venules, and finally, in mixed venous blood from where it is eliminated through the alveoli. In the blood, CO₂ is transported in three main forms: dissolved (reflected as PaCO₂, partial pressure; accounts for approximately 5% of transported CO₂), bicarbonate ion (HCO₃⁻; almost 90%), and carbamino CO₂ (CO₂ bound to terminal amino groups in Hb molecules; approximately 5%).¹⁰ The usual quantities of CO₂ in the arterial and (mixed) venous blood are approximately 21.5 and 23.3 mmol of CO₂ per liter of blood, respectively.

Breathing O₂ can sometimes induce hypercapnia, as occurs in patients with severe chronic lung disease who are breathing supplemental O₂. Although traditionally thought to occur because increased PaO₂ reduces ventilatory drive, this is now thought not to be the case,¹⁵ resulting instead from the Haldane effect, as well as from impairment of hypoxic pulmonary vasoconstriction (HPV). The Haldane effect¹⁶ is the difference in the amount of CO₂ carried in oxygenated versus deoxygenated blood, and two mechanisms explain this. First, increased PaO₂ decreases the ability to form carbamino compounds—reducing the amount of CO₂ bound to Hb—thereby raising the amount of dissolved CO₂ (i.e., elevated PaCO₂). Second, the amino acid histidine, which has an imidazole group that is an effective H⁺ buffer at physiologic pH, is an important linking molecule between heme groups and the Hb chains. Increasing the partial pressure of oxygen (PO₂) increases the amount of O₂ bound to Hb; this changes the conformation of the Hb molecule, which in turn alters the heme-linked histidine and reduces its H⁺ buffering capacity. Therefore, more H⁺ is free (not buffered) and binds to HCO₃⁻, releasing stored CO₂. Impairment of HPV by elevated O₂ allows increased perfusion to poorly ventilated regions; this has the effect of decreasing perfusion (and delivery of CO₂) to better ventilated regions, diminishing the efficiency of CO₂ exhalation. Patients with impaired ability to increase alveolar ventilation (V_A) cannot compensate for the increased CO₂ availability, and therefore, in these patients, adding supplemental O₂ can result in elevated PaCO₂.

OXYGENATION IN THE PULMONARY ARTERY

Systemic venous blood (central venous blood) enters the right ventricle via the right atrium. The O₂ saturation (SO₂) differs among the major veins: higher venous SO₂ reflects greater blood flow, less tissue oxygen uptake, or both.¹⁷ SO₂ is usually higher in the inferior vena cava (IVC) than in the superior vena cava (SVC), possibly because of the high renal and hepatic flow relative to O₂ consumption. In the right ventricle, the central venous blood (S_{cv}O₂) from the SVC and IVC is joined by additional venous blood from the coronary circulation (via the coronary sinuses). In the right ventricle, an additional small amount of venous drainage from the myocardium enters through the thebesian veins, and as all this

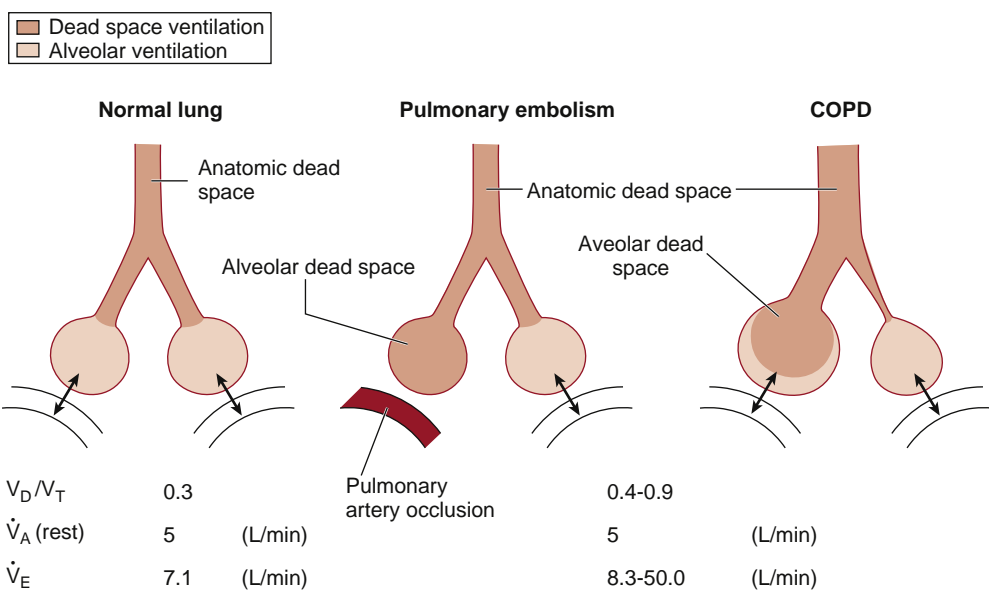


Fig. 13.1 Dead space and alveolar ventilation in normal and diseased lungs. Either cessation of blood flow or excessive alveolar ventilation relative to perfusion will cause an increase in dead space (V_D). If V_D is increased, a large compensatory increase in minute ventilation is required to preserve \dot{V}_A . V_D/V_T , dead space to tidal volume ratio; \dot{V}_A , alveolar ventilation; \dot{V}_E , minute ventilation. $\dot{V}_E = \dot{V}_A + f \times V_D$. Double arrows indicate normal CO_2 exchange. COPD, Chronic obstructive pulmonary disease. (From Hedenstierna G. *Respiratory measurement*. London: BMJ Books; 1998:184; see also book review of *Respiratory Measurement in Thorax* 1998;53:1096.)

venous blood enters the pulmonary artery, it is well mixed and is termed *mixed-venous blood* ($S_v\text{O}_2$); thus $S_v\text{O}_2 < S_{cv}\text{O}_2$, although the trends of each usually run in parallel.¹⁸

Ventilation

Ventilation refers to the movement of inspired gas into and exhaled gas out of the lungs.

ALVEOLAR VENTILATION

Fresh gas enters the lung by cyclic breathing at a rate and depth (tidal volume, V_T) determined by metabolic demand, usually 7 to 8 L/min.¹⁹ While most inspired gas reaches the alveoli, some (100-150 mL) of each V_T remains in the airways and cannot participate in gas exchange. Such dead space (V_D) constitutes approximately one third of each V_T .²⁰ Anatomic V_D is the fraction of the V_T that remains in the “conducting” airways, and physiologic V_D is any part of a V_T that does not participate in gas exchange (Fig. 13.1).

For a single tidal volume (V_T , mL), the following is true:

$$V_T = \dot{V}_A + V_D$$

The product of V_T (mL) times the respiratory rate (per minute) is the minute ventilation (\dot{V}_E). Aggregated over time, minute ventilation (\dot{V}_E , mL/min) is:

$$\dot{V}_E = \dot{V}_A + f \times V_D$$

The portion of the \dot{V}_E that reaches the alveoli and respiratory bronchioles each minute and participates in gas exchange is called the *alveolar ventilation* (\dot{V}_A), and it is approximately 5 L/min. Because this is similar to the blood flow through the lungs (i.e., the cardiac output, also 5 L/min), the overall alveolar ventilation-perfusion ratio is approximately 1.

DEAD SPACE VENTILATION

Maintenance of Paco_2 is a balance between CO_2 production ($\dot{V}\text{CO}_2$, reflecting metabolic activity) and alveolar ventilation (\dot{V}_A). If \dot{V}_E is constant but V_D is increased, \dot{V}_A will naturally be reduced, and the Paco_2 will therefore rise. Therefore, if V_D is increased, \dot{V}_E must also increase to prevent a rise in Paco_2 . Such elevations in V_D occur when a mouthpiece or facemask is used, and in such cases, the additional V_D is termed “apparatus deadspace” (which can be up to 300 mL; anatomic V_D of the airways is 100-150 mL).²¹

Increases in the volume of the conducting airways (e.g., bronchiectasis) increase the overall V_D only slightly. Far more significant increases in V_D occur when perfusion to a large number of ventilated alveoli is interrupted, as occurs in a pulmonary embolus (see Fig. 13.1). Indeed, with multiple pulmonary emboli, V_D/V_T can exceed 0.8 (2.7-fold normal). In such a case, to maintain a normal \dot{V}_A (5 L/min), the \dot{V}_E would have to increase (also 2.7-fold) to almost 20 L/min. This effort would cause considerable dyspnea, in addition to the dyspnea induced by the lowered PaO_2 .

Obstructive lung disease can result in diversion of inspired air into (nonobstructed) ventilated, but poorly perfused, regions of the lung. This results in local excesses of ventilation versus perfusion (high \dot{V}_A/\dot{Q} ratio) in such regions,²² which is equivalent to an increase in V_D/V_T (see Fig. 13.1). Patients with severe chronic obstructive pulmonary disease (COPD) may have a V_D/V_T ratio of up to 0.9, and would have to hyperventilate massively (30-50 L/min) to maintain normal Paco_2 , which is not possible where ventilator reserve is diminished. Such patients demonstrate reduced \dot{V}_A but often have an elevated \dot{V}_E . An important compensatory mechanism is that a lower level of \dot{V}_A will maintain stable CO_2 excretion where the Paco_2 is increased (Box 13.1).

BOX 13.1 Alveolar Gas Equations

Alveolar Oxygen Tension (P_{AO_2})

$$P_{AO_2} = P_{IO_2} - \frac{P_{ACO_2}}{R} + \left[P_{ACO_2} \times FiO_2 \times \frac{1-R}{R} \right]$$

where P_{IO_2} is inspired oxygen tension, P_{ACO_2} is alveolar CO_2 tension (assumed to equal arterial P_{CO_2}), R is the respiratory exchange ratio (normally in the range of 0.8-1.0), and FiO_2 is the inspired oxygen fraction. The term within brackets compensates for the larger O_2 uptake than CO_2 elimination over the alveolar capillary membranes.

A simplified equation can be written without the compensation term:

$$P_{AO_2} = P_{IO_2} - \frac{P_{ACO_2}}{R}$$

Alveolar Ventilation

Alveolar ventilation (\dot{V}_A) can be expressed as

$$\dot{V}_A = f \times (V_T - V_{DS})$$

where f is breaths/min, V_T is tidal volume, and V_{DS} is physiologic dead space.

Alveolar ventilation can also be derived from:

$$\dot{V}_{CO_2} = c \times \dot{V}_A \times F_{ACO_2}$$

where \dot{V}_{CO_2} is CO_2 elimination, c is a conversion constant, and F_{ACO_2} is the alveolar CO_2 concentration.

If \dot{V}_A is expressed in L/min, \dot{V}_{CO_2} in mL/min, and F_{ACO_2} is replaced by P_{ACO_2} in mm Hg, $c = 0.863$. By rearranging:

$$\dot{V}_A = \frac{\dot{V}_{CO_2} \times 0.863}{P_{ACO_2}}$$

Static Lung Volumes—Functional Residual Capacity

The amount of air in the lungs after an ordinary expiration is called *functional residual capacity* (FRC; Fig. 13.2); it is usually 3 to 4 L and occurs because of the balance of inward (lung) forces and outward (chest wall) forces. The inward force is the “elastic recoil” of the lung and emanates from the elastic lung tissue fibers, contractile airway smooth muscle, and alveolar surface tension. The outward force is developed by passive recoil from the ribs, joints, and muscles of the chest wall. FRC is greater with increased height and age (loss of elastic lung tissue), and smaller in women and in obesity.^{19,23}

There are two reasons why maintenance of gas in the lung at end-expiration (i.e., FRC) is important. First, inflating an already opened (inflated) lung is easier than when the lung is deflated. This is because complete collapse results in liquid-only surfaces interfacing in alveoli (high surface tension), whereas alveoli in partially inflated lung have air-liquid interfaces (lower surface tension). Second, although perfusion in the lung is phasic, the frequency is rapid and the oscillations in flow are low, resulting in nearly continuous flow. Ventilation is different: the frequency is far slower and the size of the oscillations far larger. If the lung

(or large parts of it) completely deflate between breaths, the blood flowing from closed alveoli (that contain zero O_2) would have very low SO_2 (the same as mixed venous blood); this would mix into the overall blood flow from the lungs and cause a major O_2 desaturation after every exhalation.

Respiratory Mechanics

The study of respiratory mechanics tells us how inspired air is distributed within the lung and permits quantitation of the severity of lung disease. The components of overall impedance to breathing results from elastance (the reciprocal of compliance), resistance, and inertia.

COMPLIANCE OF THE RESPIRATORY SYSTEM

The lung is like a rubber balloon that can be distended by positive pressure (inside) or negative pressure (outside). Under normal circumstances, inflation of the lung is maintained because although the pressure inside (alveolar pressure) is zero, the outside pressure (i.e., the pleural pressure) is sufficiently negative. The net distending pressure, which is the difference of the (positive) airway pressure (P_{AW}) and the (negative) pleural pressure (P_{PL}) is termed the *transpulmonary pressure* (P_{TP}). Thus:

$$P_{TP} = P_{AW} - P_{PL}$$

Clearly, increasing the P_{AW} increases the P_{TP} . In addition, lowering the P_{PL} (which is usually negative and making it more negative) also increases the P_{TP} .

Compliance—the reciprocal of elastance—is the term that expresses how much distention (volume in liters) occurs for a given level of P_{TP} (pressure, cm H₂O); it is usually 0.2 to 0.3 L/cm H₂O.²⁴ However, although higher values of P_{TP} maintain greater levels of lung opening, the relationship—as with most elastic structures—between applied pressure and resultant volume is curvilinear (Fig. 13.3).²⁴ Lung compliance depends on the lung volume; it is lowest at an extremely low or high FRC (see Fig. 13.3). In lung diseases characterized by reduced compliance (e.g., ARDS, pulmonary fibrosis, or edema), the pressure-volume (PV) curve is flatter and shifted to the right (Fig. 13.4).²⁴ In contrast, although emphysema involves the loss of elastic tissue, the overall loss of lung tissue (as seen on computed tomography [CT] scanning)²⁵ means that the compliance is increased; the PV curve is therefore shifted to the left and is steeper (see Fig. 13.4).²⁴

Chest wall impedance is not noticed during spontaneous breathing because the respiratory “pump” includes the chest wall. Chest wall mechanics can be measured only if complete relaxation of the respiratory muscles can be achieved²⁶; however, during mechanical ventilation, the respiratory muscles can be completely relaxed. As the lung is inflated by P_{AW} , the properties of the chest wall will determine the resulting change in P_{PL} . Under these circumstances, the increase in lung volume per unit increase in P_{PL} is the chest wall compliance. Values of chest wall compliance are about the same as that of the lung and are reduced with obesity, chest wall edema, pleural effusions, and diseases of the costovertebral joints.²⁶

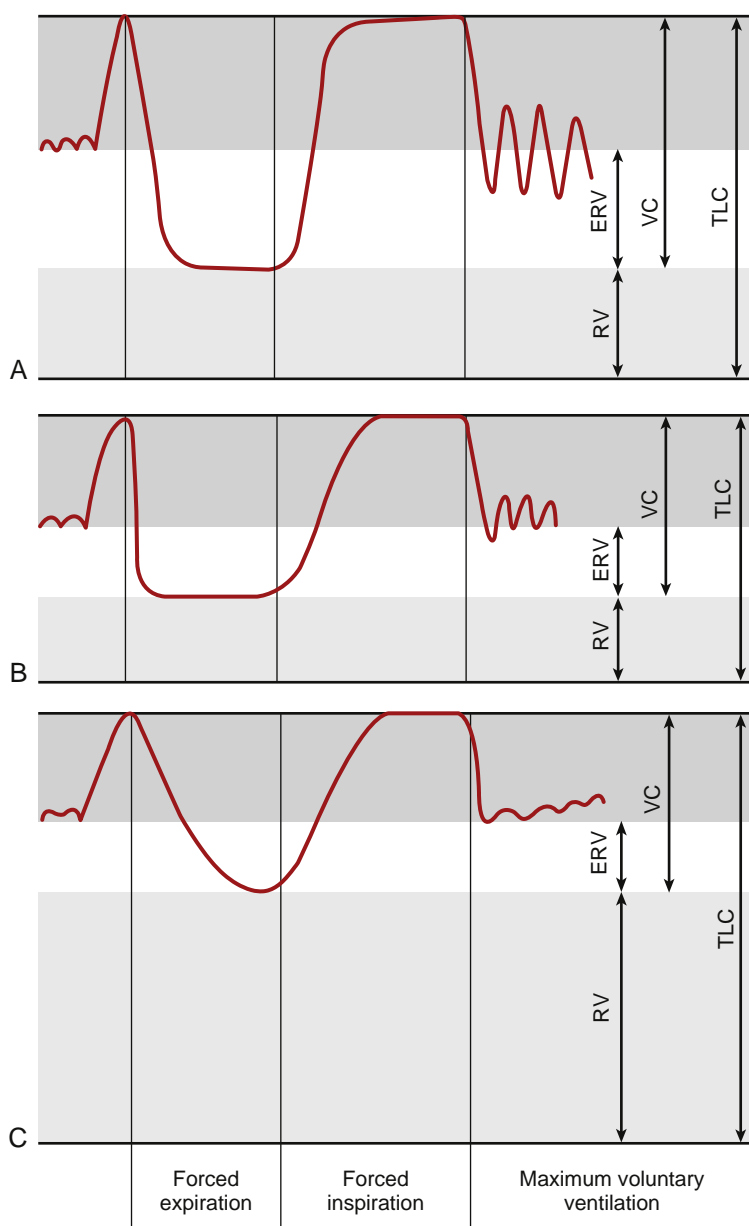


Fig. 13.2 (A) Ventilation and lung volumes in a healthy subject with normal lungs. (B) A patient with restrictive lung disease. (C) A patient with chronic obstructive pulmonary disease (COPD). In restrictive disease, the vital capacity (VC) is decreased and expiratory flow rate is increased (i.e., steeper than the normal slope of the forced expiratory curve). In COPD, the residual volume (RV) is increased, the VC is reduced, and forced expiration is slowed. ERV, Expiratory reserve volume; TLC, total lung capacity. (From Hedenstierna G. *Respiratory measurement*. London: BMJ Books; 1998:184; see also book review of *Respiratory Measurement* in *Thorax* 1998;53:1096.)

RESISTANCE OF THE RESPIRATORY SYSTEM

Airways

Resistance impedes airflow into (and out of) the lung. The major component of resistance is the resistance exerted by the airways (large and small), and a minor component is the sliding of lung and the chest wall tissue elements during inspiration (and expiration).²⁷ Resistance is overcome by (driving) pressure. In spontaneous breathing, driving pressure will be the P_{PL} ; in positive pressure ventilation, the driving pressure will be the difference between the pressures applied to the endotracheal tube (P_{AW} ; “source”) and the alveolus (P_{ALV} ; “destination”). Resistance (R) is calculated as driving pressure (ΔP) divided by the resultant gas flow (F):

$$R = \frac{\Delta P}{F}$$

The value of airway resistance is approximately 1 cm H₂O/L/sec, and is higher in obstructive lung disease (e.g., COPD, asthma); in severe asthma, it is elevated approximately tenfold.²⁸ The presence of an endotracheal tube adds a resistance of 5 (or 8) cm H₂O/L/min for a tube with internal diameter of size 8 (or 7) cm.²⁹ For any tube for which the airflow is laminar (smooth, streamlined), the resistance increases in direct proportion to the tube length and increases dramatically (to the fourth power) as the diameter of the tube is reduced.

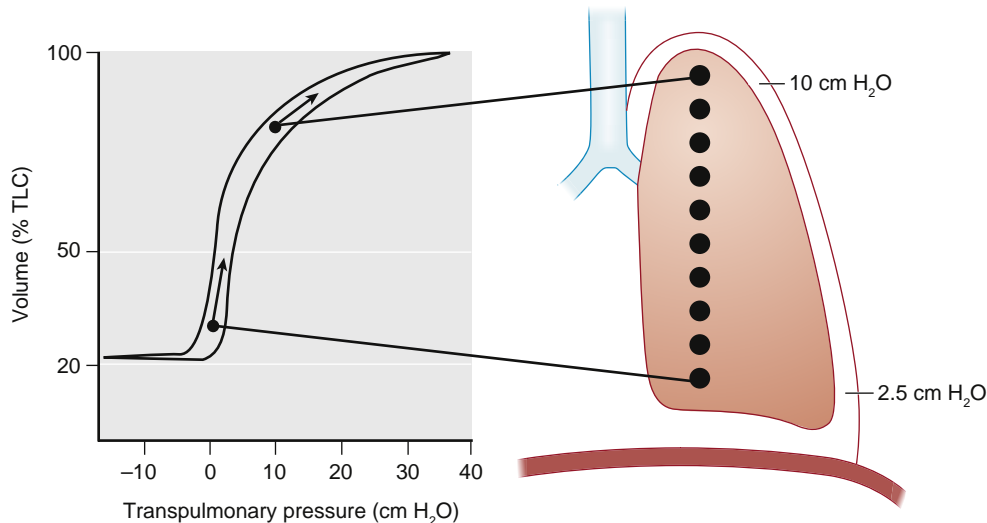


Fig. 13.3 The pressure-volume relationships of the lung. The relationship is curvilinear (typical for an elastic structure). The pleural pressure is lower (more subatmospheric) in the upper regions. In the upright subject, the transpulmonary pressure ($P_{TP} = P_{AW} - P_{PL}$) is higher in apical than in basal regions. This results in different positions on the pressure volume curve of the upper (flatter, less compliant) versus lower (steeper, more compliant) lung regions. Thus lower lung regions expand more (i.e., receive more ventilation) for a given increase in transpulmonary pressure than upper units. TLC, Total lung capacity.

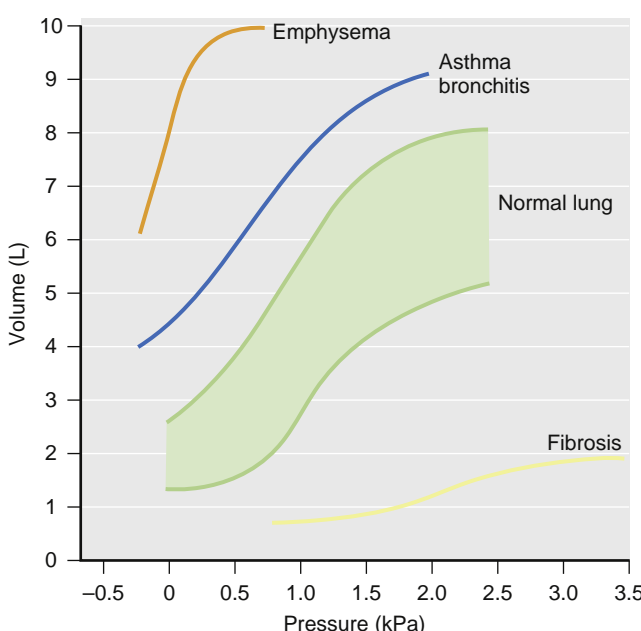


Fig. 13.4 Pressure-volume curves of the lung in healthy and lung-diseased patients. In fibrosis, the slope of the curve is flatter, reflecting considerable increases in pressure variation and in respiratory work. In asthma or bronchitis, there is a parallel (upward) shift of the pressure-volume curve, indicating an increase in lung volume but no change in compliance. In emphysema, the slope of the curve is steeper, reflecting tissue loss and possible increased compliance. However, in emphysema, asthma, or bronchitis, the airway resistance is increased; this increases work of breathing and overrides any benefit from increased compliance. (From Hedenstierna G. *Respiratory measurement*. London: BMJ Books; 1998:184; see also book review of *Respiratory Measurement in Thorax* 1998;53:1096.)

Two factors explain why most (approximately 80%) of the impedance to gas flow occurs in the large airways.²⁷ First, as bronchi progressively branch, the resistances are arranged in parallel and the total cross-sectional area at the level of the terminal bronchioles adds up to almost tenfold that at the

trachea. Second, in tubes that are large, irregular or branched, the flow is often turbulent, not laminar. When flow is laminar:

$$F_{(lam)} = \frac{\Delta P}{R}$$

In contrast, when flow is turbulent:

$$F_{(turb)} = \frac{\Delta P}{R^2}$$

Therefore, for a given radius, far more pressure is required to achieve comparable flow where flow is turbulent; thus the effort required is greater and if prolonged or severe, respiratory failure is more likely.

Several factors can alter airflow resistance. First, resistance lessens as lung volume increases; this is intuitive, as increasing volume (positive pressure or spontaneous breathing) stretches the diameter of the airways. Because this is the key determinant of resistance, the resistance falls to a small extent. The opposite occurs with exhalation (Fig. 13.5). However, as lung volume approaches residual volume (RV)—as can happen during anesthesia—the airways are narrowed in parallel with the compressing lung tissue and the resistance rises exponentially. These effects are apparent with active or passive ventilation. Second, active ventilation has additional effects. Forced expiration can compress small airways (i.e., that do not contain cartilage).²⁷ In addition, forced expiration can cause turbulent flow in small airways in patients with COPD, precipitously dropping pressure in the lumen and thereby narrowing the bronchioles³⁰ and resulting in expiratory flow limitation and, after multiple breaths, eventual “dynamic hyperinflation.”³¹ Expiratory against resistance (or pursed-lips breathing) is sometimes used by those with COPD to make breathing easier. This works by increasing expiratory resistance and slowing expiration. The slowed expiration reduces the pressure gradient driving expiration (i.e., pressure highest in the alveolus, lower toward the mouth). Therefore, the point along the airway tree at which pressure inside the airway has decreased to less than that outside the

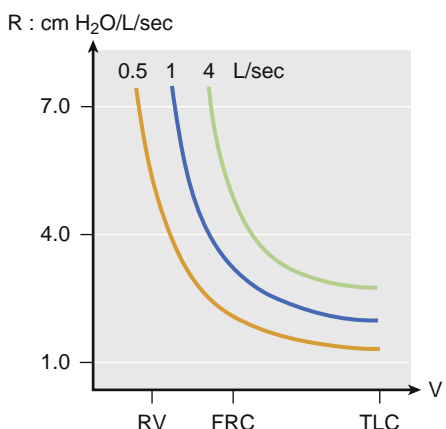


Fig. 13.5 Schematic drawing of airflow resistance against lung volume at different flow rates. As lung volume falls, the resistance to flow increases; the steepness of this increase is far greater at lung volumes below functional residual capacity (FRC). In addition, higher airflow rates are associated with greater resistance. At extremely low lung volume, the resistance is comparable to values seen in moderate to severe asthma ($6-8 \text{ cm H}_2\text{O} \times \text{l}^{-1} \times \text{s}$). *RV*, Residual volume; *TLC*, total lung capacity.

airway (equal to pleural pressure) is moved from smaller collapsible airways toward the mouth to noncollapsible, cartilaginous airways (Fig. 13.6); this prevents collapse of the smaller airways, which are vital for proper gas exchange.³²

The large airways (i.e., pharynx, larynx, and trachea) are outside the chest wall. During inspiration, the intra-thoracic airways are exposed to extraluminal pressure (i.e., P_{PL}) that is less than the lumen pressure; in contrast, the extrathoracic airways are exposed to lumen pressure that is less than the extraluminal (i.e., atmospheric) pressure.²⁷ This feature, coupled with downward stretch induced by inspiration, narrows the large extrathoracic airways; in the presence of preexisting narrowing (e.g., thyroid enlargement or tumor, paralyzed vocal cord, epiglottitis), this can critically reduce the cross-sectional area.

Tissue

Although not intuitively obvious, resistance of the lung tissue is the applied pressure on tissue divided by the resulting velocity of tissue movement. There are various approaches to determining this in humans, including separately

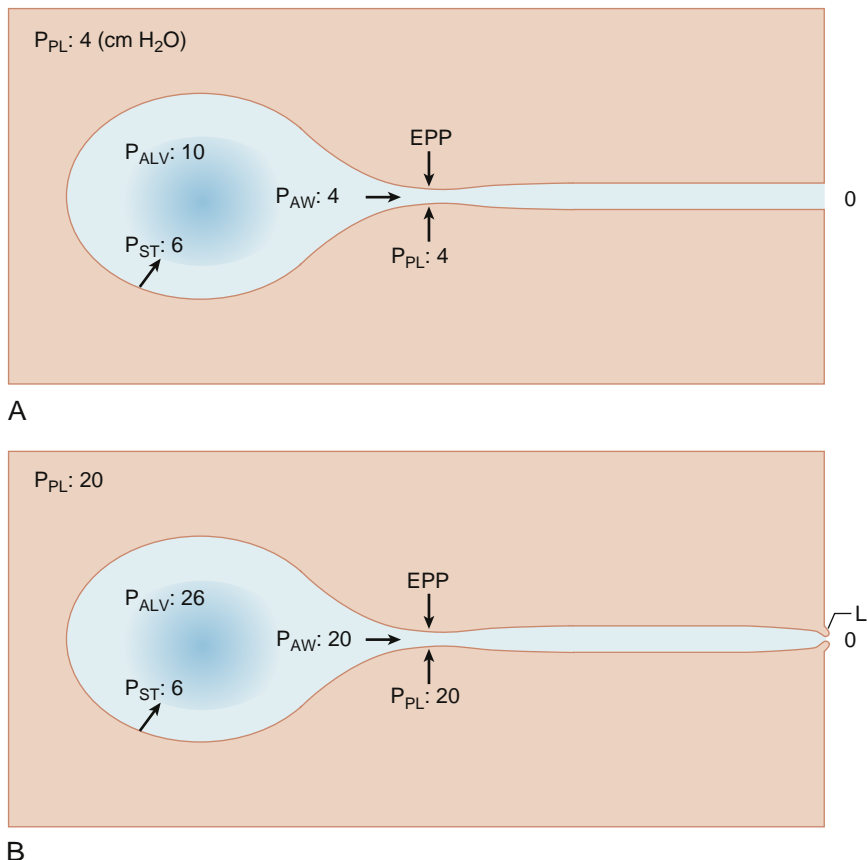


Fig. 13.6 Schematic drawings of the equal pressure point (EPP) concept and dynamic compression of airways. (A) Slightly forced expiration during otherwise normal conditions. With the application of some expiratory muscle effort, pleural pressure (P_{PL}) is positive, 4 cm H₂O (0.4 kPa). The elastic recoil pressure (P_{ST}) of the alveoli (6 cm H₂O) and the pleural pressure add together to yield intraalveolar pressure (P_{ALV}) (10 cm H₂O). This causes expiratory flow. At some point downstream toward the airway opening, airway pressure (P_{AW}) has dropped by 6 cm H₂O, so intraluminal pressure and pleural, extraluminal pressure are the same. This is the EPP. From this point to the mouth, intraluminal airway pressure is lower than the surrounding, extraluminal pressure and the airway may be compressed. (B) An attempt to stabilize the airway by so-called "pursed-lip" breathing. The increased resistance to expiratory flow requires increased expiratory effort to maintain gas flow. Thus pleural pressure is increased in comparison to the normal conditions ($P_{PL} = 20 \text{ cm H}_2\text{O}$). Alveolar elastic recoil pressure (P_{ST}) is the same as in the earlier condition, provided that lung volume is the same. If expiratory flow is of the same magnitude as during normal breathing, pressure along the airway falls to the same extent as during normal breathing. Thus the EPP will have the same location as during normal breathing, and no stabilization of the airway has been achieved. The two ways of moving the EPP toward the mouth and to less collapsible airways is by raising alveolar recoil pressure (P_{ST}) by an increase in lung volume or by lowering the expiratory flow rate so that the pressure drop along the airway tree is slowed down.

considering the PV characteristics using plethysmography (where the area of the PV curve corresponds to work against total pulmonary resistance) and esophageal pressure (where the area of the PV curve corresponds to work against “tissue” resistance).³³ Alternative approaches mathematically model the lung responses to varying respiratory frequencies.³⁴ Lung tissue resistance amounts to 20% of the total resistance to breathing; it can be increased threefold or fourfold in chronic lung disease³⁵ and is reduced by panting respirations.³⁶ Finally, in adult respiratory distress syndrome (ARDS) the chest wall resistance is increased.³⁷

INERTIA OR ACCELERATION OF GAS AND TISSUE

A final component of the total impedance to breathing is inertance, or the pressure required to accelerate air and tissue during inspiration and expiration. This component is minor, however, and can hardly be measured under normal breathing, regardless of whether the lungs are healthy. Nonetheless, tissue inertia is large during rapid ventilation,³⁸ and it could be important during the rapid, shallow breathing characteristic of weaning failure or during high-frequency oscillation.

Distribution of Inspired Gas

Inspired gas is not evenly distributed throughout the lung; naturally, more gas enters those lung units that expand

most during inspiration. In the resting lung, the basal (dependent) regions are less aerated than the apical (non-dependent) regions; therefore, they have the capacity to undergo greater expansion. During inspiration, most gas goes to the basal units (dorsal, when supine; lower right lung when in the right lateral position).³⁹ This distribution is because of the compliance properties of the lung and the effects of position on the distribution of the distending pleural pressure (i.e., the P_{PL} gradient). These changes are not related to the properties of the inspired gas.

In the upright position, the P_{PL} is less negative at the base of the lung than at the apex. Because the alveolus pressure (P_A) is uniform throughout the lung, the distending P_{TP} is greater at the apex; therefore, before inspiration commences, the apical lung is more open (and is less compliant) than the basal lung (Figs. 13.3 and 13.7). With inspiration, the contracting diaphragm lowers the P_{PL} by a comparable amount in all areas of the pleural surface (because of the fluid-like behavior of normal lung³⁹) and distends the basal more than the apical regions (see Figs. 13.3 and 13.7). Because the pleural pressure gradient is oriented according to gravity, the distribution of ventilation changes with body position.

The P_{PL} gradient exists because lung density, gravity, and conformation of the lung to the shape of the thorax⁴⁰ result in crowding of the basal lung tissue, making the local P_{PL} less negative in the basal regions. Because the density of normal lung is approximately 0.3, P_{PL} will become more positive by 0.3 cm H₂O for each downward vertical

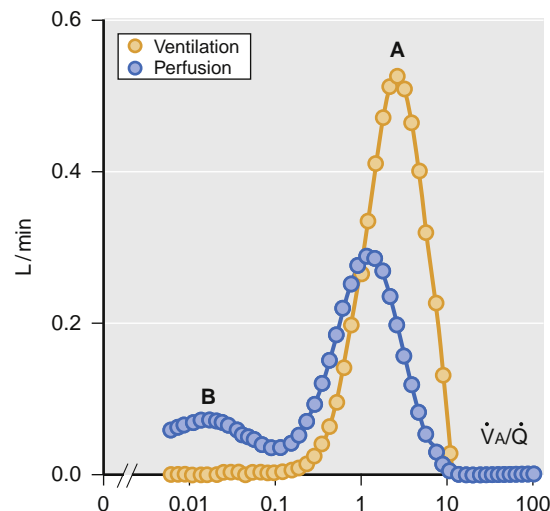
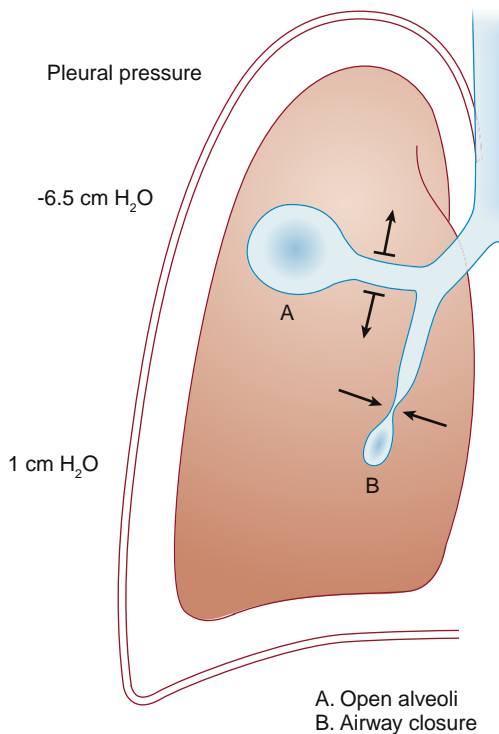


Fig. 13.7 Schematic of regional alveolar and airway volume at an upper (A) and a lower (B) lung level (left panel). There is a vertical pleural pressure (P_{PL}) gradient between the uppermost and lowermost regions (-6.5 to $1 = -7.5$ cm H₂O). Airway pressure (P_{AW}) is atmospheric, or 0 cm H₂O throughout; thus, in the upper regions, $P_{AW} > P_{PL}$ maintains airways open. In contrast, in the lower regions, $P_{PL} > P_{AW}$ causes airway closure—potentially exacerbated by subsequent alveolar gas absorption behind the occluded airway. The right panel shows the distribution of ventilation and blood flow from the multiple inert gas elimination technique. A “normal” mode of ventilation and blood flow (A) can be seen corresponding to the open and ventilated alveoli in the upper parts of the lung. In addition, there is a range of low V_A/Q ratios with more perfusion than ventilation (B). This pattern is compatible with intermittent airway closure during breathing.

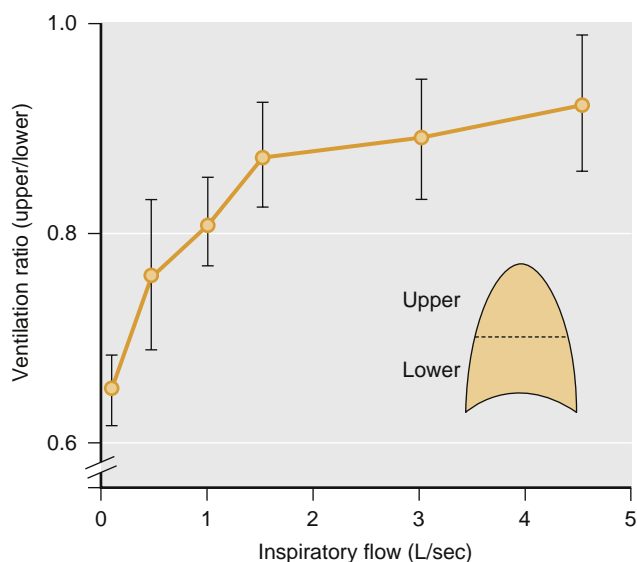


Fig. 13.8 Distribution of ventilation to upper versus lower lung regions as inspiratory flow is altered. At low flow, the bulk of the airflow goes to the lower regions. At higher flow rates (e.g., during exercise) the distribution is more even, ensuring more efficient use of all alveolar-capillary membranes for gas transfer (provided that pulmonary blood flow shows a similar distribution pattern).

centimeter, and more so with injured or edematous lungs. Indeed, experimentally induced weightlessness decreases inhomogeneity in the distribution of ventilation,⁴¹ but does not eliminate it; therefore, nongravitational (e.g., tissue, airway) factors also play a role.⁴²

Although the vertical height of the lung is the same in the prone and supine positions, the vertical gradient P_{PL} is less when prone,⁴³ perhaps because the mediastinum compresses the dependent lung when supine but rests on the sternum when prone.⁴⁴ A more even distribution of inspired gas—with improved oxygenation—in the prone position was predicted by Bryan in 1974⁴⁴; this has been confirmed experimentally.^{45,46}

During low-flow states (e.g., at rest), distribution is determined by differences in compliance and not by airway resistance. Because compliance at the start of inflation is less in the (already more aerated) apex, ventilation is preferentially directed to the base. In contrast, at high airflow, resistance (not compliance) is the key determinant of distribution; because the resistance is lower in upper, more expanded lung regions, increasing flow rate equalizes the distribution of ventilation, as shown by distribution of ^{133}Xe gas in humans (Fig. 13.8).^{47,48} This is important during exercise or stress because greater amounts of the alveolar-capillary surface area will be used.

AIRWAY CLOSURE

Expiration causes the airways to narrow, and deep expiration can cause them to close. The volume remaining above RV where expiration below FRC closes some airways is termed *closing volume* (CV), and this volume added to the RV is termed the *closing capacity* (CC; i.e., the total capacity of the lung at which closing can occur).⁴⁹ Closure of airways during expiration is normal and is potentiated by increasing P_{PL} , especially with active expiration. When P_{PL} exceeds

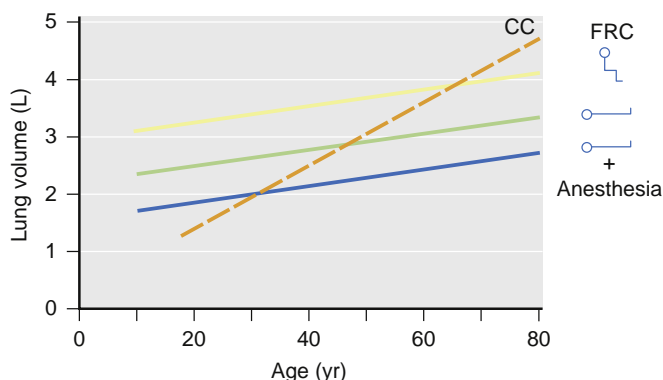


Fig. 13.9 Resting functional residual capacity (FRC) and closing capacity (CC). FRC increases with age (because of loss of elastic tissue), and superimposed upon this is a step decrease in FRC with supine position (because of diaphragm elevation by abdominal contents), and a further decrease with anesthesia in the supine position. The CC is also increased with age, but far more steeply, causing airway closure above FRC in upright subjects (>65 yr) and in supine subjects (>45 yr). This relationship between CC and FRC explains decreasing oxygenation with age.

the P_{AW} , the airway—if collapsible—will tend to close, and this usually commences at the bases because the basal P_{PL} is greatest (see Fig. 13.7).

Three applications of this important principle are of key relevance to anesthesia. First, airway closure depends on age: in youth, the closure does not occur until expiration is at or near RV, whereas with older age, it occurs earlier in expiration (i.e., at higher lung volumes). This occurs because P_{PL} is on average more “positive” (i.e., atmospheric, equal to P_{AW}) as age increases. Closing can occur at or above FRC in individuals aged 65 to 70 years,⁵⁰ such that dependent regions will undergo closure during normal expiration. This may be the major reason why oxygenation decreases with age. Second, in the supine position, FRC is less than when upright, but CC is unchanged; therefore, exhalation of a usual V_T (from FRC) encroaches on CC in a supine 45-year-old, and closure may be continuous in a supine 70-year-old (Fig. 13.9). Finally, COPD increases the lung volume at which closure occurs, possibly exacerbated by airway edema and increased bronchial tone.⁴⁹

DIFFUSION OF GAS

Gas moves in the large and medium-sized airways by bulk flow (i.e., convection), meaning that the gas molecules travel together at a given mean velocity according to a driving pressure gradient. Flow is through multiple generations of bronchi, and the net resistance falls with each division. After the 14th generation, airways merge with alveoli and participate in gas exchange (respiratory bronchioles). The cross-sectional area expands massively (trachea, 2.5 cm^2 ; 23rd generation bronchi, 0.8 m^2 ; alveolar surface, 140 m^2),⁵¹ resulting in a sharp drop in overall resistance. Because the number of gas molecules is constant, the velocity falls rapidly, which by the time the gas enters the alveoli is minuscule (0.001 mm/s); it is zero when it reaches the alveolar membrane. The velocity of the gas entering the alveolus is slower than the diffusion rates of O_2 and CO_2 ; therefore, diffusion—not convection—is necessary for transport in the distal airways and alveoli. Indeed,

CO₂ is detectable at the mouth after just seconds of breath-holding, because of rapid diffusion and because of cardiac oscillations (i.e., mixing).

Gas mixing is complete in the alveoli of a normal lung during normal breathing. However, if the alveolus expands (e.g., emphysema), the diffusion distance may be too great to allow complete mixing, potentially leaving a layer of CO₂-rich gas lining the alveolar membrane and a core of O₂-rich gas in the alveolus. This represents a “micro” version of inhomogeneous distribution of ventilation.⁵²

Perfusion

The pulmonary circulation differs from the systemic circulation: it operates at a five to tenfold lower pressure, and the vessels are shorter and wider. There are two important consequences of the particularly low vascular resistance. First, the downstream blood flow in the pulmonary capillaries is pulsatile, in contrast to the more constant systemic capillary flow.⁵³ Second, the capillary and alveolar walls are protected from exposure to high hydrostatic pressures; therefore, they can be sufficiently thin to optimize diffusion (i.e., exchange) of gas but not permit leakage of plasma or blood into the airspace. Whereas an abrupt increase in the pulmonary arterial (or venous) pressure can cause breaks in the capillaries,⁵⁴ slower increases (i.e., months to years) stimulate vascular remodeling.⁵⁵ This remodeling might protect against pulmonary edema⁵⁶ (and possibly against lung injury⁵⁷), but diffusion will be impaired.

DISTRIBUTION OF LUNG BLOOD FLOW

Pulmonary blood flow depends on driving pressure and vascular resistance; these factors (and flow) are not homogeneous throughout the lung. The traditional thinking about lung perfusion emphasized the importance of gravity;⁵⁸ however, factors other than gravity are also important.

DISTRIBUTION OF BLOOD FLOW IN THE LUNG: THE EFFECT OF GRAVITY

Blood has weight and therefore blood pressure is affected by gravity. The height (base to apex) of an adult lung is approximately 25 cm; therefore, when a person is standing, the hydrostatic pressure at the base is 25 cm H₂O (i.e., approximately 18 mm Hg) higher than at the apex. The mean pulmonary arterial pressure is approximately 12 mm Hg at the level of the heart, and the pulmonary artery pressure at the lung apex can therefore approach zero. Thus less blood flow will occur at the apex (versus the base), and in the setting of positive pressure ventilation, the apical alveoli can compress the surrounding capillaries and prevent any local blood flow.

Based on such gravitational distribution of pulmonary artery pressure, as well as the effect of alveolar expansion, West and colleagues⁵⁹ divided the lung into zones I to III (Fig. 13.10). This system is based on the principle that perfusion to an alveolus depends on the pressures in the pulmonary artery (P_{PA}), pulmonary vein (P_{PV}), and alveolus (P_{ALV}). In the apex (zone I), the key issue is that pulmonary arterial pressure is less than alveolar pressure; therefore,

$$\text{Pulmonary vascular resistance (PVR)} = \frac{P_{PA} - P_{ALV}}{Q_T}$$

(true only if lung is in zone III)

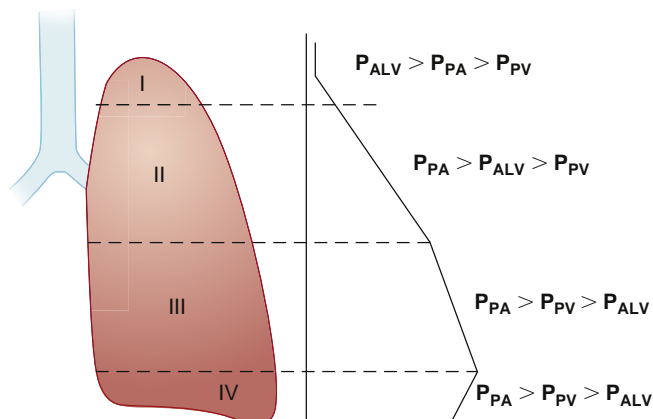


Fig. 13.10 Vertical distribution of lung blood flow. The so-called zones I, II, III, and IV are indicated. In zone I there is no perfusion, only ventilation. In zone II, pulmonary artery pressure exceeds alveolar pressure which in turn exceeds venous pressure; the driving pressure is P_{PA}–P_{ALV}. In zone III, arterial and venous pressures both exceed alveolar pressure, and here the driving pressure is P_{PA}–P_{PV}. In the lung base, blood flow is decreased possibly because of increased interstitial pressure that compresses extra alveolar vessels. P_{ALV}, intraalveolar pressure; P_{PV}, pulmonary vein pressure; P_{PA}, pulmonary artery pressure; Q_T, cardiac output.

no perfusion occurs. Zone I conditions can exist during mechanical ventilation and be exacerbated by low P_{PA}. Whenever zone I conditions exist, the nonperfused alveoli constitute additional dead space (V_D). Below the apex in zone II, P_{PV} is less than alveolar pressure, and the veins are collapsed except during flow, as in a “vascular waterfall.” Although P_{ALV} is always greater than P_{PV}, perfusion occurs when P_{PA} exceeds P_{ALV} (i.e., intermittently, during systole). Below this zone is zone III, in which there are two important differences: P_{PA} and P_{PV} both always exceed P_{ALV}. As a result, there is perfusion throughout systole and diastole (and inspiration and expiration). Gravity results in equal increases in both P_{PA} and P_{PV} toward the lung base; therefore, gravity cannot affect flow throughout zone III by increasing the P_{PA} to P_{PV} pressure gradient alone. Nonetheless, it is possible that the greater weight of the blood nearer the base results in vessel dilatation, thereby lowering vascular resistance and increasing flow.⁵⁸ It was subsequently recognized that there is also a decrease in perfusion in the lung base, or zone IV, that is thought to occur because of the effects of gravity compressing the lung at the bases—and the blood vessels therein—and thereby increasing vascular resistance.⁶⁰

Finally, additional evidence for the effect of gravity comes from volunteer experiments in which gravity was increased or abolished by altering the flight pattern of a jet aircraft.⁶¹ In these experiments, zero gravity decreased cardiac oscillations of O₂ and CO₂ during a breath-hold, indicating development of more homogeneous perfusion. In contrast, more recent experiments of exhaled gas analysis (on the Mir space station) reported that the heterogeneity of lung perfusion was reduced, but not eliminated, in the presence of

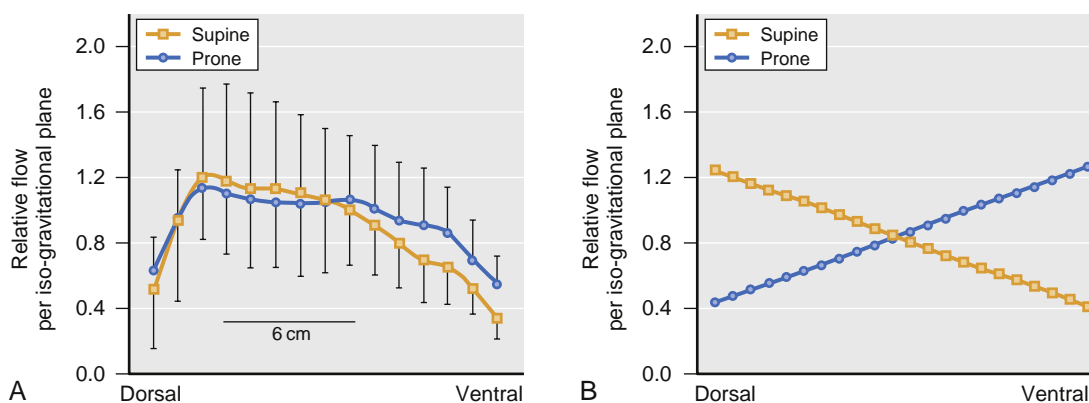


Fig. 13.11 Distribution of blood flow (ventral, dorsal) in supine versus prone position. The distributions from ventral to dorsal are similar, irrespective of position, suggesting that the anatomic features (and not simply gravity) determine the distribution of flow. The magnitude of the variability in either the prone (or in the supine) position (i.e., nongravitational inhomogeneity) is far greater than the differences in distribution between the prone and the supine positions (i.e., gravitational inhomogeneity). (From Glenny RW, Lamm WJ, Albert RK, Robertson HT. Gravity is a minor determinant of pulmonary blood flow distribution. *J Appl Physiol*. 1991;71:620-629.)

microgravity, indicating that gravity contributes to the heterogeneity of blood flow distribution but does not explain it entirely.⁶² While the precise role of gravity is disputed, it is likely to play a smaller role when supine versus when upright.

DISTRIBUTION OF BLOOD FLOW IN THE LUNG: INFLUENCE OF FACTORS NOT RELATED TO GRAVITY

Key experiments have reconsidered the effects of gravity. Blood flow measured in the same gravitational plane was less per unit of lung tissue at the apex than at the base.⁶³ In addition, microsphere assessment demonstrated significant variability within iso-gravitational planes, and lung height appeared to account for less than 10% of the distribution of flow in either the prone or supine positions.⁶⁴ In addition, inhomogeneity in the horizontal planes can exceed that in the vertical direction (Fig. 13.11).⁶⁵ Other studies have reported a preponderance of perfusion to the central lung (versus peripheral) tissue,⁶⁶ which can be reversed by the application of positive end-expiratory pressure (PEEP).⁶⁷ Although greater length of radial blood vessels was considered to explain this central-peripheral difference, others have suggested that it is not significant.⁶⁴ Finally, differences have been reported among lung regions in local vascular resistance.⁶⁸

Fractal distribution of blood flow may be more important than the influence of gravity.⁶⁹ A fractal pattern of perfusion means that in any given region, there will be “spatial correlation” (similarity) of the blood flow between neighboring regions.

Although the methods to study lung perfusion are complex—and there is a spectrum of opinion⁷⁰—the aggregate data suggest that factors other than gravity contribute to the heterogeneity of the distribution of perfusion.

HYPOXIC PULMONARY VASOCONSTRICION

HPV is a compensatory mechanism that diverts blood flow away from hypoxic lung regions toward better oxygenated regions.⁷¹ The major stimulus for HPV is low alveolar

oxygen tension (P_{AO_2}), whether caused by hypoventilation or by breathing gas with a low PO_2 , and is more potent when affecting a smaller lung region. The stimulus of hypoxic mixed venous blood is weaker.^{72,73} Whereas in humans older volatile anesthetics were thought to inhibit HPV more than intravenously based anesthesia, modern volatile anesthetics, including sevoflurane⁷⁴ and desflurane,⁷⁵ have little effect. During intravenously based anesthesia, exposure of one lung to an FiO_2 of 1.0 and the contralateral lung to a hypoxic gas mixture (FiO_2 , 0.12 to 0.05) reduced perfusion to the hypoxic lung to 30% of the cardiac output.⁷⁶ Pulmonary hypertension, because of vascular remodeling owing to ongoing HPV, can develop in humans at high altitude⁷⁷ or in the presence of chronic hypoxic lung disease.

Clinical Assessment of Lung Function

SPIROMETRY—TOTAL LUNG CAPACITY AND SUBDIVISIONS

The gas volume in the lung after a maximum inspiration is called the *total lung capacity* (TLC; usually 6 to 8 L). TLC can be increased in COPD either by overexpansion of alveoli or by destruction of the alveolar wall, resulting in loss of elastic tissue, as in emphysema (see Fig. 13.4).⁷⁸ In extreme cases, TLC can be increased to 10 to 12 L. In restrictive lung disease, TLC is reduced, reflecting the degree of fibrosis, and can be as low as 3 to 4 L (see Fig. 13.4).⁷⁸

Following maximum expiratory effort, some air is left in the lung and constitutes the RV (approximately 2 L). However, usually no region develops collapse because distal airways (<2 mm) close before alveoli collapse,⁷⁹ trapping gas and preventing further alveolar emptying. In addition, there is a limit to how much the chest wall, rib cage, and diaphragm can be compressed. The importance of preventing collapse of lung tissue was presented earlier (see Fig. 13.6).

The maximum volume that can be inhaled and then exhaled is the *vital capacity* (VC; 4-6 L), and this is the

difference between TLC and RV. VC is reduced in both restrictive and obstructive lung disease. In restriction, VC reduction reflects the loss of lung volume, such as from the constricting (i.e., shrinking) effects of fibrosis. In obstructive lung disease, long-term trapping of air increases the RV and can occur either by encroaching on (and reducing) the VC or in association with a (proportionally smaller) increase in FVC.⁷⁸

Tidal volume (V_T , usually 0.5 L) is inspired from the resting lung volume reached at end-expiration (FRC, 2.0 L). With increased ventilation, as in exercise, V_T is increased and FRC may be reduced by approximately 0.5 L. However, in airway obstruction, exhalation is impeded such that inspiration commences before the usual resting lung volume is reached; thus end-expiratory volume is increased.⁷⁸ Such air trapping reduces the resistance to gas flow in the narrowed airways, but because the lung tissue is hyperinflated and mechanically disadvantaged, the work of breathing overall is increased.

FRC increases with age as elastic lung tissue is lost; this reduces the lung recoil force countering the outward chest wall force, and the lung assumes a higher volume. The rate of this aging process is accelerated in COPD because of the contributions of chronic air trapping and marked loss of elastic tissue.¹⁹ FRC is reduced in fibrotic lung diseases,⁷⁸ sometimes to 1.5 L (see Fig. 13.4). Lung resection also reduces FRC, but the remaining lung will expand to fill the lung tissue void partially; this is called *compensatory emphysema* (see Chapter 53).

DIFFUSING CAPACITY (DL_{CO})—DIFFUSION ACROSS ALVEOLAR-CAPILLARY MEMBRANES

The diffusing capacity for carbon monoxide (DL_{CO}) test integrates many phenomena that are central to respiratory physiology. The test and the factors affecting its interpretation are described here. In the lungs, O_2 and CO_2 diffuse passively: O_2 from alveolar gas into plasma and red cells, where it binds to hemoglobin, and CO_2 in the opposite direction, from plasma to the alveoli. The amount that can diffuse across a membrane in a given period is the diffusing capacity, and it is determined with the following equation:

$$Diffusing\ capacity = \frac{(SA \times \Delta P \times Sol)}{(h \times \sqrt{MW})}$$

where SA is the surface area of the membrane exposed to gas, ΔP is the gradient of partial pressure between administered gas versus blood tension, Sol is the solubility of the gas in the membrane, h is the thickness of the membrane, and MW is the molecular weight of the gas.

Assessment of diffusing capacity (sometimes called *transfer factor*) uses CO as the test gas; it is inhaled at a small concentration (0.3%) to TLC just after a maximal expiration, filling the lung as much as possible with the dilute CO. The breath is held and then deeply exhaled to RV. The difference between the quantity of CO exhaled versus inhaled will therefore either be taken up by the perfusing blood (i.e., hemoglobin) or remain in the lung (RV). The latter can be determined if the CO is coadministered with an insoluble gas (e.g., helium) that remains in the lung.

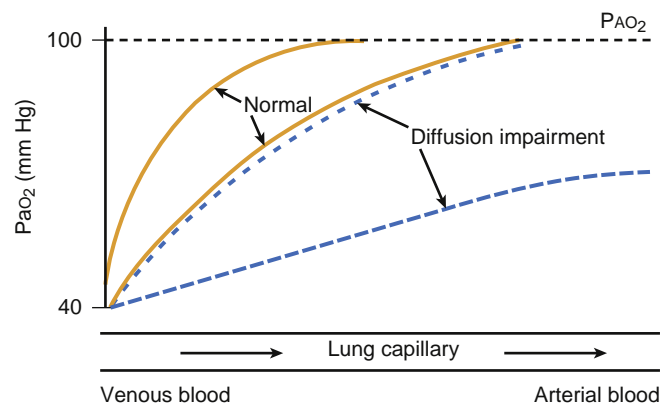


Fig. 13.12 Schematic of oxygenation of pulmonary capillary blood. In a healthy subject, there is a rapid equilibration (<30% capillary length) of the oxygen tension in capillary blood than that in alveolar gas; however, during exercise, the flow rate is greater (i.e., transit time shorter) and most of the capillary distance is used before equilibration is reached. This effect can be offset by distention and recruitment of pulmonary capillaries. If diffusion is impaired, equilibration takes longer, and it might not occur with exercise.

Surface Area

The surface area is taken as the area that is capable of exchanging gas on the alveolar and the capillary sides; thus it assumes a ventilated and perfused lung (i.e., not dead space). It will be lower in small lungs, lung fibrosis (restriction), after lung resection, or in cases of lung tissue destruction, such as emphysema.

Membrane Thickness

Thicker membranes reduce the CO transfer because the longer diffusion distance lowers the diffusion capacity, and the solubility of O_2 (and CO_2) is lower in fibrotic tissue than in plasma. Differentiating between effects of the volume of capillary blood and the membrane thickness can be difficult, but because oxygen and CO compete for binding to hemoglobin, distinguishing between these issues may be possible by measuring CO transfer with altered FiO_2 (see review by Hughes and colleagues).^{80,81}

Pressure Gradient

The larger the O_2 or CO_2 tension difference (ΔP) between the gas phase (alveolus) and the plasma (capillary), the greater the rate of diffusion. The mixed venous blood entering the pulmonary capillary has a PO_2 of 40 mm Hg (5.3 kPa), and alveolar PO_2 is approximately 100 mm Hg (13.3 kPa); therefore, the driving pressure (ΔP) is 60 mm Hg (8 kPa).

When blood flows through the capillary, it takes up oxygen and delivers CO_2 , but because oxygen pressure builds up in capillary blood, the diffusion rate slows down and becomes zero when pressure is equilibrated across the alveolar-capillary wall. At rest, equilibrium is usually reached within 25% to 30% of the capillary length, and almost no gas transfer occurs in the remaining capillary (Fig. 13.12). However, during exercise or stress (i.e., high cardiac output), blood flow through the capillary is faster, and a longer capillary distance is required before equilibrium is reached. Thickened alveolar-capillary membranes will also prolong the equilibration process and, if severe, can prevent

equilibration occurring and increasing the propensity to hypoxemia. If the mixed venous PO_2 ($P_{\text{mv}}\text{O}_2$) is lower than normal, the driving pressure increases and partially compensates toward achieving equilibrium with alveolar O_2 . The driving pressure is expressed:

$$\Delta P = (Pa\text{O}_2 - P_{\text{mv}}\text{O}_2) \text{ mm Hg}$$

Most of the oxygen that dissolves in plasma diffuses into the red cell and binds to hemoglobin; therefore, 1 L of blood (Hb 150 g/L) with a saturation of 98%—normal in arterial blood—carries 200 mL of Hb-bound O_2 , compared with 3 mL that is dissolved (PaO_2 100 mm Hg). The Hb-bound oxygen creates no pressure in plasma, which is important because it allows much more oxygen to diffuse over the membranes before a pressure equilibration is reached. Anemia (or prior CO exposure) reduces—and polycythemia increases—diffusion capacity.

Molecular Weight and Solubility

The rate of diffusion of a gas is inversely related to the square root of its MW; the larger the molecule, the slower the diffusion. O_2 is a light gas (MW 32), and CO_2 is heavier (MW 44). However, diffusion is also directly proportional to solubility in tissue, and CO_2 is almost 30-fold more soluble than O_2 . The aggregate effect is that CO_2 diffuses about 20-fold faster than O_2 ⁸²; therefore, there is no lung disease compatible with life that measurably impairs CO_2 diffusion.

Intraoperative Respiratory Events

RESPIRATORY FUNCTION DURING ANESTHESIA

Anesthesia impairs pulmonary function, whether the patient is breathing spontaneously or is receiving mechanical ventilation. Impaired oxygenation of blood occurs in most subjects who are anesthetized,⁸³ and this is why supplemental O_2 (FiO_2 usually 0.3–0.5) is almost invariably used. Mild to moderate hypoxemia (SaO_2 , 85% to 90%) is common and lasts from seconds to minutes; sometimes it is severe, and approximately 20% of patients may suffer from SaO_2 less than 81% for up to 5 minutes.⁸⁴ Indeed, greater than 50% of claims in anesthesia-related deaths relate to hypoxemia during anesthesia.² Beyond the operating room, the alterations in lung function acquired during anesthesia persist: clinically significant pulmonary complications can be seen in 1% to 2% of patients after minor surgery, and in up to 20% of patients after more major upper abdominal or thoracic surgery.⁸⁵ Such consequences of anesthesia place prime importance on ascertaining the causes of perioperative respiratory dysfunction and the clinical approaches to treatment.

In this section, we describe the effects of anesthesia and mechanical ventilation on lung function. The arrangement of this section parallels the sequence of events involved in oxygenating the blood and removing CO_2 . Thus the first phenomenon that might be seen with anesthesia is loss of muscle tone with a subsequent change in the balance between outward forces (i.e., respiratory muscles) and inward forces (i.e., elastic tissue in the lung) leading to a fall in FRC. This causes or is paralleled by an increase in

the elastic behavior of the lung (reduced compliance) and an increase in respiratory resistance. The decrease in FRC affects the patency of lung tissue with the formation of atelectasis (made worse with the use of high concentrations of inspired oxygen) and airway closure. This alters the distribution of ventilation and matching of ventilation and blood flow and impedes oxygenation of blood and removal of CO_2 .

LUNG VOLUME AND RESPIRATORY MECHANICS DURING ANESTHESIA

Lung Volume

Resting lung volume (i.e., FRC) is reduced by almost 1 L by moving from upright to supine position; induction of anesthesia further decreases the FRC by approximately 0.5 L.⁸⁶ This reduces the FRC from approximately 3.5 to 2 L, a value close to RV. General anesthesia causes a fall in FRC (approximately 20%), whether breathing is controlled or spontaneous^{87,88} and whether the anesthetic is inhalational or intravenous;⁸⁹ this is a major contributor to lowered oxygenation (discussed later). Muscle paralysis in the context of general anesthesia does not cause additional reduction in FRC.

The anatomic basis of the FRC reduction is not well understood. A landmark experiment on three volunteers using two-dimensional tomography suggested that a cephalad shift of the diaphragm, induced by anesthesia and paralysis, was responsible.⁹⁰ Recent studies using CT scanning also suggest cephalad diaphragm shift, as well as a decrease in the transverse chest area.^{89,91} However, other data suggest little role for the diaphragm, with possible caudal (not cephalad) shift of its anterior aspect.⁹² Simple CT suggests a cranial displacement, except in severe obstructive lung disease. Although the anatomic components of reduced FRC are debatable, the mechanism appears to be related to loss of respiratory muscle tone. FRC is maintained by a balance of the forces inward (lung recoil) versus forces outward (chest wall recoil, chest wall muscles, diaphragm). For example, maintenance of muscle tone using ketamine as the anesthetic does not reduce FRC.⁸⁹ Because patients are usually supine, the FRC will already have been reduced, and in elderly patients, this is particularly the case; in this context, the effects of anesthesia are more marked (see Fig. 13.9). As can be seen in the figure, FRC decreases with age assuming that weight does not change.

Compliance and Resistance of the Respiratory System

Static compliance of the total respiratory system (lungs and chest wall) is reduced on average from 95 to 60 mL/cm H_2O during anesthesia.⁹³ Most studies of lung compliance during anesthesia indicate a decrease compared with the awake state, and pooled data from several studies suggest that anesthesia is associated with a reduction in mean static compliance from almost 190 to approximately 150 mL/cm H_2O .⁹³ Data on changes in respiratory resistance are less clear. Although most studies suggest that anesthesia increases respiratory resistance, especially during mechanical ventilation,⁹³ no studies have corrected for lung volume and flow rates (both affect resistance considerably), and it is possible that changes in resistance occur merely because of volume (i.e., FRC) loss (Fig. 13.13).

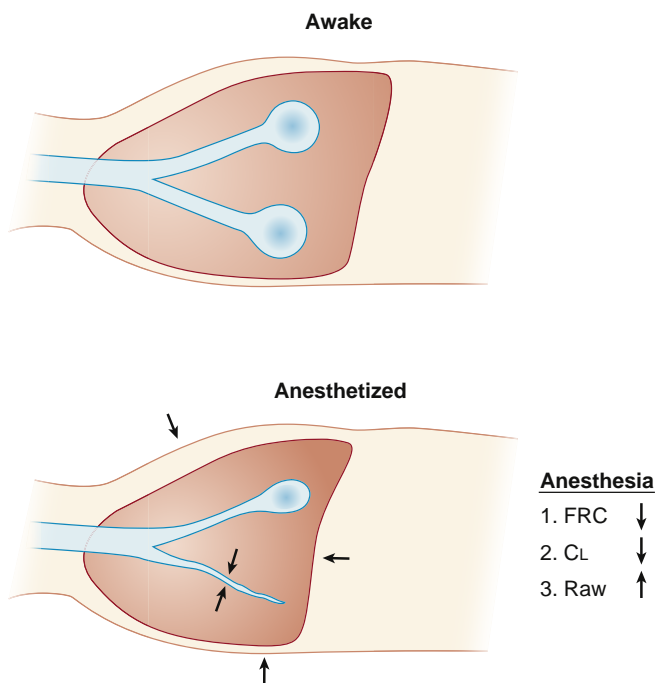


Fig. 13.13 Anesthesia induces cranial shift of the diaphragm and a decrease of transverse diameter of the thorax. These effects contribute to a lowered functional residual capacity (FRC). The decreased ventilated volume (atelectasis and airway closure) can contribute to reduced compliance (C_V). Decreased airway dimensions by the lowered FRC can contribute to increased airway resistance (Raw).

ATELECTASIS AND AIRWAY CLOSURE DURING ANESTHESIA

The classic article by Bendixen and colleagues⁹⁴ proposed “a concept of atelectasis” as a cause of impaired oxygenation and reduced respiratory compliance during anesthesia.⁹⁴ That study described a progressive decrease in compliance that paralleled decreases in oxygenation in both anesthetized humans and experimental animals, which was interpreted as progressive of atelectasis. However, others noticed an abrupt decrease in compliance and PaO_2 during induction of anesthesia, and yet atelectasis could not be shown on conventional chest radiography.

Since then, CT scanning has improved our knowledge of the nature of anesthesia-induced atelectasis, and the technique reveals prompt development of densities in the dependent regions of both lungs during anesthesia (data up to 1990 reviewed by Moller and associates).^{84,95} Morphologic studies of these densities in various animals supported the diagnosis of atelectasis. An example of atelectasis as seen on a CT scan is shown in [Fig. 13.14](#).

Atelectasis develops in approximately 90% of patients who are anesthetized, but it is unrelated to the choice of anesthesia.⁹⁶ It is seen during spontaneous breathing and after muscle paralysis, and with either intravenous or inhaled anesthetics.⁸⁹ The atelectatic area near the diaphragm is usually 5% to 6% of the total lung area, but can easily exceed 20%. The amount of lung tissue that is collapsed is larger, because the atelectatic area consists mostly of lung tissue, whereas normal aerated lung consists of 20% to 40% tissue (the rest being air). Thus 15% to 20% of the lung is atelectatic during uneventful anesthesia, before surgery has

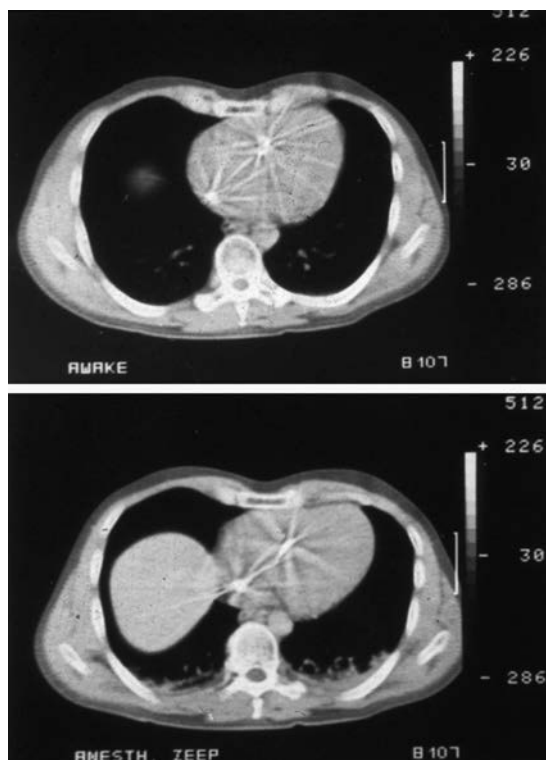


Fig. 13.14 Computed tomography with transverse exposures of the chest when the subject is awake (upper panel) and anesthetized (lower panel). In the awake condition, the lung is well aerated (radiations from a pulmonary artery catheter are seen in the heart). During anesthesia, atelectasis has developed in the dependent regions (grey/white irregular areas). The large grey/white area in the middle of the right lung field is caused by a cranial shift of the diaphragm and the underlying liver.

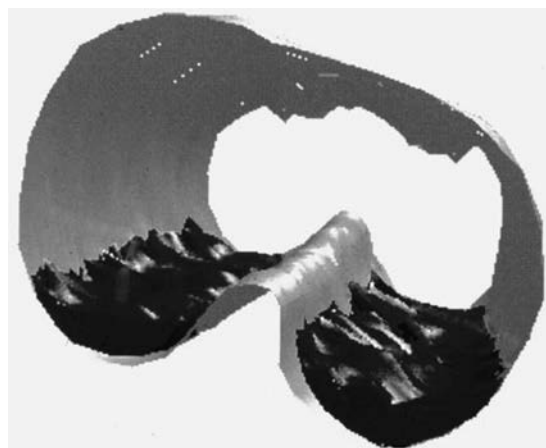


Fig. 13.15 A three-dimensional reconstruction of the thorax of an anesthetized patient with atelectasis in the dependent regions of both lungs. There is a slight decrease in the degree of atelectasis toward the apex (distal in this image). (Data from Reber A, Nylund U, Hedenstierna G. Position and shape of the diaphragm: implications for atelectasis formation. *Anaesthesia*. 1998;53:1054–1061.)

commenced; it decreases toward the apex, which usually remains aerated ([Fig. 13.15](#)). However, this degree of atelectasis is larger (upward of 50% of lung volume) after thoracic surgery or cardiopulmonary bypass, and can last for several hours.⁹⁷ Abdominal surgery adds little to the atelectasis, but after such surgery, it can persist for several days.⁹⁸

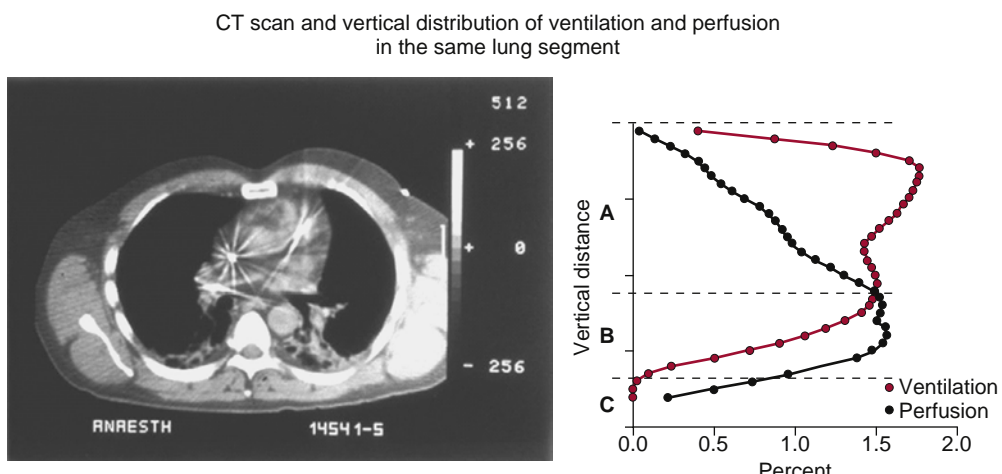


Fig. 13.16 Atelectasis and distribution of ventilation and blood flow. The left panel is a cross-sectional slice of a computed tomographic image of the chest of an anesthetized patient, illustrating atelectasis in the basal (dorsal) regions. The right panel illustrates the distribution of ventilation and perfusion throughout that slice. The bulk of the ventilation is to the upper lung region (zone A), in contrast to the awake subject without atelectasis, and it exceeds the level of local perfusion; this results in wasted ventilation (i.e., dead space) in the upper regions. In the lower region (zone B), the ventilation is less (probably because of intermittent airway closure) and is exceeded by the local perfusion, resulting in areas of low V_A/Q , causing hypoxemia. In the next lowest region (zone C), there is complete cessation of ventilation because of atelectasis, but some perfusion exists and causes a shunt. The farther from the top of the lung, the higher the perfusion; however, in the lowermost regions perfusion decreases (see text). (Data from Hedenstierna G. Alveolar collapse and closure of airways: regular effects of anaesthesia. *Clin Physiol Funct Imaging*. 2003;23:123–129.)

Atelectasis is an important cause of hypoxemia: there is a strong and significant correlation between the degree of atelectasis and the size of the pulmonary shunt ($R = 0.81$), where atelectasis is expressed as the percentage of lung area just above the diaphragm on CT scan and shunt is expressed as the percentage of cardiac output using the multiple inert gas elimination technique (MIGET).⁹⁶ The site of the increased shunt has been colocalized to the areas of atelectasis, using a technique that combines CT scanning and single photon emission computed tomography (SPECT; Fig. 13.16).⁹⁹ In addition to shunt, atelectasis may form a focus of infection and can certainly contribute to pulmonary complications.¹⁰⁰

Aside from anesthesia (and the type of surgery), it is difficult to predict the development of atelectasis. The magnitude of atelectasis is often directly related to the body mass index (BMI) and inspired oxygen concentration.^{87,89} Moreover, neither age⁹⁶ nor the presence of COPD¹⁰¹ predicts the development or extent of atelectasis. In COPD, it may be that airway closure precedes (and therefore prevents) alveolar closure. Alternatively, the greater loss of lung (elastic recoil) versus chest wall tissue may serve to protect against atelectasis.

PREVENTION OF ATELECTASIS DURING ANESTHESIA

Several interventions can help prevent atelectasis⁹⁵ or even reopen collapsed tissue, as discussed in the following sections.

Positive End-Expiratory Pressure

The application of PEEP (10 cm H₂O) has been repeatedly demonstrated to reexpand atelectasis in part (Fig. 13.17). Some atelectasis may persist and might require higher PEEP and inspiratory airway pressure.⁸⁹ The application of larger levels of PEEP can have complex effects. Reversal of hypoxemia is not proportionally associated with applied

PEEP, and a threshold exists in many cases. In addition, SaO_2 may decrease during the application of increased PEEP for two reasons. First, the increased P_{PL} owing to the PEEP can impair venous return, especially in the presence of hypovolemia, lowering the cardiac output and oxygen delivery (DO_2) and thereby reducing mixed venous O₂ content (CvO_2). In the presence of an intrapulmonary shunt, such as with atelectasis, the mixed venous blood is shunted directly into pulmonary venous blood causing arterial desaturation. Second, increased PEEP can cause redistribution of blood flow away from the aerated, expanded regions (distended by PEEP) toward atelectatic areas (not distended by PEEP; Fig. 13.18).¹⁰² In this context, persisting atelectasis in a dependent lung receives a larger proportion of the total pulmonary blood flow than without PEEP.⁵⁸ Finally, anesthesia-induced atelectasis rapidly reemerges after discontinuation of PEEP.⁸⁹ Indeed, Hewlett and coworkers¹⁰³ in 1974 cautioned against the “indiscriminate use of PEEP in routine anesthesia.”

To avoid negative circulatory effects, the magnitude of PEEP should just be enough to open up a collapsed lung. A PEEP of 7 cm H₂O in normal-weight patients (BMI < 25 kg/m²) without cardiopulmonary disease will recruit most of the lung, and keep it open with better oxygenation than in a comparable group without PEEP.¹⁰⁴ Thus a forceful dedicated recruit maneuver should not be needed. This effect was seen in nonabdominal surgery, and whether similar beneficial effect will be seen in abdominal surgery remains to be shown.

Recruitment Maneuvers

A sigh maneuver, or a large V_T , has been suggested for reversing atelectasis¹⁰; however, atelectasis is not uniformly reduced by a V_T increase or sigh up to P_{AW} of 20 cm H₂O.¹⁰⁵ Instead, a P_{AW} of 30 cm H₂O is required for initial opening, and 40 cm H₂O for more complete reversal (Fig. 13.19). In the presence of normal lungs, such inflation is equivalent to a VC and can therefore be called a VC

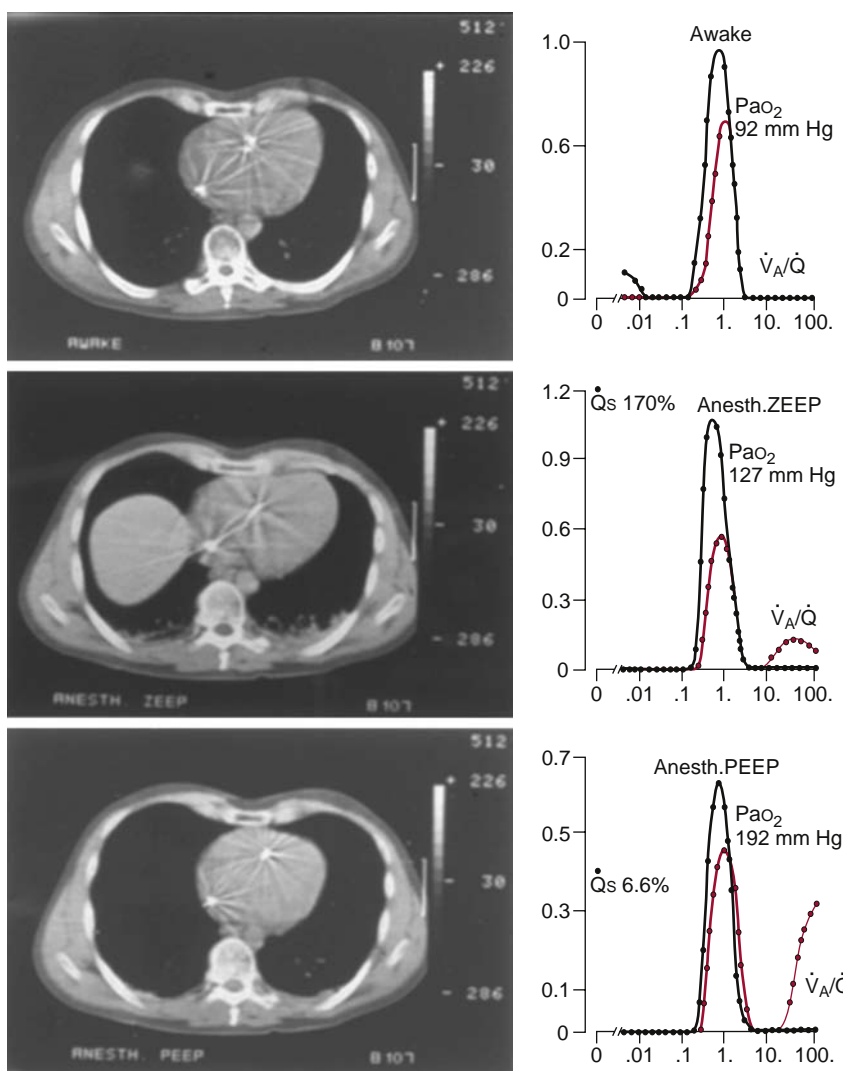


Fig. 13.17 Computed tomographic scans and \dot{V}_A/\dot{Q} distributions in the lung of a healthy, awake subject during anesthesia (zero positive end-expiratory pressure [ZEEP]) and during anesthesia (10 cm H_2O positive end-expiratory pressure [PEEP]). In the awake state, there is no atelectasis and the corresponding minor low \dot{V}_A/\dot{Q} distribution (left side of plot) may reflect intermittent airway closure. During anesthesia with ZEEP, atelectasis is apparent in the lung bases (and the diaphragm has been pushed cranially). The low \dot{V}_A/\dot{Q} has been replaced by atelectasis and large shunt; in addition, a small "high" \dot{V}_A/\dot{Q} mode (right side of plot) may reflect alveolar dead space in upper lung regions. With the addition of PEEP during anesthesia, the collapsed lung tissue has been recruited and the shunt has been reduced considerably. Moreover, the "high" \dot{V}_A/\dot{Q} mode (right side of plot) has significantly increased; this may reflect additional inflation of nonperfused upper lung.

maneuver (albeit achieved with positive P_{AW}). In addition, a significant hemodynamic effect is likely if the VC maneuver is sustained; in fact, inflation with a P_{AW} of 40 cm H_2O for 7 to 8 seconds appears to successfully open almost all anesthesia-induced atelectasis.¹⁰⁶

Minimizing Gas Resorption

Although recruitment of anesthesia-induced atelectasis is completely possible with either PEEP or a VC maneuver, continuous application of some level of PEEP is required to prevent rapid recurrence of the atelectasis.¹⁰⁷ However, nitrogen (N_2)—an insoluble gas that is not absorbed into the blood—can “splint” the alveolus if the alveolus is already opened. As a result, in anesthetized patients, a VC maneuver followed by ventilation with a gas mixture containing 60% N_2 (40% O_2) reduced the propensity for reaccumulation of atelectasis, with only 20% reappearing 40 minutes after recruitment.¹⁰⁷

The same principles apply in the practice of preoxygenation of patients during induction of anesthesia. Here, the aim is to prevent O_2 desaturation (i.e., gain an O_2 safety margin) during induction before the airway has been secured when the anesthesiologist can better manage ventilation and oxygenation. Traditionally, the application of FiO_2 1.0 has been used. Although the SaO_2 is usually well maintained with this approach, atelectasis inevitably forms. The use of 30% versus 100% O_2 during induction was demonstrated in a clinical study to eliminate the formation of atelectasis.¹⁰⁸ Later, a comparison of breathing 100%, 80%, and 60% O_2 during induction demonstrated ubiquitous atelectasis with 100%, less with 80%, and even less with 60% O_2 (Fig. 13.20); however, the trade-off for less atelectasis was a shorter safety margin before occurrence of O_2 desaturation.¹⁰⁹

An alternative approach may be continuous positive airway pressure (CPAP). Application of CPAP 10 cm

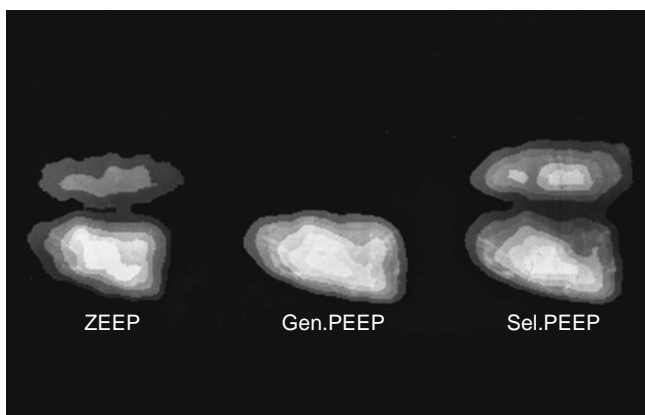


Fig. 13.18 Gamma camera images of lung blood flow in an anesthetized subject in the lateral position. During mechanical ventilation with zero end-expiratory pressure (ZEEP), perfusion is predominantly (60–70% of cardiac output) to the lower lung. Applying PEEP (10 cm H₂O) to both lungs forces more perfusion to the lower lung, leaving almost no perfusion to the upper lung (i.e., major increase in V_D). In contrast, selective application of PEEP to the lower lung causes redistribution of perfusion to the upper lung. Of course, the image presented is perfused tissue (not total anatomic lung tissue; in the right lateral position the upper-right lung would be larger). *PEEP*, Positive end-expiratory pressure. (From Hedenstierna G, Baehrendtz S, Klingstedt C, et al. Ventilation and perfusion of each lung during differential ventilation with selective PEEP. *Anesthesiology*. 1984;61:369–376.)

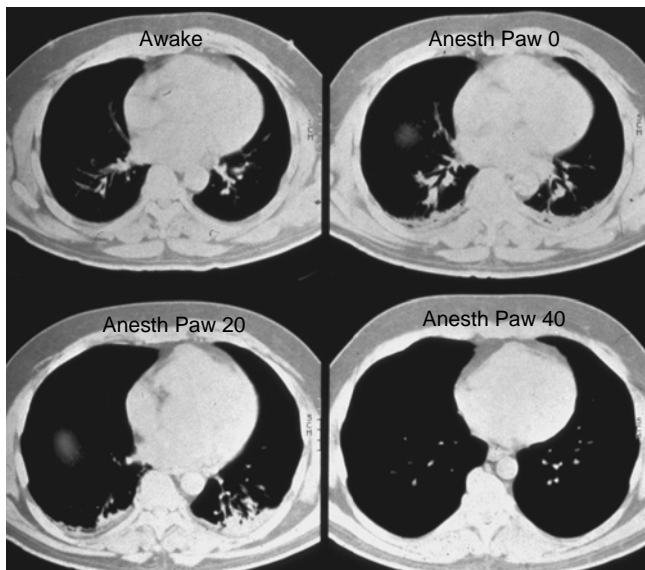


Fig. 13.19 Computed tomographic (CT) scans during awake and anesthetized states with altered airway pressure (P_{AW}). The CT scan in the awake subject (upper left panel) shows normal vasculature and no atelectasis. During anesthesia (P_{AW} , 0 cm H₂O; upper right panel), bilateral basal atelectasis is seen; the P_{AW} is increased in increments (20 cm H₂O shown), but the atelectasis is not reversed until a P_{AW} of 40 cm H₂O is applied (lower right panel). Thus a vital capacity maneuver was required to open the lung. (From Rothen HU, Sporre B, Engberg G, Wegenius G, Hedenstierna G. Re-expansion of atelectasis during general anaesthesia: a computed tomography study. *Br J Anaesth*. 1993;71:788–795.)

H₂O permitted the use of 100% inspired O₂ without formation of significant degrees of atelectasis.¹¹⁰ This might provide an ideal combination of minimal risk of either O₂ desaturation or atelectasis, but it has not been repeatedly verified.

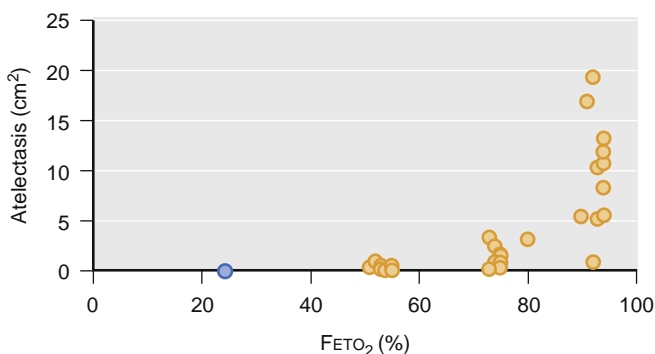


Fig. 13.20 Atelectasis formation in anesthetized subjects following preoxygenation with different inspired oxygen concentrations. Increasing the F_{O₂} during preoxygenation increases the propensity to subsequent atelectasis (closed symbols), although there is much variability. The blue circle at around an expired oxygen concentration (F_EO₂) of 25% represents data from anesthesia being induced while breathing 30% O₂. *FETO₂*, Expiratory oxygen fraction. (From Rothen HU, Sporre B, Engberg G, Wegenius G, Reber A, Hedenstierna G. Prevention of atelectasis during general anaesthesia. *Lancet*. 1995;345:1387–1391.)

Maintenance of Muscle Tone

Because loss of muscle tone in the diaphragm or chest wall appears to increase the risk of atelectasis, techniques that preserve muscle tone may have advantages. Intravenous ketamine does not impair muscle tone and is the only individual anesthetic that does not cause atelectasis. If neuromuscular blockade is added, atelectasis occurs as with other anesthetics.⁹⁰ Ketamine is an extremely useful anesthetic in special circumstances but has challenges with widespread use.

An experimental approach is restoration of respiratory muscle tone by diaphragm pacing. This approach is achieved with phrenic nerve stimulation, and it can modestly reduce the degree of atelectasis; however, the effect is minor and the approach is complicated.¹¹¹

Atelectasis Following Surgery

Hypoxemia is common after anesthesia and surgery. It is enhanced by breathing oxygen before induction of anesthesia and suctioning of the airway (negative pressure) before extubation of the trachea. In addition, splinting and inhibition of coughing associated with pain can cause atelectasis postoperatively. Several approaches have been tried to address such atelectasis-associated hypoxemia following surgery. Administration of 100% O₂ coupled with a VC maneuver is not effective; this is probably because while the VC maneuver recruits the lung, the alveolar opening is not maintained (in fact closure is encouraged by the N₂-free O₂).¹¹¹ However, a VC maneuver followed by a lower O₂ concentration (40% O₂ in N₂) can maintain an open lung until the end of anesthesia.¹⁰⁶ Oxygenation is sustained for a longer period following ventilation with 50% O₂ in air (i.e., N₂) compared with 100%, following cardiopulmonary bypass.¹¹³ In addition, use of 100% inspired oxygen before extubation increases the propensity to atelectasis¹¹² and treatment of postoperative hypoxemia, considered to be due to atelectasis, is associated with better outcomes when CPAP is used instead of 100% O₂.¹¹⁴

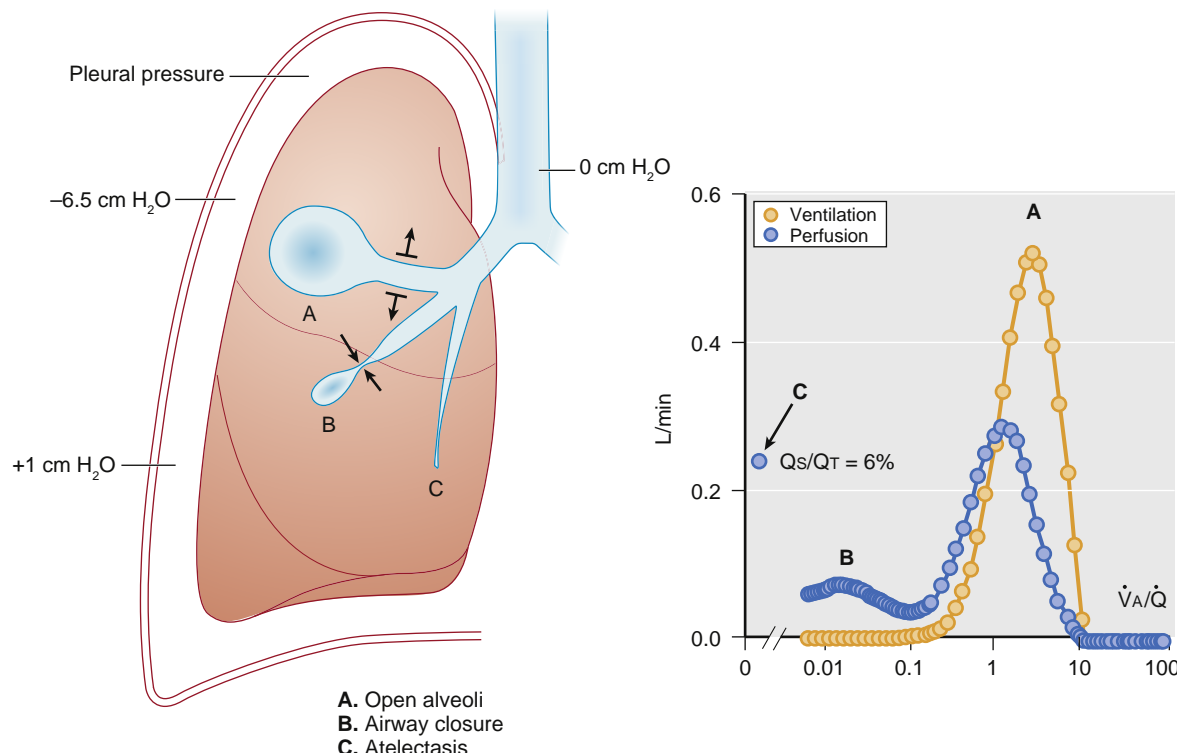


Fig. 13.21 A three-compartment model of ventilation and perfusion during anesthesia. In the upper regions, the alveoli and airways are open (left panel, A). In the middle region, the airways are intermittently closed (B), and atelectasis is present in the lower region (C). The corresponding ventilation-perfusion distribution (multiple inert gas elimination technique) is illustrated in the right panel. Mode A reflects good ventilation and perfusion, whereas mode B reflects intermittent airway closure. In addition, there is a shunt in the atelectatic region (mode C). Q_s/QT , Venous admixture, or shunt equation.

AIRWAY CLOSURE

Intermittent airway closure reduces ventilation of the affected alveoli. Such lung regions can become regions of low \dot{V}_A/\dot{Q} if perfusion is maintained or is not reduced to the same degree as ventilation. The propensity to airway closure increases with age (see Fig. 13.9),⁴⁹ as does perfusion to low \dot{V}_A/\dot{Q} regions.¹¹⁵ Anesthesia reduces FRC by about 0.5 L,⁸⁷ which increases airway closure during tidal ventilation.^{116,117} In fact, the reduction in ventilation in the nonatelectatic lung (Fig. 13.21) is caused by airway closure. In addition, ventilation in these regions is less than perfusion (i.e., regions of low \dot{V}_A/\dot{Q}) and contributes to impaired oxygenation during anesthesia. Taken together, the combination of atelectasis and airway closure explain about 75% of the overall impairment in oxygenation.⁸⁸ In addition, where (CV-ERV) indicates the amount of airway closure occurring above FRC (and ERV is expiratory reserve volume), this value increased with induction of anesthesia, and there is good correlation between low \dot{V}_A/\dot{Q} and the extent of airway closure.⁸⁸ In summary, a simple three-compartment lung model (normal \dot{V}_A/\dot{Q} matching regions, region of airway closure, and atelectatic lung) describes well the components contributing to impairment of oxygenation during anesthesia (see Fig. 13.21).

DISTRIBUTION OF VENTILATION AND BLOOD FLOW DURING ANESTHESIA

Distribution of Ventilation

Redistribution of inspired gas away from dependent to nondependent lung regions has been demonstrated, using isotope

techniques in anesthetized supine humans. Radiolabeled aerosol and SPECT demonstrate that ventilation is distributed mainly to the upper lung regions, with a successive decrease toward the lower lung regions, and an absence of ventilation in the lower-most regions, a finding consistent with the atelectasis demonstrable using CT (see Fig. 13.16).¹⁰⁰

Recruitment maneuvers increase dependent lung ventilation in anesthetized subjects in the lateral¹¹⁸ and supine¹¹⁹ positions, restoring the distribution of ventilation to that in the awake state. Thus restoration of overall FRC toward the awake level returns gas distribution toward the awake pattern. The explanations are recruitment of atelectatic lung, reopening of closed airways, and further expansion of already expanded (upper) lung regions, decreasing regional compliance and lessening incremental ventilation.

Distribution of Lung Blood Flow

The distribution of lung blood flow has been studied by injection of radioactively labeled macroaggregated albumin and SPECT.⁹⁹ During anesthesia, a successive increase in perfusion occurs from upper toward lower regions, with a slight drop in perfusion in the lowermost portion of the lung, which is atelectatic on simultaneous CT (see Fig. 13.16). PEEP will impede venous return to the right heart and reduce cardiac output. It can also affect pulmonary vascular resistance, although this would have little effect on cardiac output. In addition, PEEP redistributes blood flow toward dependent lung regions,^{59,119} reducing flow (and increasing dead space) in the upper lung; the increased dependent flow may increase shunt through atelectatic lung.¹⁰²

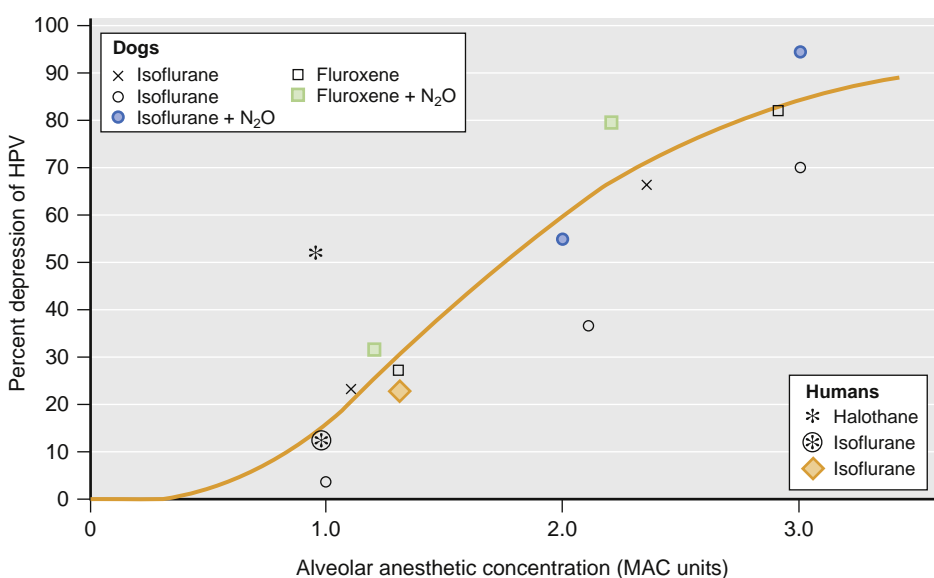


Fig. 13.22 Effect of inhaled anesthetics on hypoxic pulmonary vasoconstriction (HPV). A concentration of 1 MAC causes a 20% to 30% depression of HPV, and the HPV depression decreases sharply with higher concentrations. The effect is that the shunt (i.e., perfusion through nonventilated regions) will be less reduced during inhalational anesthesia. MAC, Minimum alveolar concentration. (From Marshall BE. Hypoxic pulmonary vasoconstriction. *Acta Anaesthesiol Scand Suppl*. 1990;94:37–41.)

HYPOXIC PULMONARY VASOCONSTRICTION

Several inhaled—but not intravenous—anesthetics inhibit HPV in isolated lung preparations.¹²⁰ Human studies of HPV are complex with multiple parameters changing simultaneously, thereby confounding the HPV response with changes in cardiac output, myocardial contractility, vascular tone, blood volume distribution, pH, PCO_2 , and lung mechanics. However, studies with no obvious changes in cardiac output indicated that isoflurane and halothane depress the HPV response by 50% at a minimum alveolar concentration (MAC) of 2 (Fig. 13.22).¹²¹

Ventilation-Perfusion Matching During Anesthesia

DEAD SPACE, SHUNT, AND VENTILATION-PERFUSION RELATIONSHIPS

CO_2 Elimination

Anesthesia impairs CO_2 elimination and oxygenation of blood. The explanation for reduced CO_2 elimination is reduced minute ventilation (\dot{V}_E) because of respiratory depression, or where this is preserved, because of an increase in the V_D/V_T . Single-breath wash out recordings demonstrate that “anatomic” dead space is unchanged, indicating that increased V_D/V_T is alveolar and confirmed by MIGET scan (Fig. 13.23).¹⁰ Such high \dot{V}_A/\dot{Q} can be explained by the perfusion of small corner vessels in interalveolar septa in the upper lung regions, where alveolar pressure can exceed pulmonary vascular pressure (zone I).⁸⁴ The impaired CO_2 elimination is most easily corrected by increasing the ventilation and is seldom a problem in routine anesthesia with mechanical ventilation.

Oxygenation

The impairment in arterial oxygenation during anesthesia is more marked with increased age, obesity, and

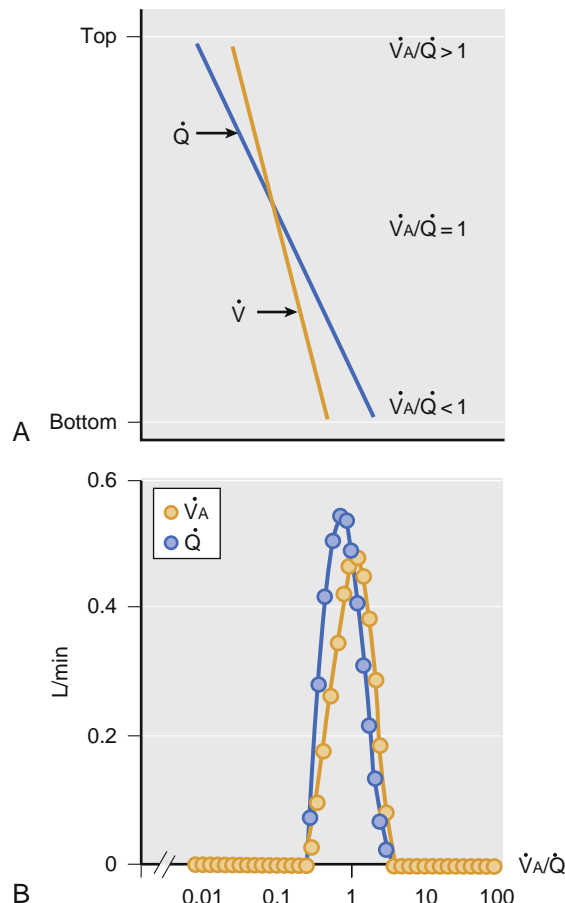


Fig. 13.23 A schematic drawing of (A) the vertical distributions of ventilation (\dot{V}_A) and blood flow through the lung (\dot{Q}) and (B) the resulting ventilation-perfusion distribution (\dot{V}_A/\dot{Q}). The \dot{V}_A/\dot{Q} distribution is centered at a ratio of 1, corresponding to the intersection of the ventilation and perfusion distribution curves. The slightly larger ventilation than perfusion in upper lung regions contribute to the high \dot{V}_A/\dot{Q} ratios greater than 1, whereas the larger perfusion than ventilation in the lower part of the lung is the cause of the lower \dot{V}_A/\dot{Q} ratios, less than 1. Although there is a moderate increase in ventilation down the lung, the increase in perfusion is greater.

BOX 13.2 Derivation of the Venous Admixture (Shunt) Equation

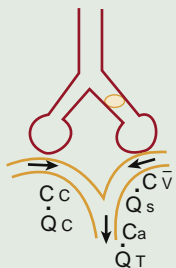
$$Ca \times \dot{Q}_T = (Cc' \times \dot{Q}_C) + (Cv \times \dot{Q}_S) \quad (1)$$

$$\dot{Q}_C = \dot{Q}_T - \dot{Q}_S \quad (2)$$

By inserting Equation (2) (accounts for all blood flow through the lungs) into Equation (1) (accounts for all oxygen carriage through the lungs),

$$Ca \times \dot{Q}_T = (Cc \times [\dot{Q}_T - \dot{Q}_S]) + (Cv \times \dot{Q}_S)$$

Rearranging,



$$\frac{\dot{Q}_S}{\dot{Q}_T} = \frac{Cc' - Ca}{Cc' - Cv}$$

where Cc' , Ca , and Cv are oxygen content in pulmonary end-capillary, arterial, and mixed venous blood, respectively; \dot{Q}_T is cardiac output; \dot{Q}_C is capillary flow; and \dot{Q}_S is shunt.

smoking.^{122,123} Venous admixture, as calculated by the standard oxygen shunt equation, is also increased during anesthesia to approximately 10% of cardiac output. However, this is an averaged calculation that considers hypoxia caused by pure shunt only, when actually it is due to a combination of “true” shunt (i.e., perfusion of nonventilated lung), poor ventilation of some regions, and regions that are ventilated but are perfused in excess of their ventilation (low \dot{V}_A/\dot{Q} regions). The combination of these effects is called *venous admixture*. The shunt equation (derived in Box 13.2) assumes that all blood flow through the lung goes to either of two compartments: in one (the non-shunt fraction), all the blood is oxygenated; and in the other (the shunt fraction), all blood is shunted.

The shunt equation (or venous admixture) can be written:¹²⁴

$$\frac{\dot{Q}_S}{\dot{Q}_T} = \frac{(CcO_2 - CaO_2)}{(CcO_2 - CvO_2)}$$

Because pulmonary end-capillary blood is assumed to be maximally saturated (therefore, $S_cO_2 = 1$), the quantity of dissolved O_2 can be ignored, and it can be assumed that the difference between CvO_2 and C_cO_2 is small ($CvO_2 = C_cO_2$):

$$\frac{\dot{Q}_S}{\dot{Q}_T} = \frac{(1 - S_aO_2)}{(1 - S_vO_2)}$$

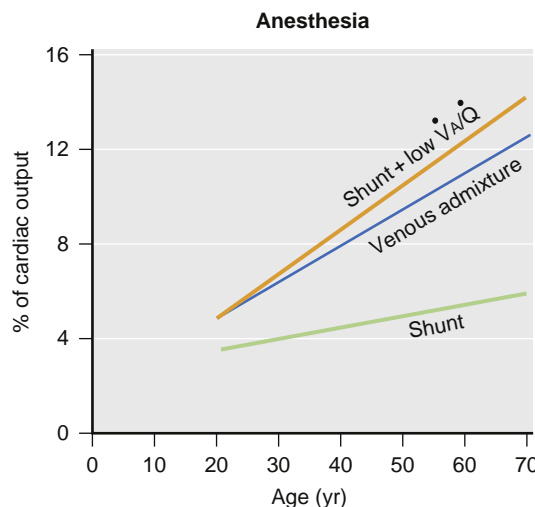


Fig. 13.24 The effect of age on oxygenation during anesthesia. The combination of shunt with low \dot{V}_A/\dot{Q} increases sharply with age (as does the degree of venous admixture). The increase in shunt with age, while significant, is less striking. (From Gunnarsson L, Tokics L, Gustavsson H, Hedenstierna G. Influence of age on atelectasis formation and gas exchange impairment during general anaesthesia. *Br J Anaesth*. 1991;66:423–432.)

Thus the effect of interventions on estimated shunt can be calculated easily from the changes in SaO_2 and SvO_2 .

The extent of venous admixture depends on the inspired oxygen fraction (FiO_2). The higher the inspired oxygen fraction, the less there are of the low \dot{V}_A/\dot{Q} regions. However, with high FiO_2 , regions with low \dot{V}_A/\dot{Q} may collapse because of gas adsorption and be transformed to shunt regions.¹²⁵ A good correlation between venous admixture versus the sum of “true” shunt and perfusion of low \dot{V}_A/\dot{Q} regions was seen in a study involving 45 anesthetized subjects (Fig. 13.24).⁹⁷ Derivation of the “oxygen shunt” or venous admixture is shown in Box 13.2.

In young healthy volunteers during anesthesia with thiopental and methoxyflurane, both ventilation and perfusion were distributed to wider ranges of \dot{V}_A/\dot{Q} ratios, which can be expressed as an increase in the logarithmic standard deviation of the perfusion distribution ($\log SDQ$). In a similar group of patients studied during halothane anesthesia and muscle paralysis, $\log SDQ$ was almost doubled (0.43 awake, 0.80 during anesthesia). In addition, true shunt was increased to a mean of 8%. A similar increase in shunt from 1% awake to a mean of 9% during anesthesia was recorded in a study on middle-aged (37 to 64 years) surgical patients, and there was a widening of the distribution ($\log SDQ$: 0.47 awake, 1.01 during anesthesia). In older patients with more severe impairment of lung function, halothane anesthesia with muscle paralysis, with or without nitrous oxide, caused considerable widening of the \dot{V}_A/\dot{Q} distribution ($\log SDQ$ 0.87 awake, 1.73 during anesthesia). In addition, shunt increased to a mean of 15%, with large variation among patients (0% to 30%). Thus the most consistent findings during anesthesia are an increased \dot{V}_A/\dot{Q} mismatch, expressed as an increased $\log SDQ$, and an increase in shunt. For review, see the article by Hedenstierna.⁸³

Spontaneous ventilation is frequently reduced during anesthesia because inhaled anesthetics¹²⁶ or

barbiturates¹²⁷ reduce sensitivity to CO₂. The response is dose-dependent and ventilation decreases with deepening anesthesia. Anesthesia also reduces the response to hypoxia, possibly because of effects on the carotid body chemoreceptors.¹²⁸

The effects of anesthesia on respiratory muscle function are becoming better understood.¹²⁹ The effects are not uniform. Rib cage excursions diminish with deepening anesthesia.¹³⁰ The predominant ventilatory response to CO₂ is produced by the intercostal muscles,^{131, 132} but with no clear increase in rib cage motion with CO₂ rebreathing during halothane anesthesia. Thus the reduced ventilatory response to CO₂ during anesthesia is due to impeded function of the intercostal muscles.

Factors that Influence Respiratory Function During Anesthesia

SPONTANEOUS BREATHING

Most studies of lung function have been performed on anesthetized, mechanically ventilated subjects or animals. Spontaneous breathing has been studied rarely. FRC decreases to the same extent during anesthesia, regardless of whether a muscle relaxant is used,^{90, 91} and atelectasis occurs to almost the same extent in anesthetized, spontaneously breathing subjects as during muscle paralysis.¹³³ Furthermore, the cranial shift of the diaphragm, as reported by Froese and Bryan,⁹⁰ was of the same magnitude both during general anesthesia with spontaneous breathing and with muscle paralysis, even though a difference in movement of the diaphragm from the resting position was noted. Thus, during spontaneous breathing, the lower, dependent portion of the diaphragm moved the most, whereas with muscle paralysis, the upper, nondependent part showed the largest displacement.

All these findings have raised the question of whether regional ventilation is different between spontaneous breathing and mechanical ventilation and whether mechanical ventilation worsens \dot{V}_A/Q as a consequence of poor ventilation of well-perfused, dependent lung regions. However, there is not much support for worsening of gas exchange by muscle paralysis if the lungs are normal (in contrast to injured lungs); there is also little support from the few studies of \dot{V}_A/Q distribution that have been performed. Dueck and colleagues¹³⁴ found the same increase in \dot{V}_A/Q mismatch in anesthetized sheep during anesthesia, regardless of whether they were spontaneously breathing or ventilated mechanically. The log SDQ, indicating the degree of mismatch, increased (0.66 [awake], 0.83 [inhaled anesthesia with spontaneous breathing], 0.89 [mechanical ventilation]). Shunt is also increased during anesthesia from 1% (awake) to 11% (anesthetized, spontaneous breathing) or 14% (anesthetized, mechanical ventilation). In a study of anesthetized human subjects, shunt and log SDQ increased from 1% and 0.47 while awake to 6% and 1.03 during anesthesia with spontaneous breathing and 8% and 1.01 during mechanical ventilation.⁸³ Thus most of the gas exchange effects of anesthesia occurs during spontaneous breathing, with little or no further derangement added by muscle paralysis and mechanical ventilation.

INCREASED OXYGEN FRACTION

In the studies cited thus far, an inspired oxygen fraction (FiO₂) of approximately 0.4 was used. Anjou-Lindskog and colleagues¹³⁵ induced anesthesia in subjects breathing air (FiO₂, 0.21) in middle-aged to older patients during intravenous anesthesia before elective lung surgery and found only small shunts of 1% to 2%, although log SDQ increased from 0.77 to 1.13. When FiO₂ was increased to 0.5, the shunt increased (by 3% to 4%). In another study of older patients during halothane anesthesia,⁸³ an increase in FiO₂ from 0.53 to 0.85 caused an increase in shunt from 7% to 10% of cardiac output. Thus increasing FiO₂ increases shunt, possibly because of attenuation of HPV by increasing FiO₂¹²¹ or further development of atelectasis and shunt in lung units with low \dot{V}_A/Q ratios.¹²⁵

BODY POSITION

FRC is reduced dramatically by the combined effect of the supine position and anesthesia. The effects on the FRC of inducing anesthesia in the upright position were tested by Heneghan and associates,¹³⁶ and there was no difference in oxygenation in the semirecumbent versus supine position. Decreased cardiac output and inhomogeneity of blood flow can outweigh any effects of posture. Fractional perfusion of the most dependent lung regions—likely poorly or not ventilated—may actually have been increased in the semi-recumbent position. In the lateral position, differences in lung mechanics, resting lung volumes, and atelectasis formation between the dependent and nondependent portions of the lung have been demonstrated¹³⁷ and shown to result in further disturbance of the ventilation-perfusion match, with severe impairment in oxygenation. However, there are large and unpredictable inter-individual variations.¹³⁸ Using isotope techniques, an increase in \dot{V}_A/Q mismatch was also demonstrated in anesthetized, paralyzed patients in the lateral position,¹³⁹ and an improvement was noticed in the prone position.¹⁴⁰ In addition, the vertical inhomogeneity of perfusion distribution is less marked in the prone position,⁶⁸ possibly reflecting regional differences in vascular configuration that promote perfusion of dorsal lung regions, regardless of whether they are in a dependent or nondependent position. Finally, distribution of ventilation may be uniform in anesthetized subjects when prone.¹⁴¹

AGE

Oxygenation is less efficient in older patients.¹⁰ However, the formation of atelectasis does not increase with age in adults, and the few CT studies of infants during anesthesia suggest greater degrees of atelectasis.⁹⁶ In addition, shunt is independent of age between 23 and 69 years. However, \dot{V}_A/Q mismatch increases with age, with enhanced perfusion of low \dot{V}_A/Q regions when awake and when anesthetized. The major cause of impaired gas exchange during anesthesia in those younger than 50 years is shunt, whereas beyond 50 years, \dot{V}_A/Q mismatch (i.e., increased log SDQ) becomes increasingly important (see Fig. 13.24). Because the correlation between log SDQ and age during anesthesia is almost parallel with that during the awake state, it can be said that anesthesia worsens \dot{V}_A/Q matching to the same extent as 20 years of aging.

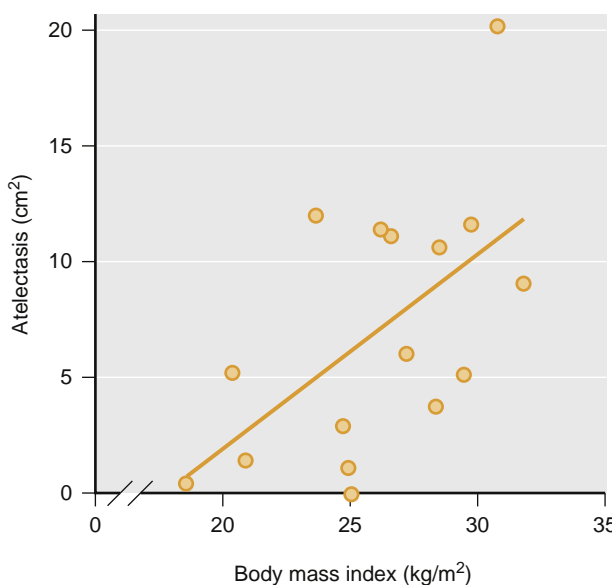


Fig. 13.25 Relationship between body mass index (BMI) and extent of atelectasis during general anesthesia. As BMI increases, so does the extent of atelectasis (although there is considerable variability). (From Rothen HU, Sporre B, Engberg G, Wegenius G, Hedenstierna G. Re-expansion of atelectasis during general anaesthesia: a computed tomography study. *Br J Anaesth*. 1993;71:788–795.)

OBESITY

Obesity worsens oxygenation^{142,143} predominantly because of reduced FRC resulting in a greater propensity to airway closure.¹⁴⁴ In addition, the use of high inspired oxygen concentrations promotes rapid atelectasis formation in alveoli distal to closed airways,^{87,109} and the atelectasis seems to be larger than in normal weight subjects (Fig. 13.25).^{144,145}

Preventing a decrease in FRC by applying CPAP during induction of anesthesia probably reduces atelectasis formation, and thereby maintains oxygenation.^{123,146,147} Indeed, the reduced “safety window” (the time taken to develop desaturation following breathing oxygen before induction of anesthesia) is much reduced in obese patients, and this may be prolonged by PEEP or CPAP¹⁴⁸ increasing lung volume and increasing the reservoir of O₂ available for diffusion into the capillary blood.

The use of high levels of inspired oxygen concentration, often almost 100%, to keep an acceptable level of oxygenation during anesthesia and surgery may be the simplest but not necessarily the best approach. It will promote further atelectasis formation,¹⁰⁸ and if the shunt is larger than 30%, which may be the case in these patients, additional oxygen will add little to arterial oxygenation.¹⁴⁹ The application of PEEP has been advocated, and it may reduce the atelectasis^{122,144,146} but may also have adverse effects, such as propensity for aspiration, reduced cardiac output, and redistribution of blood flow toward residual collapsed lung regions. Ventilation with inflations close to VC to reopen collapsed tissue, followed by ventilation with added PEEP, is another option. Recruitment of the lung with inflation to 55 cm H₂O opened essentially all collapsed lung tissue in patients with a BMI of 40 kg/m² or more.¹⁵⁰ However, a recruitment alone did not keep the lung open for more than a few minutes. To keep the lung open, a PEEP of 10 cm H₂O after the recruitment was needed, and PEEP of 10 was not

enough to open up the lung.¹⁵⁰ Body position can have a substantial effect on lung volume and should be considered to the extent that surgery allows.¹⁵¹

PREEEXISTING LUNG DISEASE

Smokers and patients with chronic lung disease have impaired gas exchange in the awake state, and anesthesia-associated deterioration in oxygenation is greater than in healthy individuals.¹⁰ Interestingly, smokers with moderate airflow limitation may have less shunt as measured by MIGET than in subjects with healthy lungs. Thus, in patients with mild to moderate bronchitis who were to undergo lung surgery or vascular reconstructive surgery in the leg, only a small shunt was noticed, but log SDQ was increased.⁸³ In patients with chronic bronchitis studied by MIGET and CT, no or limited atelectasis developed during anesthesia and no or only minor shunt;¹⁰¹ however, a considerable mismatch was seen with a large perfusion fraction to low V_A/Q regions. Consequently, arterial oxygenation was more impaired than in lung-healthy subjects, but the cause was different from that in healthy subjects. A possible reason for the absence of atelectasis and shunt in these patients is chronic hyperinflation, which changes the mechanical behavior of the lungs and their interaction with the chest wall such that the tendency to collapse is reduced. It should be kept in mind that a patient with obstructive lung disease may have large regions with low V_A/Q ratios that can be converted over time to resorption atelectasis. Thus the protection against atelectasis formation during anesthesia by the obstructive lung disease might not last long. Regions with low V_A/Q can be replaced by atelectasis as a result of slow absorption of gas behind occluded airways later during surgery and in the postoperative period.

REGIONAL ANESTHESIA

The ventilatory effects of regional anesthesia depend on the type and extension of motor blockade. With extensive blocks that include all the thoracic and lumbar segments, inspiratory capacity is reduced by 20% and expiratory reserve volume approaches zero.^{152,153} Diaphragmatic function, however, is often spared, even in cases of inadvertent extension of subarachnoid or epidural sensory block up to the cervical segments.¹⁵² Skillfully handled regional anesthesia affects pulmonary gas exchange only minimally. Arterial oxygenation and CO₂ elimination are well maintained during spinal and epidural anesthesia. This is in line with the findings of an unchanged relationship of CC and FRC,¹⁵⁴ and unaltered distributions of ventilation-perfusion ratios as assessed by MIGET during epidural anesthesia.⁸³

CAUSES OF HYPOXEMIA AND HYPERCAPNIA

In the previous sections, we discussed ventilation, gas distribution, and the respiratory mechanics that govern distribution, diffusion, and pulmonary perfusion. All these components of lung function can affect the oxygenation of blood, and all except diffusion can also measurably affect CO₂ elimination. The different mechanisms behind hypoxemia and CO₂ retention, or hypercapnia or hypercarbia, have been mentioned previously but will be analyzed in more detail here.

TABLE 13.1 Causes of Hypoxemia

Disturbance	Pao ₂ (Breathing Air) at Rest	Pao ₂ (Breathing Oxygen) at Rest	Pao ₂ (Breathing Air) With Exercise (Versus Rest)	Paco ₂
Hypoventilation	Reduced	Normal	No change or further decrease	Increased
̇V _A /̇Q mismatch	Reduced	Normal	No change or minor increase or decrease	Normal
Shunt	Reduced	Reduced	No change or further decrease	Normal
Diffusion impairment	Reduced	Normal	Small to large decrease	Normal

TABLE 13.2 Mechanisms of Hypoxemia in Different Lung Disorders

Disorder	Hypoventilation	Diffusion Impairment	̇V _A /̇Q Mismatch	Shunt
Chronic bronchitis	(+)	—	++	—
Emphysema	+	++	+++	—
Asthma	—	—	++	—
Fibrosis	—	++	+	+
Pneumonia	—	—	+	++
Atelectasis	—	—	—	++
Pulmonary edema	—	+	+	++
Pulmonary emboli	—	—	++	+
Acute respiratory distress syndrome	—	—	+	+++

+++ Most Important; ++ Important; + Somewhat Important; – Unimportant.

Causes of hypoxemia include hypoventilation, ̇V_A/̇Q mismatch, impaired diffusion, and right-to-left shunt (Table 13.1). Hypercapnia is usually caused by hypoventilation, although it can be caused by ̇V_A/̇Q mismatch and shunt (Table 13.2). Increased ̇VCO₂ occurs in hypermetabolic conditions (e.g., fever, malignant hyperthermia, thyroid crisis) or with the use of CO₂-generating buffers such as sodium bicarbonate (NaHCO₃).

Hypoventilation

If ventilation is low relative to metabolic demand, elimination of CO₂ will be inadequate, and CO₂ will accumulate in the alveoli, blood, and other body tissues. Hypoventilation is often defined as ventilation that results in a Paco₂ greater than 45 mm Hg (6 kPa). Thus hypoventilation could be present even when minute ventilation is high, provided the metabolic demand or dead space ventilation is increased to a greater extent.

The increased alveolar Paco₂ reduces the alveolar space available for oxygen. Alveolar PO₂ (PAO₂) can be estimated by the alveolar gas equation (see Box 13.1). The simplified equation is expressed:

$$PAO_2 = P_{lO_2} - \left(\frac{PACO_2}{R} \right)$$

Assuming that the respiratory exchange ratio (R) is 0.8 (more or less true at rest), PAO₂ can be estimated. In the ideal lung, PaO₂ equals PAO₂. For example, if PiO₂ is 149 mm Hg (19.9 kPa) and Paco₂ is 40 mm Hg (5.3 kPa), then PaO₂ is 99 mm Hg (13.2 kPa). If hypoventilation develops

and the Paco₂ rises to 60 mm Hg (8 kPa) and there is no other gas exchange impairment, the PaO₂ will fall to 74 mm Hg (9.9 kPa). Clearly, a decrease in PaO₂ caused by hypoventilation is easily overcome by increasing PiO₂ (i.e., by increasing FiO₂). If there is a gap between the PAO₂ (estimated from this equation) and the measured (actual) PaO₂, then a cause of hypoxemia in addition to hypoventilation is present. These causes are discussed in the following sections.

Ventilation-Perfusion Mismatch

For optimal gas exchange, ventilation and perfusion must match each other in all lung regions. At rest, both ventilation and perfusion increase downward through the lung. However, perfusion increases more than ventilation, the difference between the uppermost and lowermost 5-cm segments being threefold for ventilation and tenfold for perfusion. This change results in a mean ̇V_A/̇Q ratio of approximately 1 somewhere in the middle of the lung and a range of ̇V_A/̇Q ratios (0.5 at the bottom, 5.0 in the apex; see Fig. 13.23, upper panel, the perfusion distribution being a simplified drawing of Fig. 13.11).

Another way of showing the matching between ventilation and blood flow is by illustrating a multicompartimental analysis of ventilation and distribution of blood flow against ̇V_A/̇Q ratios. This can be achieved with MIGET.¹⁵⁵ In short, MIGET is based on the constant intravenous infusion of a number of inert gases (usually six) with differing solubilities in blood. When passing through the lung capillaries, the different gases are eliminated via the alveoli and expired in indirect proportion to their solubility. A poorly

TABLE 13.3 Mean (SD) Ventilation-Perfusion Relationships With No Cardiopulmonary Disease (Normal, $N = 45$), Awake and During General Anesthesia and Muscle Paralysis

	Q̄ mean	log SDQ̄	V̄ mean	log SDV̄	Shunt (% QT)	Dead Space (% VT)	Pao ₂ /Fio ₂ (kPa)
Awake	0.76 (0.33)	0.68 (0.28)	1.11 (0.52)	0.52 (0.15)	0.5 (1.0)	34.8 (14.2)	59.5 (8.1)
Anesthetized	0.65 (0.34)	1.04 (0.36)	1.38 (0.76)	0.76 (0.31)	4.8 (4.1)	35.0 (9.9)	50.9 (15.2)

log SDQ̄, Standard deviations of the logarithmic distribution of perfusion; log SDV̄, standard deviations of the logarithmic distribution of ventilation; Q̄ mean, mean \dot{V}_A/\dot{Q} of the perfusion distribution; V̄ mean, mean \dot{V}_A/\dot{Q} of ventilation distribution. (Gunnarsson L, Tokics L, Gustavsson H, Hedenstierna G. Influence of age on atelectasis formation and gas exchange impairment during general anaesthesia. Br J Anaesth. 1991;66:423–432).

soluble gas will rapidly leave the bloodstream and be more or less completely eliminated and exhaled (e.g., sulfur hexafluoride); a gas with a high solubility in the blood will be almost completely retained in the blood and will not be exhaled (e.g., acetone); and a gas of intermediate solubility will be retained (and expired) to an intermediate extent (e.g., halothane).

As a result, the concentration of the different gases in arterial blood will differ, with higher concentrations of gases with high solubility. Retention can be calculated as the ratio between arterial and mixed venous blood concentrations. Similarly, the ratio of the concentrations (i.e., expired:mixed venous) can be calculated and gives the excretion for each gas. With knowledge of the retention, excretion, and solubility of each gas, an essentially continuous distribution of blood flow against \dot{V}_A/\dot{Q} ratios can be constructed. The lower panel in Fig. 13.23 shows an example from a healthy subject. Note that ventilation and blood flow are well matched, being distributed to a limited number of compartments centered on a \dot{V}_A/\dot{Q} ratio of 1. MIGET has a high discriminatory capacity of detecting different \dot{V}_A/\dot{Q} disturbances, but does not provide topographic information. Several variables that reflect the degree of mismatch can be calculated and are shown in Table 13.3. In the following paragraphs, examples of \dot{V}_A/\dot{Q} mismatch are discussed.

If ventilation and perfusion are not matched, gas exchange will be affected. The most common cause of impaired oxygenation is \dot{V}_A/\dot{Q} mismatch. Low \dot{V}_A/\dot{Q} will impede oxygenation because ventilation is insufficient to fully oxygenate the blood, and the degree of impairment is dependent on the degree of \dot{V}_A/\dot{Q} mismatch; in fact, even normal lung regions \dot{V}_A/\dot{Q} (0.5–1) cannot completely saturate the blood. Thus PaO_2 cannot equal alveolar PO_2 , and a difference ($\text{PAO}_2 - \text{PaO}_2$) of 3 to 5 mm Hg (0.4–0.7 kPa) is normal. With greater \dot{V}_A/\dot{Q} mismatch, the $\text{PAO}_2 - \text{PaO}_2$ difference is further increased. The \dot{V}_A/\dot{Q} mismatch can account for all the hypoxemia seen in a patient with severe obstruction.¹¹⁵ Shunt (\dot{Q} , but no \dot{V}_A), which is often claimed to exist in patients with COPD, is mostly absent when analyzed with a more sophisticated technique such as MIGET. Indeed, shunt in a patient with obstruction likely represents a complicating factor in the disease (Fig. 13.26).

In severe asthma, a distinct bimodal pattern of low ratios occurs when using MIGET (see Fig. 13.26).¹⁵⁶ The reason may be that alveoli behind airways obstructed by edema (or a mucous plug or spasm) can still be ventilated by collateral ventilation (i.e., alveolar pores, interbronchial communications); these regions would otherwise be shunt (no \dot{V}_A , some \dot{Q}), resulting in the additional peak in \dot{V}_A/\dot{Q} explaining the bimodal distribution. Such collateral ventilation

might be part of the reason that true shunt is not normally seen in COPD. Of course, if the standard shunt equation is used to explain hypoxemia, there is no capacity to distinguish between the contributions of low \dot{V}_A/\dot{Q} versus shunt to hypoxemia (the net effect is best called *venous admixture*).

Airway obstruction is distributed unevenly, and a large variation in \dot{V}_A/\dot{Q} ratios results. Indeed, ventilation is redistributed from regions with high airway resistance to other regions that can then become overventilated in proportion to their perfusion; this causes high \dot{V}_A/\dot{Q} ratios. There are normally regions in the apex that have ratios of up to 5, but ratios of 100 or more exist in patients with obstruction, making the regions practically indistinguishable from true dead space; this is what causes the increase in physiologic dead space in obstructive lung disease. The effect of high \dot{V}_A/\dot{Q} is also the same as for airway dead space—that is, ventilation that seems not to participate in gas exchange (“wasted ventilation”). Consequently, a patient with COPD has low \dot{V}_A/\dot{Q} (impedes oxygenation) and high \dot{V}_A/\dot{Q} (mimics dead space, impedes CO_2 elimination). However, MIGET is a complex, research-orientated tool, and the calculation of dead space for clinical purposes relies instead on expired CO_2 . Derivation of the CO_2 dead space is shown in Box 13.3.

\dot{V}_A/\dot{Q} mismatch exists to varying degrees in all patients with COPD, and it fully explains hypoxemia in most of them. Hypoventilation can also contribute, whereas impaired diffusion or shunt rarely contributes to hypoxemia. Diffusion capacity, or transfer test, can be reduced markedly in severe COPD, in particular in emphysema; in this case the decrease is not caused by thickened alveolar-capillary membranes but rather by reduced capillary blood volume and reduced area for diffusion.

Pulmonary vessels can be affected by lung disease and can cause \dot{V}_A/\dot{Q} mismatch by impeding regional blood flow. Systemic diseases with vascular involvement can cause severe pulmonary dysfunction because of \dot{V}_A/\dot{Q} mismatch, impaired diffusion, and shunt. \dot{V}_A/\dot{Q} mismatch causes most of the hypoxemia in pulmonary fibrosis.¹⁵⁷ In addition, hypoxemia can be caused by impaired diffusion (in particular, during exercise, when it can dominate) and a varying degree of shunt (discussed later).

Pulmonary emboli cause \dot{V}_A/\dot{Q} mismatch in three ways. First, vascular beds are occluded, causing extremely high \dot{V}_A/\dot{Q} locally; this is manifest as increased dead space. Second, the occluded vascular bed diverts blood flow to other, already ventilated regions, thus converting these into low \dot{V}_A/\dot{Q} regions. Finally, if P_{PA} (pulmonary artery pressure) is markedly increased, then any propensity to shunt will be increased.¹⁵⁸ In patients with acute pulmonary embolism,¹⁵⁹ hypoxemia appears to be principally caused by increased variability of \dot{V}_A/\dot{Q} , and this has been confirmed experimentally.¹⁶⁰

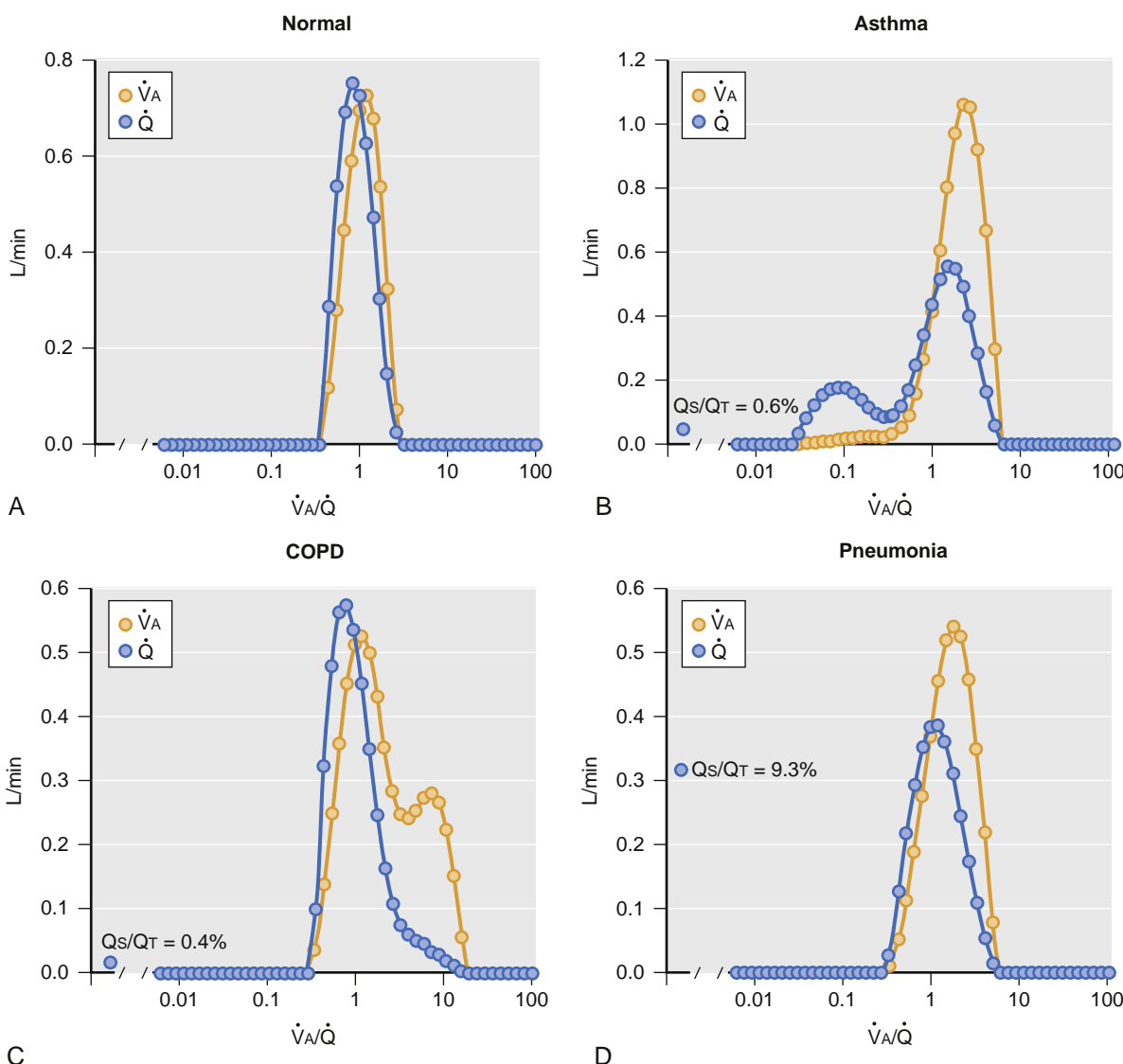


Fig. 13.26 Distribution of ventilation and perfusion in normal lungs, asthma, chronic obstructive pulmonary disease (COPD), and pneumonia. In normal lungs (A) there is good matching between ventilation (orange circle) and perfusion (blue circle) with a mode centered around a \dot{V}_A/\dot{Q} ratio of 1. This results in near optimal oxygenation of blood and CO_2 removal. In asthma (B) there is broader distribution of \dot{V}_A/\dot{Q} with some regions being ventilated well in excess of perfusion ($\dot{V}_A/\dot{Q} = 10$ and greater), with another mode of low \dot{V}_A/\dot{Q} centered around a ratio of 0.1. This mode can be explained by collateral ventilation maintaining gas exchange in alveoli behind occluded airways. There is no shunt seen in asthma. In COPD (C) the pattern is similar to asthma, but with an additional "high" \dot{V}_A/\dot{Q} mode that adds to dead space such as ventilation. Shunt is not present, and the pattern of \dot{V}_A/\dot{Q} distribution is not associated with significant hypoxemia. In lobar pneumonia (D) the major finding is pure shunt (consolidated, perfused, and poorly ventilated lobe); there is only minor widening of the \dot{V}_A/\dot{Q} distribution.

Pneumonia involving large areas of consolidated, edematous, or atelectatic (i.e., all non-aerated) lung involves significant shunt, and areas of partial aeration contribute to \dot{V}_A/\dot{Q} mismatch (see Fig. 13.26).¹⁴⁹ In bacterial pneumonia, HPV appears to be inhibited, which is an important mechanism that worsens hypoxemia.^{161,162}

EFFECT OF \dot{V}_A/\dot{Q} ON CO_2 ELIMINATION

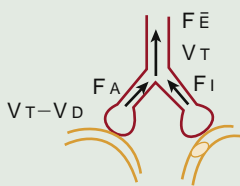
A common misconception is that although \dot{V}_A/\dot{Q} impedes oxygenation, it has little effect on CO_2 clearance. Actually, elimination of CO_2 is even more limited by \dot{V}_A/\dot{Q} mismatch than is oxygenation of blood⁸²; however, this seldom results in hypercapnia because minimal increases in \dot{V}_A rapidly correct PaCO_2 . If alveolar ventilation is already impaired

and cannot be increased, the addition of \dot{V}_A/\dot{Q} mismatch will increase PaCO_2 .

IMPAIRED DIFFUSION

Hypoxemia can occur because of impaired diffusion in fibrosis or vascular diseases because of severely thickened alveolar-capillary membranes. Diffusion is slowed down and the entire length of capillary may be required before the capillary blood has been fully oxygenated, even in resting conditions. On the other hand, this means that a diffusion barrier is unlikely to cause hypoxemia provided the perfusion time and distance permits O_2 equilibration (see Fig. 13.12); however, when these reserves are spent, PaO_2 begins to fall. This decrease is particularly noticeable in patients with

BOX 13.3 Derivation of the Physiologic Dead Space Equation



The quantity of CO_2 expired in an exhaled tidal volume = $\text{FeCO}_2 \times V_T$

This comes from perfused lung and from nonperfused lung.

CO_2 exhaled from perfused lung = $\text{FACO}_2 \times V_A = \text{FACO}_2 \times (V_T - V_D)$

CO_2 from nonperfused (dead space) lung is derived from inspired gas = $\text{FICO}_2 \times V_D$

Thus, $\text{FeCO}_2 \times V_T = \text{FACO}_2(V_T - V_D) + (\text{FICO}_2 \times V_D)$

By rearranging,

$$\frac{V_{DS}}{V_T} = \frac{F_A - F_E}{F_A - F_I}$$

If $F_I = 0$, F is replaced by P , and P_A is replaced by P_a , for CO_2 ,

$$\frac{V_{DS}}{V_T} = \frac{PaCO_2 - PECO_2}{PaCO_2}$$

where F_E , F_A , and F_I are mixed expired, alveolar, and inspired gas concentration, respectively, and V_T , V_{DS} , and V_A are tidal volume, dead space, and part of the tidal volume to perfused alveoli, respectively.

pulmonary fibrosis, who might have normal PaO_2 at rest but show dramatic decreases during exercise.^{82,115} Development of -or increasing- right-to-left shunting in the heart, such as with an atrial septal defect, can also cause this exercise-induced hypoxemia because the left-to-right shunt at rest becomes right-to-left (or a small right-to-left shunt increases) because of increased P_{PA} .

RIGHT-TO-LEFT SHUNT

If blood passes through the lung without contacting ventilated alveoli, then the blood will not oxygenate or release CO_2 . This condition is called a *shunt*, and it lowers PaO_2 and can increase Paco_2 . Healthy people have a small shunt (2%-3% of cardiac output) that is caused by venous drainage of the heart muscle into the left atrium by the thebesian veins. In pathologic states, the shunt ranges from 2% to 50% of cardiac output.

Shunt is often confused with \dot{V}_A/\dot{Q} mismatch. While a \dot{V}_A/\dot{Q} of zero (some perfusion, no ventilation) constitutes a shunt, there are two clear and important differences between low \dot{V}_A/\dot{Q} and shunt. First, the anatomy of a shunt differs from an area of low \dot{V}_A/\dot{Q} . Regions with low \dot{V}_A/\dot{Q} are characterized by narrowing of the airways and vasculature, which reduces ventilation and blood flow in some regions and increases them in others. Examples are obstructive lung disease and vascular disorders. Shunt is caused by the complete cessation of ventilation in a region, usually as a result of collapse (atelectasis) or consolidation (e.g., pneumonia). Asthma or COPD does not involve the formation of a shunt¹¹⁵; if a shunt is present, it indicates a complication.

Second, supplemental O_2 improves the hypoxemia caused by low \dot{V}_A/\dot{Q} , but it has little effect on hypoxemia caused by shunt. Although aeration may be poor in regions of low \dot{V}_A/\dot{Q} , aeration does exist in these regions, and the concentration of O_2 in these alveoli can be enriched by increasing FiO_2 . In contrast, supplemental O_2 cannot access the alveoli in a true (anatomic) shunt.

Anatomic shunt and low \dot{V}_A/\dot{Q} usually coexist, and the net effect is sometimes referred to as *percent shunt* (per the standard shunt equation). In this situation, the low \dot{V}_A/\dot{Q} component will contribute to the response from increasing FiO_2 , and the regions of anatomic (true) shunt will not; therefore, shunt will always lower PaO_2 (at any FiO_2). When the calculated fraction increases to 25%, the response to increased FiO_2 will be small; when it increases to 30% or greater, the response will be negligible.¹⁴⁹ This varying response is the net effect of mixing blood with normal pulmonary end-capillary PO_2 and shunt blood, which has the same PO_2 as mixed venous blood. If shunt is a large enough fraction of total lung blood flow, the additional O_2 that can be physically dissolved by the raised FiO_2 is so small that it is almost immeasurable; such a shunt is said to be refractory.

RESPIRATORY FUNCTION DURING ONE-LUNG VENTILATION

Oxygenation can be a challenge during one-lung surgery. One lung is not ventilated but is still perfused, and in the postoperative period, restoration of lung integrity and ventilation-perfusion matching can take time.¹⁶³

The technique of one-lung anesthesia and ventilation means that only one lung is ventilated and that the lung provides oxygenation of—and elimination of CO_2 from—the blood. Persisting perfusion through the nonventilated lung causes a shunt and decreases PaO_2 (Fig. 13.27); measures can be taken to reduce this blood flow.^{164,165}

During one-lung anesthesia, there are two main contributors to impaired oxygenation: (1) the persisting blood flow through nonventilated lung and (2) development of atelectasis in the dependent lung, resulting in local shunt and low \dot{V}_A/\dot{Q} .¹³⁸ A recruitment maneuver can identify the influence of the dependent atelectasis;¹⁶⁶ serial increases in peak airway pressure and PEEP directed to the dependent, ventilated lung increased significantly the PaO_2 , indicating that dependent atelectasis was an important cause of hypoxemia. In this situation, diversion of perfusion from the dependent (ventilated) to the nondependent (i.e., non-ventilated) lung would have worsened oxygenation.

Recruitment can also affect V_D . Recruitment during one-lung anesthesia improved oxygenation, but also decreased V_D .¹⁶⁷ The slope of the CO_2 curve during a tidal expiration (phase III) was flatter, indicating a more even distribution of inspired gas throughout the lung and more synchronous alveolar emptying. Thus a secondary effect of recruiting collapsed lung tissue can be (presumably not when recruitment causes overinflation) more even distribution of ventilation and a decrease in the dead space fraction. This effect should facilitate the use of a smaller V_T . In contrast to an individual recruitment, the application of continuous elevated P_{AW} (PEEP titrated to optimal compliance in the ventilated lung) increased compliance by 10% but slightly worsened oxygenation, probably because of redistribution

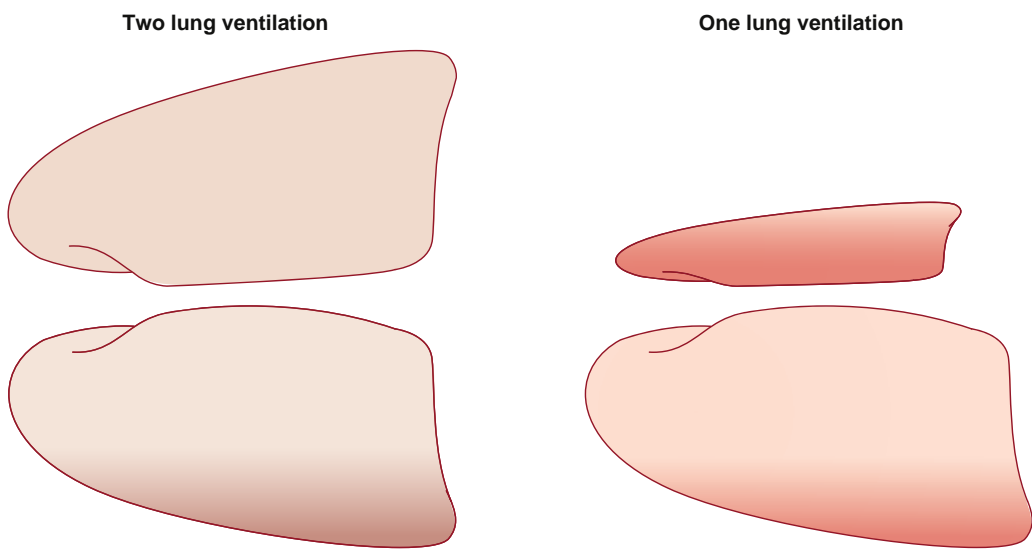


Fig. 13.27 Schematic drawing of the distribution of shunt during two-lung ventilation and one-lung ventilation during anesthesia. Shunt region is indicated by dark area in the lower lung during two-lung ventilation and in the lower lung—plus the entire upper lung—during one-lung ventilation.

of blood from the ventilated to the nonventilated (nondependent) lung.¹⁶⁸ The rationale for identifying and using optimal PEEP has also been reviewed.¹⁶⁹

Maneuvers can also be applied to the nondependent lung. The effects of compressing the nondependent lung on oxygenation were examined using an intraarterial O₂ sensor, which provides instantaneous and continuous PaO₂.¹⁷⁰ Compression resulted in increased PaO₂, suggesting a shift of blood flow from the nondependent (nonventilated) to the dependent (ventilated) lung; development of complete absorption atelectasis in the nondependent lung may have similar effects.¹⁷¹

Inhaled NO (pulmonary vasodilator) and intravenous almitrine (pulmonary vasoconstrictor) have been studied alone and in combination. NO alone has little effect,¹⁷² but oxygenation is improved when NO is combined with almitrine.^{173,174} Almitrine alone also improves oxygenation¹⁷⁵ at a dose that does not alter P_{PA} or cardiac output. Although inhaled NO increases perfusion to already ventilated regions (increasing \dot{V}_A/Q), almitrine potentiates HPV, decreasing perfusion to nonventilated (i.e., shunt) areas (reducing shunt) and potentially diverting blood flow to ventilated regions of the lung. Selective pulmonary vasodilation is reviewed.^{176,177}

Careful analysis of the mechanical obstruction caused by kinking of pulmonary vessels and by HPV has shown that HPV is the important determinant of diversion of blood flow away from nonventilated lung (though not complete).¹⁷⁸ Moreover, positioning of the patient can affect the degree of shunting.¹⁷⁹

PNEUMOPERITONEUM

Laparoscopic operations are usually performed by insufflation of CO₂ into the abdominal cavity. The effects are two-fold. First, the consequences of hypercapnic acidosis^{180,181} include depressed cardiac contractility, sensitization of the myocardium to the arrhythmogenic effects of catecholamines, pulmonary vasoconstriction and systemic vasodilation.¹⁸² There can also be long-lasting postoperative effects

on breathing control.¹⁸³ In addition, the physical effects of pneumoperitoneum are important. These include decreased FRC and VC,¹⁸⁴ formation of atelectasis,¹⁸⁵ reduced respiratory compliance,¹⁸⁶ and increased peak airway pressure.¹⁸⁷ Nonetheless, shunt is reduced and arterial oxygenation is mostly improved during CO₂ pneumoperitoneum.¹⁸⁸ This paradox—more atelectasis and less shunt—suggests that efficient redistribution of blood flow away from collapsed lung regions is attributable to hypercapnic acidosis CO₂ potentiating hypoxic pulmonary vasoconstriction. Indeed, a recent experimental study showed that if the abdomen was inflated with air, a much larger shunt developed than if CO₂ had been used for inflation.¹⁸⁹

Lung Function After Cardiac Surgery

Cardiac surgery produces the greatest degree of atelectasis in the postoperative period,¹⁹⁰ perhaps because both lungs are often collapsed. Spontaneous resolution of the atelectasis is gradual, leaving a residual shunt of up to 30% by day 1 or 2;^{97,191} however, recruitment at the end of the case is possible. In some cases, 30 cm H₂O for 20 seconds is sufficient,⁹⁷ facilitated by the chest being open. A recruitment maneuver (with zero PEEP) causes transient increase in PaO₂ and end-expiratory lung volume (EELV), and with PEEP alone, EELV was increased but PaO₂ unchanged. However, a recruitment maneuver followed by PEEP resulted in a large and sustained increase in both PaO₂ and EELV.¹⁹² The separation of effect whereby PEEP alone increases EELV to a greater extent than it increases oxygenation suggests further opening of an already opened lung rather than opening of atelectatic lung.

Head-to-head comparison of intermittent CPAP versus constant noninvasive pressure support ventilation reported intriguing findings. There was less radiographic evidence of atelectasis following pressure support, without differences in oxygenation of bedside pulmonary function testing.¹⁹³ Although the authors' conclusion was of no clinical benefit

with noninvasive pressure support ventilation, differences in FiO_2 could cause differences in propensity to atelectasis. Recruitment maneuvers up to moderately high levels of airway pressure (46 cm H_2O) do not appear to affect the pulmonary vascular resistance or right ventricular afterload,¹⁹⁴ which is an issue of considerable importance following cardiac surgery. Nonetheless, it is prudent to consider RV loading and ejection in such circumstances, especially in the setting of diminished RV reserve or tricuspid regurgitation. Finally, many cardiac surgeries are now being performed “off pump,” and the postoperative pulmonary effect is reduced, with less postoperative intrapulmonary shunt and correspondingly shorter hospital stays.¹⁹⁵

Protective Ventilation

During the last few years, a concept of “protective ventilation” has appeared, based on three tools of ventilator support: (1) low tidal volume (assumed to reduce stress and strain of the lung), (2) recruitment maneuver (assumed to reopen any collapsed alveoli), and (3) PEEP (assumed to keep a recruited lung open during ongoing anesthesia and surgery).¹⁹⁶ These three tools have been adopted from intensive care, and one may ask whether they are equally useful in the mechanically ventilated, essentially lung healthy, anesthetized patient. As for (1) low tidal volume, a small tidal volume is reasonable, and a volume of 6 to 8 mL/kg/body weight, as is generally suggested, is the same size of what a normal subject is breathing spontaneously when awake. As for (2) recruitment maneuver and (3) PEEP, opening up and keeping the lung open is also reasonable and even important. Both a recruitment maneuver and PEEP will achieve this.

“Protective ventilation” has been claimed to reduce postoperative lung complications, although results vary between studies,^{196,197} and which tool may be the most important remains also to be shown. Moreover, the protective ventilation concept covers the period from induction to emergence from anesthesia, and whether any positive effects remain in the postoperative period is unknown.¹⁹⁸ The atelectasis that develops intraoperatively may last for some days after surgery¹⁹⁹ and may be a cause of postoperative pulmonary complications. Further refinement of ventilatory support strategy may therefore rather be focused on the emergence from anesthesia and the postoperative period.

Postoperative Physiotherapy

Physiotherapy, much debated after surgery,²⁰⁰ is associated with more effective lung recruitment (seen on thoracic CT) when involving deliberate approaches, such as flow bottles following exercise.²⁰¹ In effect, large and early inspiration following surgery may be key to preventing postoperative lung complications. Whether the deep inspiration needs to be accomplished with a specific forced breathing device is uncertain.

Intraoperative Hyperoxia

It has been suggested that ventilation with hyperoxic gas, 80% O_2 , during anesthesia and for a couple of hours

postoperatively will improve wound healing and reduce postoperative complications.²⁰² Based on a larger number of studies, the World Health Organization (WHO) presented guidelines in favor of perioperative hyperoxia.²⁰³ However, the guidelines have met with criticism,²⁰⁴ and large studies that have appeared after the publication of the guidelines do not support the use of hyperoxic gas.^{205,206} Thus the potential advantage of elevating arterial oxygen tension may be offset by cellular responses with the formation of reactive oxygen species.²⁰⁷

Effect of Sleep on Respiration

Sleep has a major effect on many aspects of respiration, perhaps the most obvious being ventilation.²⁰⁸ Sleep reduces V_T and inspiratory drive, and \dot{V}_E falls by approximately 10%, depending on the sleep stage, with the most marked fall occurring during rapid-eye-movement (REM) sleep. Lung volume (i.e., FRC) is also reduced;²⁰⁹ this commences almost immediately after the onset of sleep, and the lowest levels of FRC (down to 10% of resting levels) occur in REM sleep.²¹⁰ CT studies in healthy volunteers demonstrate that the sleep-induced decrease in FRC is accompanied by reduced aeration in the dependent lung.²¹¹ Such loss in aeration was demonstrated in anesthetized patients when their FiO_2 was increased from 0.3 to 1.0; atelectasis developed rapidly. It is possible that during normal sleep, breathing with high levels of O_2 would also cause atelectasis.

 Complete references available online at expertconsult.com.

References

1. von Ungern-Sternberg BS, et al. *Lancet*. 2010;376:773.
2. Cook TM, et al. *Anaesthesia*. 2010;65:556.
3. Cheney FW, et al. *Anesthesiology*. 1991;75:932.
4. Woods BD, Sladen RN. *Br J Anaesth*. 2009;103(suppl 1):i57.
5. Pinsky MR. *Curr Opin Crit Care*. 2007;13:528. 2007.
6. Buhre W, Rossaint R. *Lancet*. 2003;362:1839.
7. Moonesinghe SR, et al. *Anesth Analg*. 2011;112:891.
8. Hennis PJ, et al. *Br J Anaesth*. 2012;109:566.
9. Poeze M, et al. *Intensive Care Med*. 2000;26:1272.
10. Nunn JF: *Nunn's Applied Respiratory Physiology*. 4th ed. London: Butterworth Heinemann; 1993.
11. Cabot JB, et al. *Pediatr Pulmonol*. 2012;47:808.
12. Shamir MY, et al. *Anesth Analg*. 2012;114:972.
13. Hampson NB, et al. *Am J Respir Crit Care Med*. 2012;186:1095.
14. Bohr C, et al. *Arch Physiol*. 1904;16:401.
15. Hanson CW, et al. *Crit Care Med*. 1996;24:23.
16. Jensen FB. *Acta Physiol Scand*. 2004;182:215.
17. Barratt-Boyes BG, Wood EH. *J Lab Clin Med*. 1957;50:93.
18. Chawla LS, Zia H, et al. *Chest*. 2004;126:1891.
19. Quanjer PH, et al. *Eur Respir J Suppl*. 1993;16:5.
20. Astrom E, et al. *Eur Respir J*. 2000;16:659.
21. Broughton SJ, et al. *Physiol Meas*. 2006;27:99.
22. Wilschut FA, et al. *Eur Respir J*. 1999;14:166.
23. Roca J, et al. *Respir Med*. 1998;92:454.
24. Grassino AE, Roussos C. Static properties of the lung and chest wall. In: Crystal RG, West JB, Weibel ER, Barnes PJ, eds. *The Lung: Scientific Foundations*. 2nd ed. Philadelphia: Lippincott-Raven; 1997:1187.
25. Goldin JG. *Radiol Clin North Am*. 2002;40:145.
26. Van Lith P, et al. *J Appl Physiol*. 1967;23:475.
27. Pedley TJ, Kamm RD. Dynamics of gas flow and pressure-flow relationships. In: Crystal RG, West JB, Weibel ER, Barnes PJ, eds. *The Lung: Scientific Foundations*. 2nd ed. Philadelphia, 1997, Lippincott Raven.
28. Slats AM, et al. *Am J Respir Crit Care Med*. 2007;176:121.

29. Holst M, et al. *Intensive Care Med*. 1990;16:384.
30. O'Donnell DE, et al. *Am Rev Respir Dis*. 1987;135:912.
31. Calverley PM, Koulouris NG. *Eur Respir J*. 2005;25:186.
32. Mead J, et al. *J Appl Physiol*. 1967;22:95.
33. Bachofen HJ. *Appl Physiol*. 1968;24:296.
34. Kaczka DW, et al. *J Appl Physiol*. 1997;82:1531.
35. Verbeken EK, et al. *J Appl Physiol*. 1992;72:2343.
36. Bachofen H, Scherrer M. *J Clin Invest*. 1967;46:133.
37. Tantucci C, et al. *Am Rev Respir Dis*. 1992;145:355.
38. Frostell C, et al. *J Appl Physiol*. 1983;55:1854.
39. Milic-Emili J. Ventilation distribution. In: Hammid Q, Shannon J, Martin J, eds. *Physiologic Bases of Respiratory Disease*. BC Decker: Hamilton, Ontario; 2005.
40. Hubmayr RD. *Am J Respir Crit Care Med*. 2002;165:1647.
41. Guy HJ, et al. *J Appl Physiol*. 1994;76:1719.
42. Prisk GK. *J Appl Physiol*. 2000;89:385.
43. Ganesan S, et al. *Respir Physiol*. 1989;78:281.
44. Bryan AC. *Am Rev Respir Dis*. 1974;110:143.
45. Mayo JR, et al. *J Thorac Imaging*. 1995;10:73.
46. Petersson J, et al. *J Appl Physiol*. 2004;96:1127.
47. Bryan AC, et al. *J Appl Physiol*. 1964;19:395.
48. Bache B, et al. *J Appl Physiol*. 1974;37:8.
49. Milic-Emili J, et al. *Eur J Appl Physiol*. 2007;99:567.
50. Teculescu DB, et al. *Lung*. 1996;174(43).
51. Haefeli-Bleuer B, Weibel ER. *Anat Rec*. 1988;220:401.
52. Adaro F, Piiper J. *Respir Physiol*. 1976;26:195.
53. Dawson CA, Linehan JH. Dynamics of blood flow and pressure-flow relationships. In: Crystal RG, West JB, Weibel ER, Barnes PJ, eds. *The Lung: Scientific Foundations*. 2nd ed. Philadelphia: Lippincott-Raven; 1997:1503.
54. Bachofen H, et al. *Am Rev Respir Dis*. 1993;147:997.
55. Jeffery PK. *Proc Am Thorac Soc*. 2004;176.
56. Townsley MI, et al. *Circ Res*. 1995;77:317.
57. Kornecki A, et al. *Anesthesiology*. 2008;108:1047.
58. Hughes JMB. In: Crystal RG, et al., ed. *The Lung: Scientific Foundations*. 2nd ed. Philadelphia: Lippincott-Raven; 1997:1523.
59. West JB, et al. *J Appl Physiol*. 1964;19:713.
60. Hughes JM, et al. *Respir Physiol*. 1968;4:58.
61. Michels DB, West JB. *J Appl Physiol*. 1978;45:987.
62. Verbandt Y, et al. *J Appl Physiol*. 2000;89:2407.
63. Reed JH Jr, Wood EH. *J Appl Physiol*. 1970;28:303.
64. Glenny RW, et al. *J Appl Physiol*. 1991;71:620.
65. Glenny RW, et al. *J Appl Physiol*. 1999;86:623.
66. Hakim TS, et al. *J Appl Physiol*. 1987;63:1114.
67. Hedenstierna G, et al. *J Appl Physiol*. 1979;47:938.
68. Hlastala MP, et al. *J Appl Physiol*. 1996;81:1051.
69. Glenny RW, Robertson HT. *J Appl Physiol*. 1991;70:1024.
70. Glenny R. Counterpoint. *J Appl Physiol*. 2008;104(1533):5–6; discussion.
71. Sylvester JT, et al. *Physiol Rev*. 2012;92:367.
72. Marshall BE, et al. *Intensive Care Med*. 1994;20:379.
73. Moudgil R, et al. *J Appl Physiol*. 2005;98:390.
74. Kerbaul F, et al. *Br J Anaesth*. 2000;85:440.
75. Kerbaul F, et al. *Can J Anaesth*. 2001;48:760.
76. Hambraeus-Jonzon K, et al. *Anesthesiology*. 1997;86:308.
77. Sartori C, et al. *Respir Physiol Neurobiol*. 2007;159:338.
78. Pellegrino R, et al. *Eur Respir J*. 1997;10:468.
79. Leith DE, Mead J. *J Appl Physiol*. 1967;23:221.
80. Hughes JM, Bates DV. *Respir Physiol Neurobiol*. 2003;138:115.
81. Aguilaniu B, et al. *Eur Respir J*. 2008;31:1091.
82. West JB. *Respiratory Physiology—The Essentials*. Baltimore: Williams & Wilkins; 1990.
83. Hedenstierna G. *Thorax*. 1995;50:85.
84. Moller JT, et al. *Lancet*. 1998;351:857.
85. Kroenke K, et al. *Chest*. 1993;104:1445.
86. Wahba RW. *Can J Anaesth*. 1991;38:384.
87. Rothen HU, et al. *Br J Anaesth*. 1998;81:681.
88. Westbrook PR, et al. *J Appl Physiol*. 1973;34:81.
89. Hedenstierna G, Edmark L. *Intensive Care Med*. 2005;31:1327.
90. Froese AB, Bryan AC. *Anesthesiology*. 1974;41:242.
91. Reber A, et al. *Anesthesia*. 1998;53:1054.
92. Warner DO, et al. *Anesthesiology*. 1996;85:49.
93. Don H. *Int Anesthesiol Clin*. 1977;15:113.
94. Bendixen HH, et al. *N Engl J Med*. 1963;269:991.
95. Duggan M, Kavanagh BP. *Anesthesiology*. 2005;102:838.
96. Gunnarsson L, et al. *Br J Anaesth*. 1991;66:423.
97. Tenling A, et al. *Anesthesiology*. 1998;89:371.
98. Lindberg P, et al. *Acta Anaesthesiol Scand*. 1992;36:546.
99. Tokics L, et al. *J Appl Physiol*. 1996;81:1822.
100. van Kaam AH, et al. *Am J Respir Crit Care Med*. 2004;169:1046.
101. Gunnarsson L, et al. *Eur Respir J*. 1991;4:1106.
102. Musch G, et al. *Anesthesiology*. 2004;100:323.
103. Hewlett AM, et al. *Br J Anaesth*. 1974;46:495.
104. Ostberg E, et al. *Anesthesiology*. 2018.
105. Rothen HU, et al. *Br J Anaesth*. 1993;71:788.
106. Rothen HU, et al. *Br J Anaesth*. 1999;82:551.
107. Rothen HU, et al. *Anesthesiology*. 1995;82:832.
108. Rothen HU, et al. *Lancet*. 1995;345:1387.
109. Edmark L, et al. *Anesthesiology*. 2003;98:28.
110. Rusca M, et al. *Anesth Analg*. 2003;97:1835.
111. Hedenstierna G, et al. *Anesthesiology*. 1994;80:751.
112. Benoit Z, et al. *Anesth Analg*. 2002;95:1777–1781.
113. Sinha PK, et al. *J Cardiothorac Vasc Anesth*. 2006;20:136.
114. Squadone V, et al. *JAMA*. 2005;293:589.
115. Agusti AG, Barbera JA. *Thorax*. 1994;49:924.
116. Hedenstierna G. *Clin Physiol Funct Imaging*. 2003;23:123.
117. Dueck R, et al. *Anesthesiology*. 1988;69:854.
118. Hedenstierna G, et al. *Anesthesiology*. 1984;61:369.
119. Hulands GH, et al. *Clin Sci*. 1970;38:451.
120. Marshall BE. *Effects of Anesthetics on Gas Exchange*. London: Kluwer Academic; 1989.
121. Marshall BE. *Acta Anaesthesiol Scand*. 1990;94(suppl):37.
122. Pelosi P, et al. *Anesthesiology*. 1999;91:1221.
123. Coussa M, et al. *Anesth Analg*. 2004;98:1491; table of contents.
124. Walley KR. *Am J Respir Crit Care Med*. 2011;184:514.
125. Dantzker DR, et al. *J Physiol*. 1974;242:72P.
126. Sakai EM, et al. *Pharmacotherapy*. 2005;25:1773.
127. von Ungern-Sternberg BS, et al. *Br J Anaesth*. 2007;98:503.
128. Ide T, et al. *Anesthesiology*. 1999;90:1084.
129. Sasani N, et al. *Anesthesiology*. 2013;118:961.
130. Morton CP, Drummond GB. *Br J Anaesth*. 1994;73:135.
131. Warner DO, Warner MA. *Anesthesiology*. 1995;82:20–31.
132. Warner DO, et al. *J Appl Physiol*. 1994;76:2802.
133. Strandberg A, et al. *Acta Anaesthesiol Scand*. 1986;30:154.
134. Dueck R, et al. *Anesthesiology*. 1984;61:55.
135. Anjou-Lindskog E, et al. *Anesthesiology*. 1985;62:485.
136. Heneghan CP, et al. *Br J Anaesth*. 1984;56:437.
137. Klingstedt C, et al. *Acta Anaesthesiol Scand*. 1990;34:315.
138. Klingstedt C, et al. *Acta Anaesthesiol Scand*. 1990;34:421.
139. Landmark SJ, et al. *J Appl Physiol*. 1977;43:993.
140. Mure M, et al. *Am J Respir Crit Care Med*. 1998;157:1785.
141. Nyren S, et al. *Anesthesiology*. 2010;112:682.
142. Yoshino J, et al. *Acta Anaesthesiol Scand*. 2003;47:742.
143. Brooks-Brunn JA. *Chest*. 1997;111:564.
144. Pelosi P, et al. *Anesth Analg*. 1998;87:654.
145. Eichenberger A, et al. *Anesth Analg*. 2002;95:1788; table of contents.
146. Cressey DM, et al. *Anesthesia*. 2001;56:680.
147. Gander S, et al. *Anesth Analg*. 2005;100:580.
148. Berthoud MC, et al. *Br J Anaesth*. 1991;67:464.
149. Melot C. *Thorax*. 1994;49:1251.
150. Reinius H, et al. *Anesthesiology*. 2009;111:979.
151. Mynster T, et al. *Anesthesia*. 1996;51:225.
152. Warner DO, et al. *Anesthesiology*. 1996;85:761.
153. Yamakage M, et al. *Acta Anaesthesiol Scand*. 1992;36:569.
154. McCarthy GS. *Br J Anaesth*. 1976;48:243.
155. Roca J, Wagner PD. *Thorax*. 1994;49:1027.
156. Rodriguez-Roisin R, Roca J. *Thorax*. 1994;49:1027.
157. Agusti AG, et al. *Am Rev Respir Dis*. 1991;143:219.
158. Manier G, Castaing Y. *Thorax*. 1994;49:1169.
159. Santolicandro A, et al. *Am J Respir Crit Care Med*. 1995;152:336.
160. Altemeier WA, et al. *J Appl Physiol*. 1998;85:2337.
161. Light RB. *Semin Respir Infect*. 1999;14:218.
162. Light RB. *Am Rev Respir Dis*. 1986;134:520.
163. Benumof JL. *Anesth Analg*. 1985;64:821.
164. Karzai W, Schwarzkopf K. *Anesthesiology*. 2009;110:1402.
165. Hedenstierna G, Reber A. *Acta Anaesthesiol Scand*. 1996;40:2.
166. Tusman G, et al. *Ann Thorac Surg*. 2002;73:1204.
167. Tusman G, et al. *Analg*. 2004;98:1604; table of contents.
168. Mascotto G, et al. *Eur J Anaesthesiol*. 2003;20:704.
169. Slinger PD, et al. *Anesthesiology*. 2001;95:1096.
170. Ishikawa S, et al. *Br J Anaesth*. 2003;90:21.

171. Pfitzer J. *Br J Anaesth*. 2003;91:153; author reply -4.
172. Schwarzkopf K, et al. *Anesth Analg*. 2001;92:842.
173. Moutafis M, et al. *Anesth Analg*. 1997;85:1130.
174. Silva-Costa-Gomes T, et al. *Br J Anaesth*. 2005;95:410.
175. Moutafis M, et al. *Anesth Analg*. 2002;94:830; table of contents.
176. Dembinski R, et al. *Minerva Anestesiol*. 2004;70:239.
177. Schilling T, et al. *Anesth Analg*. 2005;101:957; table of contents.
178. Friedlander M, et al. *Can J Anaesth*. 1994;41:26.
179. Choi YS, et al. *J Thorac Cardiovasc Surg*. 2007;134:613.
180. McMahon AJ, et al. *Lancet*. 2000;356:1632.
181. Neudecker J, et al. *Surg Endosc*. 2002;16:1121.
182. Gutt CN, et al. *Dig Surg*. 2004;21:95.
183. Bablekos GD, et al. *Arch Surg*. 2006;141:16.
184. Hirvonen EA, et al. *Anesth Analg*. 1995;80:961.
185. Andersson LE, et al. *Anesthesiology*. 2005;102:293.
186. Makinen MT, et al. *Can J Anaesth*. 1998;45:865.
187. Sharma KC, et al. *Chest*. 1996;110:810.
188. Andersson L, et al. *Acta Anaesthesiol Scand*. 2002;46:552.
189. Strang CM, et al. *Minerva Anestesiol*. 2013;79(6):617.
190. Hachenberg T, et al. *Acta Anaesthesiol Scand*. 1992;36:800.
191. Hachenberg T, et al. *Anesthesiology*. 1997;86:809.
192. Dyhr T, et al. *Acta Anaesthesiol Scand*. 2004;48:187.
193. Pasquina P, et al. *Anesth Analg*. 2004;99:1001; table of contents.
194. Reis Miranda D, et al. *Br J Anaesth*. 2004;93:327.
195. Tschermsko EM, et al. *J Thorac Cardiovasc Surg*. 2002;124:732.
196. Futier E, et al. *N Engl J Med*. 2013;369(5):428.
197. Las Vegas investigators. *Eur J Anaesthesiol*. 2017;34(8):492.
198. Hedenstierna G. *Anesthesiology*. 2015;123(3):501.
199. Lindberg P, et al. *Acta Anaesthesiol Scand*. 1992;36(6):546.
200. Pasquina P, et al. *BMJ*. 2003;327:1379.
201. Westerdahl E, et al. *Chest*. 2005;128:3482.
202. Greif R, et al. *N Engl J Med*. 2000;342(3):161.
203. Allegranzi B, et al. *Lancet Infect Dis*. 2016;16(12):e288.
204. Hedenstierna G, et al. *Anesthesiology*. 2017;126(5):771.
205. Staehr-Rye AK, et al. *Br J Anaesth*. 2017;119(1):140.
206. Kurz A, et al. *Br J Anaesth*. 2015;115(3):434.
207. Turrens JF. *J Physiol*. 2003;552(Pt 2):335.
208. Douglas NJ, et al. *Thorax*. 1982;37:840.
209. Hudgel DW, Devadatta P. *J Appl Physiol*. 1984;57:1319.
210. Ballard RD, et al. *J Appl Physiol*. 1990;68:2034.
211. Appelberg J, et al. *Chest*. 2007;131:122.

References

1. von Ungern-Sternberg BS, et al. Risk assessment for respiratory complications in paediatric anaesthesia: a prospective cohort study. *Lancet*. 2010;376:773–783.
2. Cook TM, Scott S, Mihai R. Litigation related to airway and respiratory complications of anaesthesia: an analysis of claims against the NHS in England 1995–2007. *Anaesthesia*. 2010;65:556.
3. Cheney FW, Posner KL, Caplan RA. Adverse respiratory events infrequently leading to malpractice suits. A closed claims analysis. *Anesthesiology*. 1991;75:932.
4. Woods BD, Sladen RN. Perioperative considerations for the patient with asthma and bronchospasm. *Br J Anaesth*. 2009;103(suppl 1):i57.
5. Pinsky MR. Heart-lung interactions. *Curr Opin Crit Care*. 2007; 13:528.
6. Buhre W, Rossaint R. Perioperative management and monitoring in anaesthesia. *Lancet*. 2003;362:1839.
7. Moonesinghe SR, Mythen MG, Grocott MP. High-risk surgery: epidemiology and outcomes. *Anesth Analg*. 2011;112:891.
8. Hennis PJ, et al. Cardiopulmonary exercise testing predicts postoperative outcome in patients undergoing gastric bypass surgery. *Br J Anaesth*. 2012;109:566.
9. Poeze M, et al. Pre-operative tonometry is predictive for mortality and morbidity in high-risk surgical patients. *Intensive Care Med*. 2000;26:1272.
10. Nunn JF. *Nunn's Applied Respiratory Physiology*. 4th ed. London: Butterworth Heinemann; 1993.
11. Caboot JB, et al. Non-invasive measurements of carboxyhemoglobin and methemoglobin in children with sickle cell disease. *Pediatr Pulmonol*. 2012;47:808.
12. Shamir MY, Avramovich A, Smaka T. The current status of continuous noninvasive measurement of total, carboxy, and methemoglobin concentration. *Anesth Analg*. 2012;114:972.
13. Hampson NB, et al. Practice recommendations in the diagnosis, management, and prevention of carbon monoxide poisoning. *Am J Respir Crit Care Med*. 2012;186:1095.
14. Bohr C, Hasselbach K, Krogh A. Über einen in biologischer Beziehung wichtigen Einfluss, den die Kohlensäurespannung des Blutes auf dessen Sauerstoffbindung übt. *Arch Physiol*. 1904;16:401.
15. Hanson CW 3rd, Marshall BE, Frasch HF, Marshall C. Causes of hypercarbia with oxygen therapy in patients with chronic obstructive pulmonary disease. *Crit Care Med*. 1996;24:23.
16. Jensen FB. Red blood cell pH, the Bohr effect, and other oxygenation-linked phenomena in blood O₂ and CO₂ transport. *Acta Physiol Scand*. 2004;182:215.
17. Barratt-Boyes BG, Wood EH. The oxygen saturation of blood in the venae cavae, right-heart chambers, and pulmonary vessels of healthy subjects. *J Lab Clin Med*. 1957;50:93.
18. Chawla LS, et al. Lack of equivalence between central and mixed venous oxygen saturation. *Chest*. 2004;126:1891.
19. Quanjer PH, et al. Lung volumes and forced ventilatory flows. Report working party standardization of lung function tests, European community for steel and coal. Official Statement of the European Respiratory Society. *Eur Respir J Suppl*. 1993;16:5.
20. Astrom E, et al. Partitioning of dead space—a method and reference values in the awake human. *Eur Respir J*. 2000;16:659.
21. Broughton SJ, et al. Problems in the measurement of functional residual capacity. *Physiol Meas*. 2006;27:99.
22. Wilschut FA, et al. Intrapulmonary gas mixing and the sloping alveolar plateau in COPD patients with macroscopic emphysema. *Eur Respir J*. 1999;14:166.
23. Roca J, et al. Prediction equations for plethysmographic lung volumes. *Respir Med*. 1998;92:454.
24. Grassino AE, Roussos C. Static properties of the lung and chest wall. In: Crystal RG, West JB, Weibel ER, Barnes PJ, eds. *The Lung: Scientific Foundations*. 2nd ed. Philadelphia: Lippincott-Raven; 1997:1187.
25. Goldin JG. Quantitative CT of the lung. *Radiol Clin North Am*. 2002;40:145.
26. Van Lith P, Johnson FN, Sharp JT. Respiratory elastances in relaxed and paralyzed states in normal and abnormal men. *J Appl Physiol*. 1967;23:475.
27. Pedley TJ, Kamm RD. Dynamics of gas flow and pressure-flow relationships. In: Crystal RG, West JB, Weibel ER, Barnes PJ, eds. *The Lung: Scientific Foundations*. 2nd ed. Philadelphia: Lippincott-Raven; 1997:1365.
28. Slats AM, et al. Bronchial inflammation and airway responses to deep inspiration in asthma and chronic obstructive pulmonary disease. *Am J Respir Crit Care Med*. 2007;176:121.
29. Holst M, Striem J, Hedenstierna G. Errors in tracheal pressure recording in patients with a tracheostomy tube—a model study. *Intensive Care Med*. 1990;16:384.
30. O'Donnell DE, et al. Effect of dynamic airway compression on breathing pattern and respiratory sensation in severe chronic obstructive pulmonary disease. *Am Rev Respir Dis*. 1987;135:912.
31. Calverley PM, Koulouris NG. Flow limitation and dynamic hyperinflation: key concepts in modern respiratory physiology. *Eur Respir J*. 2005;25:186.
32. Mead J, et al. Significance of the relationship between lung recoil and maximum expiratory flow. *J Appl Physiol*. 1967;22:95.
33. Bachofen H. Lung tissue resistance and pulmonary hysteresis. *Appl Physiol*. 1968;24:296.
34. Kaczka DW, et al. Partitioning airway and lung tissue resistances in humans: effects of bronchoconstriction. *J Appl Physiol*. 1997;82:1531.
35. Verbeken EK, et al. Tissue and airway impedance of excised normal, senile, and emphysematous lungs. *J Appl Physiol*. 1992;72:2343.
36. Bachofen H, Scherrer M. Lung tissue resistance in diffuse interstitial pulmonary fibrosis. *J Clin Invest*. 1967;46:133.
37. Tantucci C, et al. Flow and volume dependence of respiratory system flow resistance in patients with adult respiratory distress syndrome. *Am Rev Respir Dis*. 1992;145:355.
38. Frostell C, Pande JN, Hedenstierna G. Effects of high-frequency breathing on pulmonary ventilation and gas exchange. *J Appl Physiol*. 1983;55:1854.
39. Milic-Emili J. Ventilation distribution. In: Hammid Q, Shannon J, Martin J, eds. *Physiologic Bases of Respiratory Disease*. BC Decker: Hamilton, Ontario; 2005.
40. Hubmayr RD. Perspective on lung injury and recruitment: a skeptical look at the opening and collapse story. *Am J Respir Crit Care Med*. 2002;165:1647.
41. Guy HJ, et al. Inhomogeneity of pulmonary ventilation during sustained microgravity as determined by single-breath washouts. *J Appl Physiol*. 1994;76:1719.
42. Prisk GK. Microgravity and the lung. *J Appl Physiol*. 2000;89:385.
43. Ganesan S, Lai-Fook SJ, Schurch S. Alveolar liquid pressures in nonedematous and kerosene-washed rabbit lung by micropuncture. *Respir Physiol*. 1989;78:281.
44. Bryan AC. Conference on the scientific basis of respiratory therapy. Pulmonary physiotherapy in the pediatric age group. Comments of a devil's advocate. *Am Rev Respir Dis*. 1974;110:143.
45. Mayo JR, et al. Measurement of lung water content and pleural pressure gradient with magnetic resonance imaging. *J Thorac Imaging*. 1995;10:73.
46. Petersson J, et al. Physiological evaluation of a new quantitative SPECT method measuring regional ventilation and perfusion. *J Appl Physiol*. 2004;96:1127.
47. Bryan AC, et al. Factors affecting regional distribution of ventilation and perfusion in the lung. *J Appl Physiol*. 1964;19:395.
48. Bate B, et al. Effect of inspiratory flow rate on regional distribution of inspired gas. *J Appl Physiol*. 1974;37:8.
49. Milic-Emili J, Torchio R, D'Angelo E. Closing volume: a reappraisal (1967–2007). *Eur J Appl Physiol*. 2007;99:567.
50. Teculescu DB, et al. Computerized single-breath nitrogen washout: predicted values in a rural French community. *Lung*. 1996;174:43–55.
51. Haefeli-Bleuer B, Weibel ER. Morphometry of the human pulmonary acinus. *Anat Rec*. 1988;220:401.
52. Adaro F, Piiper J. Limiting role of stratification in alveolar exchange of oxygen. *Respir Physiol*. 1976;26:195.
53. Dawson CA, Linehan JH. Dynamics of blood flow and pressure-flow relationships. In: Crystal RG, West JB, Weibel ER, Barnes PJ, eds. *The Lung: Scientific Foundations*. 2nd ed. Philadelphia: Lippincott-Raven; 1997:1503.
54. Bachofen H, Schurch S, Weibel ER. Experimental hydrostatic pulmonary edema in rabbit lungs. Barrier lesions. *Am Rev Respir Dis*. 1993;147:997.
55. Jeffery PK. Remodeling and inflammation of bronchi in asthma and chronic obstructive pulmonary disease. *Proc Am Thorac Soc*. 2004;176.
56. Townsley MI, et al. Pulmonary microvascular permeability. Responses to high vascular pressure after induction of pacing-induced heart failure in dogs. *Circ Res*. 1995;77:317.

57. Kornecki A, et al. Vascular remodeling protects against ventilator-induced lung injury in the in vivo rat. *Anesthesiology*. 2008;108:1047.
58. Hughes JMB. In: Crystal RG, et al., ed. *The Lung: Scientific Foundations*. 2nd ed. Philadelphia: Lippincott-Raven; 1997:1523.
59. West JB, Dollery CT, Naimark A. Distribution of blood flow in isolated lung: relation to vascular and alveolar pressures. *J Appl Physiol*. 1964;19:713.
60. Hughes JM, et al. Effect of lung volume on the distribution of pulmonary blood flow in man. *Respir Physiol*. 1968;4:58.
61. Michels DB, West JB. Distribution of pulmonary ventilation and perfusion during short periods of weightlessness. *J Appl Physiol*. 1978;45:987.
62. Verbandt Y, et al. Ventilation-perfusion matching in long-term microgravity. *J Appl Physiol*. 2000;89:2407.
63. Reed JH Jr, Wood EH. Effect of body position on vertical distribution of pulmonary blood flow. *J Appl Physiol*. 1970;28:303.
64. Glenny RW, et al. Gravity is a minor determinant of pulmonary blood flow distribution. *J Appl Physiol*. 1991;71:620.
65. Glenny RW, et al. Gravity is an important but secondary determinant of regional pulmonary blood flow in upright primates. *J Appl Physiol*. 1999;86:623.
66. Hakim TS, Lisbona R, Dean GW. Gravity-independent inequality in pulmonary blood flow in humans. *J Appl Physiol*. 1987;63:1114.
67. Hedenstierna G, White FC, Wagner PD. Spatial distribution of pulmonary blood flow in the dog with PEEP ventilation. *J Appl Physiol*. 1979;47:938.
68. Hlastala MP, et al. Pulmonary blood flow distribution in standing horses is not dominated by gravity. *J Appl Physiol*. 1996;81:1051.
69. Glenny RW, Robertson HT. Fractal modeling of pulmonary blood flow heterogeneity. *J Appl Physiol*. 1991;70:1024.
70. Glenny R. Counterpoint: gravity is not the major factor determining the distribution of blood flow in the healthy human lung. *J Appl Physiol*. 2008;104(1533):5–6; discussion.
71. Sylvester JT, et al. Hypoxic pulmonary vasoconstriction. *Physiol Rev*. 2012;92:367.
72. Marshall BE, et al. Role of hypoxic pulmonary vasoconstriction in pulmonary gas exchange and blood flow distribution. 2. Pathophysiology. *Intensive Care Med*. 1994;2:379.
73. Moudgil R, Michelakis ED, Archer SL. Hypoxic pulmonary vasoconstriction. *J Appl Physiol*. 2005;98:390.
74. Kerbaul F, et al. Effects of sevoflurane on hypoxic pulmonary vasoconstriction in anaesthetized piglets. *Br J Anaesth*. 2000;85:440.
75. Kerbaul F, et al. Sub-MAC concentrations of desflurane do not inhibit hypoxic pulmonary vasoconstriction in anaesthetized piglets. *Can J Anaesth*. 2001;48:760.
76. Hambræus-Jonzon K, et al. Hypoxic pulmonary vasoconstriction in human lungs. A stimulus-response study. *Anesthesiology*. 1997;86:308.
77. Sartori C, Allemann Y, Scherzer U. Pathogenesis of pulmonary edema: learning from high-altitude pulmonary edema. *Respir Physiol Neurobiol*. 2007;159:338.
78. Pellegrino R, Brusasco V. On the causes of lung hyperinflation during bronchoconstriction. *Eur Respir J*. 1997;10:468.
79. Leith DE, Mead J. Mechanisms determining residual volume of the lungs in normal subjects. *J Appl Physiol*. 1967;23:221.
80. Hughes JM, Bates DV. Historical review: the carbon monoxide diffusing capacity (DLCO) and its membrane (DM) and red cell (Theta.Vc) components. *Respir Physiol Neurobiol*. 2003;138:115.
81. Aguilaniu B, et al. European reference equations for CO and NO lung transfer. *Eur Respir J*. 2008;31:1091.
82. West JB. *Respiratory Physiology—The Essentials*. Baltimore: Williams & Watkins; 1990.
83. Hedenstierna G. Contribution of multiple inert gas elimination technique to pulmonary medicine. 6. Ventilation-perfusion relationships during anaesthesia. *Thorax*. 1995;50:85.
84. Moller JT, et al. Long-term postoperative cognitive dysfunction in the elderly ISPOCD1 study. ISPOCD investigators. International Study of Post-Operative Cognitive Dysfunction. *Lancet*. 1998;351:857.
85. Kroenke K, et al. Postoperative complications after thoracic and major abdominal surgery in patients with and without obstructive lung disease. *Chest*. 1993;104:1445.
86. Wahba RW. Perioperative functional residual capacity. *Can J Anaesth*. 1991;38:384.
87. Rothen HU, et al. Airway closure, atelectasis and gas exchange during general anaesthesia. *Br J Anaesth*. 1998;81:681.
88. Westbrook PR, et al. Effects of anaesthesia and muscle paralysis on respiratory mechanics in normal man. *J Appl Physiol*. 1973;34:81.
89. Hedenstierna G, Edmark L. The effects of anaesthesia and muscle paralysis on the respiratory system. *Intensive Care Med*. 2005;31:1327.
90. Froese AB, Bryan AC. Effects of anaesthesia and paralysis on diaphragmatic mechanics in man. *Anesthesiology*. 1974;41:242.
91. Reber A, Nylander U, Hedenstierna G. Position and shape of the diaphragm: implications for atelectasis formation. *Anesthesia*. 1998;53:1054.
92. Warner DO, Warner MA, Ritman EL. Atelectasis and chest wall shape during halothane anaesthesia. *Anesthesiology*. 1996;85:49.
93. Don H. The mechanical properties of the respiratory system during anaesthesia. *Int Anesthesiol Clin*. 1977;15:113.
94. Bendixen HH, Hedley-Whyte J, Laver MB. Impaired oxygenation in surgical patients during general anaesthesia with controlled ventilation. A concept of atelectasis. *N Engl J Med*. 1963;269:991.
95. Duggan M, Kavanagh BP. Pulmonary atelectasis: a pathogenic perioperative entity. *Anesthesiology*. 2005;102:838.
96. Gunnarsson L, et al. Influence of age on atelectasis formation and gas exchange impairment during general anaesthesia. *Br J Anaesth*. 1991;66:423.
97. Tenling A, et al. Atelectasis and gas exchange after cardiac surgery. *Anesthesiology*. 1998;89:371.
98. Lindberg P, et al. Atelectasis and lung function in the postoperative period. *Acta Anaesthesiol Scand*. 1992;36:546.
99. Tokics L, et al. V/Q distribution and correlation to atelectasis in anaesthetized paralyzed humans. *J Appl Physiol*. 1996;81:1822.
100. van Kaam AH, et al. Reducing atelectasis attenuates bacterial growth and translocation in experimental pneumonia. *Am J Respir Crit Care Med*. 2004;169:1046.
101. Gunnarsson L, et al. Chronic obstructive pulmonary disease and anaesthesia: formation of atelectasis and gas exchange impairment. *Eur Respir J*. 1991;4:1106.
102. Musch G, et al. Mechanism by which a sustained inflation can worsen oxygenation in acute lung injury. *Anesthesiology*. 2004;100:323.
103. Hewlett AM, et al. Functional residual capacity during anaesthesia III: artificial ventilation. *Br J Anaesth*. 1974;46:495.
104. Ostberg E, Thorisson A, Enlund M, Zetterstrom H, Hedenstierna G, Edmark L. Positive end-expiratory pressure alone minimizes atelectasis formation in nonabdominal surgery: a randomized controlled trial. *Anesthesiology*. 2018.
105. Rothen HU, et al. Re-expansion of atelectasis during general anaesthesia: a computed tomography study. *Br J Anaesth*. 1993;71:788.
106. Rothen HU, et al. Dynamics of re-expansion of atelectasis during general anaesthesia. *Br J Anaesth*. 1999;82:551–556.
107. Rothen HU, et al. Influence of gas composition on recurrence of atelectasis after a reexpansion maneuver during general anaesthesia. *Anesthesiology*. 1995;82:832–842.
108. Rothen HU, et al. Prevention of atelectasis during general anaesthesia. *Lancet*. 1995;345:1387–1391.
109. Edmark L, et al. Optimal oxygen concentration during induction of general anaesthesia. *Anesthesiology*. 2003;98:28–33.
110. Rusca M, et al. Prevention of atelectasis formation during induction of general anaesthesia. *Anesth Analg*. 2003;97:1835–1839.
111. Hedenstierna G, et al. Phrenic nerve stimulation during halothane anaesthesia. Effects of atelectasis. *Anesthesiology*. 1994;80:751–760.
112. Benoit Z, et al. The effect of increased F_{IO_2} before tracheal extubation on postoperative atelectasis. *Anesth Analg*. 2002;95:1777–1781.
113. Sinha PK, et al. Effect of lung ventilation with 50% oxygen in air or nitrous oxide versus 100% oxygen on oxygenation index after cardiopulmonary bypass. *J Cardiothorac Vasc Anesth*. 2006;20:136–142.
114. Squadrone V, et al. Continuous positive airway pressure for treatment of postoperative hypoxemia: a randomized controlled trial. *JAMA*. 2005;293:589–595.
115. Agusti AG, Barbera JA. Contribution of multiple inert gas elimination technique to pulmonary medicine. 2. Chronic pulmonary diseases: chronic obstructive pulmonary disease and idiopathic pulmonary fibrosis. *Thorax*. 1994;49:924–932.
116. Hedenstierna G. Alveolar collapse and closure of airways: regular effects of anaesthesia. *Clin Physiol Funct Imaging*. 2003;23:123–129.

117. Dueck R, et al. The lung volume at which shunting occurs with inhalation anesthesia. *Anesthesiology*. 1988;69:854–861.
118. Hedenstierna G, et al. Ventilation and perfusion of each lung during differential ventilation with selective PEEP. *Anesthesiology*. 1984;61:369–376.
119. Hulands GH, et al. Influence of anaesthesia on the regional distribution of perfusion and ventilation in the lung. *Clin Sci*. 1970;38:451–460.
120. Marshall BE. *Effects of Anesthetics on Gas Exchange*. London: Kluwer Academic; 1989.
121. Marshall BE. Hypoxic pulmonary vasoconstriction. *Acta Anaesthesiol Scand*. 1990;94(suppl):37–41.
122. Pelosi P, et al. Positive end-expiratory pressure improves respiratory function in obese but not in normal subjects during anesthesia and paralysis. *Anesthesiology*. 1999;91:1221–1231.
123. Coussa M, et al. Prevention of atelectasis formation during the induction of general anesthesia in morbidly obese patients. *Anesth Analg*. 2004;98:1491–1495; table of contents.
124. Walley KR. Use of central venous oxygen saturation to guide therapy. *Am J Respir Crit Care Med*. 2011;184:514–520.
125. Dantzker DR, Wagner PD, West JB. Proceedings: instability of poorly ventilated lung units during oxygen breathing. *J Physiol*. 1974;242:72P.
126. Sakai EM, Connolly LA, Klauck JA. Inhalation anesthesiology and volatile liquid anesthetics: focus on isoflurane, desflurane, and sevoflurane. *Pharmacotherapy*. 2005;25:1773–1788.
127. von Ungern-Sternberg BS, et al. Impact of depth of propofol anesthesia on functional residual capacity and ventilation distribution in healthy preschool children. *Br J Anaesth*. 2007;98:503–508.
128. Ide T, et al. Contribution of peripheral chemoreception to the depression of the hypoxic ventilatory response during halothane anesthesia in cats. *Anesthesiology*. 1999;90:1084–1091.
129. Sasaki N, Meyer MJ, Eikermann M. Postoperative respiratory muscle dysfunction: pathophysiology and preventive strategies. *Anesthesiology*. 2013;118:961–978.
130. Morton CP, Drummond GB. Change in chest wall dimensions on induction of anaesthesia: a reappraisal. *Br J Anaesth*. 1994;73:135–139.
131. Warner DO, Warner MA. Human chest wall function while awake and during halothane anesthesia. II. Carbon dioxide rebreathing. *Anesthesiology*. 1995;82:20–31.
132. Warner DO, Joyner MJ, Ritman EL. Anesthesia and chest wall function in dogs. *J Appl Physiol*. 1994;76:2802–2813.
133. Strandberg A, et al. Atelectasis during anaesthesia and in the postoperative period. *Acta Anaesthesiol Scand*. 1986;30:154–158.
134. Dueck R, Rathbun M, Greenburg AG. Lung volume and VA/Q distribution response to intravenous versus inhalation anesthesia in sheep. *Anesthesiology*. 1984;61:55–65.
135. Anjou-Lindskog E, et al. Effects of intravenous anesthesia on VA/Q distribution: a study performed during ventilation with air and with 50% oxygen, supine and in the lateral position. *Anesthesiology*. 1985;62:485–492.
136. Heneghan CP, Bergman NA, Jones JG. Changes in lung volume and (PAO₂–PaO₂) during anaesthesia. *Br J Anaesth*. 1984;56:437–445.
137. Klingstedt C, et al. The influence of body position and differential ventilation on lung dimensions and atelectasis formation in anaesthetized man. *Acta Anaesthesiol Scand*. 1990;34:315–322.
138. Klingstedt C, Hedenstierna G, Baehrendtz S, et al. Ventilation-perfusion relationships and atelectasis formation in the supine and lateral positions during conventional mechanical and differential ventilation. *Acta Anaesthesiol Scand*. 1990;34:421–429.
139. Landmark SJ, et al. Regional pulmonary perfusion and V/Q in awake and anesthetized-paralyzed man. *J Appl Physiol*. 1977;43:993–1000.
140. Mure M, et al. Pulmonary gas exchange improves in the prone position with abdominal distension. *Am J Respir Crit Care Med*. 1998;157:1785–1790.
141. Nyren S, et al. Lung ventilation and perfusion in prone and supine postures with reference to anesthetized and mechanically ventilated healthy volunteers. *Anesthesiology*. 2010;112:682–687.
142. Yoshino J, Akata T, Takahashi S. Intraoperative changes in arterial oxygenation during volume-controlled mechanical ventilation in modestly obese patients undergoing laparotomies with general anesthesia. *Acta Anaesthesiol Scand*. 2003;47:742–750.
143. Brooks-Brunn JA. Predictors of postoperative pulmonary complications following abdominal surgery. *Chest*. 1997;111:564–571.
144. Pelosi P, et al. The effects of body mass on lung volumes, respiratory mechanics, and gas exchange during general anesthesia. *Anesth Analg*. 1998;87:654–660.
145. Eichenberger A, et al. Morbid obesity and postoperative pulmonary atelectasis: an underestimated problem. *Anesth Analg*. 2002;95:1788–1792; table of contents.
146. Cressey DM, Berthoud MC, Reilly CS. Effectiveness of continuous positive airway pressure to enhance pre-oxygenation in morbidly obese women. *Anesthesia*. 2001;56:680–684.
147. Gander S, et al. Positive end-expiratory pressure during induction of general anesthesia increases duration of nonhypoxic apnea in morbidly obese patients. *Anesth Analg*. 2005;100:580–584.
148. Berthoud MC, Peacock JE, Reilly CS. Effectiveness of preoxygenation in morbidly obese patients. *Br J Anaesth*. 1991;67:464–466.
149. Melot C. Contribution of multiple inert gas elimination technique to pulmonary medicine. 5. Ventilation-perfusion relationships in acute respiratory failure. *Thorax*. 1994;49:1251–1258.
150. Reinius H, et al. Prevention of atelectasis in morbidly obese patients during general anesthesia and paralysis: a computerized tomography study. *Anesthesiology*. 2009;111:1979–1987.
151. Mynter T, et al. The effect of posture on late postoperative oxygenation. *Anesthesia*. 1996;51:225–227.
152. Warner DO, Warner MA, Ritman EL. Human chest wall function during epidural anesthesia. *Anesthesiology*. 1996;85:761–773.
153. Yamakage M, et al. Changes in ventilatory pattern and arterial oxygen saturation during spinal anaesthesia in man. *Acta Anaesthesiol Scand*. 1992;36:569–571.
154. McCarthy GS. The effect of thoracic extradural analgesia on pulmonary gas distribution, functional residual capacity and airway closure. *Br J Anaesth*. 1976;48:243–248.
155. Roca J, Wagner PD. Contribution of multiple inert gas elimination technique to pulmonary medicine. 1. Principles and information content of the multiple inert gas elimination technique. *Thorax*. 1994;49:815–824.
156. Rodriguez-Roisin R, Roca J. Contributions of multiple inert gas elimination technique to pulmonary medicine. 3. Bronchial asthma. *Thorax*. 1994;49:1027–1033.
157. Agusti AG, et al. Mechanisms of gas-exchange impairment in idiopathic pulmonary fibrosis. *Am Rev Respir Dis*. 1991;143:219–225.
158. Manier G, Castaing Y. Contribution of multiple inert gas elimination technique to pulmonary medicine. 4. Gas exchange abnormalities in pulmonary vascular and cardiac disease. *Thorax*. 1994;49:1169–1174.
159. Santolicandro A, et al. Mechanisms of hypoxemia and hypocapnia in pulmonary embolism. *Am J Respir Crit Care Med*. 1995;152:336–347.
160. Altemeier WA, et al. Pulmonary embolization causes hypoxemia by redistributing regional blood flow without changing ventilation. *J Appl Physiol*. 1998;85:2337–2343.
161. Light RB. Pulmonary pathophysiology of pneumococcal pneumonia. *Semin Respir Infect*. 1999;14:218–226.
162. Light RB. Indomethacin and acetylsalicylic acid reduce intrapulmonary shunt in experimental pneumococcal pneumonia. *Am Rev Respir Dis*. 1986;134:520–525.
163. Benumof JL. One-lung ventilation and hypoxic pulmonary vasoconstriction: implications for anesthetic management. *Anesth Analg*. 1985;64:821–833.
164. Karzai W, Schwarzkopf K. Hypoxemia during one-lung ventilation: prediction, prevention, and treatment. *Anesthesiology*. 2009;110:1402–1411.
165. Hedenstierna G, Reber A. Manipulating pulmonary blood flow during one-lung anaesthesia. *Acta Anaesthesiol Scand*. 1996;40:2–4.
166. Tusman G, et al. Alveolar recruitment strategy increases arterial oxygenation during one-lung ventilation. *Ann Thorac Surg*. 2002;73:1204–1209.
167. Tusman G, et al. Lung recruitment improves the efficiency of ventilation and gas exchange during one-lung ventilation anesthesia. *Anesth Analg*. 2004;98:1604–1609; table of contents.
168. Mascotto G, et al. Prospective, randomized, controlled evaluation of the preventive effects of positive end-expiratory pressure on patient oxygenation during one-lung ventilation. *Eur J Anaesthesiol*. 2003;20:704–710.

169. Slinger PD, et al. Relation of the static compliance curve and positive end-expiratory pressure to oxygenation during one-lung ventilation. *Anesthesiology*. 2001;95:1096–1102.
170. Ishikawa S, Nakazawa K, Makita K. Progressive changes in arterial oxygenation during one-lung anaesthesia are related to the response to compression of the non-dependent lung. *Br J Anaesth*. 2003;90:21–26.
171. Pfizer J. Acute lung injury following one-lung anaesthesia. *Br J Anaesth*. 2003;91:153; author reply, p4.
172. Schwarzkopf K, et al. Oxygenation during one-lung ventilation: the effects of inhaled nitric oxide and increasing levels of inspired fraction of oxygen. *Anesth Analg*. 2001;92:842–847.
173. Moutafis M, et al. The effects of inhaled nitric oxide and its combination with intravenous almitrine on Pao_2 during one-lung ventilation in patients undergoing thoracoscopic procedures. *Anesth Analg*. 1997;85:1130–1135.
174. Silva-Costa-Gomes T, et al. Low- vs high-dose almitrine combined with nitric oxide to prevent hypoxia during open-chest one-lung ventilation. *Br J Anaesth*. 2005;95:410–416.
175. Moutafis M, et al. The effects of intravenous almitrine on oxygenation and hemodynamics during one-lung ventilation. *Anesth Analg*. 2002;94:830–834; table of contents.
176. Dembinski R, Henzler D, Rossaint R. Modulating the pulmonary circulation: an update. *Minerva Anestesiol*. 2004;70:239–243.
177. Schilling T, et al. The pulmonary immune effects of mechanical ventilation in patients undergoing thoracic surgery. *Anesth Analg*. 2005;101:957–965; table of contents.
178. Friedlander M, et al. Is hypoxic pulmonary vasoconstriction important during single lung ventilation in the lateral decubitus position? *Can J Anaesth*. 1994;41:26–30.
179. Choi YS, et al. Effects of head-down tilt on intrapulmonary shunt fraction and oxygenation during one-lung ventilation in the lateral decubitus position. *J Thorac Cardiovasc Surg*. 2007;134:613–618.
180. McMahon AJ, et al. Impact of laparoscopic cholecystectomy: a population-based study. *Lancet*. 2000;356:1632–1637.
181. Neudecker J, et al. The European Association for Endoscopic Surgery clinical practice guideline on the pneumoperitoneum for laparoscopic surgery. *Surg Endosc*. 2002;16:1121–1143.
182. Gutt CN, et al. Circulatory and respiratory complications of carbon dioxide insufflation. *Dig Surg*. 2004;21:95–105.
183. Bablekos GD, et al. Changes in breathing control and mechanics after laparoscopic vs open cholecystectomy. *Arch Surg*. 2006;141:16–22.
184. Hirvonen EA, Nuutinen LS, Kauko M. Ventilatory effects, blood gas changes, and oxygen consumption during laparoscopic hysterectomy. *Anesth Analg*. 1995;80:961–966.
185. Andersson LE, et al. Effect of carbon dioxide pneumoperitoneum on development of atelectasis during anesthesia, examined by spiral computed tomography. *Anesthesiology*. 2005;102:293–299.
186. Makinen MT, Yli-Hankala A. Respiratory compliance during laparoscopic hiatal and inguinal hernia repair. *Can J Anaesth*. 1998;45:865–870.
187. Sharma KC, et al. Cardiopulmonary physiology and pathophysiology as a consequence of laparoscopic surgery. *Chest*. 1996;110:810–815.
188. Andersson L, et al. Effect of CO_2 pneumoperitoneum on ventilation-perfusion relationships during laparoscopic cholecystectomy. *Acta Anaesthesiol Scand*. 2002;46:552–560.
189. Strang CM, et al. Improved ventilation-perfusion matching by abdominal insufflation (pneumoperitoneum) with CO_2 but not with air. *Minerva Anestesiol*. 2013;79(6):617.
190. Hachenberg T, et al. Gas exchange impairment and pulmonary densities after cardiac surgery. *Acta Anaesthesiol Scand*. 1992;36:800–805.
191. Hachenberg T, et al. The ventilation-perfusion relation and gas exchange in mitral valve disease and coronary artery disease. Implications for anesthesia, extracorporeal circulation, and cardiac surgery. *Anesthesiology*. 1997;86:809–817.
192. Dyhr T, et al. Both lung recruitment maneuver and PEEP are needed to increase oxygenation and lung volume after cardiac surgery. *Acta Anaesthesiol Scand*. 2004;48:187–197.
193. Pasquina P, et al. Continuous positive airway pressure versus non-invasive pressure support ventilation to treat atelectasis after cardiac surgery. *Anesth Analg*. 2004;99:1001–1008; table of contents.
194. Reis Miranda D, et al. The open lung concept: effects on right ventricular afterload after cardiac surgery. *Br J Anaesth*. 2004;93:327–332.
195. Tscherkno EM, et al. Intrapulmonary shunt after cardiopulmonary bypass: the use of vital capacity maneuvers versus off-pump coronary artery bypass grafting. *J Thorac Cardiovasc Surg*. 2002;124:732–738.
196. Futier E, Constantin JM, Paugam-Burtz C, et al. A trial of intraoperative low-tidal-volume ventilation in abdominal surgery. *N Engl J Med*. 2013;369(5):428–437.
197. Las Vegas investigators. Epidemiology, practice of ventilation and outcome for patients at increased risk of postoperative pulmonary complications: LAS VEGAS - an observational study in 29 countries. *Eur J Anaesthesiol*. 2017;34(8):492–507.
198. Hedenstierna G. Small tidal volumes, positive end-expiratory pressure, and lung recruitment maneuvers during anesthesia: good or bad? *Anesthesiology*. 2015;123(3):501–503.
199. Lindberg P, Gunnarsson L, Tokics L, et al. Atelectasis and lung function in the postoperative period. *Acta Anaesthesiol Scand*. 1992;36(6):546–553.
200. Pasquina P, Tramer MR, Walder B. Prophylactic respiratory physiotherapy after cardiac surgery: systematic review. *BMJ*. 2003;327:1379.
201. Westerdahl E, et al. Deep-breathing exercises reduce atelectasis and improve pulmonary function after coronary artery bypass surgery. *Chest*. 2005;128:3482–3488.
202. Greif R, Akca O, Horn EP, et al. Outcomes Research G. Supplemental perioperative oxygen to reduce the incidence of surgical-wound infection. *N Engl J Med*. 2000;342(3):161–167.
203. Allegranzi B, Zayed B, Bischoff P, et al. New WHO recommendations on intraoperative and postoperative measures for surgical site infection prevention: an evidence-based global perspective. *Lancet Infect Dis*. 2016;16(12):e288–e303.
204. Hedenstierna G, Perchiazzini G, Meyhoff CS, Larsson A. Who can make sense of the WHO guidelines to prevent surgical site infection? *Anesthesiology*. 2017;126(5):771–773.
205. Staehr-Rye AK, Meyhoff CS, Scheffenbichler FT, et al. High intraoperative inspiratory oxygen fraction and risk of major respiratory complications. *Br J Anaesth*. 2017;119(1):140–149.
206. Kurz A, Fleischmann E, Sessler DI, et al. Effects of supplemental oxygen and dexamethasone on surgical site infection: a factorial randomized trial double dagger. *Br J Anaesth*. 2015;115(3):434–443.
207. Turrens JF. Mitochondrial formation of reactive oxygen species. *J Physiol*. 2003;552(Pt 2):335–344.
208. Douglas NJ, et al. Respiration during sleep in normal man. *Thorax*. 1982;37:840–844.
209. Hudgel DW, Devadatta P. Decrease in functional residual capacity during sleep in normal humans. *J Appl Physiol*. 1984;57:1319–1322.
210. Ballard RD, et al. Influence of sleep on lung volume in asthmatic patients and normal subjects. *J Appl Physiol*. 1990;68:2034.
211. Appelberg J, et al. Lung aeration during sleep. *Chest*. 2007;131:122.

KEY POINTS

- The cardiac cycle is the sequence of electrical and mechanical events during a single heartbeat.
- Cardiac output is determined by the heart rate, myocardial contractility, and preload and afterload.
- The majority of cardiomyocytes consist of myofibrils, which are rod-like bundles that form the contractile elements within the cardiomyocyte.
- The basic working unit of contraction is the sarcomere.
- Gap junctions are responsible for the electrical coupling of small molecules between cells.
- Action potentials have four phases in the heart.
- The key player in cardiac excitation-contraction coupling is the ubiquitous second messenger calcium.
- Calcium-induced sparks are spatially and temporally patterned activations of localized calcium release that are important for excitation-contraction coupling and regulation of automaticity and contractility.
- β -Adrenoreceptors stimulate chronotropy, inotropy, lusitropy, and dromotropy.
- Hormones with cardiac action can be synthesized and secreted by cardiomyocytes or produced by other tissues and delivered to the heart.
- Cardiac reflexes are fast-acting reflex loops between the heart and central nervous system that contribute to the regulation of cardiac function and the maintenance of physiologic homeostasis.

“To err, to be deceived, is human.” This was William Harvey’s gentle repudiation to fellow physicians in his 1628 *“Exercitatio Anatomica de Motu Cordis et Sanguinis in Animalibus,”* in which he advanced the concepts of circulation with the heart as the central pump, a major break from the centuries-old anatomic teaching of Galen.^{1,2} Modern cardiac physiology includes this as well as concepts of cellular and molecular biology of the cardiomyocyte and regulation of cardiac function by neural and humoral factors. This chapter focuses on the physiology of the heart, beginning with the intact heart and advancing to cellular cardiac physiology. Finally, the various factors that regulate cardiac function are briefly discussed.

The basic anatomy of the heart consists of two atria and two ventricles that provide two separate circulations in series. The pulmonary circulation, a low-resistance and high-capacitance vascular bed, receives output from the right side of the heart, and its chief function is bidirectional gas exchange. The left side of the heart provides output for the systemic circulation. It functions to deliver oxygen (O_2) and nutrients and to remove carbon dioxide (CO_2) and metabolites from various tissue beds.

Physiology of the Intact Heart

Understanding the mechanical performance of the intact heart begins with the knowledge of the phases of the cardiac cycle and the determinants of ventricular function.

CARDIAC CYCLE

The cardiac cycle is the sequence of electrical and mechanical events during a single heartbeat. [Fig. 14.1](#) illustrates the electrical events of a single cardiac cycle represented by the electrocardiogram (ECG) with corresponding mechanical events. Left atrial and left ventricular pressures are shown correlated in time with aortic flow and ventricular volume.³

Intrinsic to the specialized cardiac pacemaker tissues is automaticity and rhythmicity. The cardiac cycle begins at the sinoatrial (SA) node with the initiation of the heartbeat. Because the SA node can generate impulses at the greatest frequency, it is the natural pacemaker.

Electrical Events and the Electrocardiogram

Electrical events of the pacemaker and the specialized conduction system are represented by the ECG at the body surface. The ECG is the result of differences in electrical potential generated by the heart at sites of the surface recording. The action potential initiated at the SA node is propagated to both atria by specialized conduction tissue that leads to atrial systole (contraction) and the P wave of the ECG. At the junction of the interatrial and interventricular septa, specialized atrial conduction tissue converges at the atrioventricular (AV) node, which is distally connected to the His bundle. The AV node is an area of relatively slow conduction, and a delay between atrial and ventricular contraction normally occurs at this locus. The PR interval represents the delay between atrial and ventricular contraction at the level of the AV node. From the distal His

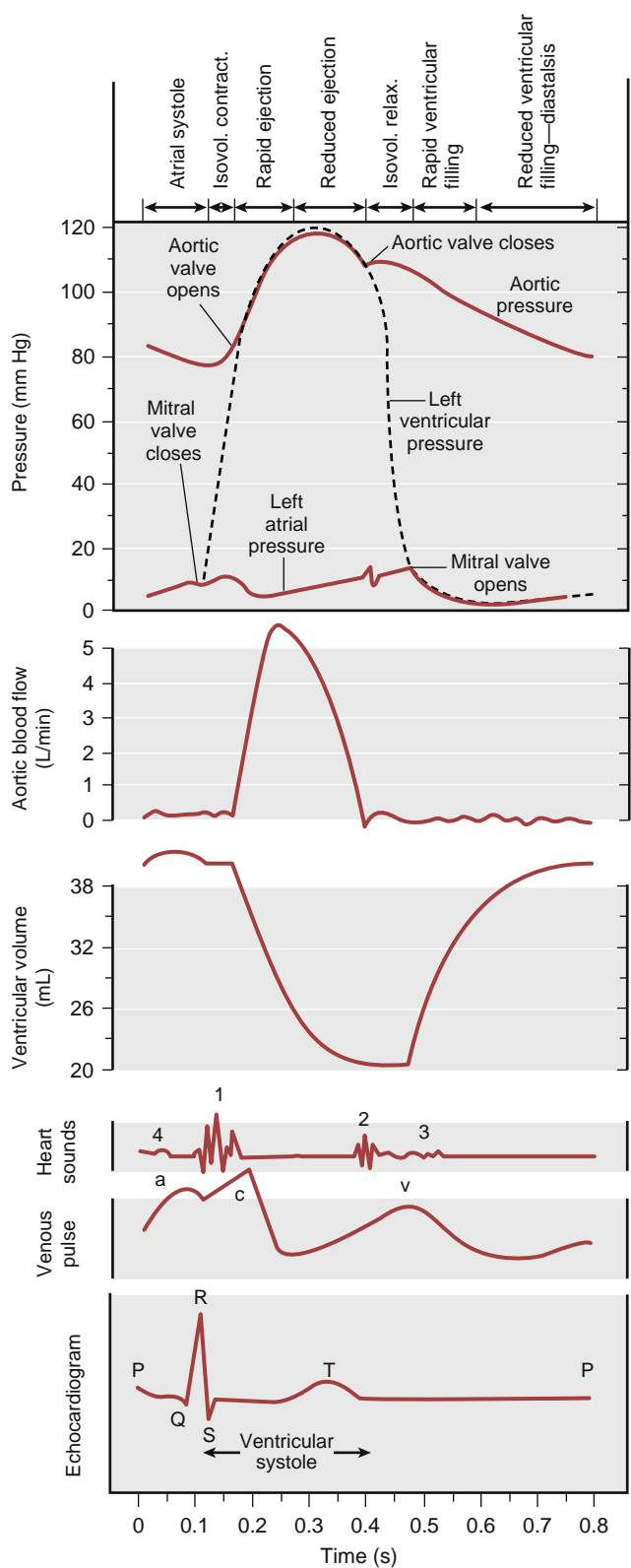


Fig. 14.1 Electrical and mechanical events during a single cardiac cycle. Aortic and atrial blood flow, ventricular volume, venous pulse, and the electrocardiogram are shown. (Berne RM, Levy MN: The cardiac pump. In *Cardiovascular physiology*, ed 8, St Louis, 2001, Mosby, pp 55-82.)

bundle, an electrical impulse is propagated through large left and right bundle branches and finally to the Purkinje system fibers, which are the smallest branches of the specialized conduction system. Finally, electrical signals are transmitted from the Purkinje system to individual ventricular cardiomyocytes. The spread of depolarization to the ventricular myocardium is exhibited as the QRS complex on the ECG. Depolarization is followed by ventricular repolarization and the appearance of the T wave on the ECG.⁴

Mechanical Events

The mechanical events of a cardiac cycle begin with the return of blood to the right and left atria from the systemic and pulmonary circulation, respectively. As blood accumulates in the atria, atrial pressure increases until it exceeds the pressure within the ventricle, and the AV valve opens. Blood passively flows first into the ventricular chambers, and such flow accounts for approximately 75% of the total ventricular filling.⁵ The remainder of the blood flow is mediated by active atrial contraction or systole, known as the atrial “kick.” The onset of atrial systole coincides with the depolarization of the SA node and the P wave. While the ventricles fill, the AV valves are displaced upward and ventricular contraction (systole) begins with closure of the tricuspid and mitral valves, which corresponds to the end of the R wave on the ECG. The first part of ventricular systole is known as isovolumic (or isometric) contraction. The electrical impulse traverses the AV region and passes through the right and left bundle branches into the Purkinje fibers, which leads to contraction of the ventricular myocardium and a progressive increase in intraventricular pressure. When intraventricular pressure exceeds pulmonary artery and aortic pressure, the pulmonic and aortic valves open and ventricular ejection occurs, which is the second part of ventricular systole.

Ventricular ejection is divided into the rapid ejection phase and the reduced ejection phase. During the rapid ejection phase, forward flow is maximal, and pulmonary artery and aortic pressure is maximally developed. In the reduced ejection phase, flow and great artery pressures taper with progression of systole. Pressures in both ventricular chambers decrease as blood is ejected from the heart, and ventricular diastole begins with closure of the pulmonic and aortic valves. The initial period of ventricular diastole consists of the isovolumic relaxation phase. This phase is concomitant with repolarization of the ventricular myocardium and corresponds to the end of the T wave on the ECG. The final portion of ventricular diastole involves a rapid decrease in intraventricular pressure until it decreases to less than that of the right and left atria, at which point the AV valve reopens, ventricular filling occurs, and the cycle repeats itself.

VENTRICULAR STRUCTURE AND FUNCTION

Ventricular Structure

The specific architectural order of the cardiac muscles provides the basis for the heart to function as a pump. The ellipsoid shape of the left ventricle (LV) is a result of the laminar layering of spiraling bundles of cardiac muscles (Fig. 14.2). The orientation of the muscle bundle is longitudinal in the subepicardial myocardium and circumferential

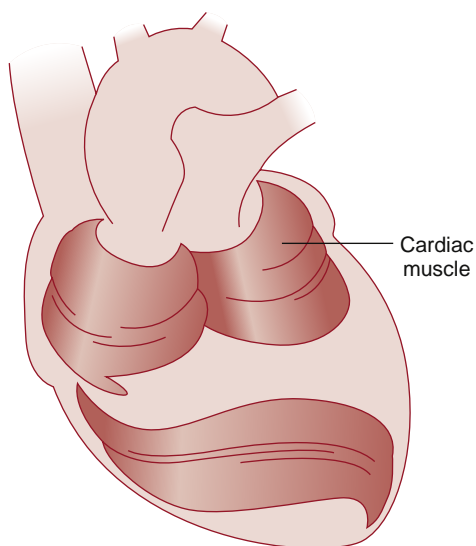


Fig. 14.2 Muscle bundles. (From Marieb EN. *Human Anatomy & Physiology*. 5th ed. San Francisco: Pearson Benjamin Cummings; 2001:684.)

in the middle segment and again becomes longitudinal in the subendocardial myocardium. Because of the ellipsoid shape of the LV, regional differences in wall thickness result in corresponding variations in the cross-sectional radius of the left ventricular chamber. These regional differences may serve to accommodate the variable loading conditions of the LV.⁶ In addition, such anatomy allows the LV to eject blood in a corkscrew-type motion beginning from the base and ending at the apex. The architecturally complex structure of the LV thus allows maximal shortening of myocytes, which results in increased wall thickness and the generation of force during systole. Moreover, release of the twisted LV may provide a suction mechanism for filling of the LV during diastole. The left ventricular free wall and the septum have similar muscle bundle architecture. As a result, the septum moves inward during systole in a normal heart. Regional wall thickness is a commonly used index of myocardial performance that can be clinically assessed, such as by echocardiography or magnetic resonance imaging.

Unlike the LV, which needs to pump against the higher-pressure systemic circulation, the right ventricle (RV) pumps against a much lower pressure circuit in the pulmonary circulation. Consequently, wall thickness is considerably less in the RV. In contrast to the ellipsoidal form of the LV, the RV is crescent shaped; as a result, the mechanics of right ventricular contraction are more complex. Inflow and outflow contraction is not simultaneous, and much of the contractile force seems to be recruited from interventricular forces of the LV-based septum.

An intricate matrix of collagen fibers forms a scaffold of support for the heart and adjacent vessels. This matrix provides enough strength to resist tensile stretch. The collagen fibers are made up of mostly thick collagen type I fiber, which cross-links with the thin collagen type III fiber, the other major type of collagen.⁷ Elastic fibers that contain elastin are in close proximity to the collagen fibers and account for the elasticity of the myocardium.⁸

Ventricular Function

The heart provides the driving force for delivering blood throughout the cardiovascular system to supply nutrients and to remove metabolic waste. Because of the anatomic complexity of the RV, the traditional description of systolic function is usually limited to the LV. Systolic performance of the heart is dependent on loading conditions and contractility. Preload and afterload are two interdependent factors extrinsic to the heart that govern cardiac performance.

Diastole is ventricular relaxation, and it occurs in four distinct phases: (1) isovolumic relaxation; (2) the rapid filling phase (i.e., the LV chamber filling at variable left ventricular pressure); (3) slow filling, or diastasis; and (4) final filling during atrial systole. The isovolumic relaxation phase is energy dependent. During auxotonic relaxation (phases 2 through 4), ventricular filling occurs against pressure. It encompasses a period during which the myocardium is unable to generate force, and filling of the ventricular chambers takes place. The isovolumic relaxation phase does not contribute to ventricular filling. The greatest amount of ventricular filling occurs in the second phase, whereas the third phase adds only approximately 5% of total diastolic volume and the final phase provides 15% of ventricular volume from atrial systole.

To assess diastolic function, several indices have been developed. The most widely used index for examining the isovolumic relaxation phase of diastole is to calculate the peak instantaneous rate of decline in left ventricular pressure ($-dP/dt$) or the time constant of isovolumic decline in left ventricular pressure (τ). The aortic closing-mitral opening interval and the isovolumic relaxation time and peak rate of left ventricular wall thinning, as determined by echocardiography, have both been used to estimate diastolic function during auxotonic relaxation. Ventricular compliance can be evaluated by pressure-volume relationships to determine function during the auxotonic phases of diastole.^{9,10}

Many different factors influence diastolic function: magnitude of systolic volume, passive chamber stiffness, elastic recoil of the ventricle, diastolic interaction between the two ventricular chambers, atrial properties, and catecholamines. Whereas systolic dysfunction is a reduced ability of the heart to eject, diastolic dysfunction is a decreased ability of the heart to fill. Abnormal diastolic function is now recognized as the predominant cause of the pathophysiologic condition of congestive heart failure.¹¹

Ventricular interactions during systole and diastole are internal mechanisms that provide feedback to modulate stroke volume (SV). Systolic ventricular interaction involves the effect of the interventricular septum on the function of both ventricles. Because the interventricular septum is anatomically linked to both ventricles, it is part of the load against which each ventricle has to work. Therefore, any changes in one ventricle will also be present in the other. In diastolic ventricular interaction, dilatation of either the LV or RV will have an impact on effective filling of the contralateral ventricle and thereby modify function.

Preload and Afterload. **Preload** is the ventricular load at the end of diastole, before contraction has started. First described by Starling, a linear relationship exists between

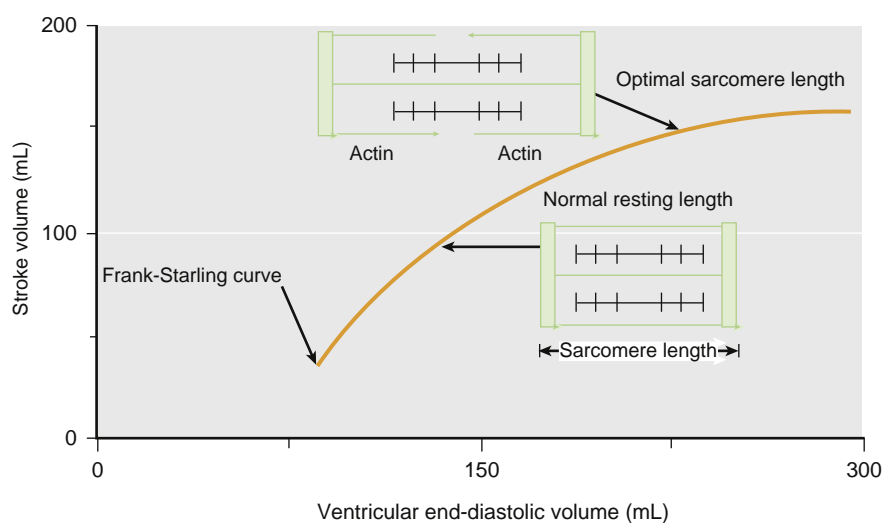


Fig. 14.3 Frank-Starling relationship. The relationship between sarcomere length and tension developed in cardiac muscles is shown. In the heart, an increase in end-diastolic volume is the equivalent of an increase in myocardial stretch; therefore, according to the Frank-Starling law, increased stroke volume is generated.

sarcomere length and myocardial force (Fig. 14.3). In clinical practice, surrogate representatives of left ventricular volume such as pulmonary wedge pressure or central venous pressure are used to estimate preload.⁵ More direct measures of ventricular volumes can be made using echocardiography.

Afterload is the systolic load on the LV after contraction has begun. Aortic compliance is an additional determinant of afterload.³ Aortic compliance is the ability of the aorta to give way to systolic forces from the ventricle. Changes in the aortic wall (dilation or stiffness) can alter aortic compliance and thus afterload. Examples of pathologic conditions that alter afterload are aortic stenosis and chronic hypertension. Both impede ventricular ejection, thereby increasing afterload. Aortic impedance, or aortic pressure divided by aortic flow at that instant, is an accurate means of gauging afterload. However, clinical measurement of aortic impedance is invasive. Echocardiography can non-invasively estimate aortic impedance by determining aortic blood flow at the time of its maximal increase. In clinical practice, the measurement of systolic blood pressure is adequate to approximate afterload, provided that aortic stenosis is not present.

Preload and afterload can be thought of as the wall stress that is present at the end of diastole and during left ventricular ejection, respectively. Wall stress is a useful concept because it includes preload, afterload, and the energy required to generate contraction. Wall stress and heart rate are probably the two most relevant indices that account for changes in myocardial O₂ demand. Laplace's law states that wall stress (σ) is the product of pressure (P) and radius (R) divided by wall thickness (h):⁵

$$\sigma = P \times R / 2h$$

The ellipsoid shape of the LV allows the least amount of wall stress such that as the ventricle changes its shape from ellipsoid to spherical, wall stress is increased. By using the ratio of the long axis to the short axis as a measure of the ellipsoid shape, a decrease in this ratio would signify a transition from ellipsoid to spherical.

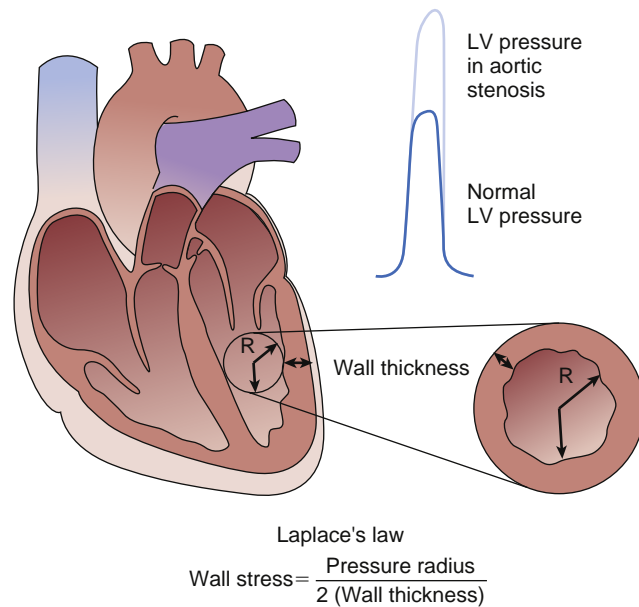


Fig. 14.4 In response to aortic stenosis, left ventricular (LV) pressure increases. To maintain wall stress at control levels, compensatory LV hypertrophy develops. According to Laplace's law, wall stress = pressure · radius (R) \div (2 × wall thickness). Therefore, the increase in wall thickness offsets the increased pressure, and wall stress is maintained at control levels. (From Opie LH. Ventricular function. In: *Heart Physiology From Cell to Circulation*. 4th ed. Philadelphia: Lippincott-Raven; 2004:355–401.)

Thickness of the left ventricular muscle is an important modifier of wall stress. For example, in aortic stenosis, afterload is increased. The ventricle must generate a much higher pressure to overcome the increased load opposing systolic ejection of blood. To generate such high performance, the ventricle increases its wall thickness (left ventricular hypertrophy). By applying Laplace's law, increased left ventricular wall thickness will decrease wall stress, despite the necessary increase in left ventricular pressure to overcome the aortic stenosis (Fig. 14.4).¹² In a failing heart, the radius of the LV increases, thus increasing wall stress.

Frank-Starling Relationship. The Frank-Starling relationship is an intrinsic property of myocardium by which stretching of the myocardial sarcomere results in enhanced myocardial performance for subsequent contractions (see Fig. 14.3). In 1895, Otto Frank first noted that in skeletal muscle, the change in tension was directly related to its length, and as pressure changed in the heart, a corresponding change in volume occurred.¹³ In 1914, E.H. Starling, using an isolated heart-lung preparation as a model, observed that “the mechanical energy set free on passage from the resting to the contracted state is a function of the length of the muscle fiber.”¹⁴ If a strip of cardiac muscle is mounted in a muscle chamber under isometric conditions and stimulated at a fixed frequency, then an increase in sarcomere length results in an increase in twitch force. Starling concluded that the increased twitch force was the result of a greater interaction of muscle bundles.

Electron microscopy has demonstrated that sarcomere length (2-2.2 μm) is positively related to the amount of actin and myosin cross-bridging and that there is an optimal sarcomere length at which the interaction is maximal. This concept is based on the assumption that the increase in cross-bridging is equivalent to an increase in muscle performance. Although this theory continues to hold true for skeletal muscle, the force-length relationship in cardiac muscle is more complex. When comparing force-strength relationships between skeletal and cardiac muscle, it is noteworthy that the reduction in force is only 10%, even if cardiac muscle is at 80% sarcomere length.¹³ The cellular basis of the Frank-Starling mechanism is still being investigated and is briefly discussed later in this chapter. A common clinical application of Starling’s law is the relationship of left ventricular end-diastolic volume and SV. The Frank-Starling mechanism may remain intact even in a failing heart.¹⁵ However, ventricular remodeling after injury or in heart failure may modify the Frank-Starling relationship.

Contractility. Each Frank-Starling curve specifies a level of contractility, or the inotropic state of the heart, which is defined as the work performed by cardiac muscle at any given end-diastolic fiber. Factors that modify contractility will create a family of Frank-Starling curves with different contractility (Fig. 14.5).¹² Factors that modify contractility are exercise, adrenergic stimulation, changes in pH, temperature, and drugs such as digitalis. The ability of the LV to develop, generate, and sustain the necessary pressure for the ejection of blood is the intrinsic inotropic state of the heart.

In isolated muscle, the maximal velocity of contraction (V_{\max}) is defined as the maximal velocity of ejection at zero load. V_{\max} is obtained by plotting the velocity of muscle shortening in isolated papillary muscle at varying degrees of force. Although this relationship can be replicated in isolated myocytes, V_{\max} cannot be measured in an intact heart because complete unloading is impossible. To measure the intrinsic contractile activity of an intact heart, several strategies have been attempted with varying success. Pressure-volume loops, albeit requiring catheterization of the left side of the heart, are currently the best way to determine contractility in an intact heart (Fig. 14.6).¹² The pressure-volume loop represents an indirect measure of the Frank-Starling relationship between force (pressure)

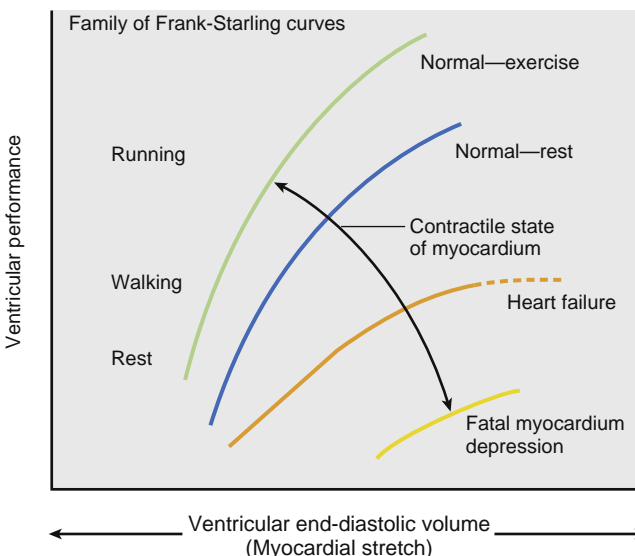


Fig. 14.5 A family of Frank-Starling curves is shown. A leftward shift of the curve denotes enhancement of the inotropic state, whereas a rightward shift denotes decreased inotropy. (From Opie LH. Ventricular function. In: *Heart Physiology From Cell to Circulation*. 4th ed. Philadelphia: Lippincott-Raven; 2004:355-401.)

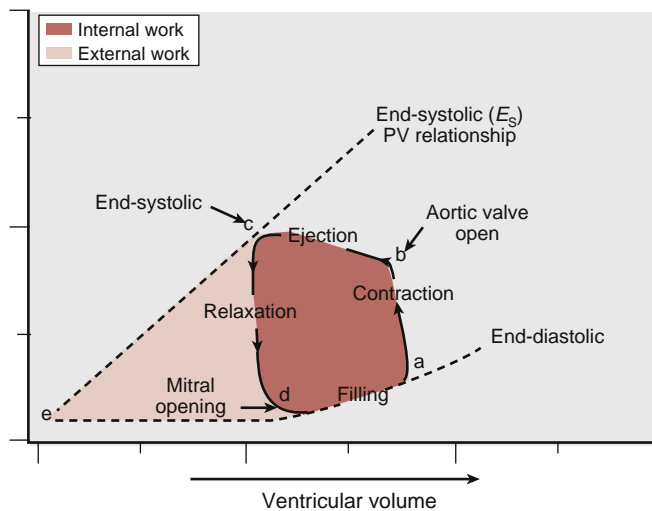


Fig. 14.6 Pressure-volume (PV) loop. Point *a* depicts the start of isovolumetric contraction. The aortic valve opens at point *b*, and ejection of blood follows (points *b*–*c*). The mitral valve opens at point *d*, and ventricular filling ensues. External work is defined by points *a*, *b*, *c*, and *d*, and internal work is defined by points *e*, *d*, and *c*. The PV area is the sum of external and internal work. (From Opie LH. Ventricular function. In: *Heart Physiology From Cell to Circulation*. 4th ed. Philadelphia: Lippincott-Raven; 2004:355-401.)

and muscle length (volume). Clinically, the most commonly used noninvasive index of ventricular contractile function is the ejection fraction, which is assessed by echocardiography, angiography, or radionuclide ventriculography.

$$\text{Ejection fraction} = (\text{LVEDV} - \text{LVESV}) / \text{LVEDV}$$

where LVESV is left ventricular end-systolic volume.

Cardiac Work. The work of the heart can be divided into external and internal work. External work is expended to eject blood under pressure, whereas internal work is

expended within the ventricle to change the shape of the heart and to prepare it for ejection. Internal work contributes to inefficiency in the performance of the heart. Wall stress is directly proportional to the internal work of the heart.¹⁶

External work, or stroke work, is a product of the SV and pressure (P) developed during ejection of the SV.

$$\text{Stroke work} = \text{SV} \times P \text{ or } (\text{LVEDV} - \text{LVESV}) \times P$$

The external work and internal work of the ventricle both consume O_2 . The clinical significance of internal work is illustrated in the case of a poorly drained LV during cardiopulmonary bypass. Although external work is provided by the roller pump during bypass, myocardial ischemia can still occur because poor drainage of the LV creates tension on the left ventricular wall and increases internal work.

The efficiency of cardiac contraction is estimated by the following formula¹⁰:

$$\text{Cardiac efficiency} = \frac{\text{External work}}{\text{Energy equivalent of } O_2 \text{ consumption}}$$

The corkscrew motion of the heart for the ejection of blood is the most favorable in terms of work efficiency, based on the architecture in a normal LV (with the cardiac muscle bundles arranged so that a circumferentially oriented middle layer is sandwiched by longitudinally oriented outer layers). In heart failure, ventricular dilation reduces cardiac efficiency because it increases wall stress, which in turn increases O_2 consumption.¹³

Heart Rate and Force-Frequency Relationship. In isolated cardiac muscle, an increase in the frequency of stimulation induces an increase in the force of contraction. This relationship is termed the *treppe*, which means *staircase* in German, and is the phenomenon of the force-frequency relationship.^{10,17} At between 150 and 180 stimuli per minute, maximal contractile force is reached in an isolated heart muscle at a fixed muscle length. Thus, an increased frequency incrementally increases inotropy, whereas stimulation at a lower frequency decreases contractile force. However, when the stimulation becomes extremely rapid, the force of contraction decreases. In the clinical context, pacing-induced positive inotropic effects may be effective only up to a certain heart rate, based on the force-frequency relationship. In a failing heart, the force-frequency relationship may be less effective in producing a positive inotropic effect.¹⁰

CARDIAC OUTPUT

Cardiac output is the amount of blood pumped by the heart per unit of time (\dot{Q}) and is determined by four factors: two factors that are intrinsic to the heart—heart rate and myocardial contractility—and two factors that are extrinsic to the heart but functionally couple the heart and the vasculature—preload and afterload.

Heart rate is defined as the number of beats per minute and is mainly influenced by the autonomic nervous system. Increases in heart rate escalate cardiac output if ventricular filling is adequate during diastole. Contractility can be defined as the intrinsic level of contractile performance

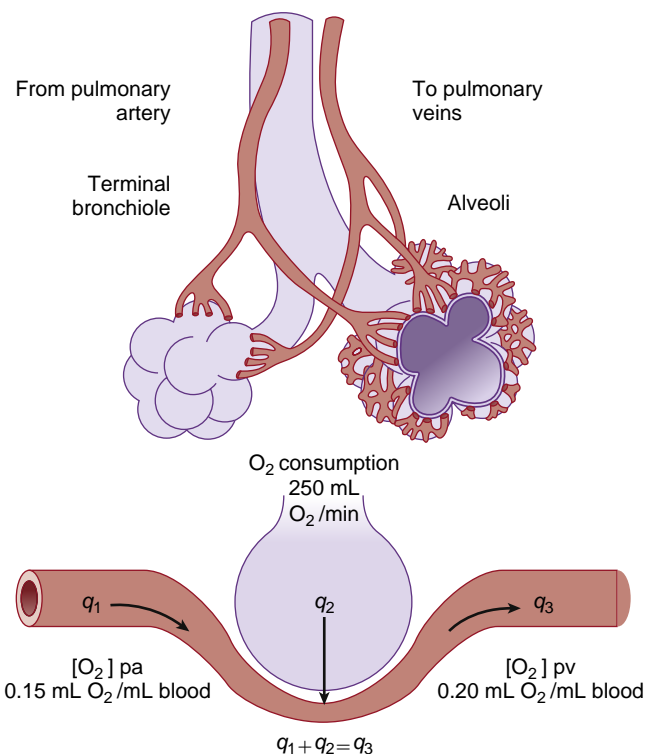


Fig. 14.7 Illustration demonstrates the principle of determination of cardiac output according to the Fick formula. If the oxygen (O_2) concentration in pulmonary arterial blood ($C_{pa}O_2$), the O_2 concentration of the pulmonary vein ($C_{pv}O_2$), and the O_2 consumption are known, then cardiac output can be calculated. *pa*, Pulmonary artery; *pv*, pulmonary vein. (Berne RM, Levy MN: The cardiac pump. In *Cardiovascular physiology*, ed 8, St Louis, 2001, Mosby, pp 55-82.)

that is independent of loading conditions. Contractility is difficult to define in an intact heart because it cannot be separated from loading conditions.^{10,17} For example, the *Frank-Starling relationship* is defined as the change in intrinsic contractile performance, based on changes in preload. Cardiac output in a living organism can be measured with the Fick principle (a schematic depiction is illustrated in Fig. 14.7).³

The Fick principle is based on the concept of conservation of mass such that the O_2 delivered from pulmonary venous blood (q_3) is equal to the total O_2 delivered to pulmonary capillaries through the pulmonary artery (q_1) and the alveoli (q_2).

The amount of O_2 delivered to the pulmonary capillaries by way of the pulmonary arteries (q_1) equals total pulmonary arterial blood flow (\dot{Q}) times the O_2 concentration in pulmonary arterial blood ($C_{pa}O_2$):

$$q_1 = \dot{Q} \times C_{pa}O_2$$

The amount of O_2 carried away from pulmonary venous blood (q_3) is equal to total pulmonary venous blood flow (\dot{Q}) times the O_2 concentration in pulmonary venous blood ($C_{pv}O_2$):

$$q_3 = \dot{Q} \times C_{pv}O_2$$

The pulmonary arterial O_2 concentration is the mixed systemic venous O_2 , and the pulmonary venous O_2

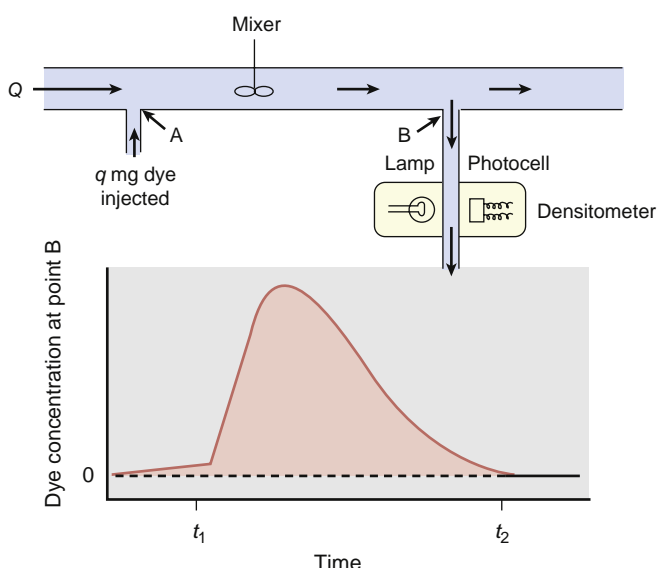


Fig. 14.8 Illustration demonstrates the principle of determining cardiac output with the indicator dilution technique. This model assumes that there is no recirculation. A known amount of dye (q) is injected at point A into a stream flowing at \dot{Q} (mL/min). A mixed sample of the fluid flowing past point B is withdrawn at a constant rate through a densitometer. The change in dye concentration over time is depicted in a curve. Flow may be measured by dividing the amount of indicator injected upstream by the area under the downstream concentration curve. (Berne RM, Levy MN: The cardiac pump. In *Cardiovascular physiology*, ed 8, St Louis, 2001, Mosby, pp 55-82.)

concentration is the peripheral arterial O_2 . O_2 consumption is the amount of O_2 delivered to the pulmonary capillaries from the alveoli (q_2). Because $q_1 + q_2 = q_3$,

$$\dot{Q}(\text{CpaO}_2) + q_2 = \dot{Q}(\text{CpvO}_2)$$

$$q_2 = \dot{Q}(\text{CpvO}_2) - \dot{Q}(\text{CpaO}_2)$$

$$q_2 = \dot{Q}(\text{CpvO}_2 - \text{CpaO}_2)$$

$$\dot{Q} = q_2 / (\text{CpvO}_2 - \text{CpaO}_2)$$

Thus, if the CpaO_2 , CpvO_2 , and O_2 consumption (q_2) are known, then the cardiac output can be determined.

The indicator dilution technique is another method for determining cardiac output also based on the law of conservation of mass. The two most commonly used indicator dilution techniques are the dye dilution and the thermodilution methods. **Fig. 14.8** illustrates the principles of the dye dilution method.³

Cellular Cardiac Physiology

CELLULAR ANATOMY

At the cellular level, the heart consists of three major components: cardiac muscle tissue (contracting cardiomyocytes), conduction tissue (conducting cells), and extracellular connective tissue. A group of cardiomyocytes with its connective tissue support network or extracellular matrix make up a myofiber (Fig. 14.9). Adjacent myofibers are connected by strands of collagen. The extracellular matrix is the synthetic product of fibroblasts and is made up of collagen,

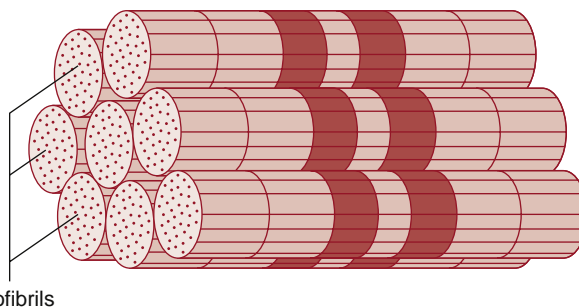


Fig. 14.9 Organization of cardiomyocytes. Fifty percent of cardiomyocyte volume is made up of myofibrils; the remainder consists of mitochondria, nucleus, sarcoplasmic reticulum, and cytosol.

which is the main determinant of myocardial stiffness, and other major matrix proteins. One of the matrix proteins, elastin, is the chief constituent of elastic fibers. The elastic fibers account for, in part, the elastic properties of the myocardium.⁸ Other matrix proteins include the glycoproteins or proteoglycans and matrix metalloproteinases. Proteoglycans are proteins with short sugar chains, and they include heparan sulfate, chondroitin, fibronectin, and laminin. Matrix metalloproteinases are enzymes that degrade collagen and other extracellular proteins. The balance between the accumulation of extracellular matrix proteins by synthesis and their breakdown by matrix metalloproteinases contributes to the mechanical properties and function of the heart.⁸

CARDIOMYOCYTE STRUCTURE AND FUNCTION

Individual contracting cardiomyocytes are large cells between 20 μm (atrial cardiomyocytes) and 140 μm (ventricular cardiomyocytes) in length. Approximately 50% of the cell volume in a contracting cardiomyocyte is made up of myofibrils, and the remainder consists of mitochondria, nucleus, sarcoplasmic reticulum (SR), and cytosol. The myofibril is the rod-like bundle that forms the contractile elements within cardiomyocytes. Within each contractile element are contractile proteins, regulatory proteins, and structural proteins. Contractile proteins make up approximately 80% of the myofibrillar protein, with the remainder being regulatory and structural proteins.^{18,19} The basic unit of contraction is the sarcomere (see discussion under **Contractile Elements** later in this chapter).

The sarcolemma, or the outer plasma membrane, separates the intracellular and extracellular space. It surrounds the cardiomyocyte and invaginates into the myofibrils through an extensive tubular network known as *transverse tubules* or *T tubules*, and it also forms specialized intercellular junctions between cells.^{20,21}

Transverse or T tubules are in close proximity to an intramembranous system and the SR, which plays an important role in the calcium (Ca^{2+}) metabolism that is critical in the excitation-contraction coupling (ECC) of the cardiomyocyte. The SR can be further divided into the longitudinal (or network) SR and the junctional SR. The longitudinal SR is involved in the uptake of Ca^{2+} for the initiation of relaxation. The junctional SR contains large Ca^{2+} -release channels (ryanodine receptors [RyRs]) that release SR Ca^{2+} stores in response to depolarization-stimulated Ca^{2+} influx through the sarcolemmal Ca^{2+} channels. The RyRs are not only

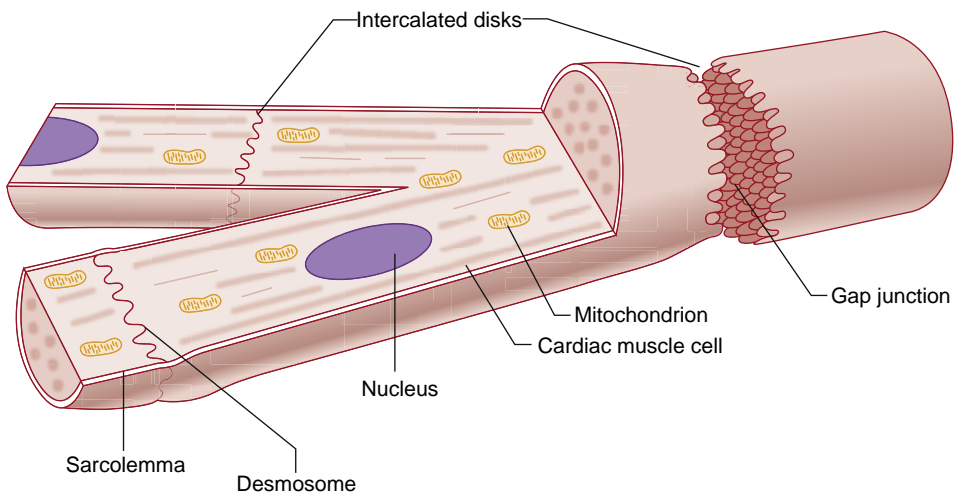


Fig. 14.10 The sarcolemma that envelops cardiomyocytes becomes highly specialized to form the intercalated disks where ends of neighboring cells are in contact. The intercalated disks consist of gap junctions and spot and sheet desmosomes.

Ca^{2+} -release channels, but they also form the scaffolding proteins that anchor many of the key regulatory proteins.²²

Mitochondria are immediately found beneath the sarcolemma, wedged between myofibrils within the cell. They contain enzymes that promote the generation of adenosine triphosphate (ATP), and they are the energy powerhouse for the cardiomyocyte. In addition, mitochondria can also accumulate Ca^{2+} and thereby contribute to the regulation of the cytosolic Ca^{2+} concentration. Nearly all the genetic information is found within the centrally located nucleus. The cytosol is the fluid-filled microenvironment within the sarcolemma, exclusive of the organelles and the contractile apparatus and proteins.

Cardiac muscle cells contain three different types of intercellular junctions: gap junctions, *spot* desmosomes, and *sheet* desmosomes (or *fasciae adherens*) (Fig. 14.10).^{20,23} Gap junctions are responsible for electrical coupling and the transfer of small molecules between cells, whereas desmosome-like junctions provide mechanical linkage. The adhesion sites formed by spot desmosomes anchor the intermediate filament cytoskeleton of the cell; those formed by the *fasciae adherens* anchor the contractile apparatus. Gap junctions consist of clusters of plasma membrane channels directly linking the cytoplasmic compartments of neighboring cells. Gap junction channels are constructed from connexins, a multigene family of conserved proteins. The principal connexin isoform of the mammalian heart is connexin 43; other connexins, notably connexins 40, 45, and 37, are also expressed but in smaller quantities.^{22,23}

The conducting cardiomyocytes, or Purkinje cells, are cells specialized for conducting propagated action potentials. These cells have a low content of myofibrils and a prominent nucleus, and they contain an abundance of gap junctions. Cardiomyocytes can be functionally separated into (1) the excitation system, (2) the ECC system, and (3) the contractile system.

Excitation System

The cellular action potential originating in the specialized conduction tissue is propagated to individual cells where it initiates the intracellular event that leads to the contraction of the cell through the sarcolemmal excitation system.

Action Potential. Ion fluxes across plasma membranes result in depolarization (attaining a less negative membrane potential) and repolarization (attaining a more negative membrane potential). They are mediated by membrane proteins with ion-selective pores. Because these ion channel proteins open and close the pores in response to changes in membrane potential, the channels are voltage gated. In the heart, sodium (Na^+), potassium (K^+), Ca^{2+} , and chloride (Cl^-) channels contribute to the action potential.

The types of action potential in the heart can be separated into two categories: (1) fast-response action potentials, which are found in the His-Purkinje system and atrial or ventricular cardiomyocytes; and (2) slow-response action potentials, which are found in the pacemaker cells in the SA and AV nodes. A typical tracing of an action potential in the His-Purkinje system is depicted in Fig. 14.11.¹⁰ The electrochemical gradient for K^+ across the plasma membrane is the determinant for the resting membrane potential. Mostly as a result of the influx of Na^+ , the membrane potential becomes depolarized, which leads to an extremely rapid upstroke (phase 0). As the membrane potential reaches a critical level (or threshold) during depolarization, the action potential is propagated. The rapid upstroke is followed by a transient repolarization (phase 1). Phase 1 is a period of brief and limited repolarization that is largely attributable to the activation of a transient outward K^+ current, i_{to} . The plateau phase (phase 2) occurs with a net influx of Ca^{2+} through L-type Ca^{2+} channels and the efflux of K^+ through several K^+ channels—the inwardly rectifying i_{k} , the delayed rectifier i_{k1} , and i_{to} . Repolarization (phase 3) is brought about when an efflux of K^+ from the three outward K^+ currents exceeds the influx of Ca^{2+} , thus returning the membrane to the resting potential. Very little ionic flux occurs during diastole (phase 4) in a fast-response action potential.

In contrast, during diastole (phase 4), pacemaker cells that show slow-response action potentials have the capability of spontaneous diastolic depolarization and generate the automatic cardiac rhythm. Pacemaker currents during phase 4 are the result of an increase in the three inward currents and a decrease in the two outward currents. The three

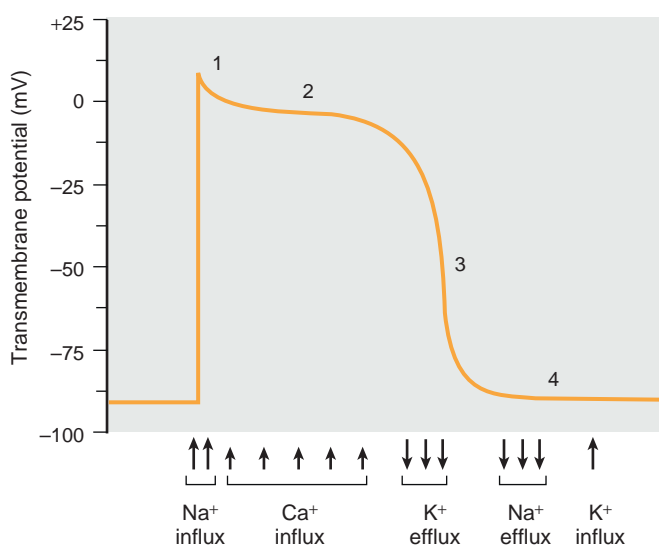


Fig. 14.11 Phases of cellular action potentials and major associated currents in ventricular myocytes. The initial phase (0) spike and overshoot (1) are caused by a rapid inward sodium (Na^+) current, the plateau phase (2) by a slow calcium (Ca^{2+}) current through L-type Ca^{2+} channels, and repolarization (phase 3) by outward potassium (K^+) currents. Phase 4, the resting potential (Na^+ efflux, K^+ influx), is maintained by Na^+ - K^+ -adenosine triphosphatase (ATPase). The Na^+ - Ca^{2+} exchanger is mainly responsible for extrusion of Ca^{2+} . In specialized conduction system tissue, spontaneous depolarization takes place during phase 4 until the voltage resulting in opening of the Na^+ channel is reached. (From LeWinter MM, Osol G. Normal physiology of the cardiovascular system. In Fuster V, Alexander RW, O'Rourke RA, eds. *Hurst's the Heart*. 10th ed. New York: McGraw-Hill; 2001:63–94.)

inward currents that contribute to spontaneous pacemaker activity include two carried by Ca^{2+} , i_{CaL} and i_{CaT} , and one that is a mixed cation current, I_f .²⁴ The two outward currents are the delayed rectifier K^+ current, i_K , and the inward rectifying K^+ current, i_{K1} . When compared with the fast-response action potential, phase 0 is much less steep, phase 1 is absent, and phase 2 is indistinct from phase 3 in the slow-response action potential.²⁵ In SA node cells, the pacemaker I_f current is the principal determinant of duration diastolic depolarization, and it is encoded by four members of the hyperpolarization-activated cyclic nucleotide-gated gene (HCN1-4) family.²⁶

During the cardiac action potential, movement of Ca^{2+} into the cell and Na^+ out of the cell creates an ionic imbalance. The Na^+ - Ca^{2+} exchanger restores cellular ionic balance by actively transporting Ca^{2+} out of the cell against a concentration gradient while moving Na^+ into the cell in an energy-dependent manner.

Excitation-Contraction Coupling

Structures that participate in cardiac ECC include the sarcolemma, transverse tubules, SR, and myofilaments (Fig. 14.12A).²⁷ The process of ECC begins with depolarization of the plasma membrane and spread of electrical excitation along the sarcolemma of cardiomyocytes.

The ubiquitous second messenger Ca^{2+} is the key player in cardiac ECC (see Fig. 14.12B).²⁵ Cycling of Ca^{2+} within the structures that participate in ECC initiates and terminates contraction. Activation of the contractile system depends on an increase in free cytosolic Ca^{2+} and its subsequent binding to contractile proteins.

Ca^{2+} enters through plasma membrane channels concentrated at the T tubules, and such entry through L-type Ca^{2+} channels (dihydropyridine receptors) triggers the release of Ca^{2+} from the SR.²⁸ This evokes a Ca^{2+} spark. Ca^{2+} sparks are considered to be the elementary Ca^{2+} signaling event of ECC in heart muscle. A Ca^{2+} spark occurs with the opening of a cluster of SR RyRs to release Ca^{2+} in a locally regenerative manner. It, in turn, activates the Ca^{2+} -release channels and induces further release of Ca^{2+} from subsarcolemmal cisternae in the SR and thus leads to a large increase in intracellular Ca^{2+} ($i\text{Ca}^{2+}$). These spatially and temporally patterned activations of localized Ca^{2+} release, in turn, stimulate myofibrillar contraction. The increase in $i\text{Ca}^{2+}$, however, is transient, inasmuch as Ca^{2+} is removed by active uptake by the SR Ca^{2+} pump adenosine triphosphatase (ATPase), extrusion of Ca^{2+} from the cytosol by the Na^+ - Ca^{2+} exchanger, and binding of Ca^{2+} to proteins.²⁹ Ca^{2+} sparks have also been implicated in pathophysiologic diseases such as hypertension, cardiac arrhythmias, heart failure, and muscular dystrophy.³⁰⁻³²

The SR provides the anatomic framework and is the major organelle for the cycling of Ca^{2+} . It is the depot for $i\text{Ca}^{2+}$ stores. The cyclic release plus reuptake of Ca^{2+} by the SR regulates the cytosolic Ca^{2+} concentration and couples excitation to contraction. The physical proximity between L-type Ca^{2+} channels and RyRs at the SR membrane makes Ca^{2+} -induced Ca^{2+} release occur easily. The foot region of the RyR is the part that extends from the SR membrane to the T tubules, where the L-type Ca^{2+} channels are located.^{19,29,33}

The SR is also concerned with the reuptake of Ca^{2+} that initiates relaxation or terminates contraction. The sarcoplasmic/endoplasmic reticulum Ca^{2+} -ATPase (SERCA) pump is the ATP-dependent pump that actively pumps the majority of the Ca^{2+} back into the SR after its release. SERCA makes up close to 90% of all the SR proteins and is inhibited by the phosphoprotein, phospholamban, at rest. Phospholamban is an SR membrane protein that is active in the dephosphorylated form. Phosphorylation by a variety of kinases as a result of β -adrenergic stimulation or other stimuli inactivates phospholamban and releases its inhibitory action on SERCA. Positive feedback ensues and leads to further phospholamban phosphorylation and greater SERCA activity. Active reuptake of Ca^{2+} by SERCA then promotes relaxation.^{19,29,33}

Once taken up into the SR, Ca^{2+} is stored until it is released during the next cycle. Calsequestrin and calreticulin are two storage proteins in the SR. Calsequestrin is a highly charged protein located in the cisternal component of the SR near the T tubules. Because it lies close to the Ca^{2+} -release channels, the stored Ca^{2+} can be quickly discharged for release once the Ca^{2+} -release channels are stimulated. Cytosolic Ca^{2+} can also be removed by extrusion through the sarcolemmal Ca^{2+} pump and the activity of the Na^+ - Ca^{2+} exchanger. The protein, calmodulin, is an important sensor and regulator of $i\text{Ca}^{2+}$.²¹

Errors in Ca^{2+} Handling. Because of the ubiquity of Ca^{2+} in cardiac signaling, changes in Ca^{2+} handling can be associated with numerous maladaptive outcomes. There is an increase in Ca^{2+} leak from the SR in the failing heart, which may be associated with removal of Ca^{2+} from the cytosole.

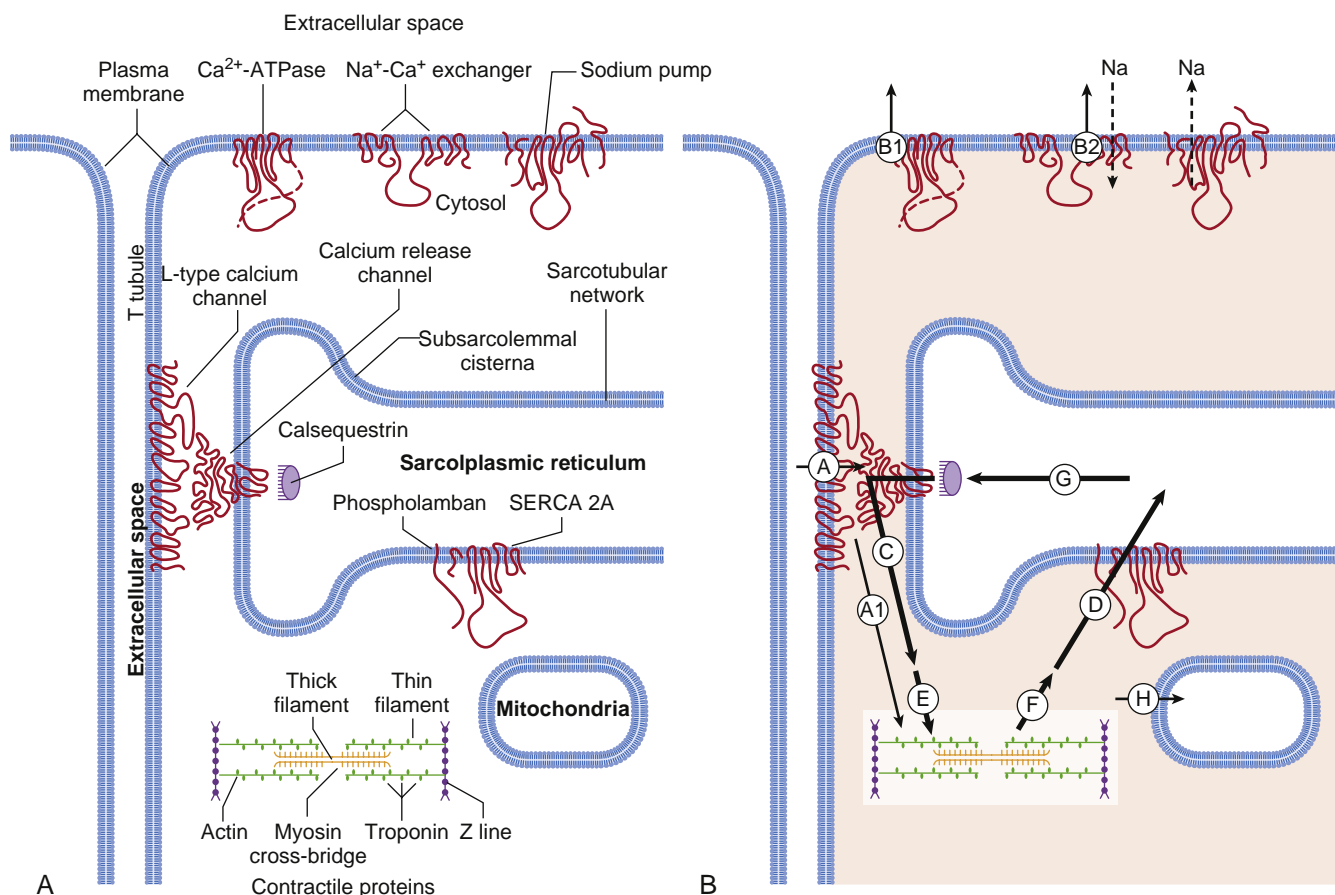


Fig. 14.12 (A) Diagram depicts the components of cardiac excitation-contraction coupling. Calcium pools are noted in **bold** letters. (B) Extracellular (arrows A, B1, B2) and intracellular calcium flux (arrows C, D, E, F, G) are shown. The thickness of the arrows indicates the magnitude of the calcium flux, and the vertical orientations describe their energetics: downward-pointing arrows represent passive calcium flux, whereas upward-pointing arrows represent energy-dependent calcium transport. Calcium entering the cell from extracellular fluid through L-type calcium channels triggers the release of calcium from the sarcoplasmic reticulum. Only a small portion directly activates the contractile proteins (arrow A1). Arrow B1 depicts active transport of calcium into extracellular fluid by means of the plasma membrane calcium adenosine triphosphatase (Ca^{2+} -ATPase) pump and the sodium-calcium (Na^{+} - Ca^{2+}) exchanger. Sodium that enters the cell in exchange for calcium (dashed line) is pumped out of the cytosol by the sodium pump. SR regulates calcium efflux from the subsarcolemmal cisternae (arrow C) and calcium uptake into the sarcotubular network (arrow D). Arrow G represents calcium that diffuses within the SR. Calcium binding to (arrow E) and dissociation from (arrow F) high-affinity calcium-binding sites of troponin C activate and inhibit interactions of the contractile proteins. Arrow H depicts movement of calcium into and out of mitochondria to buffer the cytosolic calcium concentration. SERCA 2A, Sarcoplasmic/endoplasmic reticulum Ca^{2+} -ATPase. (From Katz AM. Calcium fluxes. In: *Physiology of the Heart*. 3rd ed. Philadelphia: Lippincott-Raven; 2001:232–233.)

This Ca^{2+} leak from the SR may significantly reduce contractile force in the heart and contributes to reduced inotropy in heart failure.^{34,35} Uncoupling of β -AR activation of protein kinase A (PKA) and dysregulation of Ca^{2+} handling occurs in heart failure.³⁴ PKA, a cAMP-dependent protein kinase, is a key effector protein activated by β -AR agonists, which stimulates transsarcolemmal Ca^{2+} influx and its sequestration in the SR, leading to increased contractile function and lusitropy. Calcineurin, a Ca^{2+} -dependent signaling molecule, is consistently linked with myocardial hypertrophy via gene expression through a nuclear factor of activated T-cells pathway.^{34,35} Calcium-calmodulin-dependent protein kinase II, in addition to calcineurin, is tightly coupled with Ca^{2+} homeostasis, and its prolonged activation can be proarrhythmic.

Contractile System

Contractile Elements. The basic working unit of contraction is the sarcomere. A *sarcomere* is defined as the distance between Z lines (Z is an abbreviation for the German word,

Zuckung, meaning *contraction*), which join the sarcomeres in series. Each sarcomere consists of a central A band that is separated by one half of an I band from the Z lines on each side because the Z line bisects the I band. A schematic representation is depicted in Fig. 14.13.¹⁰ Within each sarcomere are two principal contractile proteins (see the next section, Contractile Proteins) and one noncontractile protein, titin.²⁹ The two contractile proteins are actin, the thin filament, and myosin, the thick filament. Actin filaments and titin are both tethered to the Z line, but the thick myosin filaments do not actually reach the Z lines. Titin, the third filament protein, tethers the thick-filament myosin to the Z line. The Z lines at the two ends of the sarcomere are brought closer together during contraction as the thick-filament myosin heads interact with the thin actin filaments and slide over each other.^{36,37}

Familial hypertrophic cardiomyopathy is an inherited autosomal dominant sarcomeric disease³⁸ that is the most common cause of sudden death in otherwise healthy individuals. Its clinical features are left ventricular hypertrophy

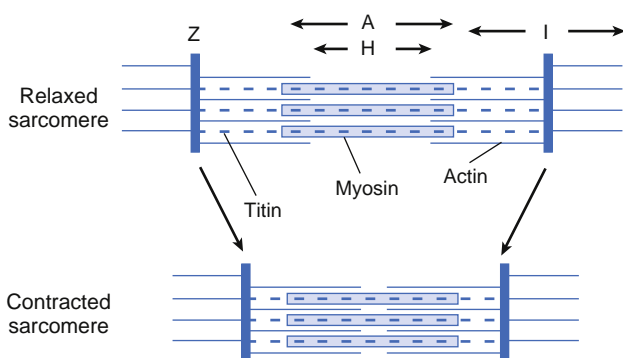


Fig. 14.13 The basic unit of contraction is the sarcomere. A contracted and relaxed sarcomere is depicted. Z lines are located at the ends of the sarcomere. The A band is the site of overlap between myosin and actin filaments. The I band is located on either side of the A band and contains only actin filament. The H zone is located in the center of the A band, and only myosin is present.

and myocyte and myofibrillar disarray. Mutations in at least eight different genes encoding sarcomere proteins have been identified as the molecular basis for the disorder. These genes are β -cardiac myosin heavy chain, cardiac troponin T (TnT), α -tropomyosin, cardiac myosin-binding protein C, essential or regulatory myosin light chain, cardiac troponin I (TnI), α -cardiac actin, and titin.³⁸

Contractile Proteins. The contractile apparatus within the cardiomyocyte consists of contractile and regulatory proteins.^{21,39,40} The thin-filament actin and the thick-filament myosin are the two principal contractile proteins. Actin contains two helical chains. Tropomyosin, a double-stranded α -helical regulatory protein, winds around the actin array and forms the backbone for the thin-filament actin. The thick-filament myosin is made up of 300 myosin molecules. Each myosin molecule has two functional domains: the body or filament and the bilobar myosin head. The myosin head is made up of one heavy chain and two light chains. The heavy head chain has two domains: the larger one interacts with actin at the actin cleft and has an ATP-binding pocket where myosin ATPase is located, and the other smaller one is flexible and attached to the two light chains. The regulatory troponin heterotrimer complex is found at regular intervals along tropomyosin. The heterotrimer troponins are made up of troponin C (TnC), the Ca^{2+} receptor; TnI, an inhibitor of actin-myosin interaction; and TnT, which links the troponin complex to tropomyosin. Tropomodulin is another regulatory protein. It is located at the end of the thin-filament actin and caps the end to prevent any excessive elongation of the thin filament.^{36,37}

Myocyte Contraction and Relaxation. At rest, cross-bridge cycling and generation of force do not occur because either the myosin heads are blocked from physically reacting with the thin filament or they are only weakly bound to actin (Fig. 14.14).¹⁸ Cross-bridge cycling is initiated on binding of Ca^{2+} to TnC, which increases TnC-TnI interaction and decreases the inhibitory TnI-actin interaction. These events, which ensue from the binding of Ca^{2+} to TnC, lead to conformational changes in tropomyosin and permit attachment of the myosin head to actin. Cross-bridging

involves the detachment of the myosin head from actin and a reattachment of myosin to another actin on hydrolysis of ATP by myosin ATPase. Binding of ATP to the nucleotide pocket of the myosin head leads to the activation of myosin ATPase,^{33,36,37} ATP hydrolysis, and changes in the configuration of the myosin head, all of which facilitate binding of the myosin head to actin and the generation of the power stroke of the myosin head. Based on this model, the rate of cross-bridge cycling is dependent on the activity of myosin ATPase.⁴⁰ Turnoff of cross-bridge cycling is largely initiated by the decrease in cytosolic Ca^{2+} .

Myocyte relaxation is an energy-dependent process because restoration of cytosolic Ca^{2+} to resting levels requires the expenditure of ATP. The decrease in cytosolic Ca^{2+} occurs through active reuptake of Ca^{2+} into the SR by SERCA and extrusion of Ca^{2+} by the Na^{+} - Ca^{2+} exchanger. This activity results in the release of Ca^{2+} binding to TnC and the separation of the myosin-actin cross-bridge. Myocyte relaxation is dependent on the kinetics of cross-bridge cycling, the affinity of Ca^{2+} for TnC, and the activity of the Ca^{2+} -reuptake mechanisms. Relaxation is enhanced by the increased kinetics of cross-bridge cycling, decreased Ca^{2+} affinity for TnC, and increased activity of Ca^{2+} -reuptake mechanisms.²⁹

Titin is a giant string-like protein that acts as the third filament within the sarcomere. A single titin molecule spans one half of the sarcomere. Structurally, titin consists of an inextensible anchoring segment and an extensible elastic segment. Its two main functions involve muscle assembly and elasticity. Titin is the principal determinant of the passive properties of the myocardium at small ventricular volumes.⁴¹

The Frank-Starling relationship states that an increase in end-diastolic volume results in enhanced systolic function.^{42,43} At the cellular level, the key component for the Frank-Starling relationship is a length-dependent shift in Ca^{2+} sensitivity.⁴⁴⁻⁴⁶ Several possible mechanisms for this change in Ca^{2+} sensitivity have been implicated, including Ca^{2+} sensitivity: as a function of myofilament lattice spacing, involving positive cooperativity in cross-bridge binding to actin, and dependence on a strain of the elastic protein titin.^{40,44}

Cytoskeleton Proteins. The cytoskeleton is the protein framework within the cytoplasm that links, anchors, or tethers structural components inside the cell.^{18,21} Microfilaments (actin filaments), microtubules, and intermediate filaments are three classes of cytoskeleton proteins found in the cytoplasm. Microfilament proteins are actin filaments, either sarcomeric or cortical, depending on their location. Sarcomeric actin filaments are the thin filaments in the contractile machinery that have been previously described. Cortical actin filaments are found below the plasma membrane at the cell surface and are linked to several other microfilament proteins, including dystrophin, vinculin, and ankyrin. Microtubules assemble by polymerization of the α - and β -dimers of tubulin. They play a major role in intracellular transport and cell division.⁴⁷ Attachment of the ends of microtubules to cellular structures causes the microtubules to expand and contract, thereby pulling and pushing these structures around the cell. The intermediate filaments are relatively insoluble. They have been demonstrated to be important in normal mitochondrial function and behavior. The desmin intermediate filament in cardiomyocytes connects the nucleus to the plasma membrane and is important in the transmission of the stress and strain of contractile force between cells.⁴⁸

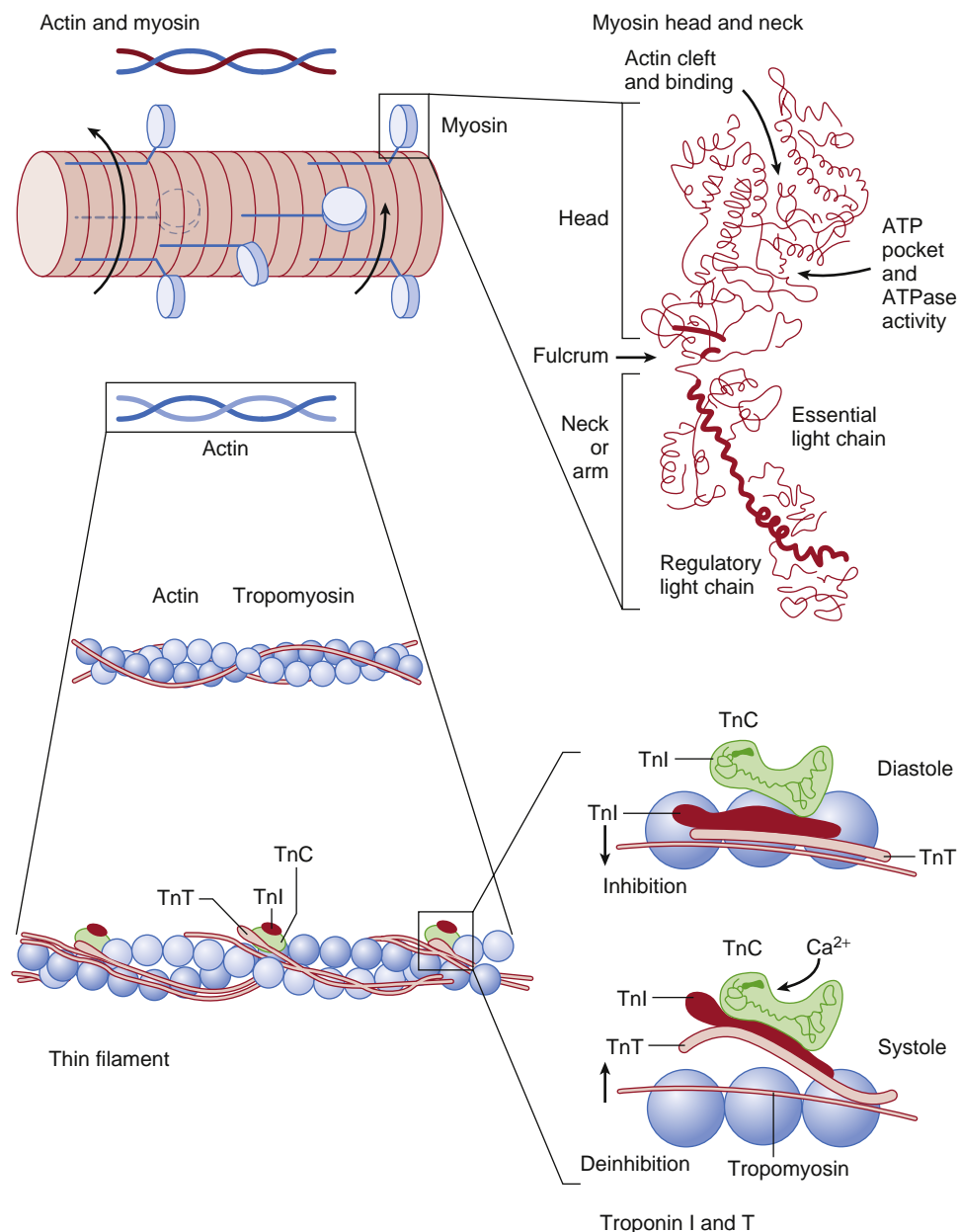


Fig. 14.14 Molecules of the contractile system, troponins C, I, and T (TnC, TnI, and TnT). ATP, Adenosine triphosphate; ATPase, adenosine triphosphatase. (From Opie LH. Ventricular function. In: *Heart Physiology From Cell to Circulation*. 4th ed. Philadelphia: Lippincott-Raven; 2004:209–231.)

The cytoskeleton provides the organization of microenvironments within the cell for enzyme and protein activity and interaction.

Whereas familial hypertrophic cardiomyopathy is a genetic sarcomeric disease, familial dilated cardiomyopathy (FDCM) is a disease of cytoskeleton proteins. The genetic basis of FDCM includes two genes for X-linked FDCM (dystrophin, G4.5) and four genes for the autosomal dominant form (actin, desmin, lamin A/C, and δ -sarcoglycan).¹⁸

Control of Cardiac Function

NEURAL REGULATION OF CARDIAC FUNCTION

The two limbs of the autonomic nervous system provide opposing input to regulate cardiac function.⁴⁹ The

neurotransmitter of the sympathetic nervous system is norepinephrine, which provides positive chronotropic (heart rate), inotropic (contractility), and lusitropic (relaxation) effects. The parasympathetic nervous system has a more direct inhibitory effect in the atria and has a negative modulatory effect in the ventricles. The neurotransmitter of the parasympathetic nervous system is acetylcholine. Both norepinephrine and acetylcholine bind to seven-transmembrane-spanning G protein-coupled receptors (GPCRs) to transduce their intracellular signals and affect their functional responses (Fig. 14.15).⁵⁰ At rest, the heart has a tonic level of parasympathetic cardiac nerve firing and little, if any, sympathetic activity. Therefore, the major influence on the heart at rest is parasympathetic. During exercise or stress, however, the sympathetic neural influence becomes more prominent.

Parasympathetic innervation of the heart is through the vagal nerve. Supraventricular tissue receives significantly more intense vagal innervation than do the ventricles. The principal parasympathetic target neuroeffectors are the muscarinic receptors in the heart.^{51,52} Activation of muscarinic receptors reduces pacemaker activity, slows AV conduction, directly decreases atrial contractile force, and exerts inhibitory modulation of ventricular contractile force. A total of five muscarinic receptors have been cloned.⁵³ M₂ receptors are the predominant subtype found in the mammalian heart. In the coronary circulation, M₃ receptors have been identified. Moreover, non-M₂ receptors have also been reported to exist in the heart. In general, for intracellular signaling, M₁, M₃, and M₅ receptors couple to G_{q/11} protein and activate the phospholipase C-diacylglycerol-inositol phosphate system. On the other hand, the M₂ and M₄ receptors couple to the pertussis toxin-sensitive G protein, G_{i/o}, to inhibit adenylyl cyclase. M₂ receptors can couple to certain K⁺ channels and influence the activity of Ca²⁺ channels, I_f current, phospholipase A₂, phospholipase D, and tyrosine kinases.

In contrast to vagal innervation, sympathetic innervation of the heart is more predominant in the ventricle than in the atrium. Norepinephrine released from sympathetic nerve terminals stimulates adrenergic receptors (adrenoceptors [AdRs]) located in the heart. The two major classes

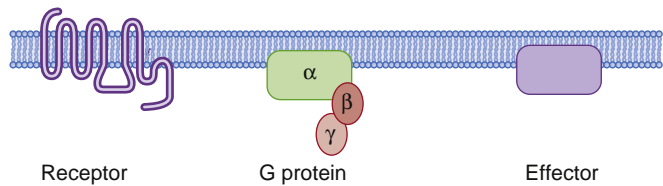


Fig. 14.15 General scheme for a G protein-coupled receptor consisting of receptor, the heterotrimeric G protein, and the effector unit. (Reprinted with permission from Bers DM. Cardiac excitation-contraction coupling. *Nature* 2002;415:198–205. Copyright MacMillan Magazines Ltd.)

of ARs are α and β , both of which are GPCRs that transduce their intracellular signals by means of specific signaling cascades (Fig. 14.16).

β -ARs can be further divided into subpopulations of β_1 , β_2 , and β_3 .⁵⁴ Although most mammalian hearts contain β_1 -ARs and β_2 -ARs, β_3 -ARs also exist in many mammalian ventricular tissues. The relative contribution of each β -AR subtype to modulation of cardiac function varies among species. In humans, β_1 -ARs are the predominant subtype in both the atria and ventricles, but a substantial proportion of β_2 -ARs are found in the atria, and approximately 20% of β_2 -ARs are found in the LV. Much less is known about β_3 -ARs, but they do exist in the human ventricle. Even though the β_1 -AR population is more intense than the β_2 -AR population, the cardiotonic effect is not proportional to the relative densities of these two subpopulations, which is largely attributable to the tighter coupling of β_2 -ARs than β_1 -ARs to the cyclic adenosine monophosphate (cAMP) signaling pathway. Both β_1 -ARs and β_2 -ARs activate a pathway that involves the stimulatory G protein (G_s), activation of adenylyl cyclase, accumulation of cAMP, stimulation of cAMP-dependent PKA, and phosphorylation of key target proteins, including L-type Ca²⁺ channels, phospholamban, and TnI.

Both β_1 -ARs and β_2 -ARs are coupled to the G_s-cAMP pathway. Additionally, β_2 -ARs can couple to G protein-independent pathways to modulate cardiac function, and also couple to the inhibitory G protein (G_i) to activate non-cAMP-dependent signaling pathways. β -AR stimulation increases both contraction and relaxation, as summarized in Fig. 14.17.

The two major subpopulations of α -ARs are α_1 and α_2 . α_1 -ARs and α_2 -ARs can be further subdivided into different subtypes. α_1 -ARs are GPCRs and include the α_{1A} , α_{1B} , and α_{1D} subtypes. The α_1 -AR subtypes are products of separate genes and differ in structure, G protein coupling, tissue distribution, signaling, regulation, and function. Both

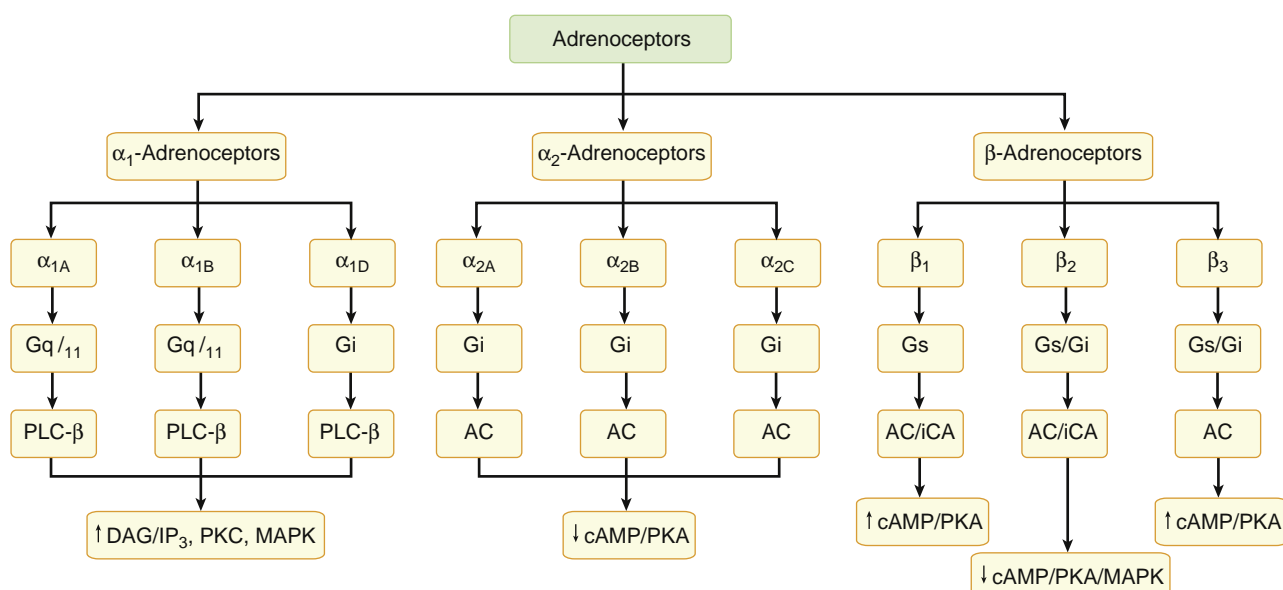


Fig. 14.16 Adrenoceptor signaling cascades involving G proteins and effectors are adenylyl cyclase (AC), L-type calcium current (iCA), and phospholipase β (PLC- β) in the heart. The intracellular signals are diacylglycerol (DAG), inositol 1,4,5-triphosphate (IP₃), protein kinase C (PKC), cyclic adenosine monophosphate (cAMP), protein kinase A (PKA), and mitogen-activated protein kinase (MAPK). G_{q/11}, Heterotrimeric G protein; G_i, inhibitory G protein; G_s, stimulatory G protein.

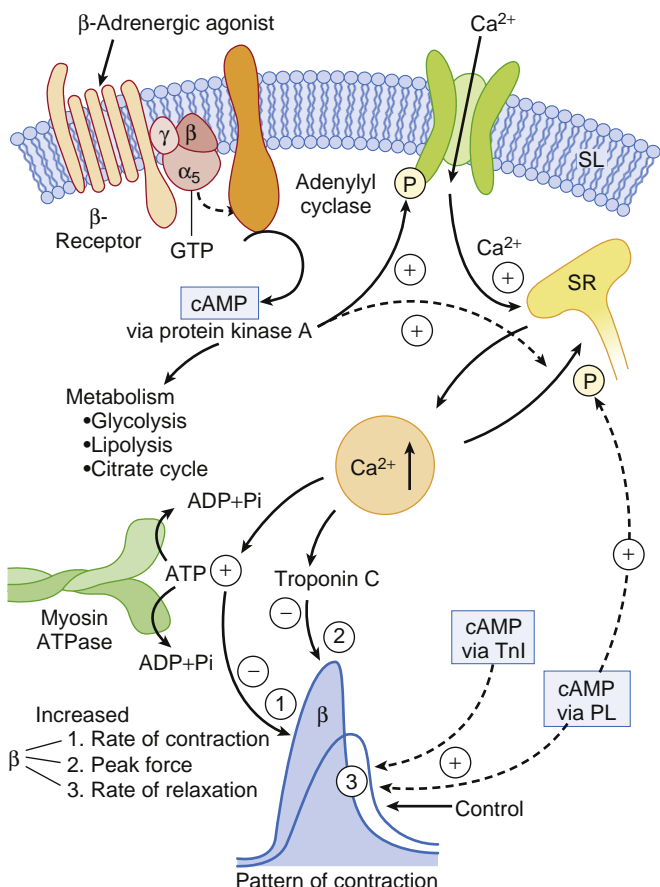


Fig. 14.17 The β -adrenoceptor signaling system leads to an increased rate and force of contraction and increased relaxation. ADP, Adenosine diphosphate; ATP, adenosine triphosphate; ATPase, adenosine triphosphatase; cAMP, cyclic adenosine monophosphate; GTP, guanosine triphosphate; Pi, phosphatidylinositol; PL, phospholipase; SL, sarcolemma; SR, sarcoplasmic reticulum; TnI, troponin I. (From Opie LH. Receptors and signal transduction. In: *Heart Physiology From Cell to Circulation*. 3rd ed. Philadelphia: Lippincott-Raven; 1998:195.)

α_{1A} -ARs and α_{1B} -ARs mediate positive inotropic responses. However, the positive inotropic effect mediated by α_{1A} -ARs is believed to be of minor importance in the heart. α_{1A} -ARs are coupled to phospholipase C, phospholipase D, and phospholipase A₂; they increase iCa^{2+} and myofibrillar sensitivity to Ca^{2+} .

Cardiac hypertrophy is primarily mediated by α_{1A} -ARs.^{55,56} Cardiac hypertrophic responses to α_1 -AR agonists involve activation of protein kinase C and mitogen-activated protein kinase through G_q-signaling mechanisms. Three subtypes of α_2 -ARs are recognized: α_{2A} , α_{2B} , and α_{2C} . In the mammalian heart, α_2 -ARs in the atrium play a role in the presynaptic inhibition of norepinephrine release. These prejunctional α_2 -ARs are believed to belong to the α_{2C} subtype.

Neural regulation of cardiac function involves a complex interaction between the different classes and subpopulations of adrenoceptors and their signaling pathways. Targeted therapeutics in cardiovascular medicine involve the clinical application and manipulation of a basic understanding of adrenoceptor pharmacology.

HORMONES AFFECTING CARDIAC FUNCTION

Many hormones have direct and indirect actions on the heart (Table 14.1). Hormones with cardiac actions can be synthesized and secreted by cardiomyocytes or produced by other tissues and delivered to the heart. They act on specific receptors expressed in cardiomyocytes. Most of these hormone receptors are plasma membrane GPCRs. Non-GPCRs include the natriuretic peptide receptors, which are guanylyl cyclase-coupled receptors, and the glucocorticoid and mineralocorticoid receptors, which bind androgens and aldosterone and are nuclear zinc finger transcription factors. Hormones can have activity in normal cardiac physiologic function or are active only in pathophysiologic conditions, or both situations can apply. Most of the new information regarding the action of hormones in the heart has been derived from the endocrine changes associated with chronic heart failure.⁵⁷

Cardiac hormones are polypeptides secreted by cardiac tissues into the circulation in the normal heart. Natriuretic peptides,^{58,59} aldosterone,⁶⁰ and adrenomedullin⁶¹ are hormones secreted by cardiomyocytes. Angiotensin II, the effector hormone in the renin-angiotensin system, is also produced by cardiomyocytes.^{62,63} The renin-angiotensin system is one of the most important regulators of cardiovascular physiology. It is a key modulator of cardiac growth and function. Angiotensin II stimulates two separate receptor subtypes, AT₁ and AT₂, both of which are present in the heart. AT₁ receptors are the predominant subtype expressed in the normal adult human heart. Stimulation of AT₁ receptors induces a positive chronotropic and inotropic effect. Angiotensin II also mediates cell growth and proliferation in cardiomyocytes and fibroblasts, and induces the release of the growth factors aldosterone and catecholamines through the stimulation of AT₁ receptors. Activation of AT₁ receptors is directly involved in the development of cardiac hypertrophy and heart failure, as well as adverse remodeling of the myocardium. In contrast, AT₂ receptor activation is counterregulatory and generally antiproliferative. Expression of AT₂ receptors, however, is relatively scant in the adult heart because AT₂ receptors are most abundant in the fetal heart and decline with development. In response to injury and ischemia, AT₂ receptors become upregulated. The precise role of AT₂ receptors in the heart remains to be defined.

The beneficial effects of blockade of the renin-angiotensin system with angiotensin-converting enzyme inhibitors in the treatment of heart failure have been attributed to an inhibition of AT₁-receptor activity. In addition to the renin-angiotensin system, other cardiac hormones that have been shown to play pathogenic roles in the promotion of cardiomyocyte growth and cardiac fibrosis, development of cardiac hypertrophy, and progression of congestive heart failure include aldosterone,⁶⁰ adrenomedullin,⁶⁴⁻⁶⁶ natriuretic peptides,^{58,59} angiotensin,⁶⁷⁻⁶⁹ endothelin,⁷⁰ and vasopressin.^{71,72}

Increased stretch of the myocardium stimulates the release of atrial natriuretic protein (ANP) and B-type natriuretic protein (BNP) from the atria and ventricles, respectively. Both ANP and BNP bind to natriuretic peptide receptors to generate the second messenger cyclic guanosine monophosphate and represent part of the cardiac

TABLE 14.1 Actions of Hormones on Cardiac Function

Hormone	Receptor	Cardiac Action	Increase (+) or Decrease (-) With CHF
Adrenomedullin	GPCR	+ Inotropy/+ chronotropy	+
Aldosterone	Cytosolic or nuclear MR		+
Angiotensin	GPCR	+ Inotropy/+ chronotropy	+
Endothelin	GPCR		+
Natriuretic peptides	GCCR		
ANP (ANF)			+
BNP			+
Neuropeptide Y*	GPCR	- Inotropy	+
Vasopressin	GPCR	+ Inotropy/+ chronotropy	+
Vasoactive intestinal peptide [†]	GPCR	+ Inotropy	No
Estrogen	ER α /ER β	Indirect	No
Testosterone	AR	Indirect	No
Progesterone	PR	Indirect	No
Thyroid hormones	NR	+ Inotropy/+ chronotropy	-
Growth hormones	IGF-1	+ Inotropy/+ chronotropy	-

ANF, Atrial natriuretic factor; ANP, atrial natriuretic peptide; AR, androgen receptor; BNP, B-type natriuretic peptide; CHF, congestive heart failure; ER, estrogen receptor; GCCR, guanylyl cyclase-coupled receptor; GPCR, G protein-coupled receptor; IGF-1, insulin growth factor 1; MR, mineralocorticoid receptor; NR, nuclear receptor; PR, progesterone receptor.

*Data from Grundemar L, Hakanson R. Multiple neuropeptide Y receptors are involved in cardiovascular regulation. Peripheral and central mechanisms. *Gen Pharmacol*. 1993;24:785–796; and Maisel AS, Scott NA, Motulsky HJ, et al. Elevation of plasma neuropeptide Y levels in congestive heart failure. *Am J Med*. 1989;86:43–48.

[†]Data from Henning RJ, Sawmiller DR. Vasoactive intestinal peptide: cardiovascular effects. *Cardiovasc Res*. 2001;49:27–37.

endocrine response to hemodynamic changes caused by pressure or volume overload. They also participate in organogenesis of the embryonic heart and cardiovascular system.^{58,59} In patients with chronic heart failure, increases of serum ANP and BNP levels are a predictor of mortality.⁷³

Adrenomedullin is a recently discovered cardiac hormone that was originally isolated from pheochromocytoma tissue. It increases the accumulation of cAMP and has direct positive chronotropic and inotropic effects.^{61,64,65} Adrenomedullin, with interspecies and regional variations, has also been shown to increase nitric oxide production, and it functions as a potent vasodilator.

Aldosterone is one of the cardiac-generated steroids, although its physiologic significance remains to be defined. It binds to mineralocorticoid receptors and can increase the expression or activity (or both) of cardiac proteins involved in ionic homeostasis or the regulation of pH, such as cardiac Na⁺/K⁺-ATPase, the Na⁺-K⁺ cotransporter, Cl⁻-bicarbonate (HCO₃²⁺), and the Na⁺-hydrogen (H⁺) antiporter.⁶⁰ Aldosterone modifies cardiac structure by inducing cardiac fibrosis in both ventricular chambers and thereby leads to impairment of cardiac contractile function.

Other hormones such as the growth hormone,⁷⁴ thyroid hormones,⁷⁵ and sex steroid hormones (see the following text) can also have cardiac effects through direct actions of nuclear receptors or indirect effects.

Sex Steroid Hormones and the Heart

Cardiac contractility is more intense in premenopausal women than in age-matched men, and withdrawal of

hormone replacement therapy in postmenopausal women leads to a reduction in cardiac contractile function. The gender dimorphism in heart function and its adaptive responses to injury and disease states are partly mediated by sex steroid hormones. Indeed, healthy premenopausal women exhibit a lower cardiovascular risk compared to men, which suggests a mechanism for sex hormones in the modulation of cardiac function.⁷⁶

The most extensively studied sex steroid hormones are estradiol-17 β (E2) and its bioactive metabolites. They bind and act on the two subtypes of estrogen receptors (ERs) in the heart: ER α and ER β . Progesterone and testosterone (two other sex steroid hormones) and the enzyme aromatase, which converts testosterone to estrogen, are much less well investigated. Progesterone and testosterone bind and act on their respective progesterone receptors and androgen receptors in the heart. Sex steroid hormones interact with their receptors to affect postsynaptic target cell responses and to influence presynaptic sympathoadrenergic function. Cardiomyocytes are not only targets for the action of sex steroid hormones, but they are also the source of synthesis and the site of metabolism of these hormones.⁷⁷

E2 is derived from testosterone and is primarily metabolized in the liver to form hydroxyestradiols, catecholestradiols, and methoxyestradiols. Estradiol metabolism also takes place in vascular smooth muscle cells, cardiac fibroblasts, endothelial cells, and cardiomyocytes. Cardiomyocytes express nuclear steroid hormone receptors that modulate gene expression and nonnuclear receptors for the nongenomic effects of sex steroid hormones. They interact with

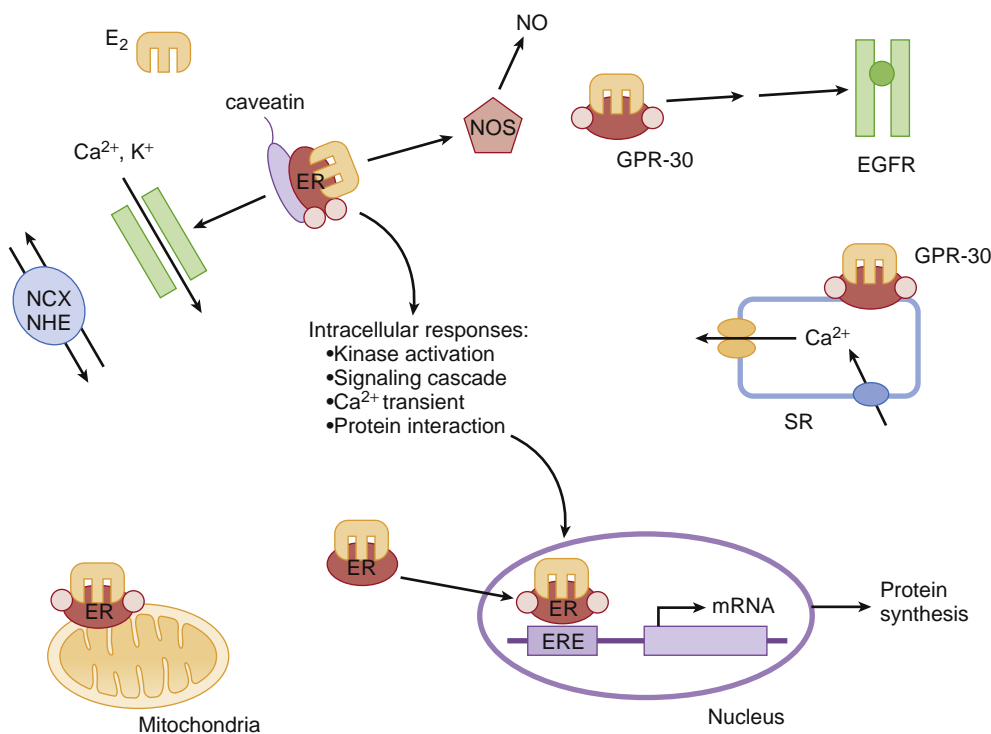


Fig. 14.18 Signaling mechanism of nuclear and nonnuclear localized estrogen receptor (ER) and the estrogen-binding receptor, GPR-30. Nuclear ER influences the transcription of target genes by binding to an ER-response element (ERE) within the promotor region of target genes. E_2 , Estrogen; EGFR, epidermal growth factor receptor; GPR, growth factor receptor; NCX, Na^+-Ca^{2+} exchanger; NHE, Na^+-H^+ exchanger; NO, nitric oxide; NOS, nitric oxide synthase; SR, sarcoplasmic reticulum. (From Du XJ, Fang L, Kiriazis H. Sex dimorphism in cardiac pathophysiology: experimental findings, hormonal mechanisms, and molecular mechanisms. *Pharmacol Ther*. 2006;111:434–475.)

many different coregulators to confer tissue and temporal specificity in their transcriptional actions. These cell-specific coactivator and corepressor proteins are known as estrogen-related receptors.⁷⁸ Sex steroid hormones can activate rapid signaling pathways without changing gene expression (Fig. 14.18). One such example is stimulation of vascular endothelial nitric oxide synthase to mediate vascular dilation. Estrogen's vasodilatory effect might explain the lower systolic blood pressures of premenopausal women when compared with age-matched men. In men, aromatase-mediated conversion of testosterone to estrogen maintains normal vascular tone. In addition to sex steroid hormone stimulation of nuclear or nonnuclear receptors, sex steroid hormone receptors could also induce rapid signaling of growth factor pathways in the absence of ligands.

Gender differences exist in cardiac electrophysiologic function. The modulatory actions of estrogen on Ca^{2+} channels might be responsible for sex-based differences in repolarization of the heart, such as the faster resting heart rate of women, as well as the increased propensity of women to have prolonged QT syndrome.⁷⁹ Estrogen, through the activation of $ER\beta$, confers protection after ischemia and reperfusion in murine models of myocardial infarction. In contrast, testosterone, in the same model, has the opposite effect. Aromatase also has protective effects, probably through its action to increase estrogen and to decrease testosterone.

Gender differences in cardiac physiology should include consideration of the cellular physiology of sex steroid hormones in males and females; intrinsic differences in the physiology of cardiomyocytes, vascular smooth muscle cells, and endothelial cells between males and females; and

gender-based differences in the autonomic modulation of cardiac physiology.

CARDIAC REFLEXES

Cardiac reflexes are fast-acting reflex loops between the heart and the central nervous system (CNS) that contribute to regulation of cardiac function and the maintenance of physiologic homeostasis. Specific cardiac receptors elicit their physiologic responses by various pathways. Cardiac receptors are linked to the CNS by myelinated or unmyelinated afferent fibers that travel along the vagus nerve. Cardiac receptors are in the atria, ventricles, pericardium, and coronary arteries. Extracardiac receptors are located in the great vessels and carotid artery. Sympathetic and parasympathetic nerve input is processed in the CNS. After central processing, efferent fibers to the heart or the systemic circulation will provoke a specific reaction. The response of the cardiovascular system to efferent stimulation varies with age and duration of the underlying condition that elicited the reflex in the first instance.

Baroreceptor Reflex (Carotid Sinus Reflex)

The baroreceptor reflex is responsible for the maintenance of arterial blood pressure. This reflex regulates arterial pressure around a preset value through a negative-feedback loop (Fig. 14.19).^{80,81} In addition, the baroreceptor reflex is capable of establishing a prevailing set point for arterial blood pressure when the preset value has been reset because of chronic hypertension. Changes in arterial blood pressure are monitored by circumferential and longitudinal stretch

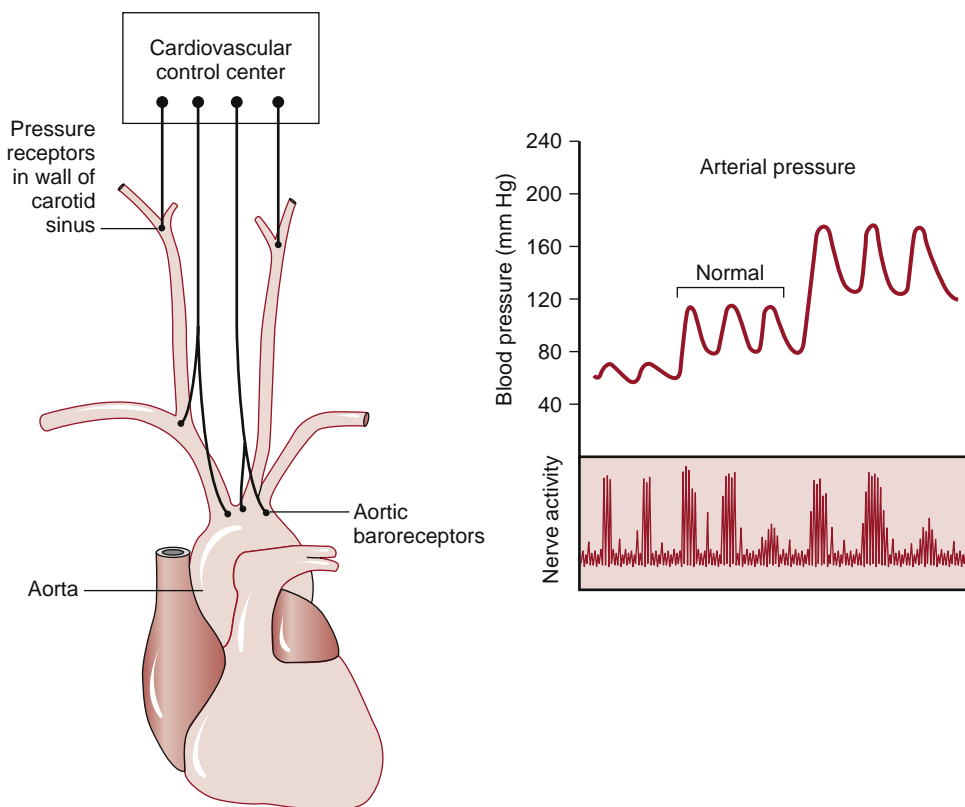


Fig. 14.19 Anatomic configuration of the baroreceptor reflex. Pressure receptors in the wall of the carotid sinuses and aorta detect changes in arterial pressure in the circulation. These signals are conveyed to afferent receptive regions of the medulla through the Hering and vagus nerves. Output from effector portions of the medulla modulates peripheral tone and heart rate. The increase in blood pressure results in increased activation of the reflex (right), which affects a decrease in blood pressure. (From Campagna JA, Carter C. Clinical relevance of the Bezold-Jarisch reflex. *Anesthesiology*. 2003;98:1250–1260.)

receptors located in the carotid sinus and aortic arch. The nucleus solitarius, located in the cardiovascular center of the medulla, receives impulses from these stretch receptors through afferents of the glossopharyngeal and vagus nerves. The cardiovascular center in the medulla consists of two functionally different areas; the area responsible for increasing blood pressure is laterally and rostrally located, whereas the area responsible for lowering arterial blood pressure is centrally and caudally located. The latter area also integrates impulses from the hypothalamus and the limbic system. Typically, stretch receptors are activated if systemic blood pressure is greater than 170 mm Hg. The response of the depressor system includes decreased sympathetic activity, leading to a decrease in cardiac contractility, heart rate, and vascular tone. In addition, activation of the parasympathetic system further decreases the heart rate and myocardial contractility. Reverse effects are elicited with the onset of hypotension.

The baroreceptor reflex plays an important beneficial role during acute blood loss and shock. However, the reflex arch loses its functional capacity when arterial blood pressure is less than 50 mm Hg. Hormonal status and therefore sex differences may alter baroreceptor responses.⁸² Furthermore, volatile anesthetics (particularly halothane) inhibit the heart rate component of this reflex.⁸³ Concomitant use of Ca^{2+} -channel blockers, angiotensin-converting enzyme inhibitors, or phosphodiesterase inhibitors will lessen the cardiovascular response of raising blood pressure through

the baroreceptor reflex. This lessened response is achieved by either their direct effects on the peripheral vasculature or, more importantly, their interference with CNS signaling pathways (Ca^{2+} , angiotensin).⁸⁴ Patients with chronic hypertension often exhibit perioperative circulatory instability as a result of a decrease in their baroreceptor reflex response.

Chemoreceptor Reflex

Chemosensitive cells are located in the carotid bodies and the aortic body. These cells respond to changes in pH status and blood O_2 tension. At an arterial partial O_2 pressure (PaO_2) of less than 50 mm Hg or in conditions of acidosis, the chemoreceptors send their impulses along the sinus nerve of Hering (a branch of the glossopharyngeal nerve) and the tenth cranial nerve to the chemosensitive area of the medulla. This area responds by stimulating the respiratory centers and thereby increasing ventilatory drive. In addition, activation of the parasympathetic system ensues and leads to a reduction in heart rate and myocardial contractility. In the case of persistent hypoxia, the CNS will be directly stimulated, with a resultant increase in sympathetic activity.

Bainbridge Reflex

The Bainbridge reflex⁸⁵⁻⁸⁷ is elicited by stretch receptors located in the right atrial wall and the cavoatrial junction. An increase in right-sided filling pressure sends vagal

afferent signals to the cardiovascular center in the medulla. These afferent signals inhibit parasympathetic activity, thereby increasing the heart rate. Acceleration of the heart rate also results from a direct effect on the SA node by stretching the atrium. The changes in heart rate are dependent on the underlying heart rate before stimulation.

Bezold-Jarisch Reflex

The Bezold-Jarisch reflex responds to noxious ventricular stimuli sensed by chemoreceptors and mechanoreceptors within the left ventricular wall by inducing the triad of hypotension, bradycardia, and coronary artery dilatation.⁸⁰ The activated receptors communicate along unmyelinated vagal afferent type C fibers. These fibers reflexively increase parasympathetic tone. Because it invokes bradycardia, the Bezold-Jarisch reflex is thought of as a cardioprotective reflex. This reflex has been implicated in the physiologic response to a range of cardiovascular conditions such as myocardial ischemia or infarction, thrombolysis, or revascularization and syncope. Natriuretic peptide receptors stimulated by endogenous ANP or BNP may modulate the Bezold-Jarisch reflex. Thus, the Bezold-Jarisch reflex may be less pronounced in patients with cardiac hypertrophy or atrial fibrillation.⁸⁸

Valsalva Maneuver

Forced expiration against a closed glottis produces increased intrathoracic pressure, increased central venous pressure, and decreased venous return. Cardiac output and blood pressure will be decreased after the Valsalva maneuver. This decrease will be sensed by baroreceptors and will reflexively result in an increase in heart rate and myocardial contractility through sympathetic stimulation. When the glottis opens, venous return increases and causes the heart to respond by vigorous contraction and an increase in blood pressure. This increase in arterial blood pressure will, in turn, be sensed by baroreceptors, thereby stimulating the parasympathetic efferent pathways to the heart.

Cushing Reflex

The Cushing reflex is a result of cerebral ischemia caused by increased intracranial pressure. Cerebral ischemia at the medullary vasomotor center induces initial activation of the sympathetic nervous system. Such activation will lead to an increase in heart rate, arterial blood pressure, and myocardial contractility in an effort to improve cerebral perfusion. As a result of the high vascular tone, reflex bradycardia mediated by baroreceptors will ensue.

Oculocardiac Reflex

The oculocardiac reflex is provoked by pressure applied to the globe of the eye or traction on the surrounding structures. Stretch receptors are located in the extraocular muscles. Once activated, stretch receptors will send afferent signals through the short- and long-ciliary nerves. The ciliary nerves will merge with the ophthalmic division of the trigeminal nerve at the ciliary ganglion. The trigeminal nerve will carry these impulses to the gasserian ganglion, thereby resulting in increased parasympathetic tone and subsequent bradycardia. The incidence of this reflex during ophthalmic surgery ranges from 30% to 90%.

Administration of an antimuscarinic drug such as glycopyrrolate or atropine reduces the incidence of bradycardia during eye surgery.

Acknowledgment

The editors, publisher, and Dr. Lena Sun would like to thank Drs. Johanna Schwarzenberger and Radhika Dinavahi for their contribution to this chapter in the prior edition of this work. It has served as the foundation for the current chapter.

 Complete references available online at expertconsult.com.

References

1. Harvey W. *On the Motion of the Heart and Blood in Animals* [Willis R, Trans]. *Scientific Papers: Physiology, Medicine, Surgery, Geology*, vol. 38. P. F. Collier & Son; 1910.
2. Shultz SG. *News Physiol Sci*. 2002;17:175–180.
3. Berne RM, Levy MN. The cardiac pump. In: *Cardiovascular Physiology*. St. Louis: Mosby; 2001:55–82.
4. Berne RM, Levy MN. Electrical activity of the heart. In: *Cardiovascular Physiology*. St. Louis: Mosby; 2001:7–32.
5. Katz AM. The heart as a muscular pump. In: *Physiology of the Heart*. Philadelphia: Lippincott-Raven; 2001:408–417.
6. Takayama Y, Costa KD, Covell JW. *Am J Physiol Heart Circ Physiol*. 2002;282:H1510.
7. Katz AM. Structure of the heart. In: *Physiology of the Heart*. Philadelphia: Lippincott-Raven; 2001:1.
8. Opie LH. Heart cells and organelles. In: *Heart Physiology From Cell to Circulation*. Philadelphia: Lippincott-Raven; 2004:42.
9. Little WC. Assessment of normal and abnormal cardiac function. In: Braunwald E, ed. *Heart Disease*. 6th ed. Philadelphia: Saunders; 2001:479.
10. LeWinter MM, Osol G. Normal physiology of the cardiovascular system. In: Fuster V, Alexander RW, O'Rourke RA, eds. *Hurst's the heart*. 10th ed. New York: McGraw-Hill; 2001:63.
11. Zile MR, Brutsaert DL. *Circulation*. 2002;105:1387.
12. Opie LH. Ventricular function. In: *Heart Physiology From Cell to Circulation*. Philadelphia: Lippincott-Raven; 2004:355.
13. Frank O. *Z Biol*. 1895;32:370.
14. Starling EH. *Linacre Lecture on the Law of the Heart*. London: Longmans Green; 1918.
15. Holubarsch CT, et al. *Circulation*. 1996;94:683.
16. Katz AM. The working heart. In: *Physiology of the Heart*. Philadelphia: Lippincott-Raven; 2001:418.
17. Opie LH. Mechanisms of cardiac contraction and relaxation. In: Braunwald E, ed. *Heart Disease*. 6th ed. Philadelphia: Saunders; 2001:443.
18. Roberts R. Principles of molecular cardiology. In: Alexander RW, O'Rourke RA, eds. *Hurst's the heart*. 10th ed. New York: McGraw-Hill; 2001:95.
19. Opie LH. Myocardial contraction and relaxation. In: *Heart Physiology From Cell to Circulation*. Philadelphia: Lippincott-Raven; 2004:221.
20. Severs NJ. *Bioessays*. 2000;22:188.
21. Katz AM. Contractile proteins and cytoskeleton. In: *Physiology of the Heart*. Philadelphia: Lippincott-Raven; 2001:123.
22. Yeager M. *J Struct Biol*. 1998;121:231.
23. Severs NJ. *Adv Myocardiol*. 1985;5:223.
24. DiFrancesco D. *Circ Res*. 2010;106:434.
25. Fill M, Copella JA. *Physiol Rev*. 2002;82:893.
26. Baruscotti M, DiFrancesco D. *Ann NY Acad Sci*. 2004;1015:111.
27. Kumar NM, Gilula NB. *Cell*. 1996;84:381.
28. Katz AM. The cardiac action potential. In: *Physiology of the Heart*. Philadelphia: Lippincott-Raven; 2001:478.
29. Katz AM. Calcium fluxes. In: *Physiology of the Heart*. Philadelphia: Lippincott-Raven; 2001:478.
30. Katz AM, Lorell BH. *Circulation*. 2000;102:69–74.
31. Cheng H, Lederer WJ. *Physiol Rev*. 2008;88:1491.
32. Cheng H, et al. *Cell Calcium*. 1996;20:129.
33. Bers DM. *Nature*. 2002;415:198.
34. Luo M, Anderson ME. *Circ Res*. 2013;113:690–708.

35. Hajjar RJ, Ishikawa K, Thum T. Molecular and cellular biology of the heart. In: Fuster V, Harrington RA, Narula J, Eapen ZJ, eds. *Hurst's The Heart*, 14e New York, NY: McGraw-Hill.
36. Opie LH. Excitation-contraction coupling. In: *Heart Physiology From Cell to Circulation*. Philadelphia: Lippincott-Raven; 2004:159.
37. de Tombe PP. *J Biomech*. 2003;36:721.
38. Bonne GL, et al. *Circ Res*. 1998;83:580.
39. Solaro RJ, Rarick HM. *Circ Res*. 1998;83:417.
40. Fuchs F, Smith SH. *News Physiol Sci*. 2001;16:5.
41. Trinick J, Tskhovrebova L. *Trends Cell Biol*. 1999;9:377.
42. Moss RL, Fitzsimons DP. *Circ Res*. 2002;90:11.
43. Alvarez BV, et al. *Circ Res*. 1999;85:716.
44. Konhilas JP, et al. *Circ Res*. 2002;90:59.
45. Konhilas JP, et al. *J Physiol*. 2002;544:225.
46. Fukuda N, et al. *Circulation*. 2001;104:1639.
47. Capetanaki Y. *Trends Cardiovasc Med*. 2002;12:339.
48. Howard J, Hyman AA. *Nature*. 2003;422:753.
49. Opie LH. Receptors and signal transduction. In: *Heart Physiology From Cell to Circulation*. Philadelphia: Lippincott-Raven; 2004:187.
50. Rockman HA, et al. *Nature*. 2002;415:206.
51. Mendelowitz D. *News Physiol Sci*. 1999;14:155.
52. Brodde OE, Michel MC. *Pharmacol Rev*. 1999;51:651.
53. Dhein S, et al. *Pharmacol Res*. 2001;44:161.
54. Kaumann AJ, Molenaar P. *Naunyn Schmiedebergs Arch Pharmacol*. 1997;355:667.
55. Endoh M. *Neurochem Res*. 1996;21:217.
56. Arteaga GMT, et al. *Ann Med*. 2002;34:248.
57. van der Horst IC, et al. *Neth Heart J*. 2010;18:190.
58. Cameron VA, Ellmers LJ. *Endocrinology*. 2003;144:2191.
59. de Bold AJ, et al. *Cardiovasc Res*. 1996;31:7.
60. Delcayre C, Silvestre JS. *Cardiovasc Res*. 1999;42:7.
61. Martinez A. *Microsc Res Tech*. 2002;57:1.
62. Dinh DT, et al. *Clin Sci*. 2001;100:481.
63. Schuijt MP, Jan Danser AH. *Am J Hypertens*. 2002;15:1109.
64. Kitamura K, et al. *Microsc Res Tech*. 2002;57:3.
65. Minamino N, et al. *Microsc Res Tech*. 2002;57:28.
66. Smith DM, et al. *Biochem Soc Trans*. 2002;30:432.
67. Mello De WC. *J Mol Med*. 2001;79:103.
68. Opie LH, Sack MN. *Circ Res*. 2001;88:654.
69. Scicchitano P, et al. *Molecules*. 2012;17:4225.
70. Kramer BK, et al. *J Mol Med*. 1997;75:886.
71. Chandrashekhar Y, et al. *J Mol Cell Cardiol*. 2003;35:495.
72. Walker BR, et al. *Am J Physiol*. 1988;255:H261.
73. Giannakoulas G, et al. *Am J Cardiol*. 2010;105:869.
74. Palmeiro CR, et al. *Cardiol Rev*. 2012;20:197.
75. Danzi S, Klein I. *Med Clin North Am*. 2012;96:257.
76. Clerico A, et al. *Am J Physiol Heart Circ Physiol*. 2011;301:H12–H20.
77. Mendelsohn ME. *Science*. 2005;308:1583.
78. Du XJ, et al. *Pharmacol Ther*. 2006;111:434.
79. Pham TV, Rosen MR. *Cardiovasc Res*. 2002;53:740.
80. Campagna JA, Carter C. *Anesthesiology*. 2003;98:1250.
81. Parlow JL, et al. *Anesthesiology*. 1999;90:681.
82. Huikuri HV, et al. *Circulation*. 1996;94:122.
83. Keyl C, et al. *Anesth Analg*. 2002;95:1629.
84. Devlin MG, et al. *Clin Exp Pharmacol Physiol*. 2002;29:372.
85. Crystal GJ, Salem MR. *Anesth Analg*. 2012;114:520.
86. Hakumaki MO. *Acta Physiol Scand*. 1987;130:177.
87. Ludbrook J. *Annu Rev Physiol*. 1983;45:155.
88. Thomas CJ, Woods RL. *Hypertension*. 2003;41:279.

References

1. Harvey W. *On the Motion of the Heart and Blood in Animals* [Willis R, Trans]. *Scientific Papers; Physiology, Medicine, Surgery, Geology*, vol. 38. P. F. Collier & Son; 1910.
2. Shultz Stanley G. William Harvey and the circulation of the blood: the birth of a scientific revolution and modern physiology. *News Physiol Sci*. 2002;17:175–180.
3. Berne RM, Levy MN. The cardiac pump. In: *Cardiovascular Physiology*. St. Louis: Mosby; 2001:55–82.
4. Berne RM, Levy MN. Electrical activity of the heart. In: *Cardiovascular Physiology*. St. Louis: Mosby; 2001:7–32.
5. Katz AM. The heart as a muscular pump. In: *Physiology of the Heart*. Philadelphia: Lippincott-Raven; 2001:408–417.
6. Takayama Y, Costa KD, Covell JW. Contribution of laminar myofiber architecture to load-dependent changes in mechanics of LV myocardium. *Am J Physiol Heart Circ Physiol*. 2002;282:H1510–H1520.
7. Katz AM. Structure of the heart. In: *Physiology of the Heart*. Philadelphia: Lippincott-Raven; 2001:1–38.
8. Opie LH. Heart cells and organelles. In: *Heart Physiology From Cell to Circulation*. Philadelphia: Lippincott-Raven; 2004:42–69.
9. Little WC. Assessment of normal and abnormal cardiac function. In: Braunwald E, ed. *Heart Disease*. 6th ed. Philadelphia: Saunders; 2001:479–502.
10. LeWinter MM, Osol G. Normal physiology of the cardiovascular system. In: Alexander RW, O'Rourke RA, eds. *Hurst's the Heart*. 10th ed. New York: McGraw-Hill; 2001:63–94.
11. Zile MR, Brutsaert DL. New concepts in diastolic dysfunction and diastolic heart failure. *Circulation*. 2002;105:1387–1393.
12. Opie LH. Ventricular function. In: *Heart Physiology From Cell to Circulation*. Philadelphia: Lippincott-Raven; 2004:355–401.
13. Frank O. Zur Dynamik des Herzmuskels. *Z Biol*. 1895;32:370.
14. Starling EH. *Linacre Lecture on the Law of the Heart*. London: Longmans Green; 1918.
15. Holubarsch C, Ruf T, Goldstein D, et al. Existence of the Frank-Starling mechanism in the failing human heart. *Circulation*. 1996;94:683–689.
16. Katz AM. The working heart. In: *Physiology of the Heart*. 3rd ed. Philadelphia: Lippincott-Raven; 2001:418–443.
17. Opie LH. Mechanisms of cardiac contraction and relaxation. In: Braunwald E, ed. *Heart Disease*. 6th ed. Philadelphia: Saunders; 2001:443–478.
18. Roberts R. Principles of molecular cardiology. In: Alexander RW, O'Rourke RA, eds. *Hurst's the Heart*. 10th ed. New York: McGraw-Hill; 2001:95–112.
19. Opie LH. Myocardial contraction and relaxation. In: *Heart Physiology From Cell to Circulation*. Philadelphia: Lippincott-Raven; 2004:221–245.
20. Severs NJ. The cardiac muscle cell. *Bioessays*. 2000;22:188–199.
21. Katz AM. Contractile proteins and cytoskeleton. In: *Physiology of the Heart*. Philadelphia: Lippincott-Raven; 2001:123–150.
22. Yeager M. Structure of cardiac gap junction inter-cellular channels. *J Struct Biol*. 1998;121:231–245.
23. Severs NJ. Intercellular junctions and the cardiac intercalated disk. *Adv Myocardiol*. 1985;5:223–242.
24. DiFrancesco D. The role of the funny current in pacemaker activity. *Circ Res*. 2010;106(3):434–446.
25. Fill M, Copella JA. Ryanodine receptor calcium release channels. *Physiol Rev*. 2002;82:893–922.
26. Baruscotti M, DiFrancesco D. Pacemaker channels. *Ann N Y Acad Sci*. 2004;1015:111–121.
27. Kumar NM, Gilula NB. The gap junction communication channel. *Cell*. 1996;84:381–388.
28. Katz AM. The cardiac action potential. In: *Physiology of the Heart*. Philadelphia: Lippincott-Raven; 2001:478–516.
29. Katz AM. Calcium fluxes. In: *Physiology of the Heart*. Philadelphia: Lippincott-Raven; 2001:478–516.
30. Katz AM, Lorell BH. Regulation of cardiac contraction and relaxation. *Circulation*. 2000;102:69–74.
31. Cheng H, Lederer WJ. Calcium sparks. *Physiol Rev*. 2008;88:1491–1545.
32. Cheng H, Lederer MR, Xiao RP, et al. Excitation-contraction coupling in heart: new insights from Ca²⁺ sparks. *Cell Calcium*. 1996;20:129–140.
33. Bers DM. Cardiac excitation-contraction coupling. *Nature*. 2002;415:198–205.
34. Luo M, Anderson ME. Mechanisms of altered Ca²⁺ handling in heart failure. *Circulation Research*. 2013;113:690–708.
35. Hajjar RJ, Ishikawa K, Thum T. Molecular and cellular biology of the heart. In: Fuster V, Harrington RA, Narula J, Eapen ZJ, eds. *Hurst's The Heart*, 14th ed. New York, NY: McGraw-Hill.
36. Opie LH. Excitation-contraction coupling. In: *Heart Physiology From Cell to Circulation*. Philadelphia: Lippincott-Raven; 2004:159–185.
37. de Tombe PP. Cardiac myofilaments: mechanics and regulation. *J Biomed*. 2003;36:721–730.
38. Bonne G, Carrier L, Richard P, et al. Familial hypertrophic cardiomyopathy, from mutations to functional defect. *Circ Res*. 1998;83:580–593.
39. Solaro RJ, Rarick HM. Troponin and tropomyosin. *Circ Res*. 1998;83:417–480.
40. Fuchs F, Smith SH. Calcium, cross-bridges, and the Frank-Starling relationship. *News Physiol Sci*. 2001;16:5–10.
41. Trinick J, Tskhovrebova L. Titin: a molecular control freak. *Trends Cell Biol*. 1999;9:377–380.
42. Moss RL, Fitzsimons DP. Frank-Starling relationship. *Circ Res*. 2002;90:11–13.
43. Alvarez BV, Perez NG, Ennis IL, et al. Mechanisms underlying the increase in force and Ca²⁺ transient that follow stretch of cardiac muscle. *Circ Res*. 1999;85:716–722.
44. Konhilas JP, Irving TC, de Tombe PP. Myofilament calcium sensitivity in skinned rat cardiac trabeculae. *Circ Res*. 2002;90:59–65.
45. Konhilas JP, Irving TC, de Tombe PP. Length-dependent activation in three striated muscle types of the rat. *J Physiol*. 2002;544:225–236.
46. Fukuda N, Sasaki D, Ishiwata S, Kurihara S. Length dependence of tension generation in rat skinned cardiac muscle. *Circulation*. 2001;104:1639–1645.
47. Capetanaki Y. Desmin cytoskeleton: a potential regulator of muscle mitochondrial behavior and function. *Trends Cardiovasc Med*. 2002;12:339–348.
48. Howard J, Hyman AA. Dynamics and mechanics of the microtubule plus end. *Nature*. 2003;422:753–758.
49. Opie LH. Receptors and signal transduction. In: *Heart Physiology From Cell to Circulation*. Philadelphia: Lippincott-Raven; 2004:187.
50. Rockman HA, Koch WJ, Lefkowitz RJ. Seven-transmembrane-spanning receptors and heart function. *Nature*. 2002;415:206–212.
51. Mendelowitz D. Advances in parasympathetic control of heart rate and cardiac function. *News Physiol Sci*. 1999;14:155–161.
52. Brodde OE, Michel MC. Adrenergic and muscarinic receptors in the human heart. *Pharmacol Rev*. 1999;51:651–689.
53. Dhein S, Van Koppen CJ, Brodde OE. Muscarinic receptors in the mammalian heart. *Pharmacol Res*. 2001;44:161–182.
54. Kaumann AJ, Molenaar P. Modulation of human cardiac function through 4 beta-adrenoceptor populations. *Naunyn Schmiedebergs Arch Pharmacol*. 1997;355:667–681.
55. Endoh M. Cardiac alpha(1)-adrenoceptors that regulate contractile function: subtypes and subcellular signal transduction mechanisms. *Neurochem Res*. 1996;21:217–229.
56. Arteaga GM, Kobayashi T, Solaro RJ. Molecular actions of drugs that sensitize cardiac myofilaments to Ca²⁺. *Ann Med*. 2002;34:248–258.
57. van der Horst IC, et al. Neurohormonal profile of patients with heart failure and diabetes. *Neth Heart J*. 2010;18(4):190–196.
58. Cameron VA, Ellmers LJ. Minireview: natriuretic peptides during development of the fetal heart and circulation. *Endocrinology*. 2003;144:2191–2194.
59. de Bold AJ, Bruneau BG, Kuroski de Bold M. Mechanical and neuroendocrine regulation of the endocrine heart. *Cardiovasc Res*. 1996;31:7–18.
60. Delcayre C, Silvestre JS. Aldosterone and the heart: towards a physiological function? *Cardiovasc Res*. 1999;42:7–12.
61. Martinez A. Biology of adrenomedullin. Introduction. *Microsc Res Tech*. 2002;57:1–2.
62. Dinh DT, et al. Angiotensin receptors: distribution, signalling and function. *Clin Sci*. 2001;100:481–492.
63. Schuijt MP, Jan Danser AH. Cardiac angiotensin II: an intracrine hormone? *Am J Hypertens*. 2002;15:1109–1116.
64. Kitamura K, Kangawa K, Eto T. Adrenomedullin and PAMP: discovery, structures, and cardiovascular functions. *Microsc Res Tech*. 2002;57:3–13.
65. Minamino N, Kikumoto K, Isumi Y. Regulation of adrenomedullin expression and release. *Microsc Res Tech*. 2002;57:28–39.

66. Smith DM, Coppock HA, Withers DJ, et al. Adrenomedullin: receptor and signal transduction. *Biochem Soc Trans*. 2002;30:432–437.
67. De Mello WC. Cardiac arrhythmias: the possible role of the renin-angiotensin system. *J Mol Med*. 2001;79:103–108.
68. Opie LH, Sack MN. Enhanced angiotensin II activity in heart failure. *Circ Res*. 2001;88:654–658.
69. Scicchitano P, Carbonara S, Ricci G, et al. HCN channels and heart rate. *Molecules*. 2012;17:4225–4235.
70. Kramer BK, Ittner KP, Beyer ME, et al. Circulatory and myocardial effects of endothelin. *J Mol Med*. 1997;75:886–890.
71. Chandrashekhar Y, Prahast AJ, Sen A, et al. The role of arginine vasopressin and its receptors in the normal and failing rat heart. *J Mol Cell Cardiol*. 2003;35:495–504.
72. Walker BR, Childs ME, Adamas EM. Direct cardiact effects of vasopressin: role of V1 and V2 vasopressinergic receptors. *Am J Physiol*. 1988;255:H261–H265.
73. Giannakoulas G, Dimopoulos K, Bolger AP, et al. Usefulness of natriuretic peptide levels to predict mortality in adults with congenital heart disease. *Am J Cardiol*. 2010;105:869–873.
74. Palmeiro CR, Anand R, Dardi IK, et al. Growth hormone and the cardiovascular system. *Cardiol Rev*. 2012;20:197–207.
75. Danzi S, Klein I. Thyroid hormone and the cardiovascular system. *Med Clin North Am*. 2012;96(2):257–268.
76. Clerico Aldo, Giannoni Alberto, Vittorini Simona, Passino Claudio. Thirty years of the heart as an endocrine organ: physiological role and clinical utility of cardiac natriuretic hormones. *Am J Physiol Heart Circ Physiol*. 2011;301:H12–H20.
77. Mendelsohn ME. Molecular and cellular basis of cardiovascular gender differences. *Science*. 2005;308:1583–1587.
78. Du XJ, Fang L, Kiriazis H. Sex dimorphism in cardiac pathophysiology: experimental findings, hormonal mechanisms, and molecular mechanisms. *Pharmacol Ther*. 2006;111:434–475.
79. Pham TV, Rosen MR. Sex, hormones and repolarization. *Cardiovasc Res*. 2002;53:740–751.
80. Campagna JA, Carter C. Clinical relevance of the Bezold-Jarisch reflex. *Anesthesiology*. 2003;98:1250–1260.
81. Parlow JL, Begou G, Sagnard P, et al. Cardiac baroreflex during the postoperative period in patients with hypertension. *Anesthesiology*. 1999;90:681–692.
82. Huikuri HV, Pikkujamsa SM, Airaksinen KE, et al. Sex-related differences in autonomic modulation of heart rate in middle-aged subjects. *Circulation*. 1996;94:122–125.
83. Keyl C, Schneider A, Hobbhahn J, Bernardi L. Sinusoidal neck suction for evaluation of baroreflex sensitivity during desflurane and sevoflurane anesthesia. *Anesth Analg*. 2002;95:1629–1636.
84. Devlin MG, Angus JA, Wilson KM, Wright CE. Acute effects of L- and T-type calcium channel antagonists on cardiovascular reflexes in conscious rabbits. *Clin Exp Pharmacol Physiol*. 2002;29:372–380.
85. Crystal GJ, Salem MR. The Bainbridge and the “reverse” Bainbridge reflexes: history, physiology, and clinical relevance. *Anesth Analg*. 2012;114:520–532.
86. Hakumaki MO. Seventy years of the Bainbridge reflex. *Acta Physiol Scand*. 1987;130:177–185.
87. Ludbrook J. Reflex control of blood pressure during exercise. *Annu Rev Physiol*. 1983;45:155–168.
88. Thomas CJ, Woods RL. Guanylyl cyclase receptors mediate cardiopulmonary vagal reflex actions of ANP. *Hypertension*. 2003;41:279–285.

KEY POINTS

- The gastrointestinal (GI) tract forms a long tube from mouth to anus and its main functions are motility, digestion, absorption, excretion, and circulation. Each component of the GI tract has specific functions.
- The layers of the GI tract wall are (outermost to innermost): serosa, longitudinal muscle, circular muscle, submucosa, and mucosa. Within the mucosa is (outermost to innermost): muscularis mucosae, lamina propria, and epithelium.
- The GI tract is innervated by the autonomic nervous system. The extrinsic nervous system consists of the sympathetic, which is primarily inhibitory, and parasympathetic, which is primarily excitatory on GI tract motility. The enteric nervous system controls motility, secretion, and blood flow.
- Mixing movements and propulsive movements are the two primary movements within and along the GI tract. The mechanisms for each are altered significantly in the diseased state and there are multiple modalities for evaluating these alterations.
- The effect of general anesthesia on the GI tract is multifaceted and everything from the medications administered to the hemodynamic side effects can alter GI tract function. Opioids, in particular, have an adverse effect on the bowel and there are many efforts underway to decrease the use of opioids in GI surgery.
- Hemodynamic changes, bowel manipulation, and open abdominal surgeries can produce major effects on the anatomy and function of the GI tract including postoperative ileus, inflammatory states, mesenteric ischemia, and partial or total disruption of myogenic continuity.
- The innervation of the GI organs up to the proximal transverse colon is supplied by the celiac plexus, whereas the innervation of the descending colon and distal GI tract comes from the inferior hypogastric plexus.
- The celiac plexus can be blocked via different approaches, including: transcrural, intraoperative, endoscopic ultrasound-guided, and peritoneal lavage.
- Epidural anesthesia can suppress sympathetic mediated GI reflexes and reduce the incidence of postoperative ileus.
- Pain management strategies that use regional anesthetic techniques and avoid the use of systemic opioids help reduce the incidence of postoperative nausea and vomiting.
- The Enhanced Recovery after GI Surgery (ERAS) protocol and evidence-based practices helps to preserve natural GI physiology and is associated with shorter hospitalizations.
- The ERAS protocol focuses on: optimal perioperative pain control; nutrition; avoidance of unnecessary tubes, lines, and drains; temperature; fluid management; and early ambulation.

Introduction

The purpose of this chapter is to gain an understanding of the various components of gastrointestinal (GI) anatomy and their respective functions. This understanding of the GI system in the healthy state will pave the way for an understanding of how it is affected in different and common disease states. The chapter then transitions into a discussion of perioperative considerations for the anesthetist, including the effects of various anesthetic medications and surgical conditions on bowel function and physiology. The remainder of the chapter will focus on gastrointestinal innervation and how various regional anesthesia and pain management strategies are used when dealing with GI conditions and surgeries.

Gastrointestinal Anatomy and Function

The GI tract constitutes approximately 5% of the total human body mass. Its main functions are motility, digestion, absorption, excretion, and circulation. This section is composed of two parts. In the first part, the basic anatomy and innervation common to all parts of the GI tract are discussed. In the second part the specific anatomy and function of the esophagus, stomach, small bowel, and large bowel are discussed. The pancreas, liver, and biliary tract are covered in Chapter 16.

Common to all parts of the GI tract are the layers of the wall, but the functions of each layer differ from organ to organ.

From outermost to innermost these layers are the serosa, longitudinal muscle layer, circular muscle layer, submucosa, and mucosa. Within the mucosa is (outermost to innermost) the muscularis mucosae, lamina propria, and epithelium. The serosa is a smooth membrane of thin connective tissue and cells that secrete serous fluid that serves to enclose the cavity and reduce friction between muscle movements. The longitudinal muscle layer contracts in order to shorten the length of the intestinal segment whereas the circular muscle layer contracts to decrease the diameter of the intestinal lumen. These two layers work together to allow for gut motility. Between these smooth muscle layers is the myenteric (Auerbach) plexus, which regulates the gut smooth muscle. The submucosa contains the submucosal (Meissner) plexus, which transmits information from the epithelium to the enteric and central nervous systems (CNS). The mucosa is composed of a thin layer of smooth muscle called the muscularis mucosa, which functions to move the villi; the lamina propria, which contains blood vessels, nerve endings, and immune and inflammatory cells; and the epithelium, which is where the GI contents are sensed and where secretion of enzymes, absorption of nutrients, and excretion of waste products occur.

The GI tract is innervated by the autonomic nervous system. This is composed of the extrinsic nervous system, which has sympathetic and parasympathetic components, and the enteric nervous system. The extrinsic sympathetic nervous system is primarily inhibitory as stimulation can decrease or cease GI motility. The preganglionic fibers originate at the T5 to L2 segments of the spinal cord. They travel to the sympathetic chain of ganglia and synapse with postganglionic neurons. Then they travel to the gut where they terminate at the enteric nervous system. The primary neurotransmitter is norepinephrine. Vasoactive intestinal polypeptide (VIP) also transmits sympathetic signals. The extrinsic parasympathetic nervous system is primarily excitatory as it activates GI motility and function. Parasympathetic preganglionic fibers originate in the medulla and sacral region of the spinal cord. Vagus nerve fibers innervate the esophagus, stomach, pancreas, small intestine, and the first half of the large intestine. Pelvic nerve fibers innervate the second half of the large intestine, sigmoid, rectal, and anal regions. The primary neurotransmitter is acetylcholine.

The enteric nervous system is the independent nervous system of the GI tract, which controls motility, secretion, and blood flow. Two plexuses constitute the enteric nervous system: the myenteric (Auerbach) plexus and the submucosal (Meissner) plexus. The myenteric plexus controls motility, which is carried out by enteric neurons, interstitial cells of Cajal (pacemaker cells that generate intrinsic electrical activity of the GI tract), and smooth muscle cells. The submucosal plexus controls absorption, secretion, and mucosal blood flow. Both of these plexuses respond to sympathetic and parasympathetic stimulation. Sympathetic stimulation is inhibitory so it will increase the tone of the intestinal wall whereas parasympathetic stimulation is excitatory and will induce intestinal contractions and movement. Additionally, there are a variety of reflexes in the enteric nervous system. For example, when there is sympathetic stimulation the tone of the wall

increases, the sphincters contract, and, reflexively, the amount of excitatory acetylcholine released is reduced. The mechanism is via α -2 activation, which inhibits the release of acetylcholine and through β activation which contracts sphincter muscles and relaxes intestinal muscles. These two actions work together to slow the transit of contents through the GI tract.

This next section serves to briefly discuss the anatomy and function of the various components of the GI tract. Only the esophagus, stomach, small intestine, and large intestine are covered. See Table 15.1 for an overview of GI tract anatomy and function.

The esophagus is a muscular tube that connects the pharynx to the stomach. It is the first passageway for food entry into the digestive system. It is approximately 18 to 25 cm in length and extends from the level of the hypopharynx at the C6 vertebrae down to the gastroesophageal (GE) junction at the T11 level.¹ The esophagus has three regions: cervical, thoracic, and abdominal. The cervical esophagus is approximately 4 to 5 cm long and is surrounded by the trachea anteriorly, the vertebral column posteriorly, and the carotid sheaths and thyroid gland laterally. The thoracic esophagus spans from the suprasternal notch to the diaphragmatic hiatus and lies posterior to the trachea. At the level of the carina, it deviates right to allow room for the aortic arch and runs posteriorly and underneath the left mainstem bronchus. From T8 to the diaphragmatic hiatus (T10) the esophagus runs anterior to the aorta. The abdominal esophagus extends from the diaphragmatic hiatus to the cardia of the stomach. The upper one-third of the esophagus is composed of striated muscle and the remaining two-thirds is smooth muscle. There are two areas of high pressure: the upper esophageal sphincter (UES) and the lower esophageal sphincter (LES). The UES lies at the level of the cricoid cartilage and is made up of the cricopharyngeal, inferior constrictor, and circular esophageal muscles. Resting tone ranges from 30–200 mm Hg. Opening and closing of the UES is coordinated with the pharyngeal pushing of food downstream. The LES is formed intrinsically by circular esophageal muscle and extrinsically by the diaphragm muscle. It has both sympathetic and parasympathetic innervation. Resting tone is 10–45 mm Hg.²

The stomach is a J-shaped dilation of the alimentary tract. It is divided into four regions: the cardia, fundus, body or corpus, and antrum. The stomach has three main functions: store large quantities of food (up to 1.5–2 liters), mix food with gastric secretions to form chyme and break down particle size, and slow emptying into the small intestine. The proximal stomach is the reservoir for undigested food and produces smooth, tonic contractions. The distal stomach grinds, mixes, and sieves food particles via high-amplitude contractions. Notable cell types in the stomach that aid in digestion are the mucous cells, which protect against harsh hydrochloric acid; parietal cells, which secrete hydrochloric acid; chief cells, which secrete pepsin; and G cells, which secrete gastrin. Together these cells' secretions break down and partially digest the food into chyme as well as reduce particle dimension to an appropriate size (2 mm or less) before it enters the small intestine.²

TABLE 15.1 Table of Gastrointestinal Components, Locations, and Functions

Component	Location	Function
Esophagus	Extends from C6 to T11	Propels food from the pharynx to the stomach
Stomach	Left upper abdominal cavity. Diaphragm along the top, pancreas posteriorly, greater omentum laterally	Receives food from the esophagus and initiates digestion. Breaks down food into chyme through physical and chemical mechanisms
Duodenum	Inferior to stomach, approximately 25–30 cm long	Chemically digests chyme for absorption in the small intestine
Jejunum	Between duodenum and ileum	Absorption of nutrients from chyme
Ileum	Between jejunum and cecum	Further nutrient absorption
Cecum	Lower right quadrant of abdominal cavity, inferior and lateral to the ileum	A space for mixing of chyme with bacteria to form fecal matter
Ascending colon	Runs superiorly from the cecum to the right inferior border of the liver where it turns 90 degrees to become the transverse colon	Peristaltic waves move the feces superiorly where bacteria digest the waste and further nutrients, water, and vitamins are absorbed
Transverse colon	Crosses abdominal cavity right to left just below the stomach	Fecal formation
Descending colon	Runs inferiorly along the left side of the abdominal cavity	Stores fecal matter prior to elimination. Further absorbs water, nutrients, vitamins
Sigmoid colon	Lower left quadrant of the abdominal cavity	Stores fecal matter prior to elimination
Rectum	Posterior pelvic cavity. Along the anterior surface of the sacrum and coccyx	Stores fecal matter prior to elimination. Distention will activate stretch receptors allowing the internal anal sphincter to relax and allow for defecation.

The duodenum is the first and smallest section of the small intestine. It is between 25 and 30 cm long and it forms a C-shaped loop around the pancreas. Its main function is to chemically digest the chyme received from the stomach in preparation for absorption. The pancreas, liver, and gallbladder secrete digestive enzymes through the ampulla of Vater into the middle portion of the duodenum.²

The jejunum is the second section of the small intestine and its primary function is to absorb nutrients. The digested chyme from the duodenum enters the jejunum where it is mixed and circulated for exposure to the jejunal walls for nutrient absorption. The walls of the jejunum are folded many times over to increase its surface area and allow for maximal absorption of nutrients. By the time chyme enters the ileum, almost 90% of all available nutrients are absorbed.²

The ileum is the final section of the small intestine. It serves to absorb vitamin B12 and other products of digestion that were not previously absorbed in the jejunum. It ends at the ileocecal valve—a circular muscle that serves to prevent reflux of colonic contents into the small intestine. It contracts in response to colonic dilation and relaxes in response to ileal dilation.²

The large intestine is composed of the cecum, appendix, ascending colon, transverse colon, descending colon, sigmoid colon, and rectum. Briefly, the cecum is a pouch at the beginning of the large intestine that allows for mixing of the chyme from the small intestine with bacteria to form fecal matter. The ascending colon transports the fecal matter superiorly along the right side up to the transverse colon. Along the way the ascending colonic wall absorbs water, nutrients, and vitamins. The transverse colon, the longest portion of the large intestine, crosses the abdominal cavity. Its contractions serve to mix the feces and allow bacteria to ferment the waste.

Further absorption of water and nutrients also take place. The feces then enter the descending colon, which stores the feces until it is ready for transport, inferiorly and along the left side of the abdominal cavity to the sigmoid colon. Again, the walls of the descending colon allow for further absorption of water and nutrients. The sigmoid colon is an S-shaped, curved region that stores then transports fecal matter from the descending colon to the rectum and anus for elimination. The final portion of the large intestine is the rectum where feces are stored until elimination. As fecal matter accumulates it exerts pressure on the walls of the rectum. This activates stretch receptors and leads to relaxation of the internal anal sphincter allowing for elimination.²

Transit Time in Health and Disease

This section serves to discuss motility in the esophagus, stomach, small intestine, and large intestine. Emphasis is placed on mechanism, how motility and transit are altered by various disease states, and methods for evaluating motility.

Mixing movements and propulsive movements are the two primary movements within and along the GI tract. Mixing movements keep the contents of the intestine appropriately and thoroughly mixed throughout, while the propulsive movements, consisting of periodic contractions of certain GI tract segments (peristalsis), move the contents of the intestine along the tract.

Transit through the esophagus starts with swallowing. Swallowing starts with the oropharynx pushing food backward and downward while the muscles of the nasopharynx prevent food from entering the nasal passages. When ready

to be swallowed the food is squeezed and rolled into the posterior pharynx by the tongue. The epiglottis moves upward in a protective mechanism over the larynx and trachea to prevent aspiration. The act of swallowing inhibits the respiratory center to protect from aspiration but it is so short-lived it is unnoticeable. Food enters the esophagus through the UES, which then constricts to prevent reflux back into the pharynx. The UES produces pressures around 30–200 mm Hg. Two waves of peristalsis move the food into the stomach through the LES, which also produces pressures between 20 and 60 mm Hg. Afferent nerve fibers transmit to the dorsal vagal complex activating efferent fibers that terminate either on the striated muscle of the esophagus or on the nerves of the enteric nervous system. Release of acetylcholine contracts the muscle while VIP and nitric oxide (NO) relax it. The LES responds to esophageal distention via myogenic and neurohormonal mechanisms.

Diseases of the esophagus are varied. Etiologies can be grouped into anatomical, mechanical, and neurologic, although many disease states involve overlap between two or all three. Anatomical etiologies include the presence of diverticula, hiatal hernia, and changes associated with chronic acid reflux. These anatomical abnormalities interrupt the normal pathway of food as it travels to the stomach which, in turn, changes many of the pressure zones of the esophagus. This can have dangerous sequelae as the luminal pressures may increase enough to overcome the resting pressures of the UES and LES allowing for reflux. Mechanical etiologies include achalasia, diffuse esophageal spasm, and hypertensive LES. There is also a neurologic component to these diseases but the result is the same—the esophagus is unable to relax properly for food travel. In achalasia the smooth muscles are unable to relax and move food down and the increased tone of the LES does not allow for complete relaxation. This results in dysphagia, regurgitation, and significant pain. In diffuse esophageal spasm the muscle contractions are uncoordinated and, as a result, food does not properly move downward. A hypertensive LES is defined as an LES with a mean pressure of 45 mm Hg or higher leading to dysphagia and chest pain. Neurologic disorders such as stroke, vagotomy, or hormone deficiencies will alter the nerve pathways such that the appropriate sensing and feedback are disrupted. A common result of neurologic disorders in the esophagus is dysphagia.

In evaluating esophageal function, it is important to select a study with an appropriate clinical correlation—is it a problem with motility or is it an anatomical abnormality? If it is a questionable motility problem, then an esophageal manometry study is best. A special catheter detects changes in pressure in the esophagus at various levels. First the pressure of the LES is recorded. The catheter is then pulled back into the esophagus and pressure measurements are made at different levels. Esophageal motor function between swallows is also evaluated. Finally the motor function of the UES is recorded and then the catheter is pulled out. Questionable anatomical problems are best studied using an upper GI series and ingested barium. These evaluate the act of swallowing and visualize the lining of the esophagus for anatomic abnormalities.

Before discussing the transit of food through the stomach and small intestine it is important to understand their actions during the fasting state. The migrating motor

complex (MMC) occurs only during fasting, and is composed of waves of electrical activity in regular cycles originating in the stomach and terminating in the distal ileum.³ Vagal stimulation releases motilin, which triggers an MMC leading to peristaltic waves. They occur every 45 to 180 minutes and are composed of four phases. Phase I is a period of quiescence. Phase II is composed of increased action potentials and low-amplitude smooth muscle contractility. Phase III is the most active as it is the time of peak electrical and mechanical activity producing bursts of regular, high-amplitude contractions. Phase IV demonstrates declining activity and will merge into the following MMC's phase I. The MMC is significant because it moves residual undigested food through the GI tract and also moves bacteria from the small intestine to the large intestine. Feeding interrupts it, and this is discussed next.

As described previously, the stomach is a J-shaped sac that serves as a reservoir for large volumes of food, mixes and breaks down food to form chyme, and slows emptying into the small intestine. Solids must be broken down into 1 to 2 mm particles before entering the duodenum, and they take approximately 3 to 4 hours to empty from the stomach. Liquids empty faster than solids. The motility of the stomach is controlled by intrinsic and extrinsic neural regulation. Parasympathetic stimulation to the vagus nerve increases the number and force of contractions whereas sympathetic stimulation inhibits these contractions via the splanchnic nerve. The intrinsic nervous system provides the coordination for motility. Neurohormonal control is also at play in that gastrin and motilin will increase the strength and frequency of contractions and the gastric inhibitory peptide will inhibit them.

Emptying of the stomach is controlled by neural and hormonal mechanisms as well as the composition of ingested food. Gastric distention, gastrin, and NO will promote emptying. Duodenal distention decreases the gastric tone to slow emptying, and increased fat content triggers the release of cholecystokinin to further inhibit stomach motility.

Gastric motility disorders that slow its emptying can increase the incidence of GE reflux disease. These disorders can be drug-induced, neurologic, or a result of critical illness. Drug-induced conditions include the administration of opioids (to be discussed later in the chapter), and the use of vasoactive agents. Vasoactive drugs increase catecholamine concentrations leading to sympathetic stimulation and, therefore, decreased motility. These drugs are often given intraoperatively or to critically ill patients for blood pressure control. Neurologic disorders resulting in decreased gastric motility include vagal neuropathies and gastroparesis. Finally, conditions that are commonly present in severely compromised patients, such as those with hyperglycemia, increased intracranial pressure, and mechanical ventilation can decrease gastric motility. Efforts to increase motility using drugs like erythromycin and metoclopramide have been used with some success.

The most prevailing test to evaluate gastric motility is the gastric emptying study. The patient fasts for at least 4 hours prior to the study then consumes a meal with a tightly bound radiotracer, commonly egg albumin. Continuous or frequent imaging occurs for the next 60 to 120 minutes and the measurement of time for 50% of the ingested meal to empty is determined. It is important to note that while

gastric emptying scintigraphy has long been the standard study, it is affected by multiple factors including meal composition and data acquisition parameters.⁴ Gastric motility studies can also be paired with small intestinal motility studies such as the small bowel manometry test. This will be discussed later.

Small intestinal motility mixes the contents of the stomach with digestive enzymes, further reducing particle size and increasing solubility. However, the major function of the small intestine is to circulate the contents and expose them to the mucosal wall in order to maximize absorption of water, nutrients, and vitamins before entering the large intestine. Again, there are mixing contractions and propulsive contractions. The circular and longitudinal muscle layers work in a coordinated fashion to achieve segmentation. Segmentation occurs when two nearby areas contract and thereby isolate a segment of intestine. Then a contraction occurs in the middle of that isolated segment, further dividing it. Contractions in the middle of those segments continue to occur and the process ensues. Segmentation allows the contents to remain in the intestine long enough for the essential substances to be absorbed into the circulation. It is controlled mainly by the enteric nervous system with modulation of motility by the extrinsic nervous system.

When considering small bowel dysmotility it is helpful to distinguish etiologies based on reversible and nonreversible causes. For reversible causes, mechanical obstruction should be the first to come to mind. In this case, there is a physical obstruction the muscles of the intestine cannot overcome. Hernias, malignancy, adhesions, and volvuluses are all examples. Bacterial overgrowth should be another consideration. Although the large intestine is rich with bacteria, the small intestine usually has fewer than 100,000 organisms per milliliter. Disrupting this condition with bacterial overgrowth leads to alterations in absorptive function leading to diarrhea. It is treated with antibiotics. Other reversible causes include ileus, electrolyte abnormalities, and critical illness. Nonreversible causes can be classified as structural or neuropathic. In structural causes there may be abnormalities with the intestinal smooth muscle, in which it cannot produce proper contractions. This occurs in diseases such as scleroderma and connective tissue disorders. In patients with an inflammatory bowel disease (IBD), there is a structural abnormality in the mucosa leading to decreased absorption of nutrients. Short bowel syndrome can be considered a structural etiology in that a large portion of the small intestinal structure is simply not present. In patients who have had a section of their small bowel resected, the remaining portion may not provide sufficient functional compensation, resulting in diarrhea, malnutrition, and weight loss. Neuropathic etiologies can produce a pseudo-obstruction in which the intrinsic and extrinsic nervous systems are altered in such a way that the intestines can only produce weak or uncoordinated contractions. This leads to symptoms of bloating, nausea, vomiting, and abdominal pain. Regardless of etiology, small intestinal dysmotility adversely affects nutrient absorption leading to malnutrition.

The most common test used to evaluate small intestine motility is small bowel manometry. This test is useful in patients with unexplained nausea, vomiting, abdominal pain, and manifested signs of obstruction without a clear

obstructive cause. Similar to esophageal manometry, this test uses a small catheter with pressure sensors to evaluate the contractions of the intestine. The study evaluates contractions during three periods: fasting, during a meal, and postprandial. Normally the recording time is four hours for fasting, followed by ingestion of a meal, and two hours postprandial. Abnormal results are grouped into myopathic and neuropathic causes. In myopathic results, the MMC is absent or phase III exhibits very low amplitudes (normal phase III amplitude is 40 mm Hg). In neuropathic results, the contraction amplitude is adequate but either the contractions are uncoordinated (enteric neuropathy) or there is an inappropriate postprandial response, meaning postprandial antral hypomotility is present (extrinsic neuropathy). This manometry test is reported to result in a change of diagnosis in 8% to 15% of patients with unexplained nausea, vomiting, and abdominal pain.⁵

The large intestine acts as a reservoir for waste and indigestible material before elimination and extracts any remaining electrolytes and water. It plays an essential role in regulating defecation and consistency of stools. Distention of the ileum will relax the ileocecal valve to allow intestinal contents to enter the colon and subsequent cecal distention will contract it. The contractions of the colon are different from the rest of the gut. While there are still mixing and propulsive movements by the circular and longitudinal muscles, respectively, the colon also exhibits giant migrating complexes. The giant migrating complexes serve to produce mass movements across the large intestine. In the healthy state, these complexes occur approximately 6 to 10 times within 24 hours with mean amplitude of 115 mm Hg at a distance of about 1 cm/s for approximately 20 seconds each.⁶ These complexes, as well as the mixing and propulsive movements, serve to transfer contents to the rectum. The giant migrating complexes that originate in the sigmoid colon will produce the urge to defecate. Rectal distention as well as VIP and NO release will promote relaxation of the internal anal sphincter and allow for defecation.

Colonic dysmotility manifests with two primary symptoms: altered bowel habits and intermittent abdominal cramping. The most common diseases associated with colonic dysmotility are irritable bowel syndrome (IBS) and IBD, both of which are clinical diagnoses. Rome II criteria define IBS as having abdominal pain/discomfort along with at least two of the following three features: defecation relieves pain or discomfort, onset of pain is associated with an abnormal frequency of stools (more than three times per day or fewer than three times per week), and onset of pain is associated with a change in the form of the stool.⁷ In IBS with predominantly diarrheal symptoms, there is an increase in the frequency and amplitude of spontaneous giant migrating complexes, and this increase is directly proportional to the severity of symptoms. In IBS with predominantly constipation, there is a decreased amplitude and frequency of giant migrating complexes. In severe cases the giant migrating complexes may be completely absent. In addition, there is a depression of overall contractile activity in the colon leading to colonic distention and the sensation of pain. This phenomenon is exacerbated by stress in which there is significant motor dysfunction and visceral hypersensitivity as well as an increase in plasma norepinephrine stimulating the sympathetic nervous system. In IBD

the mixing and propulsive movements as well as the tonic contractions are suppressed due to colonic wall compression by the inflamed mucosa, but the giant migrating complexes remain. There is an increased frequency of the giant migrating complexes and their large pressure effect further compresses the inflamed mucosa, which can lead to hemorrhage, thick mucus secretion, and significant erosions.

Methods of Evaluating Colonic Motility

Studies evaluating giant migrating complexes in patients with IBS and IBD are not routine but are performed only on patients with known diagnoses to help understand the physiology and mechanism causing them. There are, however, tests to evaluate the function and anatomy of the large intestine. The lower GI series, for example, involves the administration of a barium enema to a patient. The barium outlines the intestine and it is visible on radiograph. This allows for detection of colon and rectal anatomical abnormalities.

The Effects of General Anesthesia on Bowel Function

GI effects of the anesthetics are multifaceted and encompass a wide array of hemodynamic and physiological changes. This section is broken down into the various components that make up a general anesthetic and the GI effects of each of these components. Emphasis is placed on the effects of preoperative sedation, induction of anesthesia, hypnotic agents, volatile agents, paralysis, and reversal. Opioids will be discussed in another section. Please note that this discussion applies to the healthy state.

In the preoperative setting patients are often nervous and sympathetic stimulation is high. Inhibition of GI tract activity is directly proportional to the amount of norepinephrine secreted from sympathetic stimulation, so the higher the anxiety the higher the inhibition. Even though a good bedside manner and the use of behavioral approaches are beneficial, these may not be sufficient and patients are often given premedication with a benzodiazepine, usually midazolam, to alleviate anxiety. Midazolam acts by enhancing the effect of neurotransmitter, GABA, on GABA-A receptors. A study by Castedal and associates looked at the effect of midazolam on small bowel motility using antroduodenal manometry.⁸ The vast majority of the studied variables were not affected by the use of midazolam, but one significant change was noted—an increased duration of phase III of the MMC in the proximal and distal parts of the duodenum, which shortened the MMC by 27%. A clear explanation for this is not evident but there are a couple of considerations. One, the sedative effect of midazolam may be the reason for the change in MMC activity because MMC activity differs between awake and sleep states. Another consideration is that the resultant reduced anxiety decreases sympathetic stimulation allowing for less inhibition and higher activity. However, when applied clinically, there was no real difference seen in small intestinal motility patterns. Of the premedications, midazolam is widely used and considered well tolerated.

General anesthesia causes a loss of all protective reflexes. This is achieved with a variety of medications including

opioids, hypnotics, and neuromuscular blocking agents. As mentioned, the effect of opioids will be discussed in a later section. Volatile anesthetics affect bowel function through various mechanisms including depression of spontaneous activity and changes in intestinal tissue oxygenation. Volatile anesthetics depress the spontaneous, electrical, contractile, and propulsive activity in the stomach, small intestine, and colon as demonstrated in many animal and human studies. The small intestine is the first part of the GI tract to recover, followed by the stomach in approximately 24 hours and then the colon 30 to 40 hours postoperatively. Between the various volatile anesthetics there are minor differences. One difference worth noting is that rapid increases in the concentration of desflurane induces greater sympathetic activation, as compared to other volatile agents, which coupled with sympathetic nervous system hyperactivity during surgical procedures can inhibit GI function and motility. In a study comparing desflurane and isoflurane, rapid increases in desflurane caused significantly greater effects on sympathetic and renin-angiotensin system activity as well as increases in blood pressure and heart rate as compared to isoflurane. However, this effect is short-lived as it is only seen with rapid increases in concentration and the surge in sympathetic stimulation tapers off quickly. This transient phenomenon is unlikely to have a lasting effect on bowel function.⁹ The volatile anesthetics also affect splanchnic circulation and oxygenation in a dose-dependent manner, which is known to have an effect on bowel function. In horses receiving isoflurane for maintenance of anesthesia, microperfusion and intestinal tissue oxygenation decreased when isoflurane reached 2%.¹⁰ In a human study by Muller and associates, the effects of desflurane and isoflurane on intestinal tissue oxygenation during colorectal surgery were evaluated. It was found that desflurane and isoflurane had comparable effects on intestinal tissue oxygenation. However, during periods of ischemia for resection and anastomosis, reactive hyperemia was better preserved in the patients given isoflurane.¹¹ This may have important implications in regaining coordinated and appropriate bowel function postoperatively and may determine maintenance with volatile versus total intravenous anesthesia. Whereas the volatile anesthetics depress spontaneous activity and affect blood flow, there is no clear-cut relationship between adverse GI effects and the use of volatile anesthetics. Also, when considering their use in clinical practice, there is very little difference between desflurane, isoflurane, and sevoflurane's effects on bowel function.

An alternative to maintenance with volatile anesthetics is total intravenous anesthesia. Propofol is the most common drug used for this purpose. When used intraoperatively, propofol-remifentanil anesthetic produced increased intestinal motility as compared to sevoflurane-remifentanil.¹² No adverse GI effects were reported, but it did cause a higher degree of surgeon dissatisfaction. A study by Jensen and colleagues looked at bowel recovery after open procedures and did not find a difference in overall recovery and bowel function when comparing isoflurane/nitrous oxide, propofol/air, and propofol/nitrous oxide.¹³ Even in colorectal cancer patients there was no difference in inflammatory response among patients receiving either total intravenous anesthesia with propofol and remifentanil or inhalational anesthesia with sevoflurane and fentanyl.^{14,15} There are few data on the effect of propofol on GI smooth muscle and many of

the established studies show various and conflicting results when it comes to the recovery of bowel functions.

Nitrous oxide is 30 times more soluble than nitrogen in the blood and as such will diffuse into gas-containing cavities from the blood faster than the nitrogen already present in those cavities can diffuse out. This is especially important in the bowels as gut distention is correlated with the amount of gas already present in the bowel, the duration of nitrous oxide administration, and the concentration of nitrous oxide administered. Although it has been established that nitrous oxide causes bowel distention and it is prudent to avoid nitrous oxide in lengthy abdominal surgeries or when the bowel is already distended, the most recent ENIGMA trial did not relate the use of nitrous oxide to any significant adverse outcomes.¹⁶

Paralysis to achieve favorable surgical conditions is produced by administration of neuromuscular blocking agents. Neuromuscular blocking drugs only affect skeletal muscle so GI motility remains intact. However, special mention of the depolarizing neuromuscular blocker succinylcholine should be made. Succinylcholine mimics acetylcholine in that it produces an initial muscle contraction, which is visible as fasciculations. This contraction increases intragastric pressure, which may be so strong as to overcome the tone of the LES and allow reflux of gastric contents. Aspiration is certainly a concern, but this should not necessarily preclude the use of succinylcholine. Patient condition, including body habitus, technical difficulty of intubation, nothing by mouth (NPO) status, and comorbidities should be the determining factors in assessing the risk of aspiration.

Reversal of paralysis using the anticholinesterase, neostigmine, will increase parasympathetic activity and bowel peristalsis by increasing the frequency and intensity of contractions. In cases of fresh bowel anastomoses, this can be of concern as the increase in activity could result in dehiscence. This is partially offset by simultaneous administration of the anticholinergic medications, glycopyrrolate or atropine, which are used to attenuate the bradycardia from neostigmine. This effect is not seen with sugammadex, which may be a more prudent choice for reversal in situations of tenuous bowel anastomoses. There is some data to support the use of neostigmine in treating postoperative ileus but the adverse effects of bradycardia, vomiting, and abdominal cramps may preclude its use.

Surgical procedures on the GI tract produce an exaggerated stress response that may predispose to postoperative bowel dysfunction. Goals of anesthetic care should be to attenuate the stress response, optimize hemodynamic and fluid status, and maintain normothermia.^{17,18} At present there is no evidence for recommendations on specific anesthetic and analgesic agents to avoid adverse GI effects.

Effect of Opioids on Bowel Function

Much attention has been given to the use and effects (beneficial and adverse) of opioid administration. There is a desire to only use adjunct techniques and nonopioid medications; however, opioids are often necessary to control perioperative pain. A major adverse effect, and one that is not associated with the development of opioid tolerance, is reduced GI motility and constipation. Opioids exert their function on both central and peripheral receptors, namely mu, delta, and kappa. It is the

central effects that primarily mediate analgesia and produce the favorable effects. The peripheral effects are the adverse effects. There is a high density of peripheral mu-opioid receptors in the myenteric and submucosal plexuses. Activation of these mu-opioid receptors in the myenteric plexus has a dual effect on the neural pathways controlling motility—it inhibits excitatory pathways that depress peristaltic contraction and it also inhibits inhibitory pathways. These inhibitions increase GI muscular activity and increase resting muscle tone including tone in the ileocecal valve and internal anal sphincters. This produces spasm and nonrhythmic or propulsive motility. Activation of these receptors is also linked to the inhibition of acetylcholine release and promotion of nitrous oxide release that inhibits propulsive motility.¹⁹ Together these effects will delay gastric emptying and slow transit through the intestine. Activation of these receptors in the submucosal plexus decreases nutrient secretion and increases fluid absorption. Coupled with reduced motility the stool will remain in the gut for a longer period of time and as more water is absorbed the stool becomes hard and dry leading to constipation.²⁰ Other adverse sequelae include nausea, anorexia, delayed digestion, abdominal pain, excessive straining during bowel movements, and incomplete evacuation.

Many efforts have been made and are currently underway to attenuate or avoid opioid-induced bowel dysfunction. The use of laxatives, stool softeners, and prokinetic agents, such as metoclopramide and neostigmine, have shown some success in alleviating opioid-induced constipation. Potentially switching to a different opioid is also offered as a treatment option. Tassinari and associates performed a meta-analysis demonstrating strong evidence supporting opioid switch in alleviating constipation, most strongly for morphine to transdermal fentanyl.²¹ Another option is combining opioids with enteral opioid receptor antagonists. Naloxone was the first used. It is a nonselective, competitive opioid receptor antagonist. While its effect on the peripheral receptors in the gut produced favorable results of reversing gut motility inhibition, its nonselective profile meant it also worked on the central receptors and reversed the beneficial analgesic effect of opioids. Therefore, new attention is given to pure peripherally acting opioid receptor antagonists. Methylnaltrexone is a peripheral mu-opioid receptor antagonist and does not cross the blood-brain barrier. In healthy volunteers, the use of methylnaltrexone prevented delay in orocecal transit time after morphine administration.²² Subsequent systematic reviews demonstrated that methylnaltrexone and alvimopan were better than placebo in reversing opioid-induced increased GI transit time and constipation.^{23–25} However, long-term efficacy and safety have not been clearly established. Further studies are underway.

Effect of Open Abdominal Surgery, Ischemia, Stomas, and Bowel Anastomosis on Gastrointestinal Physiology and Function

The surgical procedure itself, even with purposes of correcting GI pathology, significantly affects GI physiology and function and predisposes to postoperative ileus. Recently, a standardized definition of postoperative ileus was established as “a

transient cessation of coordinated bowel motility after surgical intervention, which prevents effective transit of intestinal contents and/or tolerance of oral intake.”²⁶ Manipulation of the intestines is the main factor that initiates postoperative ileus. Additional contributors include immobility, electrolyte imbalance from fluid shifts and insensible losses, and intestinal wall swelling from excessive fluid administration. In open abdominal procedures, the surgical manipulation of the bowel induces a degree of trauma that sets in motion the whole process of postoperative ileus. There are two phases to uncomplicated postoperative ileus (i.e., in the absence of complications, such as perforation, bleeding, peritonitis). The first phase is an early neurogenic phase and the second is an inflammatory phase. In total, an uncomplicated postoperative ileus lasts about 3 to 4 days.²⁶

The early neurogenic phase results when the intestine is manipulated, which is more extensive in open procedures than laparoscopic ones. This manipulation activates the sympathetic nervous system, increasing the inhibitory neural input that leads to decreased propulsive movements and almost complete cessation of GI motility. This lasts about 3 to 4 hours after surgery.

The late inflammatory phase also begins with surgical manipulation of the intestines. Surgical manipulation increases sympathetic stimulation of the myenteric plexus, which promotes the influx of leukocytes into the “traumatized” areas of the gut. Further release of cytokines, chemokines, and leukocytes as well as phagocytosis in the traumatized area occurs and eventually spreads through the entire GI tract. This inflammatory cascade increases permeability and allows for translocation of intraluminal bacteria, which further exacerbates the inflammatory process. However, peritonitis does not always develop because the mast cells and neutrophils are very effective in eliminating the translocated bacteria in the peritoneal cavity. This process occurs about 3 hours after intestinal manipulation and continues throughout the manipulated segment and the rest of the GI tract for the next 24 hours. It eventually subsides and within 3 to 4 days this uncomplicated ileus is usually resolved.^{27,28}

Mesenteric ischemia, if left untreated, will lead to 100% mortality. This occurs when the supply of oxygen is insufficient to meet the oxygen demand of the intestines. It affects the small and large intestine and is classified as occlusive or nonocclusive. Etiologies of mesenteric ischemia include: strangulation, emboli (seen commonly in patients with atrial fibrillation), complications of aortic surgery or during cross-clamping, trauma, drug-induced, atherosclerosis, and inflammatory diseases. There are four stages of mesenteric ischemia. The first is the hyperactive stage when blood flow to the intestine is abruptly occluded. This produces severe pain and overactive peristalsis. There may be passage of loose stool with blood. The second stage is a paralytic stage that spreads diffusely across the intestines. The third stage involves leakage of fluid, proteins, and electrolytes through the bowel wall into the peritoneum. If the bowel becomes necrotic then peritonitis develops. The fourth stage is shock. End-organ damage is apparent and contributes to altered hemodynamics and critical illness. Treatment involves reperfusion of the occluded vessel through revascularization and possibly bowel resection.²⁹

Bowel resections vary in terms of their effect on the remaining bowel. The degree of GI dysfunction depends on

the portion of bowel resected. The colon primarily absorbs water and a full colonic resection is compatible with life. However, when the small intestine is resected the effect on the GI system is much more pronounced. The small intestine is responsible for absorbing vitamins and nutrients. This can be properly maintained if at least a third of the small bowel remains. The jejunum is the primary site for digestion and absorption of nutrients. After a jejunal resection, the ileum is usually able to adapt to fulfill its functions. The ileum absorbs vitamin B12 and bile salts. If the ileum is resected (especially more than 100 cm), the remaining small intestine cannot compensate for the loss of its function and severe malabsorption and diarrhea will result. The unabsorbed bile salts enter the colon and stimulate fat and water secretion. Small intestinal resection will increase gastric motility but this depends on the site and amount resected. If the terminal ileum and ileocecal valve are resected then intestinal content transit speeds up.³⁰

Bowel anastomoses can significantly alter bowel function in that they disrupt normal motor activity. Partial transection usually preserves the wave of activity, though complete transection will interrupt it. There is a loss in myogenic continuity in that the intestine distal to the transection will no longer receive signals or respond to the pacemaker in the proximal duodenum. Now the part distal to transection has to rely on its own intrinsic slow-wave transmission. This can be attenuated by close approximation of the muscle layers. There is motor asynchrony across the anastomotic site but long-term studies report reasonable MMC activity is ultimately achieved with time. The mechanism explaining why this recovery occurs remains uncertain. The transection and anastomosis have little effect on intestinal homeostasis and are not associated with significant digestion or absorption side effects.²

Gastrointestinal System Nociception

Abdominal visceral pain and its associated symptoms are common in the GI perioperative period. For an understanding of GI nociception, a detailed knowledge of the anatomy and physiology of abdominal visceral innervation is essential.

ABDOMINAL VISCERA INNERVATION

Abdominal visceral pain signals are carried in both sympathetic and parasympathetic autonomic fibers.^{31,32} Innervation of the parietal peritoneum, abdominal wall muscles, and skin is supplied by the ventral rami of thoracoabdominal nerves, which are part of the somatosensory system.

Sympathetic fibers for the upper abdomen, including the liver, stomach, pancreas, small bowel, and proximal part of the colon, originate from spinal cord segments T5 to L2. Those preganglionic fibers exit the cord as gray rami communicants to enter the sympathetic chain in the paravertebral region. These fibers terminate in the prevertebral (subdiaphragmatic) ganglia through splanchnic nerves and generate the celiac plexus, where they synapse with a large number of postganglionic, predominantly unmyelinated fibers. Postganglionic fibers will then innervate the

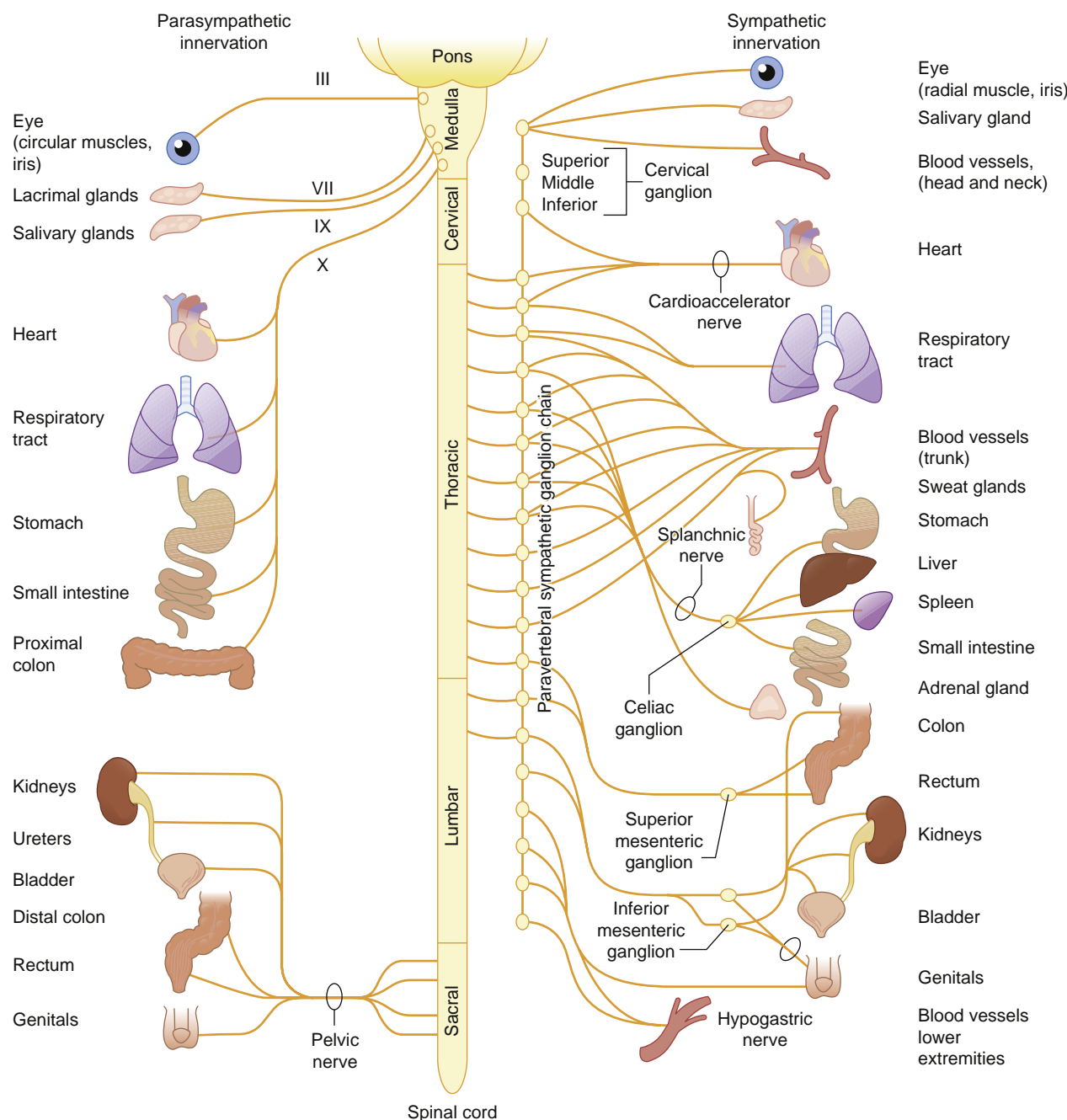


Fig. 15.1 Schematic diagram of sympathetic and parasympathetic innervation to the gastrointestinal (GI) tract. Sympathetic innervation of majority of the GI tract up to the rectum is supplied by the celiac plexus. (From Glick DB. The autonomic nervous system. In: Miller RD, ed. *Miller's Anesthesia*. 7th ed. Philadelphia: Elsevier; 2010.)

organs (see **Fig. 15.5**).³³ Innervation of the lower abdomen including the descending colon, sigmoid and rectum, bladder, and lower ureter originates from T9 to L3 and forms the inferior mesenteric and hypogastric ganglia and plexus.

Sympathetic afferent fibers transmit visceral pain, whereas sympathetic efferent nerves inhibit peristalsis and gastric distention as well as cause GI vasoconstriction.³³

The parasympathetic nervous system supplies the abdominal viscera proximal to the splenic flexure of the colon via the vagus nerve. Some of the vagal fibers pass through the prevertebral fibers (celiac plexus). The parasympathetic postganglionic neurons are located in the myenteric and submucosal

plexuses. Visceral afferent parasympathetic nerve fibers transmit the sensations of satiety, nausea, and distention, whereas efferent parasympathetic nerve fibers increase functions such as secretion, sphincter relaxation, and peristalsis.^{34–36}

The colon, rectum, internal and external genitalia, and bladder are innervated by fibers from spinal cord segments S2 to S4, which run with the pelvic nerves (**Fig. 15.1**).^{37–40}

Some of the characteristics of abdominal visceral innervation are: (1) they are almost exclusively myelinated A-delta and unmyelinated C fibers; (2) they have “dual-function” properties (sensory that carry sensory evoked potentials and afferent that regulate autonomic flow);⁴²

(3) there are an abundance of connections between nerves, ganglia, and plexuses; (4) there is not a fine and distinct nerve; (5) considerable variation in anatomy can be found; (6) visceral innervation anatomy is affected by intraabdominal pathology; and (7) visceral innervation distribution is diffuse and capable of amplification. Once stimulated, it could be difficult to stop (self-aggravation).^{41–46}

In summary, the innervation of the GI organs up to the proximal transverse colon is supplied by the celiac plexus, and innervation of the descending colon and distal GI tract comes from the inferior hypogastric plexus. Although each organ looks like it is innervated from specific cord segments, the fibers frequently communicate with each other (Table 15.2).

CELIAC PLEXUS ANATOMY

The celiac plexus is normally composed of two or three splanchnic nerves:

The greater (superior thoracic) splanchnic nerve comes from T5 to T9 (fibers can arise as high as T1 and as low as T11). The greater splanchnic nerve is usually anterolateral to the T12 vertebral body. It perforates the crura of the diaphragm and enters the retroperitoneal space where it joins the celiac plexus.

The lesser splanchnic nerve is formed from T9 to T11. In 30% of cases this nerve is not present. Two or more celiac ganglia are generated, which lie ventrolaterally to the aorta between the origin of the celiac arterial trunk and the renal arteries.

The celiac ganglia can vary considerably in size and number on each side. Usually they are oval shaped and can vary from 0.5 to 4.5 cm in width.

Fusion of these ganglia form a fine nerve plexus that may extend to the inferior border of the T12 vertebra and lower border of L2. They are mostly located close to the celiac artery trunk.⁴⁶

The plexus and related nervous structures are contained in the prevertebral retroperitoneal space along with the aorta, inferior vena cava (IVC), veins of azygos system, lymph nodes, the cisterna chyli, and diaphragmatic crura (Fig. 15.2).

ABDOMINAL VISCERAL PAIN

Despite the fact that abdominal pain of visceral origin is a very common finding during the perioperative period, our knowledge and practice to control this pain are very limited.⁴⁷

Visceral pain is different from somatic pain in many aspects; not all organs respond similarly to stimuli, some organs are more sensitive. For example, the pancreas is more sensitive than the stomach. Tissue destruction, ischemia, and inflammation will not always cause pain.⁴⁸ The most remarkable difference between visceral and superficial structures is the fact that visceral pain is poorly localized, produces strong affective responses, and refers to other locations with intense regional or muscle spasms and autonomic instability.^{49–51}

The referral properties of visceral pain have been attributed to the conjunction of visceral and somatic inputs to the spinal cord and CNS. For the same reason, visceral pain can have somatic components. Merging of these inputs can modify pain sensation distal to the site of visceral inflammation, or pain from one intraabdominal organ can refer to another.⁴⁰

Visceral pain is fervently associated with emotional fluctuation. IBS is thought to be related to gut-brain interaction and autonomic dysregulation.⁵²

It was found that induced sadness was attenuated by fatty acid infusion, and increased neural activity in the part of the brain processing emotions was also observed.⁵³ Probiotic bacteria are beneficial in stress-related disorders, such as anxiety and depression, and during the course of common comorbidities and some bowel disorders.⁵⁴

VISCERAL PAIN TREATMENT

Opioids are still the mainstay of visceral pain treatment, although their usage has been limited by many side effects such as decreased gut motility and constipation, sedation, nausea, and vomiting. In addition, prolonged usage of narcotics is associated with opioid-induced hyperalgesia and tolerance.⁵⁵ Usage of acetaminophen, nonsteroidal anti-inflammatory drugs, and serotonin components have been suggested, but the results are not specific.⁵⁶

VISCERAL PAIN BLOCK TECHNIQUES

Noxious pain impulses originating from abdominal viscera can be blocked by the following regional anesthesia techniques (Fig. 15.3)

1. Spinal anesthesia extending to at least the level of T5
2. Epidural anesthesia covering T5 to T12 dermatomes
3. Paravertebral blocks comprising T5 to L2 spinal segments
4. Selective T5 to L2 sympathetic chain block
5. Celiac/splanchnic nerve block

TABLE 15.2 Summary of Visceral Innervation on Gastrointestinal Tract⁴⁷

Organ	Sympathetic Sensory Supply	Parasympathetic Sensory Supply
Liver and biliary tract	T5-T10 via Celiac plexus	Vagus nerve
Stomach	T7-T9 via Celiac plexus	Vagus nerve
Pancreas	T6-T10 via Celiac plexus	Vagus nerve
Small bowel	T9-L1 via Celiac plexus	Vagus nerve
Cecum, ascending and transverse colon	T9-L1 via Celiac plexus	Vagus nerve
Descending colon	T9-T12 via Celiac plexus	S2-S4 via Pelvic nerves
Sigmoid, rectum	T11-L1 via Inferior hypogastric plexus	S2-S4 via Pelvic nerves

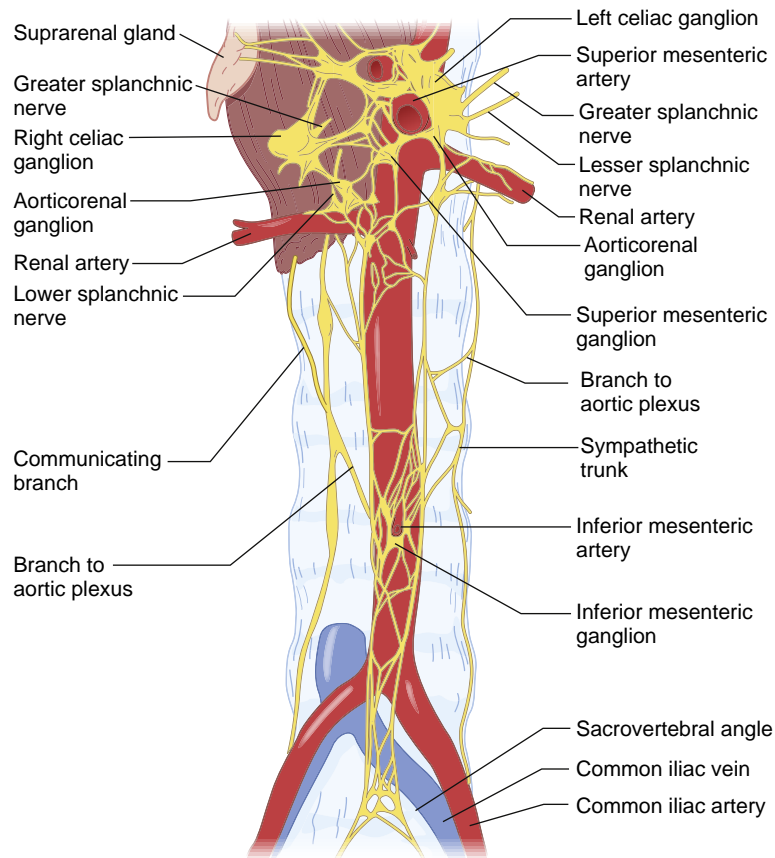


Fig. 15.2 Anatomy of the abdominal sympathetic trunk. (Redrawn from <http://commons.wikimedia.org/wiki/File:Gray847.png#mediaviewer>.)

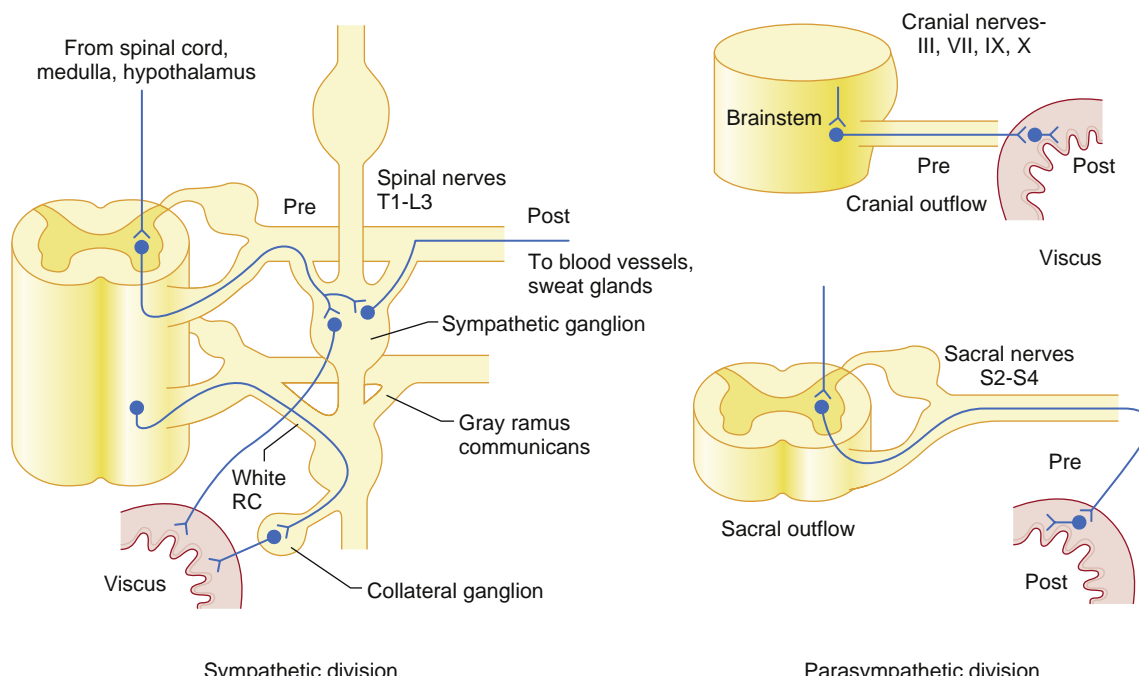


Fig. 15.3 Regional anesthetic techniques on gastrointestinal (GI) visceral sympathetic innervation: different regional techniques which can block sympathetic innervation of the GI tract at different levels. (From Glick DB. The autonomic nervous system. In: Miller RD, ed. *Miller's Anesthesia*. 7th ed. Philadelphia: Elsevier; 2010.)

Based on the type and extent of the regional technique, its effect on the GI physiology is different. Of note, the aforementioned regional anesthesia techniques are associated with the blockade of the sympathetic nervous system, whereas the parasympathetic system usually remains intact.

VISCERAL/CELIAC PLEXUS BLOCK

Blockage of the splanchnic/celiac plexus has been approached in many ways:

Intraperitoneal Regional Anesthesia or Peritoneal Lavage

Abdominal visceral pain can be blocked simply by instilling local anesthetic into the peritoneal cavity. A recent meta-analysis by Boddy and associates of intraperitoneal regional anesthesia in laparoscopic surgeries found an overall benefit, although there was no consistent analgesia, but also a remarkable absence of complications and side effects.⁵⁷

Celiac Plexus Block—Posterior and Trans-Crural Approach

Radiography, fluoroscopy, or computed tomography scan is usually needed to perform this block safely, especially in lytic blocks.

This approach requires a special needle, usually a 15-cm, 20- or 22-G Chiba needle. The patient is in the prone or lateral position and the needle is inserted below the tip of the 12th rib on the left side. The needle is aimed at a 45-degree angle to touch the lateral side of the L1 vertebral body at a depth of 7 to 9 cm. Subsequently, the needle is nearly fully redirected 5 to 10 degrees and advanced to a depth of 11 to 14 cm. In this situation the pulsation of the aorta on the needle can sometimes be felt (Fig. 15.4).

Determination of the correct vertebral level is imprecise in patients with absence of the 12th rib, a markedly downslipping of the rib, or in other congenital abnormalities.

Celiac Plexus Block—Anterior Approach

The abdomen is opened and the left lobe of the liver is retracted upward. The stomach is pulled gently downward and to the left thereby exposing and stretching the lesser omentum. The index finger of the operator is then inserted at the highest possible point of the incision, palpating the pulsating aorta through the lesser omentum. The aorta is pushed aside to the left by passing the tip of the finger to the vertebrae whereby it is separated from the vena cava. A fine 22-G spinal needle is inserted alongside the finger and in the loose, retroperitoneal, prevertebral tissue between the IVC and aorta. Diluted local anesthetic is injected in this area after careful aspiration. The tip of the needle should be close to the diaphragm, above the origin of the celiac trunk, in the midline. A similar approach was described by Lillemoe in 1992 for postoperative pain control in pancreatic cancer patients: after lesser omentum exposure, the left index and middle fingers are placed on either side of the aorta and pulled caudad until the upper border of the pancreas is identified and 20 mL of solution is injected on either side of the aorta (Fig. 15.5).⁵⁸

Endoscopic Ultrasound-Guided Celiac Plexus Block

Recent recognition that the celiac ganglia can be visualized and accessed by endoscopic ultrasound (EUS) now allows for a direct injection into the celiac plexus. The patient is placed in the left lateral decubitus position and under conscious sedation. From the posterior side of the lesser curvature of the gastric fundus EUS can visualize the aorta in a longitudinal plane. The aorta is traced distally to the celiac trunk, and the injection delivered around the celiac trunk. Meta-analysis has shown that EUS-guided celiac plexus blocks are safe and efficient (Fig. 15.6).⁵⁹

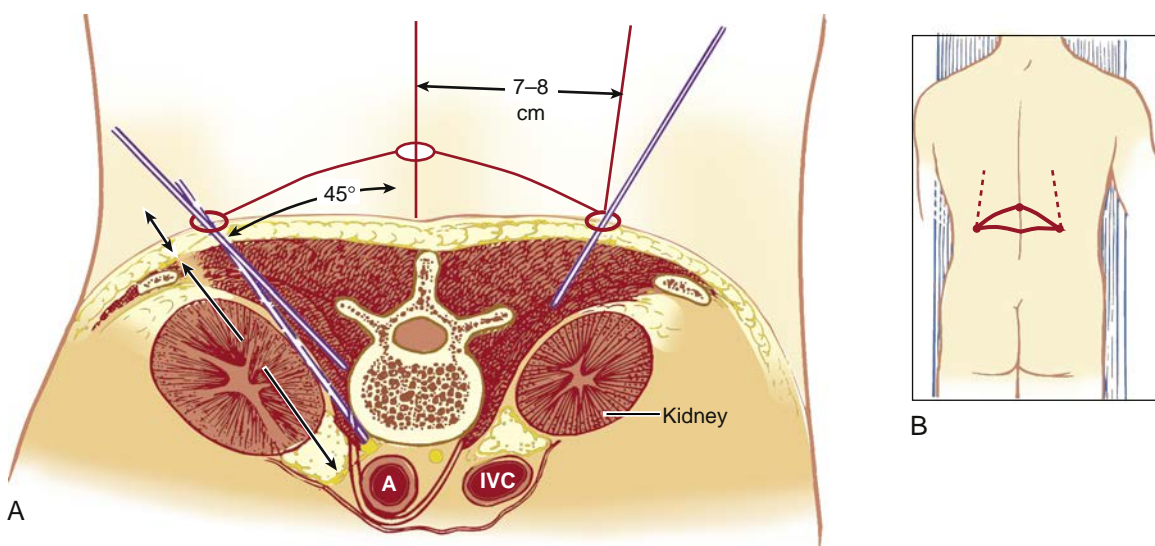


Fig. 15.4 (A) Schematic view of the posterior approach. Celiac plexus can be blocked by insertion of a 20- to 22-gauge 15-cm spinal needle (Chiba needle) at the level of T12. (B) Positioning and surface landmarks. (From Wedel DJ, Horlocker TT. Nerve blocks. In: Miller RD, ed. *Miller's Anesthesia*. 7th ed. Philadelphia: Elsevier; 2010.)

TECHNICAL ASPECTS OF VISCERAL PLEXUS BLOCKS

There is no established standard technique. It is important to completely disrupt all of the impulse traffic in the visceral innervation, as these impulses are widely spread and can be reinstated via very fine nerves.

Unfortunately, the success of splanchnic nerve and celiac plexus blocks cannot be verified by any objective signs. Hypotension is not a regular finding. If patients do have upper abdominal pain, analgesia typically results within a few minutes after the block. Failure of pain to subside is not only due to inappropriate technique but also due to the involvement of visceral plexuses, such as the hypogastric plexus.

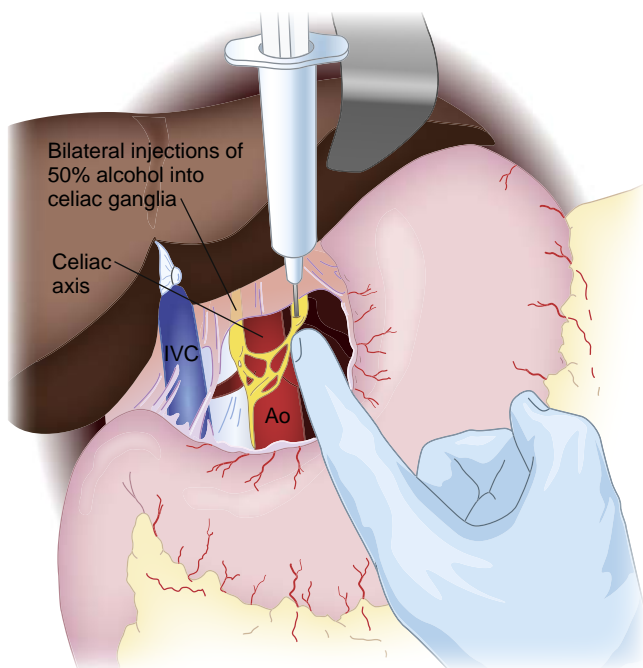


Fig. 15.5 Celiac plexus block (anterior approach): intraoperative celiac plexus block is performed using a 20- to 22-gauge spinal needle. Injection is performed at each side of the aorta and the level of celiac axis. (Redrawn from Lillemoe KD, Cameron JL, Kaufman HS, et al. Chemical splanchnicectomy in patients with unresectable pancreatic cancer. A prospective randomized trial. *Ann Surg*. 1993;217:447-457.)

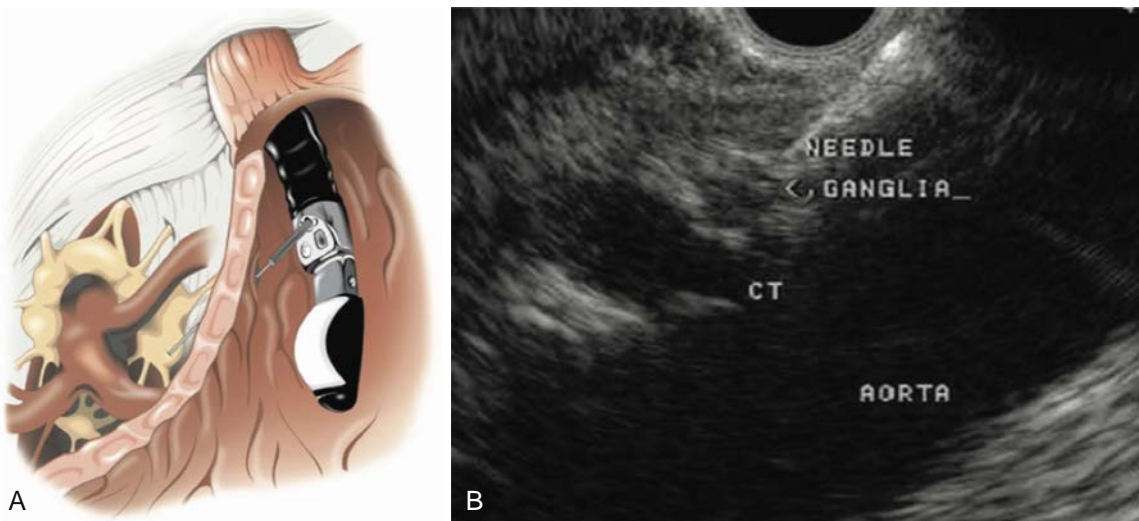


Fig. 15.6 Endoscopic ultrasound-guided celiac plexus block: (A) Ultrasound beams use lesser curvature of the gastric fundus as media to visualize the celiac trunk. (B) Ultrasonic image of celiac ganglia and needle during performance of endoscopic ultrasound-guided celiac plexus block. CT, Celiac trunk. (From Levy M, Wiersema M. EUS-guided celiac plexus neurolysis and celiac plexus block. *Gastrointest Endosc*. 2003;57(7):923-930.)

BOX 15.1 Complications of Celiac Plexus Blocks

- Hypotension
- Diarrhea
- Intravascular injection and vascular trauma
- Subarachnoid or epidural injection and paraplegia
- Renal injury
- Pneumothorax
- Chylothorax
- Damage to surrounding structures and retroperitoneal hematoma
- Peritonitis and abscess

There is little information about the duration of a successful block induced by local anesthetics. Most of the blocks have been a combination of local anesthetic and lytic therapy for chronic pain. In order to avoid toxic side effects, local anesthetic doses must be reduced when the block is combined with another major regional anesthetic technique such as abdominal wall blocks.

COMPLICATIONS OF VISCERAL PAIN BLOCKS

The complication rate is between 0.5% and 32%, depending on the method, as radiologic methods are associated with a reduced rate of complications (Box 15.1).

Dilation of the capacitance vessels in the splanchnic area will cause hypotension. Subarachnoid injection happens mostly with a posterior approach, and an alcohol injection can cause paraplegia.

A chylothorax can result from damage of the retroperitoneal lymph nodes.

The most devastating complication occurs with vascular trauma, thrombosis, and retroperitoneal hematoma.⁶⁰

INDICATIONS FOR A VISCERAL PAIN BLOCK

Post-Laparotomy Pain Relief

Visceral pain blocks are usually associated with somatosensory pain controls using central neuroaxial regional anesthesia techniques, such as epidural analgesia or paravertebral analgesia. A combination of a celiac plexus block with any other regional anesthesia technique is rarely used.

Cancer Pain

Splanchnic/celiac plexus blocks have been used for biliary and pancreatic cancers. The details of this indication of visceral pain control are discussed in the chronic pain management chapter (Chapter 51).

EFFECTS OF REGIONAL ANESTHESIA ON GASTROINTESTINAL PHYSIOLOGY

The degree to which the GI tract is affected by regional anesthesia depends on the type and extent of the block. Epidural analgesia, especially thoracic epidural analgesia (TEA), has been used extensively for a wide variety of GI surgeries. The clinical outcome of TEA after GI surgeries has been reviewed extensively in the literature; the focus of this chapter is its effect on GI physiology.

Effect on Gastrointestinal Motility and Postoperative Ileus

As described, postoperative ileus is a very common phenomenon in patients who undergo major abdominal surgery. Postoperative ileus is a temporary state of GI motor dysfunction that occurs after surgery in the abdominal cavity. This includes disruption of normal coordinated movements of the GI tract,⁶¹ nonmechanical obstruction of the bowel, activation of the inhibitory reflexes, inflammatory mediators, bowel manipulation, electrolyte disturbances, opioid administration, sympathetic overactivity with surgical pain, and postoperative pain.⁶²⁻⁶⁶ Transit time of the stomach may extend 24 to 48 hours and colon transfer time may increase 48 to 72 hours. Some of these effects may continue for up to 3 to 4 days after surgery.^{67,68}

The main pathophysiologic event in postoperative ileus is neuroimmuno interaction, which is based on the bidirectional communication between the immune system within and outside the GI tract and the autonomic nervous system.⁶⁹

Manipulation of the intestines and the stress response associated with postoperative pain are the key factors initiating postoperative ileus. The surgical stress response is a multifaceted, neurohumoral response to a surgical stimulation and can be associated with considerable morbidity, including a systemic inflammatory response syndrome, which is associated with the release of systemic inflammatory response and adrenaline and noradrenaline hormones. This sympathetic overactivity will constrain mobility and directly inhibit gut smooth muscle via activation of α - and β -adrenergic receptors resulting in postoperative ileus.⁷⁰ Epidural administration of local anesthetic or opioids has been shown to suppress these responses.⁷¹⁻⁷³

Epidural block with deposition of local anesthetic within the epidural space results in blockade of the afferent and efferent sympathetic-mediated GI reflexes, but parasympathetic innervation is left intact. The effect of an imbalanced sympathetic and parasympathetic nervous system has been associated with improved GI blood flow and anastomotic mucosal perfusion. This controls pain and decreases the need for opioids.⁷⁴⁻⁷⁸

However, it should be noted that severe hypotension (>50% reduction in systolic blood pressure) may be associated with worsened local perfusion.^{79,80} Vasoactive drugs, such as norepinephrine, can attenuate this effect and improve colonic perfusion.⁸¹

In general, epidural analgesia can effectively decrease the incidence of postoperative ileus. A Cochrane review showed that epidural usage reduces postoperative ileus by 36 hours when a local anesthetic regimen was used as compared to an opioid-based regimen.⁸²

Effect on Enteric Anastomosis Dehiscence

Unopposed parasympathetic activity with blockage of sympathetic fibers has increased concerns among clinicians that the increased mobility and intraluminal pressures will lead to anastomotic leaks and possibly rupture.⁸³ However, animal studies have failed to show any difference in anastomotic bursting pressure when epidural anesthesia is compared to general anesthesia.⁸⁴ In fact, it could be argued

that with improvement of GI blood flow and tissue oxygenation the neuroaxial block can actually reduce the risk of anastomotic breakdown. However, the effect of neuroaxial blocks after GI procedures and laparotomies on enteric anastomotic leakage is not supported in the literature.^{81,85}

Effect on Nutrition

The early postoperative period after GI surgery is characterized by a systemic stress response and catabolic activity. This effect, in conjunction with a lack of nutrition, results in postoperative weakness and muscle wasting. As discussed previously, epidural analgesia has been shown to decrease opioid requirements and reduce postoperative ileus. This, in turn, enhances enteral feeding.⁸⁶ Therefore, blockade of afferent stimuli and the endocrine metabolic responses, as well as the improvement in catabolism seen with epidural analgesia, are part of an enhanced recovery after surgery (ERAS) protocol for major GI surgeries to facilitate oral nutrition.⁸⁷

Effect on Postoperative Nausea and Vomiting

Pain management plays a large role in postoperative nausea and vomiting therapy.⁸⁸ Avoiding systemic opioids and the use of epidural analgesia helps to reduce the incidence of nausea and vomiting. However, in the setting of regional anesthesia, attention should be paid to unopposed vagal activity, local anesthetic systemic toxicity, hypotension, and medication administration.

Spinal anesthesia poses the highest risk for the development of nausea and vomiting and is seen in 20% of patients. The effects of spinal anesthesia, especially with T6 to L1 blockade, include sympathetic innervation and unopposed vagal activity and result in GI hyperperistalsis, nausea, and vomiting.⁸⁹ In addition, TEA or spinal anesthesia that results in systemic hypotension severe enough to cause cerebral ischemia can cause nausea and vomiting.⁹⁰

Effect on Gastrointestinal Blood Flow and Volume

The degree of arterial hypotension induced by spinal or epidural anesthesia is directly related to the extent of the blockade, the dose of local anesthetic used, and baseline hemodynamics.⁹¹ Lumbar epidural anesthesia leads to arterial and venous dilation at the segments affected by the anesthetic. The constriction of the proximal part of the splanchnic vasculature shifts blood volume from the splanchnic system into the systemic circulation and usually results in preservation of stressed volume and blood pressure. TEA is associated with pronounced mesenteric vaso-dilation and arterial hypotension, while intestinal blood flow and oxygen consumption are maintained. A study using labeled red cells demonstrated that epidural anesthesia with sensory block at T4 to T5 increased blood volume in both the intrathoracic and splanchnic vasculature. The addition of a vasoconstrictor decreased volume within the splanchnic region, but increased volume within the thorax. The authors estimated that the use of a vasoconstrictor during TEA led to a shift of approximately 1 L of blood from the splanchnic area into the thoracic and systemic circulation.⁹² Infusion of fluid or the use of adrenergic agonists apparently increases stressed volume. Infusion of fluid increases total (stressed and unstressed) blood volume, whereas adrenergic agonists move existing blood volume from unstressed to stressed.⁹³ In many situations, the use of α -adrenergic

agonists might be more beneficial than infusion of fluid. Because veins are much more sensitive to adrenergic stimulation than arteries are, small doses of α -adrenergic agonists in normovolemic patients would constrict veins (increasing stressed volume) without affecting arteries or jeopardizing tissue perfusion.

ENHANCED RECOVERY AFTER SURGERY FOR GASTROINTESTINAL PROCEDURES—PHYSIOLOGIC BASIS

ERAS is an interdisciplinary, multimodal concept aimed at accelerating postoperative convalescence and reducing general morbidity by simultaneously applying several interventions. ERAS represents a paradigm shift in perioperative care. It reexamines traditional practice by replacing it with evidence-based practices.⁹⁴

ERAS for GI procedures highlights a perioperative regimen with emphasis on^{95,96}:

1. Regional anesthesia
2. Avoidance of opioids
3. Multimodal analgesia
4. Nutrition and preoperative carbohydrates
5. Selective bowel preparation
6. Fluid optimization
7. Temperature control
8. Early removal of drains and tubes
9. Early mobilization
10. Early oral intake

The use of ERAS protocols has been associated with shorter hospitalizations.⁹⁷

PHYSIOLOGIC BASIS OF ERAS

Perioperative Pain Control

Many aspects of regional anesthesia, opioid-sparing anesthesia, and multimodal analgesia have already been discussed. The effect of pain control on postoperative outcomes has also been evaluated in multiple studies and is an inseparable part of ERAS protocols for many surgeries including GI procedures.^{98–100} The favorable physiologic effects on the respiratory and cardiovascular systems by epidural analgesia may serve as yet another reason as to why epidural analgesia is a devoted part of ERAS protocols.^{101–102}

Preoperative Carbohydrate Loading and Early Postoperative Feeding

There is strong evidence in animal studies demonstrating that fed animals tolerate stress much better than fasted animals. Perioperative oral carbohydrates raise insulin sensitivity by 50%. This means there is 50% less insulin resistance in the postoperative period, which also ameliorates ileum barrier failure. There is also less risk of development of hyperglycemic events and an improvement in retention of protein and lean body mass.^{103,105} Enteric feeding is associated with prevention of bacterial translocation¹⁰⁴ or gut barrier failure.¹⁰⁵ Carbohydrate loading shifts the cellular metabolism to an anabolic state that will support postoperative nutrition.^{106–108}

Most of the national and international societies now recommend a 6-hour preoperative fast for solids and a

2-hour fast for clear fluids, which includes carbohydrate drinks.^{109–112}

In order to maintain metabolic and nutritional homoeostasis, early postoperative feeding has been suggested. A small study on patients after major colorectal surgery showed that immediate postoperative enteral feeding does not result in a net loss of body nitrogen.¹¹³

Temperature Control

In addition to the adverse effects of hypothermia (<35°C) on coagulation, cardiac, respiratory, and neurologic function, hypothermia triggers a whole-body thermoregulatory vasoconstriction response. Consequently, it reduces cutaneous flow and can result in tissue hypoxia and failure of the humoral immune defense system.^{114–116} Hypothermia is associated with a threefold increase in the incidence of surgical site infection.¹¹⁷

Nasogastric Tubes

Regular use of nasogastric tubes following major intraabdominal surgery is for gastric decompression, thereby preventing anastomotic leakage and promoting early return of bowel function. However, routine use has been questioned as it is very uncomfortable for the patient and there is an associated risk of developing pulmonary complications, delays in the return of bowel function, and increasing the rate of wound infections.¹¹⁸ In addition, the presence of gastric tubes is associated with increased gastric secretion and motility—a physiologic response to the presence of a foreign body.

Bowel Preparation

Bowel preparation for major GI procedures has been implemented in order to reduce postoperative complications related to infected bowel content,¹¹⁹ with polyethylene glycol a most popular preparation. Adverse physiologic effects of this bowel preparation include decreased exercise capacity, lower weight, increased plasma osmolality, decreased urea and phosphate, and reduced plasma calcium and potassium.¹²⁰ These effects along with fasting can produce a very unpleasant experience for the patient.

The routine use of bowel preparation has been questioned repeatedly. In fact, recent studies have shown that mechanical bowel preparation can be safely omitted before elective colorectal surgery.^{121,122}

Drains

Intraabdominal drains are placed to prevent accumulations of intraabdominal collections, to quickly discover postoperative bleeding, to diagnose anastomotic leakage, and to drain intraabdominal abscesses. However, routine use of drains simply placed prophylactically after major abdominal surgeries has recently been questioned. These drains are not innocuous as they can be associated with bacterial contamination, wound infection, incisional hernia, intestinal obstruction and fistula formation, and bleeding.¹²³ There is insufficient evidence to support the notion that routine use of drainage after colorectal anastomoses can prevent anastomotic leakage or any other related complications.¹²⁴

Fluid Management

All patients having elective surgery undergo a preoperative starvation period that results in a fluid deficit. Typically, it is not enough to produce major fluid shifts, but it may stimulate the production of antidiuretic hormone, atrial natriuretic peptide, the renin-angiotensin-aldosterone system, and an increase in sympathetic activity. This relative hypovolemia is also more pronounced in patients who receive bowel preparation, experience diarrhea or vomiting, are exposed to high temperatures, or have high nasogastric tube output.

Recent NPO guidelines allow patients to have clear fluids up to 2 hours prior to surgery.¹²⁵ Intraoperative fluid management takes into account the preoperative fluid deficit, the presence of a regional anesthesia technique, hemorrhage, and third-space losses. However, prudent administration of intravenous fluids is necessary as free and rapid administration of salt and water will increase capillary hydrostatic pressure, cause tissue and bowel edema, and adversely affect anastomotic integrity. Optimizing fluid administration should focus on increasing tissue perfusion and oxygen delivery, and modulation of the hormonal and inflammatory response.¹²⁶

Mobilization and Early Ambulation

Early postoperative ambulation is recommended for prevention and treatment of postoperative ileus.^{127,128} It is believed that early ambulation helps with the restoration of normal bowel function. However, studies demonstrate that GI myoelectrical activity patterns are not always expedited by early postoperative ambulation; at least there is no correlation with the extent of ambulation.¹²⁹ Yet, early ambulation confers many other advantages, specifically prevention of postoperative thromboembolism and pulmonary complications.^{130,131}

Acknowledgment

The editors and publisher would like to thank Drs. Matthias F. Stopfkuchen-Evans and Simon Gelman for contributing a chapter on this topic in the prior edition of this work. It has served as the foundation for the current chapter.

 Complete references available online at expertconsult.com.

References

1. Agur A, et al. *Grant's Atlas of Anatomy*. Baltimore: Lippincott Williams & Wilkins; 2005.
2. Andreoli TE, Carpenter CCJ, Cecil RL. *Andreoli and Carpenter's Cecil Essentials of Medicine*. Philadelphia: Saunders; 2007. Print.
3. Quigley EM, et al. *Braz J Med Biol Res*. 1998;31:889–900.
4. Seok JW. *J Neurogastroenterol Motil*. 2011;17(2):189–191.
5. Patcharatrakul T, Gonlachanvit S. *J Neurogastroenterol Motil*. 2013;19(3):395–404.
6. Sarna SK. *Colonic Motility: From Bench to Bedside*. San Rafael: Morgan & Claypool Life Sciences; 2010.
7. Thompson W, et al. *Gut*. 1999;45(suppl 2):1143–1147.
8. Castedal M, et al. *Aliment Pharmacol Ther*. 2000;14(5):571–577.
9. Weiskopf RB, et al. *Anesthesiology*. 1994;80(5):1035–1045.
10. Hopster K, et al. *Vet J*. 2015;205(1):62–68.
11. Muller M, et al. *Anesthesia*. 2002;57(2):110–115.
12. Desmet M, et al. *Acta Anaesthesiologica Scandinavica*. 2016.
13. Jensen AG, et al. *Can J Anaesth*. 1992;39(9):938–943.

14. Tylman M, et al. *Minerva Anestesiol*. 2011;77:275–282.
15. Lee TL, et al. *Anesthesia & Analgesia*. 1999;89(5):1246–1249.
16. Leslie K, et al. *Anesth Analg*. 2011;112(2):387–393.
17. Patel S, et al. *J Anaesthesiol Clin Pharmacol*. 2012;28(2):162–171.
18. Woerlee GM. *Common Perioperative Problems and the Anaesthetist. Developments in Critical Care Medicine and Anaesthesiology*. Vol. 18. Springer Netherlands; 1988.
19. Galligan J, Akbarali H. *Am J Gastroenterol Suppl*. 2014;2(1):17–21.
20. Leppert W. *Contem Oncol (Pozn)*. 2012;16(2):125–131.
21. Tassinari D, et al. *J Palliat Med*. 2008;11:492–502.
22. Yuan CS, et al. *Clin Pharmacol Ther*. 1997;61: 467–475.
23. McNicol E, et al. *Pain Med*. 2008;9:634–659.
24. McNicol E, et al. *Cochrane Database Syst Rev*. 2008;(2):CD006332.
25. Keller D, Stein SL. *Clin Colon Rectal Surg*. 2013;26(3):186–190.
26. Delaney C, et al. In: Bosker G, ed. *Clinical Consensus Update in General Surgery*. Roswell(GA): Pharmatecture, LLC; 2006.
27. Kumar C, Bellamy M. *Gastrointestinal and Colorectal Anesthesia*. New York: Taylor & Francis; 2006. Print.
28. Zeinali F, et al. *Can J Surg*. 2009;52:153–157.
29. Holzheimer RG, et al, eds. *Surgical Treatment: Evidence-Based and Problem-Oriented*. Munich: Zuckschwerdt; 2001.
30. Jeejeebhoy KN. *CMAJ*. 2002;166(10):1297–1302.
31. McSwiney BA. *Annu Rev Physiol*. 1944;6(6):365–390.
32. Cervero F. *Physiol Rev*. Jan. 1994;74(1):95–138.
33. Scratcheder T, Grundy D. *Br J Anesth*. 1984;56:3–18.
34. Procacci P, et al. *Prog Brain Res*. 1986;67:21–28.
35. Paintal AS. *Prog Brain Res*. 1986;67:3–19.
36. Jäning W, Morrison JFB. *Prog Brain Res*. 1986;67:78–114.
37. Kuntz A. *The Autonomic Nervous System*. Philadelphia: Lea & Febiger; 1953.
38. Bornica JJ. *Anesthesiology*. 1968;29:793–813.
39. Gebhart GF. *Gut*. 2000;47(suppl 4):iv54–iv55; discussion iv8. PMID 11076915.
40. Altschuler SM, et al. *J Comp Neurol*. 1989;283(2):248–268.
41. Sengupta JN, Gebhart GF. Mechanosensitive afferent fibres in the gastrointestinal and lower urinary tracts. In: Gebhart GF, ed. *Visceral Pain*. Seattle: IASP Press; 1995:75–98.
42. Langley JN. *Brain*. 1903;(26):1–16.
43. Michell GAC. *Anatomy of the Autonomous Nervous System*. Livingstone: Edinburgh; 1953.
44. Sengupta JN, Gebhart GF. *J Neurophysiol*. 1994;71(6):2046–2060.
45. Al-Chaer ED, Traub RJ. *Pain*. 2002;96(3):221–225.
46. Renck H. Management of abdomino-visceral pain by nerve block techniques. *H Mediglobe*. 1992.
47. Sikandar S, Dickenson AH. *Curr Opin Support Palliat Care*. 2012;6(1):17–26.
48. Fields HL, Liebeskind JC. *Pharmacological Approaches to the Treatment of Chronic Pain: New Concepts and Critical Issues*. Seattle: 1994:11–30.
49. Procacci P, Zoppi M, Maresca M. Visceral sensation. In: Cervero F, Morrison JFB, eds. *Progress in Pain Research*. Amsterdam: Elsevier; 1986;39:21–28.
50. Hardy JD, et al. *J Clin Invest*. 1950;29(1):115–140.
51. Gebhart GF. *Visceral Pain, Progress in Pain Research and Management*. Seattle: IASP Press; 1995:3–23.
52. Mayer EA. *Am J Med*. 1999;107(5A). 12S–9S.
53. Van Oudenhoove L, et al. *J Clin Invest*. 2011;121(8):3094–3099.
54. Mayer EA. *Nat Rev Neurosci*. 2011;12(8):453–466.
55. Chu LF, et al. *Clin J Pain*. 2008;24(6):479–496.
56. Castro-Lopes J, Raja SN, Schmelz M. *Pain 2008 Refresher Course Syllabus*. Seattle: IASP Press; 2008:381–389.
57. Boddy AP, et al. *Anesth Analg*. 2006;103(3):682–688.
58. Lillemoen KD, et al. *Ann Surg*. 1993;217:447–457.
59. Puli SR, et al. *Dig Dis Sci*. 2009;54(11):2330–2337.
60. Rana MV, et al. *Curr Pain Headache Rep*. 2014;18(2):394.
61. Liu SS, et al. *Anesthesiology*. 1995;83(4):757–765.
62. Leslie JB, et al. *Adv Prev Med*. 2011;1:1–10.
63. Yukioka H, et al. *Br J Anaesth*. 1987;59:581–584.
64. Wilder-Smith CH, et al. *Anesthesiology*. 1999;91:639–647.
65. Ingram DM, Sheiner HJ. *Br J Surg*. 1981;68:572–576.
66. Nimmo WS, et al. *Br J Clin Pharm*. 1975;2:509–513.
67. Desborough JP. *Br J Anaesth*. 2000;85(1):109–117.
68. Guha A, et al. *Eur J Anaesthesiol*. 2002;19(09):652.
69. Boeckxstaens GE, de Jonge WJ. *Gut*. 2009;58:1300.
70. Desborough JP. *Br J Anaesth*. 2000;85(1):109–117.
71. Kehlet H. *Br J Anaesth*. 1989;63:189–195.
72. Carli F, et al. *Br J Anaesth*. 1991;67:729–734.
73. Kouraklis G, et al. *Int Surg*. 2000;85:353–357.
74. Liu S, et al. *Anesthesiology*. 1995;82(6):1474–1506.
75. Holte K, Kehlet H. *Br J Surg*. 2000;87(11):1480–1493.
76. Shi WZ, et al. *Acta Anaesthesiol Scand*. 2014;58(8):923–932.
77. Steinbrook RA. *Anesth Analg*. 1998;86(4):837–844.
78. Guay J, et al. *Anesth Analg*. 2016;123(6):1591–1602.
79. Steinbrook RA. *Anesth Analg*. 1998;86:837–844.
80. Carpenter RL. *Reg Anesth*. 1996;21:13–17.
81. Michelet P, et al. *Chest*. 2005;128(5):3461–3466.
82. Jorgensen H, et al. *Cochrane Database Syst Rev*. 2000;4:CD001893.
83. Holte K, Kehlet H. *Reg Anesth Pain Med*. 2001;26:111–117.
84. Schnitzler M, et al. *Reg Anesth*. 1992;17:143–147.
85. Ryan P, et al. *Eur J Surg*. 1992;158:45–49.
86. Holte K, Kehlet H. *Clin Nutr*. 2002;21(3):199–206.
87. Lewis KS, et al. *Am J Hosp Pharm*. 1994;51(12):1539–1554.
88. Watcha MF, White PF. *Anesthesiology*. 1992;77(1):162–184.
89. Carpenter RL, et al. *Anesthesiology*. 1992;76(6):906–916.
90. Freise H, Fischer LG. *Curr Opin Anaesthesiol*. 2009;22(5):644–648.
91. Clemente A, Carli F. *Minerva Anestesiol*. 2008;74(10):549–563.
92. Stanton-Hicks M, et al. *Anesthesiology*. 1987;66(3):317–322.
93. Holte K, et al. *Anesthesiology*. 2004;100(2):281–286.
94. Ljungqvist O, JPEN J Parenter Enteral Nutr. 2014;38(5):559–566.
95. Varadhan KK, et al. *Clin Nutr*. 2010;29(4):434–440.
96. Ljungqvist O, et al. *JAMA Surg*. 2017;152(3):292–298.
97. Nygren J, et al. *Current Opinion in Clinical Nutrition and Metabolic Care*. 2003;6:593–597.
98. Pöpping DM, et al. *Ann Surg*. 2014;259(6):1056–1067.
99. Hughes MJ, et al. *JAMA Surg*. 2014;149(12):1224–12230.
100. Khan SA, et al. *Surg Endosc*. 2013;27(7):2581–2591.
101. Popping DM, et al. *Arch Surg*. 2008;143:990–999; discussion 1000.
102. Popping DM, et al. *Ann Surg*. 2014;259:1056–1067.
103. Soop M, et al. *Br J Surg*. 2004;91(9):1138–1145.
104. Wildhaber BE, et al. *J Surg Res*. 2005;123(1):8–16.
105. Mosenthal AC, et al. *Crit Care Med*. 2002;30(2):396–402.
106. Wang ZG, et al. *Br J Surg*. 2010;97:317–327.
107. Yuill KA, et al. *Clin Nutr*. 2005;24:32–37.
108. Bardram L, et al. *Lancet*. 1995;345(8952):763–764.
109. Smith MD, et al. *Cochrane Database Syst Rev*. 2014;8:CD009161.
110. American Society of Anesthesiologists Committee. *Anesthesiology*. 2011;114:495–511.
111. Soreide E, et al. *Acta Anaesthesiol Scand*. 2005;49:1041–1047.
112. Spies CD, et al. *Anaesthesia*. 2003;52:1039–4.
113. Soop M, et al. *Br J Surg*. 2004;91:1138–1145.
114. Hart SR, et al. *Ochsner J*. 2011;11(3):259–270.
115. van Oss CJ, et al. *J Reticuloendothel Soc*. 1980;27(6):561–565. PubMed.
116. Sheffield CW, et al. *Wound Repair Regen*. 1996;4(3):339–345.
117. Kurz A, et al. *N Engl J Med*. 1996;334(19):1209–1215.
118. Nelson R, et al. *Br J Surg*. 2005;92(6):673–680.
119. Nichols RL, Condon RE. *Surg Gynecol Obstet*. 1971;132(2):323–337.
120. Bucher P, et al. *Dis Colon Rectum*. 2004;47(8):1397–1402.
121. Slim K, et al. *Gastroenterol Clin Biol*. 2002;26:667–669. 8–9.
122. Guenaga KF, et al. *Cochrane Database Syst Rev*. 2005;1:CD001544.
123. Jesus EC, et al. *Cochrane Database Syst Rev*. 2004;4:CD002100.
124. Merad F, et al. *Surgery*. 1999;125(5):529–535.
125. Practice guidelines for preoperative fasting and the use of pharmacologic agents to reduce the risk of pulmonary aspiration: application to healthy patients undergoing elective procedures an updated report by the American Society of Anesthesiologists Task Force on Preoperative Fasting and the Use of Pharmacologic Agents to Reduce the Risk of Pulmonary Aspiration. *Anesthesiology*. 2017;126 (3):376–393.
126. Scott MJ, et al. *Acta Anaesthesiol Scand*. 2015;59(10):1212–1231.
127. Story SK, Chamberlain RS. *Dig Surg*. 2009;26(4):265–275.
128. Brieger GH. *Ann Surg*. 1983;197:443–449.
129. Waldhausen JH, Schirmer BD. *Ann Surg*. 1990;212(6):671–677.
130. Wenger NK. *Cardiovascular Clinics*. 1978;9(3):107–115.
131. Parker HG, et al. *Surg Clin N Am*. 1976;56(3):667–672.

References

1. Agur A, Dalley A. *Grant's Atlas of Anatomy*. Baltimore: Lippincott Williams & Wilkins; 2005.
2. Andreoli TE, Charles C, Carpenter J, Cecil Russell L. *Andreoli and Carpenter's Cecil Essentials of Medicine*. Philadelphia: Saunders; 2007.
3. Quiqueley EM, Thompson JS. The effects of surgery on gastrointestinal motor activity. *Braz J Med Biol Res*. 1998;31:889–900.
4. Seok JW. How to interpret gastric emptying scintigraphy. *J Neurogastroenterol Motil*. 2011;17(2):189–191.
5. Patcharatrakul T, Gonlachanvit S. Technique of functional and motility test: how to perform antroduodenal manometry. *J Neurogastroenterol Motil*. 2013;19(3):395–404.
6. Sarna SK. *Colonic Motility: From Bench to Bedside*. San Rafael (CA): Morgan & Claypool Life Sciences; 2010.
7. Thompson W, Longstreth G, Drossman D, et al. Functional bowel disorders and functional abdominal pain. *Gut*. 1999;45(suppl 2):1143–1147.
8. Castedal M, Björnsson E, Abrahamsson H. Effects of midazolam on small bowel motility in humans. *Aliment Pharmacol Ther*. 2000;14(5):571–577.
9. Weiskopf RB, Moore MA, Eger EI, et al. Rapid increase in desflurane concentration is associated with greater transient cardiovascular stimulation than with rapid increase in isoflurane concentration in humans. *Anesthesiology*. 1994;80(5):1035–1045.
10. Hopster K, Hopster-Iversen C, Geburek F, et al. Temporal and concentration effects on isoflurane anaesthesia on intestinal tissue oxygenation and perfusion in horses. *Vet J*. 2015;205(1):62–68.
11. Muller M, Schindler E, Roth S, et al. Effects of desflurane and isoflurane on intestinal tissue oxygen pressure during colorectal surgery. *Anaesthesia*. 2002;57(2):110–115.
12. Desmet M, Vander Cruyssen P, Pottel H, et al. The influence of propofol and sevoflurane on intestinal motility during laparoscopic surgery. *Acta Anaesthesiologica Scandinavica*. 2016.
13. Jensen AG, Kalman SH, Nystrom PO, et al. Anaesthetic technique does not influence postoperative bowel function: a comparison of propofol, nitrous oxide and isoflurane. *Can J Anaesth*. 1992;39(9):938–943.
14. Tylman M, Sarbinowski R, Bengtson JP, Kvarnström A, Bengtsson A. Inflammatory response in patients undergoing colorectal cancer surgery: the effect of two different anesthetic techniques. *Minerva Anestesiol*. 2011;77:275–282.
15. Lee TL, Ang SB, Dambisya YM, et al. The effect of propofol on human gastric and colonic muscle contractions. *Anesth Analg*. 1999;89(5):1246–1249.
16. Leslie K, et al. Nitrous oxide and long-term morbidity and mortality in the ENIGMA trial. *Anesth Analg*. 2011;112(2):387–393.
17. Patel S, Lutz J, Panchagnula U, et al. Anesthesia and perioperative management of colorectal surgical patients—a clinical review (Part 1). *J Anaesthesiol Clin Pharmacol*. 2012;28(2):162–171.
18. Woerlee GM. *Common Perioperative Problems and the Anaesthetist. Developments in Critical Care Medicine and Anaesthesiology*. Vol. 18. Springer Netherlands; 1988.
19. Galligan J, Akbarali H. Molecular physiology of enteric opioid receptors. *Am J Gastroenterol Suppl*. 2014;2(1):17–21.
20. Leppert W. The impact of opioid analgesics on the gastrointestinal tract function and the current management possibilities. *Contem Oncol (Pozn)*. 2012;16(2):125–131.
21. Tassinari D, et al. Adverse effects of transdermal opiates treating moderate-severe cancer pain in comparison to long-acting morphine: a meta-analysis and systematic review of the literature. *J Palliat Med*. 2008;11:492–502.
22. Yuan CS, et al. The safety and efficacy of oral methynaltrexone in preventing morphine-induced delay in oral-cecal transit time. *Clin Pharmacol Ther*. 1997;61: 467–475.
23. McNicol E, et al. Efficacy and safety of mu-opioid antagonists in the treatment of opioid-induced bowel dysfunction: systematic review and meta-analysis of randomized controlled trials. *Pain Med*. 2008;9:634–659.
24. McNicol E, et al. Mu-opioid antagonists for opioid-induced bowel dysfunction. *Cochrane Database Syst Rev*. 2008;2:CD006332.
25. Keller D, Stein SL. Facilitating return of bowel function after colorectal surgery: alvimopan and gum chewing. *Clin Colon Rectal Surg*. 2013;26(3):186–190.
26. Delaney C, Kehlet H, Senagore A, et al. Postoperative ileus: profiles, risk factors, and definitions—a framework for optimizing surgical outcomes in patients undergoing major abdominal colorectal surgery. In: Bosker G, ed. *Clinical Consensus Update in General Surgery*. Roswell (GA): Pharmatecure, LLC; 2006.
27. Kumar C, Bellamy M. *Gastrointestinal and Colorectal Anesthesia*. New York: Taylor & Francis; 2006.
28. Zeinali F, Stulberg JJ, Delaney CP. Pharmacological management of postoperative ileus. *Can J Surg*. 2009;52:153–157.
29. Holzheimer RG, Mannick JA, eds. *Surgical Treatment: Evidence-Based and Problem-Oriented*. Munich; 2001.
30. Jeejeebhoy KN. Short bowel syndrome: a nutritional and medical approach. *CMAJ*. 2002;166(10):1297–1302.
31. McSwiney BA. Visceral functions of the nervous system. *Annu Rev Physiol*. 1944;6:365–390.
32. Cervero F. Sensory innervation of the viscera: peripheral basis of visceral pain. *Physiol Rev*. 1994;74(1):95–138.
33. Sengupta JN, Gebhart GF. Mechanosensitive afferent fibres in the gastrointestinal and lower urinary tracts. In: Gebhart GF, ed. *Visceral Pain*. Seattle: IASP Press; 1995:75–98.
34. Scratches T, Grundy D. The physiology of intestinal motility and secretion. *Br J Anesth*. 1984;56:3–18.
35. Procacci P, Zoppi M, Maresca M. Clinical approach to visceral pain. *Prog Brain Res*. 1986;67:21–28.
36. Paintal AS. The visceral sensations—some basic mechanism. *Prog Brain Res*. 1986;67:3–19.
37. Jähnig W, Morrison JFB. Functional properties of spinal visceral afferents supplying abdominal and pelvic organs with special emphasis on visceral nociception. *Prog Brain Res*. 1986;67:78–114.
38. Kuntz A. *The Autonomic Nervous System*. Philadelphia: Lea & Febiger; 1953.
39. Bornica JJ. Autonomic innervation of the viscera in relation to nerve block. *Anesthesiology*. 1968;29:793–813.
40. Gebhart GF. Visceral pain–peripheral sensitisation. *Gut*. 2000;47(suppl 4):iv54–iv55; discussion iv8. PMID 11076915.
41. Altschuler SM, Bao XM, Bieger D, Hopkins DA, Miselis RR. Viscerotopic representation of the upper alimentary tract in the rat: sensory ganglia and nuclei of the solitary and spinal trigeminal tracts. *J Comp Neurol*. 1989;283(2):248–268.
42. Langley JN. The autonomic nervous system. *Brain*. 1903;(26):1–16.
43. Michell GAC. *Anatomy of the Autonomic Nervous System*. Edinburgh: Livingstone; 1953.
44. Sengupta JN, Gebhart GF. Characterization of mechanosensitive pelvic nerve afferent fibers innervating the colon of the rat. *J Neurophysiol*. 1994;71(6):2046–2060.
45. Al-Chaer ED, Traub RJ. Biological basis of visceral pain: recent developments. *Pain*. 1996;3(3):221–225.
46. Renck H. *Management of Abdomino-visceral Pain by Nerve Block Techniques*. H Mediglobe; 1992.
47. Sikandar S, Dickenson AH. Visceral pain – the ins and outs, the ups and downs. *Curr Opin Support Palliat Care*. 2012;6(1):17–26.
48. Fields HL, Liebeskind JC. *Pharmacological Approaches to the Treatment of Chronic Pain: New Concepts and Critical Issues*. Seattle: 1994;11–30.
49. Procacci P, Zoppi M, Maresca M. Visceral sensation. In: Cervero F, Morrison JFB, eds. *Progress in Pain Research*. Amsterdam: Elsevier; 1986;39:21–28.
50. Hardy JD, Wolff HG, Goodell H. Experimental evidence on the nature of cutaneous hyperalgesia. *J Clin Invest*. 1950;29(1):115–140.
51. Gebhart GF. *Visceral Pain, Progress in Pain Research and Management*. Seattle: IASP Press; 1995:3–23.
52. Mayer EA. Emerging disease model for functional gastrointestinal disorders. *Am J Med*. 1999;107(5A):12S–19S.
53. Van Oudenhove L, McKie S, Lassman D, et al. Fatty acid-induced gut-brain signaling attenuates neural and behavioral effects of sad emotion in humans. *J Clin Invest*. 2011;121(8):3094–3099.
54. Mayer EA. Gut feelings: the emerging biology of gut-brain communication. *Nat Rev Neurosci*. 2011;12(8):453–466.
55. Chu LF, Angst MS, Clark D. Opioid-induced hyperalgesia in humans: molecular mechanisms and clinical considerations. *Clin J Pain*. 2008;24(6):479–496.
56. Castro-Lopes J, Raja SN, Schmelz M. *Pain 2008 Refresher Course Syllabus*. Seattle: IASP Press; 2008:381–389.

57. Boddy AP, Mehta S, Rhodes M. The effect of intraperitoneal local anesthesia in laparoscopic cholecystectomy: a systematic review and meta-analysis. *Anesth Analg.* 2006;103(3):682–688.
58. Lillemoe KD, Cameron JL, Kauffman HS, et al. Chemical splanchnectomy in patients with unresectable pancreatic cancer. A prospective randomized trial. *Ann Surg.* 1993;217:447–457.
59. Puli SR, Reddy JB, Bechtold ML, Antillon MR, Brugge WR. EUS-guided celiac plexus neurolysis for pain due to chronic pancreatitis or pancreatic cancer pain: a meta-analysis and systematic review. *Dig Dis Sci.* 2009;54(11):2330–2337.
60. Rana MV, Candido KD, Raja O, Knezevic NN. Celiac plexus block in the management of chronic abdominal pain. *Curr Pain Headache Rep.* 2014;18(2):394.
61. Liu SS, Carpenter RL, Mackey DC, et al. Effects of perioperative analgesic technique on rate of recovery after colon surgery. *Anesthesiology.* 1995;83(4):757–765.
62. Leslie JB, Viscusi ER, Pergolizzi JV, Panchal SJ. Anesthetic routines: the anesthesiologist's role in gi recovery and postoperative ileus. *Adv Prev Med.* 2011;1:1–10.
63. Yukioka H, Bogod DG, Rosen M. Recovery of bowel motility after surgery. Detection of time to first flatus from carbon dioxide concentration and patient estimate after nal-buphine and placebo. *Br J Anaesth.* 1987;59:581–584.
64. Wilder-Smith CH, Hill L, Wilkins J, et al. Effects of morphine and tramadol on somatic and visceral sensory function and gastrointestinal motility after abdominal surgery. *Anesthesiology.* 1999;91:639–647.
65. Ingram DM, Sheiner HJ. Postoperative gastric emptying. *Br J Surg.* 1981;68:572–576.
66. Nimmo WS, Heading RC, Wilson, et al. Inhibition of gastric emptying and drug absorption by narcotic analgesics. *Br J Clin Pharm.* 1975;2:509–513.
67. Desborough JP. The stress response to trauma and surgery. *Br J Anaesth.* 2000;85(1):109–117.
68. Guha A, Scawn ND, Rogers SA, Pennefather SH, Russell GN. Gastric emptying in post-thoracotomy patients receiving a thoracic fentanyl-bupivacaine epidural infusion. *Eur J Anaesthesiol.* 2002;19(09):652.
69. Boeckxstaens GE, de Jonge WJ. Neuroimmune mechanisms in postoperative ileus. *Gut.* 2009; 58:1300.
70. Desborough JP. The stress response to trauma and surgery. *Br J Anaesth.* 2000;85(1):109–117.
71. Kehlet H. Surgical stress, the role of pain and analgesia. *Br J Anaesth.* 1989;63:189–195.
72. Carli F, Webster J, Pearson M, et al. Protein metabolism after abdominal surgery: effect of 24 hour extradural block with local anaesthetic. *Br J Anaesth.* 1991;67:729–734.
73. Kouraklis G, Glinavou A, Raftopoulos L, et al. Epidural analgesia attenuates the systemic response to upper abdominal surgery: a randomized trial. *Int Surg.* 2000;85:353–357.
74. Liu S, Carpenter RL, Neal JM. Epidural anesthesia and analgesia: their role in postoperative outcome. *Anesthesiology.* 1995;82(6):1474–1506.
75. Holte K, Kehlet H. Postoperative ileus: a preventable event. *Br J Surg.* 2000;87(11):1480–1493.
76. Shi WZ, Miao YL, Yakoob MY, et al. Recovery of gastrointestinal function with thoracic epidural vs. systemic analgesia following gastrointestinal surgery. *Acta Anaesthesiol Scand.* 2014;58(8):923–932.
77. Steinbrook RA. Epidural anesthesia and gastrointestinal motility. *Anesth Analg.* 1998;86(4):837–844.
78. Guay J, Nishimori M, Kopp SL. Epidural local anesthetics versus opioid based analgesic regimens for postoperative gastrointestinal paralysis, vomiting, and pain after abdominal surgery: a Cochrane review. *Anesth Analg.* 2016;123(6):1591–1602.
79. Steinbrook RA. Epidural anesthesia and gastrointestinal motility. *Anesth Analg.* 1998;86:837–844.
80. Carpenter RL. Gastrointestinal benefits of regional anesthesia/analgesia. *Reg Anesth.* 1996;21:13–17.
81. Michelet P, D'Journo XB, Roch A, et al. Perioperative risk factors for anastomotic leakage after esophagectomy: influence of thoracic epidural analgesia. *Chest.* 2005;128(5):3461–3466.
82. Jorgensen H, Wetterslev J, Moiniche S, et al. Epidural local anesthetic versus opioid-based analgesic regimens on postoperative gastrointestinal paralysis, PONV and pain after abdominal surgery. *Cochrane Database Syst Rev.* 2000;4:CD001893.
83. Holte K, Kehlet H. Epidural analgesia and risk of anastomotic leakage. *Reg Anesth Pain Med.* 2001;26:111–117.
84. Schnitzler M, Kilbride MJ, Senagore A. Effect of epidural analgesia on colorectal anastomotic healing and colonic motility. *Reg Anesth.* 1992;17:143–147.
85. Ryan P, Schweitzer SA, Woods RJ. Effects of epidural and general anesthesia compared with general anesthesia alone in large bowel anastomosis. A prospective study. *Eur J Surg.* 1992;158:45–49.
86. Holte K, Kehlet H. Epidural anaesthesia and analgesia—effects on surgical stress responses and implications for postoperative nutrition. *Clin Nutr.* 2002;21(3):199–206.
87. Lewis KS, Whipple JK, Michael KA, Quebbeman EJ. Effect of analgesic treatment on the physiological consequences of acute pain. *Am J Hosp Pharm.* 1994;51(12):1539–1554.
88. Watcha MF, White PF. Postoperative nausea and vomiting. Its etiology, treatment, and prevention. *Anesthesiology.* 1992;77(1):162–184.
89. Carpenter RL, Caplan RA, Brown DL, Stephenson C, Wu R. Incidence and risk factors for side effects of spinal anesthesia. *Anesthesiology.* 1992;76(6):906–916.
90. Freise H, Fischer LG. Intestinal effects of thoracic epidural anesthesia. *Curr Opin Anaesthesiol.* 2009;22(5):644–648.
91. Clemente A, Carli F. The physiological effects of thoracic epidural anesthesia and analgesia on the cardiovascular, respiratory and gastrointestinal systems. *Minerva Anestesiol.* 2008;74(10):549–563.
92. Stanton-Hicks M, Höck A, Stühmeier KD, Arndt JO. Venoconstrictor agents mobilize blood from different sources and increase intrathoracic filling during epidural anesthesia in supine humans. *Anesthesiology.* 1987;66(3):317–322.
93. Holte K, Foss NB, Svensén C, Lund C, Madsen JL, Kehlet H. Epidural anesthesia, hypotension, and changes in intravascular volume. *Anesthesiology.* 2004;100(2):281–286.
94. Ljungqvist O. ERAS—enhanced recovery after surgery: moving evidence-based perioperative care to practice. *J Parenter Enteral Nutr.* 2014;38(5):559–566.
95. Varadhan KK, Neal KR, Dejong CH, Fearon KC, Ljungqvist O, Lobo DN. The enhanced recovery after surgery (ERAS) pathway for patients undergoing major elective open colorectal surgery: a meta-analysis of randomized controlled trials. *Clin Nutr.* 2010;29(4):434–440.
96. Ljungqvist O, Scott M, Fearon KC. Enhanced recovery after surgery: a review. *JAMA Surg.* 2017;152(3):292–298.
97. Nygren J, Thorell A, Ljungqvist O. New developments facilitating nutritional intake after gastrointestinal surgery. *Curr Opin Clin Nutr Metab Care.* 2003;6:593–597.
98. Pöpping DM, Elia N, Van Aken HK, et al. Impact of epidural analgesia on mortality and morbidity after surgery: systematic review and meta-analysis of randomized controlled trials. *Ann Surg.* 2014;259(6):1056–1067.
99. Hughes MJ, Ventham NT, McNally S, Harrison E, Wigmore S. Analgesia after open abdominal surgery in the setting of enhanced recovery surgery: a systematic review and meta-analysis. *JAMA Surg.* 2014;149(12):1224–1230.
100. Khan SA, Khokhar HA, Nasr AR, Carton E, El-Masry S. Effect of epidural analgesia on bowel function in laparoscopic colorectal surgery: a systematic review and meta-analysis. *Surg Endosc.* 2013;27(7):2581–2591.
101. Pöpping DM, Elia N, Marret E, Remy C, Tramer MR. Protective effects of epidural analgesia on pulmonary complications after abdominal and thoracic surgery: a meta-analysis. *Arch Surg.* 2008;143:990–999; discussion 1000.
102. Pöpping DM, Elia N, Van Aken HK, et al. Impact of epidural analgesia on mortality and morbidity after surgery: systematic review and meta-analysis of randomized controlled trials. *Ann Surg.* 2014;259:1056–1067.
103. Soop M, Carlson GL, Hopkinson J, et al. Randomized clinical trial of the effects of immediate enteral nutrition on metabolic responses to major colorectal surgery in an enhanced recovery protocol. *Br J Surg.* 2004;91(9):1138–1145.
104. Wildhaber BE, Yang H, Spencer AU, et al. Lack of enteral nutrition—effects on the intestinal immune system. *J Surg Res.* 2005;123(1):8–16.
105. Mosenthal AC, Xu D, Deitch EA. Elemental and intravenous total parenteral nutrition diet-induced gut barrier failure is intestinal site specific and can be prevented by feeding nonfermentable fiber. *Crit Care Med.* 2002;30(2):396–402.
106. Wang ZG, Wang Q, Wang WJ, Qin HL. Randomized clinical trial to compare the effects of preoperative oral carbohydrate versus

- placebo on insulin resistance after colorectal surgery. *Br J Surg.* 2010;97:317–327.
107. Yuill KA, Richardson RA, Davidson HI, Garden OJ, Parks RW. The administration of an oral carbohydrate-containing fluid prior to major elective upper-gastrointestinal surgery preserves skeletal muscle mass postoperatively—a randomised clinical trial. *Clin Nutr.* 2005;24:32–37.
108. Bardram L, Funch-Jensen P, Jensen P, Crawford ME, Kehlet H. Recovery after laparoscopic colonic surgery with epidural analgesia, and early oral nutrition and mobilisation. *Lancet.* 1995;345(8952):763–764.
109. Smith MD, McCall J, Plank L, Herbison GP, Soop M, Nygren J. Preoperative carbohydrate treatment for enhancing recovery after elective surgery. *Cochrane Database Syst Rev.* 2014;8:CD009161.
110. American Society of Anesthesiologists Committee. Practice guidelines for preoperative fasting and the use of pharmacologic agents to reduce the risk of pulmonary aspiration: application to healthy patients undergoing elective procedures: an updated report by the American Society of Anesthesiologists Committee on Standards and Practice Parameters. *Anesthesiology.* 2011;114:495–511.
111. Soreide E, Eriksson LI, Hirlekar G, et al. Pre-operative fasting guidelines: an update. *Acta Anaesthesiol Scand.* 2005;49:1041–1047.
112. Spies CD, Breuer JP, Gust R, et al. Klinik für Anästhesiologie und operative Intensivmedizin C-UB [Preoperative fasting. An update]. *Anaesthetist.* 2003;52:1039–4.
113. Soop M, Carlson GL, Hopkinson J, et al. Randomized clinical trial of the effects of immediate enteral nutrition on metabolic responses to major colorectal surgery in an enhanced recovery protocol. *Br J Surg.* 2004;91:1138–1145.
114. Hart SR, Bordes B, Hart J, Corsino D, Harmon D. Unintended perioperative hypothermia. *Ochsner J.* 2011;11(3):259–270.
115. van Oss CJ, Absolom DR, Moore LL, Park BH, Humbert JR. Effect of temperature on the chemotaxis, phagocytic engulfment, digestion and O₂ consumption of human polymorphonuclear leukocytes. *J Reticuloendothel Soc.* 1980;27(6):561–565.
116. Sheffield CW, Sessler DI, Hopf HW, et al. Centrally and locally mediated thermoregulatory responses after subcutaneous oxygen tension. *Wound Repair Regen.* 1996;4(3):339–345.
117. Kurz A, Sessler DI, Lenhardt R. Perioperative normothermia to reduce the incidence of surgical-wound infection and shorten hospitalization. Study of wound infection and temperature group. *N Engl J Med.* 1996;334(19):1209–1215.
118. Nelson R, Tse B, Edwards S. Systematic review of prophylactic nasogastric decompression after abdominal operations. *Br J Surg.* 2005;92(6):673–680.
119. Nichols RL, Condon RE. Preoperative preparation of the colon. *Surg Gynecol Obstet.* 1971;132(2):323–337.
120. Bucher P, Gervaz P, Soravia C, et al. Physiologic effects of bowel preparation. *Dis Colon Rectum.* 2004;47(8):1397–1402.
121. Slim K, Panis Y, Chipponi J. Mechanical colonic preparation for surgery or how surgeons fight the wrong battle. *Gastroenterol Clin Biol.* 2002;26:667–669.
122. Guenaga KF, Matos D, Castro AA, et al. Mechanical bowel preparation for elective colorectal surgery. *Cochrane Database Syst Rev.* 2005;1:CD001544.
123. Jesus EC, Karliczek A, Matos D, et al. Prophylactic anastomotic drainage for colorectal surgery. *Cochrane Database Syst Rev.* 2004;4:CD002100.
124. Merad F, Hay JM, Fingerhut A, et al. Is prophylactic pelvic drainage useful after elective rectal or anal anastomosis? A multicenter controlled randomized trial. French Association for Surgical Research. *Surgery.* 1999;125(5):529–535.
125. Practice guidelines for preoperative fasting and the use of pharmacologic agents to reduce the risk of pulmonary aspiration: application to healthy patients undergoing elective procedures an updated report by the American Society of Anesthesiologists Task Force on Preoperative Fasting and the Use of Pharmacologic Agents to Reduce the Risk of Pulmonary Aspiration. *Anesthesiology.* 2017;126(3):376–393.
126. Scott MJ, Baldini G, Fearon KC, et al. Enhanced Recovery After Surgery (ERAS) for gastrointestinal surgery, part 1: pathophysiological considerations. *Acta Anaesthesiol Scand.* 2015;59(10):1212–1231.
127. Story SK, Chamberlain RS. A comprehensive review of evidence-based strategies to prevent and treat postoperative ileus. *Dig Surg.* 2009;26(4):265–275.
128. Brieger GH. Early ambulation a study in the history of surgery. *Ann Surg.* 1983;197:443–449.
129. Waldhausen JH, Schirmer BD. The effect of ambulation on recovery from postoperative ileus. *Ann Surg.* 1990;212(6):671–677.
130. Wengen NK. The physiologic basis for early ambulation after myocardial infarction. *Cardiovascular Clinics.* 1978;9(3):107–115.
131. Parker HG, et al. Changing patterns in fracture management emphasizing early motion and function. *Surg Clin N Am.* 1976;56(3):667–672.

DOLORES B. NJOKU, HOVIG V. CHITILIAN, and KATE KRONISH

KEY POINTS

- The liver is the largest abdominal organ and carries out a number of vital functions including metabolism and detoxification.
- The liver receives approximately 25% of the resting cardiac output. The hepatic artery is responsible for 25% to 30% of the blood supply to the liver while the portal vein is responsible for 70% to 75%. They each deliver 50% of the total oxygen to the liver.
- For the purpose of hepatic resection, the liver can be divided into eight segments based on independent blood supply and drainage of blood and bile. A segment can be resected without compromising the blood flow and biliary drainage of other segments.
- The acinus is the basic functional unit of the liver. It is organized around the flow of blood from the portal triad to the central vein through the sinusoids. Hepatocytes in the acinus are organized into zones based on their proximity to the portal triad or central vein. Zone 1 or periportal hepatocytes are closer to the portal triads and receive oxygen and nutrient-rich blood. Zone 3 or perivenous hepatocytes are closer to the central veins and receive oxygen-poor blood. Hepatocytes in different zones serve different anatomic functions.
- The liver plays an integral role in carbohydrate, protein, lipid, and bile metabolism. It is also responsible for protein synthesis. Albumin is the most abundant plasma protein produced by the liver.
- Drug and toxin excretion is carried out by the hepatocytes by first polarizing the molecules then conjugating them to make them more hydrophilic. Drugs excreted in the bile may be reabsorbed through enterohepatic circulation leading to prolonged effects.
- Standard laboratory panels used to evaluate the hepatobiliary system help define broad categories of hepatobiliary pathology: hepatitis, hepatobiliary dysfunction, or insufficient protein synthesis. Specific diagnoses often require clinical context and radiologic studies.
- Cirrhosis is the result of chronic hepatic disease and can ultimately result in portal hypertension and liver failure. Liver failure can lead to significant dysfunction in all organ systems, giving rise to coagulopathy, thrombocytopenia, hyperdynamic circulation, esophageal varices, hepatic encephalopathy, hepatopulmonary syndrome, portopulmonary hypertension, and hepatorenal syndrome. The definitive treatment for hepatic failure is liver transplantation.
- Volatile anesthetics reduce mean arterial pressure and cardiac output, leading to a reduction in portal blood flow in a dose-dependent manner. The hepatic arterial buffer response is preserved with isoflurane, sevoflurane, and desflurane leading to the preservation total hepatic blood flow, but not with halothane.
- Advanced liver disease impairs the elimination of many drugs including vecuronium, rocuronium, morphine, meperidine, and benzodiazepines. Dosing should be adjusted in the setting of liver failure.
- Elective surgery is contraindicated in patients with acute hepatitis or liver failure. Patients with chronic hepatitis can safely undergo elective surgery. Hepatotoxic drugs should be avoided and hepatic perfusion maintained. Child-Turcotte-Pugh class and Model for End-Stage Liver Disease score can be used to predict risk of perioperative mortality.

Anatomy of the Liver

The liver is the second largest organ in the human body and is responsible for a host of functions to maintain homeostasis. The liver acts as the interface between the gastrointestinal tract and remainder of the body. It is responsible for

metabolic, synthetic, immunologic, and hemodynamic functions. As a result, hepatic dysfunction has profound effects on all organ systems and introduces significant challenges to anesthetic management. It is therefore essential for the anesthesiologist to have a firm grasp of the anatomy, physiology, and pathophysiology of the liver.

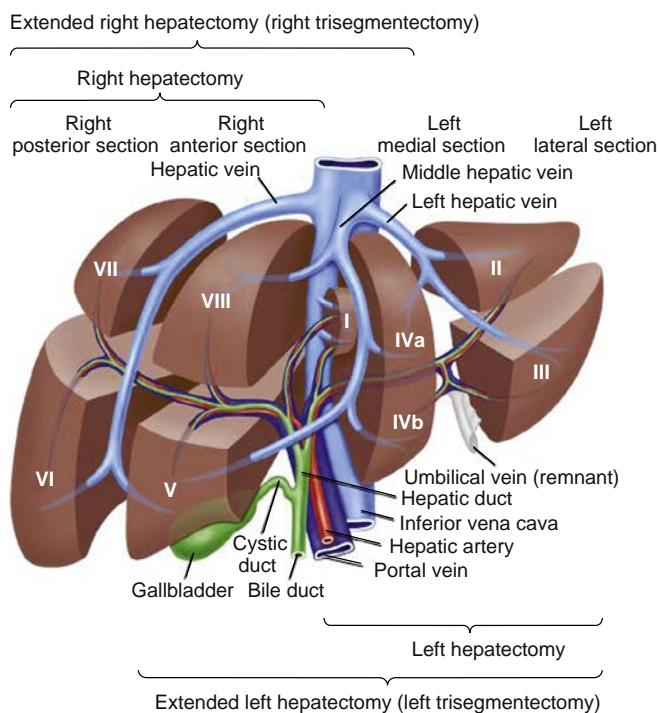


Fig. 16.1 Schematic depiction of Couinaud segmental liver anatomy and the normal portal venous structures. Bracketed text shows hepatic segments resected during partial hepatectomies. (Modified from Venook AP, Curley SA. Management of potentially resectable colorectal cancer liver metastases. <http://www.uptodate.com/contents/management-of-potentially-resectable-colorectal-cancer-liver-metastases>.)

SURGICAL ANATOMY, HEPATIC BLOOD FLOW, AND THE BILIARY TREE

The adult liver can range from around 600 to over 1800 g making the liver one of the heaviest organs in the body. In healthy females the liver ranges in size from 603 to 1767 g,¹ while in healthy males, the liver ranges in size from 968 to 1860 g.² In newborns, infants, and children, the liver is also one of the largest organs and the contribution of its weight to total body weight decreases with age. Thus the liver in a term 3 to 3.5 kg newborn can weigh 150 to 170 g,³ which represents around 5% of the total body weight. In sharp contrast the adult liver represents 2% to 2.5% of the total body weight.

The liver receives approximately 25% of the resting cardiac output (CO).⁴ The blood supply is through both the arterial and venous systems in the form of the hepatic artery and the portal vein (Fig. 16.1). The hepatic artery is responsible for 25% to 30% of the blood supply to the liver whereas the portal vein is responsible for 70% to 75%. The hepatic artery arises from the celiac trunk in 80% of the population. In the remainder, it arises from the superior mesenteric artery. After giving rise to the gastroduodenal artery, the common hepatic artery enters the hilum of the liver (porta hepatis) where it further branches into the right and left hepatic arteries, supplying the right and left sides of the liver, respectively. The right hepatic artery gives rise to the cystic artery that supplies the gallbladder.⁴ The arteries continue to branch throughout the liver ultimately running through the portal tracts and terminating in the hepatic sinusoids (capillaries). Although part of the venous system,

the portal vein is the primary source of oxygenated blood to the liver. The portal vein carries blood from the gastrointestinal tract, pancreas, and spleen to the liver. It drains the superior mesenteric, splenic, and inferior mesenteric veins. It also drains the gastric, cystic, and pancreaticoduodenal veins. The portal vein enters the hilum and, like the hepatic artery, branches into the right and left portal veins, supplying the respective sides of the liver.⁴ The portal veins continue to branch throughout the liver in conjunction with the hepatic arteries. As with the arteries, they terminate in the hepatic sinusoids.

Venous drainage of the liver is through the hepatic veins directly into the inferior vena cava (IVC). The right and middle hepatic veins serve the right half and middle portions of the liver, respectively, while the left hepatic vein drains the left half of the liver. The biliary system removes bile from the liver and delivers it to the duodenum through the ampulla of Vater. The intrahepatic bile ducts typically travel with the portal veins, draining into right and left collections systems that ultimately form the common bile duct (CBD; see Fig. 16.1).⁴

From a historical perspective, the description of the gross anatomy of the liver has evolved from being rooted in the surface anatomy of the organ to its functional organization. Traditionally, the liver was divided into four lobes based on its surface features: right lobe, left lobe, quadrate, and caudate. The right and left lobes were divided by the falciform ligament, when viewed anteriorly. When viewed from below, the quadrate lobe was bounded by the porta hepatis posteriorly, the gallbladder fossa on the right, and the ligamentum teres on the left.⁴ The caudate lobe was bounded by the porta hepatis anteriorly, the IVC on the right, and the ligamentum venosum fissure on the left. In the late 1800s, Sir James Cantlie demonstrated that the right and left hemilivers were defined by independent portal circulations and thus the functional midline of the liver was at the bifurcation of the portal vein, along a line connecting the gallbladder bed and the IVC ("Cantlie's line"), lateral to the falciform ligament. Cantlie recognized that the line defined a vascular watershed and described its implications for surgical resection of the liver.⁵ With advances in hepatic surgery, anatomic descriptions of the liver were developed that further divided the hemilivers into segments based on the vascular distribution and biliary drainage. Each segment has its own independent vascular inflow and outflow, and biliary drainage. As a result, surgical resection of a segment does not compromise adjacent segments. The most commonly used organizational system was developed by Couinaud (see Fig. 16.1).⁶ In the Couinaud model, the liver is divided into eight segments. The right and left hemilivers are divided at the bifurcation of the portal vein, along the middle hepatic vein. The right, middle, and left hepatic veins divide the liver vertically into four sectors: right posterior, right anterior, left medial, and left lateral sectors. The four sectors are divided in the horizontal plane by the branches of the portal vein, giving rise to the eight segments. In this system, the caudate lobe is referred to as segment 1 and the remainder of the segments are numbered in a clockwise fashion. Segments 2 and 3 are medial to the left hepatic vein, with segment 2 superior to segment 3. Segment 4 lies between the middle and left hepatic vein and is subdivided into 4a (superior) and 4b (inferior) subsegments. Segments 8 (superior) and 5 (inferior) are located between

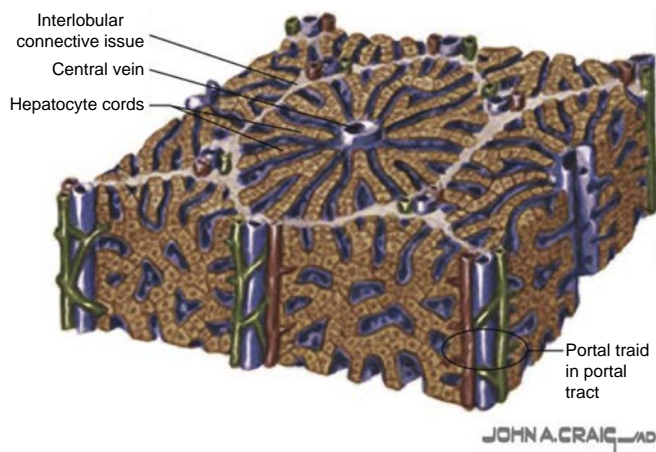


Fig. 16.2 Hepatic lobule. Liver arranged as a series of hexagonal lobules, each composed of a series of hepatocyte cords (plates) interspersed with sinusoids. Each lobule surrounds a central vein and is bounded by six peripheral portal triads (low magnification).

the middle and right hepatic veins. Segments 6 (inferior) and 7 (superior) are located between the right hepatic vein and the edge of the liver.⁶ In clinical practice, contrast-enhanced computed tomography (CT) scanning and intraoperative ultrasound are used to define the anatomy unique to each individual and plan for the appropriate resection. To standardize the nomenclature used to describe hepatic resections, the International Hepatopancreatobiliary Association published consensus terminology in 2000 based on the Couinaud segments, known as the Brisbane 2000 terminology.⁷ This system of terminology has gained traction but has not yet been uniformly adopted.^{8,9}

CELLULAR ANATOMY

Liver Lobule and Acinus

The cellular architecture of the liver supports its functions of detoxifying the blood and metabolizing nutrients. Histologically, the liver parenchyma can be organized into anatomic units (liver lobules) or functional units (liver acinus). The liver lobule is the basic structural unit of the hepatic parenchyma (Fig. 16.2). The lobule typically appears hexagonal in shape with a portal canal at each corner and a hepatic venule (central vein) located in the center. Through each portal canal run the lymphatics, nerve fibers, and a portal triad. Each portal triad consists of a bile ductule, hepatic arteriole, and portal venule. From a functional standpoint, the acinus is the smallest unit of the liver (Fig. 16.3A). It is comprised of a portal tract at the center with central vein at the periphery. Oxygenated and nutrient-rich blood flows from the portal triads to the central hepatic veins through the hepatic sinusoids (see Fig. 16.3B). The walls of the sinusoids are composed of sinusoidal endothelial cells (SECs) that are separated by fenestrations of 50 to 150 nm in diameter. The fenestrations allow the passage of metabolites, plasma proteins, pharmaceutical molecules, lipoproteins, and other solutes into the space of Disse (SD) surrounding the sinusoids while retaining blood cells in the vessels. Larger macromolecules and potentially immunogenic peptides enter the SD by transcytosis through the SECs.¹⁰ Once in the SD, the molecules are taken up by hepatocytes.

Hepatocytes

Hepatocytes make up 75% to 80% of the total cellular volume of the liver.¹¹ They are responsible for drug, protein, carbohydrate, lipid, and heme metabolism in addition to the synthesis of a variety of proteins necessary for the maintenance of homeostasis at baseline and in response to acute insults secondary to ischemia-reperfusion, viral and bacterial infections, and toxins. Hepatocytes are polarized with heterogeneous plasma membranes to facilitate their varied functions. The basolateral (sinusoidal) portion of the membrane is in direct contact with the SD while the apical portion of the membrane makes up the bile canalculus that drains bile to the ductules.¹² Hepatocytes are divided into different zones based on their proximity to the portal triad. Zone 1 is periportal, zone 3 is around the central vein (perivenous or pericentral), and zone 2 is in between (midzone). Zone 3 hepatocytes are furthest away from the portal tracts and thus receive blood with a lower oxygen tension and nutrient content.¹³ The metabolic functions of the hepatocytes differ based on the zone in which they are located (see Fig. 16.3C). This metabolic zonation increases the efficiency of carbohydrate, amino acid, lipid, and xenobiotic metabolism. Periportal (zone 1) hepatocytes are the major sites of aerobic metabolism, and process such as glycogen synthesis and sulfation whereas perivenous (zone 3) hepatocytes are the major sites of anaerobic metabolism, glycolysis, and glucuronidation. By virtue of their location, zone 3 hepatocytes are most sensitive to hypoxia.¹³

Hepatic Stellate Cells

Hepatic stellate cells (HSCs) make up 8% to 10% of all resident liver cells.¹⁴ These specialized cells reside in the SD between liver sinusoidal endothelial cells (LSECs) and the hepatocytes. In the normal liver, HSCs are believed to be in a quiescent state. In the setting of liver injury, these cells become activated in response to cytokines and chemokines generated by hepatocytes, LSECs, as well as leukocytes and Kupffer cells. The stellate cells proliferate and differentiate into myofibroblasts participating in hepatic inflammation and fibrosis.¹⁵

MYELOID CELLS

The myeloid cells that can be found in the liver consist primarily of Kupffer cells (20%-30%) also known as resident tissue macrophages, in addition to dendritic cells and myeloid-derived suppressor cells. At first glance, it may seem that these cells have a less important role than hepatocytes and LSEC. However, while Kupffer cells constitute around 20% to 30% of nonparenchymal cells, they constitute 80% to 90% of all tissue macrophages.¹⁶ Kupffer cells reside in the portal and lobular liver sinusoids where they engulf both infectious and noninfectious particles by phagocytosis. Once phagocytosed, these particles are unable to induce proinflammatory responses in the liver. Thus by prevalence and location, these cells serve critical roles in innate and adaptive immunity by detoxification where they down-regulate potentially proinflammatory triggers that could disrupt hepatic homeostasis.¹⁷

Dendritic cells and myeloid-derived suppressor cells are the least abundant of myeloid cells. Hepatic dendritic cells are present in the normal liver and reside in the portal area and are believed to promote tolerance to phagocytosed

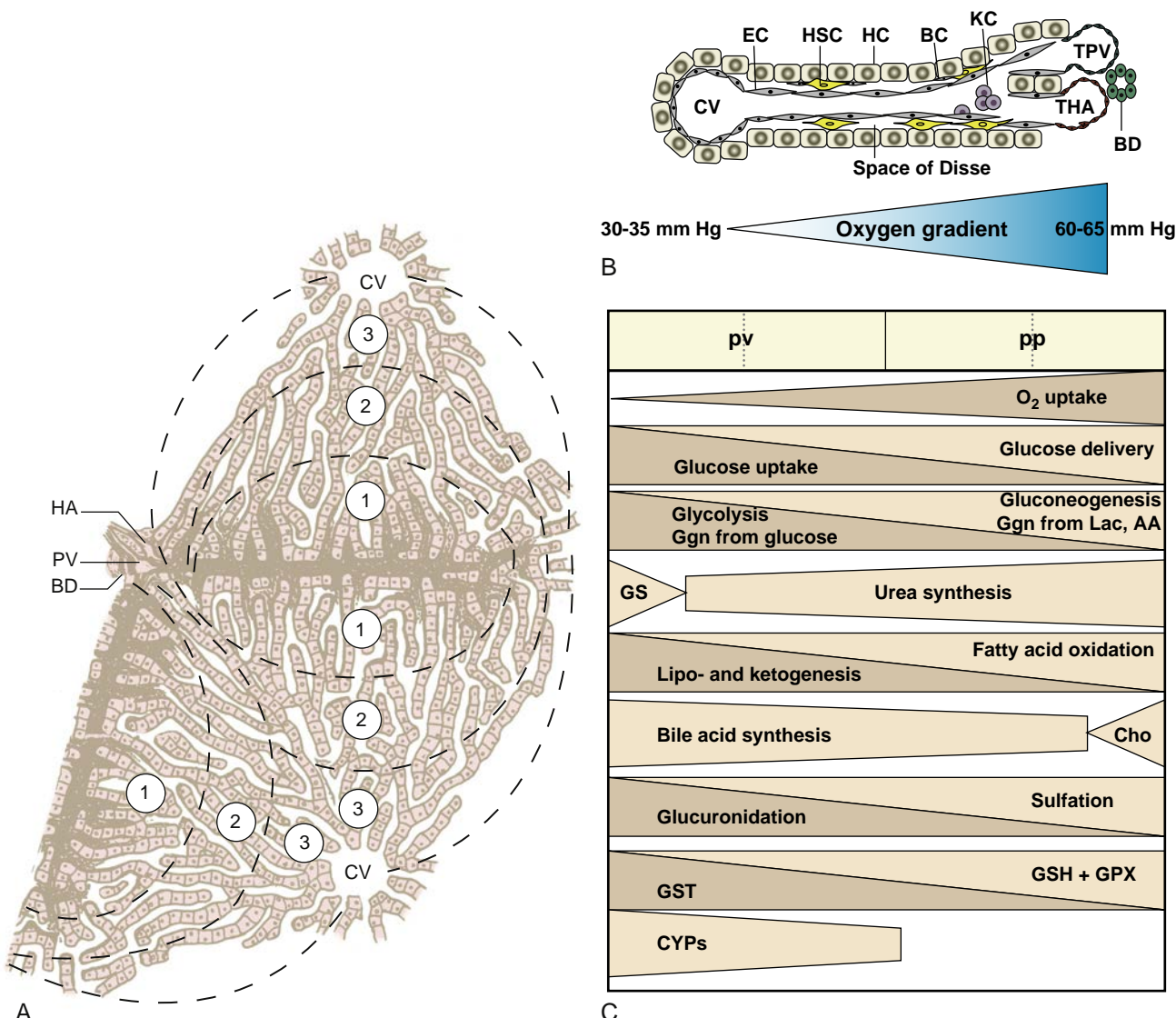


Fig. 16.3 (A) Blood supply of a liver acinus. Schematic representation of the acinus and hepatocyte zones. Hepatocytes can be divided into three zones based on their location along the sinusoid from the portal triad (PT) to the central vein (CV). Zone 1—periportal zone—hepatocytes are closest to the portal triad; Zone 3—perivenous, pericentral, or perilobular zone—hepatocytes are closest to the central vein. Zone 2 (intermediary) hepatocytes are in between. (B) Diagram of the sinusoid. The sinusoid is lined with sinusoidal epithelial cells (EC) separated by fenestrations that control the passage of solutes into the space of Disse. The space of Disse contains hepatic stellate cells (HSC) and is bound by the basolateral (sinusoidal) portion of the plasma membranes of the hepatocytes (HC). The apical portion of the plasma membranes makes up the bile canaliculus (BC). Oxygen and nutrient-rich blood flows from the terminal hepatic artery (THA) and portal vein (TPV) through the sinusoid to the central vein (CV). There is an oxygen gradient along the length of the sinusoid. Kupffer cells (KC) are resident hepatic macrophages and found in the sinusoids. (C) Hepatocyte zonation. The major metabolic pathways in the hepatocytes along the sinusoid differ based on their proximity to the portal triad or the central vein. Predominant metabolic pathways are listed for the periportal (pp) hepatocytes and the perivenous (pv) hepatocytes. AA, Amino acid; Cho, cholesterol synthesis; CYPs, cytochrome P450 enzymes; Ggn, glycogen; GPX, glutathione peroxidase; GS, glutamine synthesis; GST, glutathione transferase; Lac, lactate. ([B and C] From Kietzmann T. Metabolic zonation of the liver: the oxygen gradient revisited. *Redox Biol.* 2017;11:622–630.)

particles.¹⁸ Hepatic myeloid-derived suppressor cells suppress immune response in the liver. In acute hepatitis they reduce inflammation and limit tissue injury. Their immune suppressive function has been associated with adverse effects in certain pathologic conditions. In chronic viral hepatitis, they may promote viral persistence. They have also been associated with suppression of immune response to hepatic tumors.¹⁷

LYMPHOCYTES

Cells of lymphatic origin that can be detected in the liver include natural killer (NK) cells, NK T cells (NKT), mucosal-associated invariant T cells, and $\gamma\delta$ T cells in addition

to major histocompatibility restricted CD4+ T cells, CD8+T cells, and B cells. These cells are distributed throughout the liver parenchyma and serve critical roles in the innate (NK, NKT, mucosal-associated invariant T cells, and $\gamma\delta$ T cells) and adaptive (major histocompatibility restricted CD4+ T cells, CD8+T cells, and B cells) immune responses. These cells work primarily to maintain hepatic homeostasis by promoting tolerance to foreign substances. However, when necessary, these MHC-restricted cells can promote the clearance of foreign substances by expanding in response to them while recruiting additional cells from extrahepatic sources such as the lymph nodes and the spleen.¹⁷

TABLE 16.1 List of Well-Known Substrates, Inhibitors, and Inducers for Phase I, II, and III Metabolism Pathways

Enzymes	Substrates	Inhibitors	Inducers
PHASE I			
CYP3A	Midazolam, buspirone, felodipine, lovastatin, eletriptan, sildenafil, simvastatin, triazolam	Ketoconazole, clarithromycin, itraconazole, saquinavir, fluconazole, grapefruit juice, tipranavir/ritonavir	Phenytoin, rifampin, St. John's wort, efavirenz, etravirine, naftilin, prednisone
1A2	Alosetron, caffeine, duloxetine, melatonin, ramelteon, tacrine, tizanidine	Ciprofloxacin, enoxacin, fluvoxamine, oral contraceptives, phenylpropanolamine,	Montelukast, phenytoin, smoking components of cigarettes
2C8	Repaglinide, paclitaxel	Gemfibrozil, fluvoxamine, ketoconazole, trimethoprim	Rifampin
2C9	Celecoxib, warfarin, phenytoin	Amiodarone, fluconazole, miconazole, oxandrolone, capecitabine, etravirine, fluvastatin, metronidazole, sulfapyrazone, tigecycline	Carbamazepine, rifampin, aprepitant, bosentan, phenobarbital, St. John's wort
PHASE II			
UGTs	Bilirubin, phenols, estradiols, opiates, and carboxylic acids	Paclitaxel, midazolam, cyclosporine A, ketoconazole, phenobarbital, and phenytoin	Bilirubin, phenobarbitone, rifampin
SULTs	Phenols, alcohols, and amines	Flavonoids, mefenamic acids, salicylic acids, clomiphene, and danazol	Retinoic acid, methotrexate
NATs	Para-aminobenzoic acid, para-aminosalicylic acids, para-aminoglutamate, sulfamethazine, isoniazid, hydralazine, and sulfonamides	Caffeic acid, esculetin, quercentin, genistein, scopoletin, and coumarin	Androgens, aminophylline
GSTs	Epoxides, quinone, sulfoxides, esters, and peroxides	Phenols, quinone, vitamin C derivatives, dopamine, and <i>trans</i> -retinoic acid	Extracts of broccoli, cabbage, Brussels sprouts, and grapefruit
PHASE III			
P-gp	Digoxin, loperamide, vinblastine, talinolol	Amiodarone, azithromycin, cyclosporine, diltiazem, dronedarone, erythromycin, itraconazole, ketoconazole, lopinavir/ritonavir, quinidine, verapamil	Avasimibe, carbamazepine, phenytoin, rifampin, St. John's wort, tipranavir/ritonavir

From Almazroo OA, Miah MK, Venkataraman R. Drug metabolism in the liver. *Clin Liver Dis.* 2017;21:1–20. Elsevier.

Hepatic Physiology

DRUG METABOLISM

The vast majority of drugs used in the conduct of anesthesia are metabolized in the liver. A variety of enzymes convert drug molecules into more water-soluble (hydrophilic) molecules or compounds to facilitate their excretion. These enzymes are designated as being either part of the Phase I pathway or Phase II pathway based on the types of reactions they mediate. Phase I enzymes consist of the cytochrome P450 family of enzymes that convert lipophilic drug molecules to hydrophilic molecules primarily through oxidation, reduction, or hydrolysis. Non-CYP450 enzymes include monoamine oxidases, alcohol dehydrogenases, and aldo-keto reductase. The phase II pathway consists of the conjugation of the products of the phase I pathway with hydrophilic endogenous moieties to make them more water-soluble. Polar molecules may undergo Phase II metabolism without having undergone Phase I metabolism. The most common Phase II reaction is glucuronidation, which is the conjugation of the drug compound to glucuronic acid. This reaction is carried out by a family of enzymes known as uridine 5'-diphospho-glucuronosyltransferases. Other Phase II enzymes include sulfotransferases (SULT), glutathione S-transferases (GST), and catechol O-methyltransferases.¹⁹ The phase III pathway involves the excretion of compounds into the sinusoids or canalicular bile by molecular transporters that are transmembrane proteins which facilitate the movement of large or ionized molecules across cell membranes.

The majority of these transmembrane proteins are part of a superfamily of ATP-binding cassette (ABC) transporters that use ATP to actively transport molecules. Common ABC-transporters include multidrug resistance protein (MDR), cystic fibrosis transmembrane conductance regulator, and multidrug resistance-related protein (MRP).

Some orally administered medications undergo extensive metabolism in the gut or liver prior to entering the systemic circulation. This metabolism is termed the first-pass effect and is responsible for the lower oral bioavailability of these medications.²⁰

Drug metabolism is affected by a number of factors including genetic polymorphisms of metabolic enzymes, age, gender, pregnancy, liver disease, and concomitantly administered medications. The expression and function of Phase I and Phase II enzymes are reduced in neonates. The activities of some CYP450 enzymes are increased in women compared to men. Genetic polymorphisms in drug metabolizing enzymes and transporters can lead to wide variations in the pharmacokinetics of some drugs such as warfarin, with some patients having lower rates of metabolism based on the specific CYP450 polymorphism they carry. The concomitant administration of medications may also influence drug metabolism. A number of commonly encountered medications can serve as inducers or inhibitors of the enzymes involved in the different phases of drug metabolism.²⁰ Table 16.1 lists some of the commonly used drugs, which are metabolized and excreted by each of the three phases along with drugs that may serve as inhibitors or inducers for each phase.

See the pharmacokinetics chapter for further discussion of hepatic extraction ratio.

PROTEIN METABOLISM

The liver is responsible for the synthesis and catabolism of proteins, amino acids, and peptides. It is the site of synthesis for 80% to 90% of the circulating proteins including hormones, coagulant factors, cytokines, and chemokines. As such it plays a significant role in the functioning of the body. Albumin is the predominant protein produced by the liver, accounting for over 50% of total plasma protein. It functions to transport lipids and hormones and maintain blood volume. The liver plays a central role in protein degradation. Amino acids are catabolized through one of two reactions: deamination or transamination. Both reactions lead to the production of ammonia, which the liver converts to urea through the urea cycle. Urea is then excreted by the kidneys in the urine.²¹

CARBOHYDRATE METABOLISM

The liver is primarily responsible for storing and releasing glucose to meet the body's needs. In the postprandial state, the liver stores glucose through glycogenesis. Once the glycogen stores are complete, the liver converts excess glucose into fat through lipogenesis. In the fasting state, the liver provides the body with glucose by breaking down glycogen (glycogenolysis) or by generating glucose from carbohydrate precursors (gluconeogenesis).²²

LIPID METABOLISM

The liver plays an important role in lipid metabolism. Non-esterified fatty acids can arise from the lipase-mediated breakdown of complex lipids, or from thioesterase-mediated hydrolysis of fatty acid-CoA.²³ These fatty acids can enter the liver following oral intake or they can enter the liver following the breakdown of adipose tissue. In the liver, fatty acid oxidation is regulated by two main factors: the supply of fatty acids to the liver (via lipolysis), and the amount of microsomal esterification that occurs.²³ Lipid metabolism is also influenced by the carbohydrate metabolism, as the acetyl-CoA formed during carbohydrate metabolism can be utilized to synthesize fatty acids. Fatty acids can undergo biotransformation to supply energy for the needs of the body. Alternatively, the liver can convert amino acids and intermediate products of carbohydrates into fats and transport them to the adipose tissues.

BILE AND ENTEROHEPATIC CIRCULATION

The adult liver produces approximately 400 to 600 mL of bile each day. Bile facilitates the excretion of toxins as well as the absorption of dietary fats. It is the mechanism of excretion for compounds with molecular weights greater than 300 to 500 Daltons that are not readily excreted by the kidneys. It is used to excrete a host of endogenous and exogenous compounds, including bile acids, bilirubin, phospholipids, cholesterol, drugs, toxins, steroid hormones, and water-insoluble porphyrins. **Box 16.1** lists drugs, chemicals, and their metabolites that are excreted in the bile. The other major function of bile is to assist in the digestion and

BOX 16.1 Drugs, Foreign Chemicals, and Their Metabolites That Are Excreted in the Bile

Amiodarone ¹¹⁴	Estrone ¹¹⁵	Phenol red ¹¹³
Ampicillin ^{113,116}	Ezetimibe ¹¹⁰	Phenolphthalein ¹¹⁷
Benzylpenicillin ¹¹⁸	2-Fluoro-β-alanine ¹¹⁹	Phenytoin ¹¹⁷
Bilirubin ¹²⁰	Gentamycin ¹¹⁸	Pivampicillin ¹¹⁸
Bromocresol green ¹²¹	Glibenclamide (glyburide) ⁵	Rifamide ¹¹³
Bromosulfophthalein ¹²²	Gliclazide ¹²³	Rifamycin ¹¹³
Cefixime ¹²⁴	Imipramine ¹²⁵	Roquinimex ¹²⁶
Ceftriaxone ¹²⁷	Indocyanine green ¹²²	Rose bengal ¹²¹
Cefazidime ¹²⁸	Indomethacin ¹²⁵	Spironolactone ¹²⁵
Cephaloridine ¹¹³	Irinotecan ¹²⁹	Sulfamethoxazole ¹¹³
Cephamandole ¹¹⁸	Lanatoside C ¹¹⁸	Sulindac ¹²⁵
Cephazolin ¹¹⁸	Lorazepam ¹³⁰	Sulbactam ¹¹⁶
Chenodeoxycholic acid ^{122,125}	Lomnetazepam ⁶	Temafloxacin ¹³¹
Chloramphenicol ¹¹⁸	Methotrexate ¹¹³	Testosterone ¹²⁵
Chlortetracycline ¹¹⁸	Metronidazole ¹¹⁷	Tetracycline ^{113,118}
Clindamycin ¹¹⁷	Mezlocillin ¹³²	Thiamphenicol ¹¹³
Demethylchlortetracycline ¹¹⁸	Morphine ¹³³	Tolfenamic acid ¹³⁴
Diazepam ¹¹³	Mycophenolic acid ¹³⁵	Toremifene ¹³⁶
Digitoxin ¹¹³	Mycophenolate mofetil ^{137,138}	Troglitazone ¹³⁹
Digoxin ¹¹³	Nortriptyline ¹³¹	Trovaloxacin ⁷
Doxycycline ¹¹⁸	Novobiocin ¹³¹	Ursodeoxycholic acid ^{122,125}
Erythromycin ¹¹³	Oltipraz ¹⁴⁰	Valproic acid ¹²⁵
Estradiol ¹²⁵	Pethidine (meperidine) ¹¹³	Warfarin ¹³³

Roberts MS, Magnusson BM, Bruczynski FJ. Enterohepatic circulation. *Clin Pharmacokinet*. 2002;41:751–790, Table II, page 767.

absorption of dietary fats, cholesterol, and vitamins.²⁴ Bile is 95% water by volume, with the remainder consisting of bile acids, phospholipids, cholesterol, bilirubin, as well as other exogenous and endogenous substances. The two primary bile acids are cholic acid and chenodeoxycholic acid. Bile acids are synthesized by hepatocytes from cholesterol. They are then conjugated to reduce hepatotoxicity and increase solubility and secreted into the canaliculari. The canaliculari drain into the biliary ductules, which connect to form hepatic ducts. The walls of the intrahepatic bile ducts are made up of cholangiocytes that modify the volume and composition of the bile. The ducts ultimately form the left and right hepatic ducts, which join into the common hepatic duct. Bile is stored and concentrated in the gallbladder, which connects to the biliary tree through the cystic duct. The common hepatic duct and cystic duct join to form the CBD, which connects to the duodenum through the sphincter of Oddi (hepatopancreatic sphincter).²⁴ Following the ingestion of food, fatty acids in the duodenum stimulate the release of cholecystokinin (CCK) which causes the gallbladder to contract and the sphincter of Oddi to relax leading to the release of bile into the duodenum. The bile acids

emulsify dietary fats and facilitate their absorption. The vast majority (95%) of the bile acids released into the duodenum are reabsorbed in the terminal ileum and returned to the liver to be reused. This pathway for recycling bile acids is known as the enterohepatic circulation (EHC).²⁵ Enterohepatic cycling can impact the pharmacokinetics and pharmacodynamics of drugs that undergo biliary excretion by increasing their bioavailability, reducing their elimination, as well as altering their plasma concentration curves. The effect of EHC on the properties of a drug depends on the physiologic activity of the excreted form of the drug (i.e., prodrug or activated form), the ease with which the excreted form is reabsorbed through the intestines, and whether it is recycled through the liver into the bile or the systemic circulation. In the case of some drugs, EHC can lead to secondary and tertiary peaks in plasma concentration as the drug is recycled into the system.²⁶

ROLE OF THE LIVER IN COAGULATION

The liver plays a significant role in the coagulation system. It synthesizes all coagulation factors except factors III (thromboplastin), IV (calcium), and VIII (von Willebrand factor [vWF]). It also synthesizes proteins that regulate coagulation and fibrinolysis such as protein S, protein C, plasminogen activator inhibitor, and antithrombin III. Furthermore, it removes activated clotting and fibrinolysis products through the hepatic reticuloendothelial system. A number of factors require vitamin K to become active. Coagulation factors II, VII, IX, X, as well as protein C and protein S undergo posttranslational modification with vitamin K to become active. Briefly, glutamic acid in the amino terminus of these proteins is converted to gamma-carboxyglutamic acid. These gamma-carboxylated procoagulants can then bind calcium ions and form bridges to phospholipid surfaces that are essential for the formation of activation complexes.²⁷ Warfarin acts by inhibition gamma-carboxylation. In addition to these vitamin K-dependent factors, hepatocytes also synthesize factor V, XIII, fibrinogen, antithrombin, α_2 plasmin inhibitor, and plasminogen.²⁸ Thrombomodulin, tissue plasminogen activator, tissue factor plasma inhibitor, vWF, and urokinase are not synthesized in the liver. Instead these proteins are synthesized in endothelial cells, whereas urokinase is expressed by endothelial cells, macrophages, and renal epithelial cells. Tissue plasminogen activator is primarily removed from the bloodstream through the hepatic reticuloendothelial system.²⁹

HEME METABOLISM, BILIRUBIN, AND PORPHYRIAS

The liver is involved in both heme synthesis and metabolism. Eighty to 90% of heme synthesis takes place in the bone marrow with the resultant heme used to produce hemoglobin. Most of the remainder of the heme is produced in the liver and used primarily to synthesize cytochrome P450 enzymes. Whereas the rate of heme synthesis in the bone marrow is a function of the availability of iron, the rate of synthesis in the liver is a function of the available free heme pool in the body.³⁰ Heme is synthesized through an eight-step enzymatic cascade known as the Shemin pathway. Synthesis begins with glycine and succinyl CoA

and proceeds through porphyrinogen intermediaries. A deficiency in any of the enzymes involved in heme synthesis leads to the development of porphyria. The specific type of porphyria and its clinical manifestations depend on the specific enzyme that is deficient and the substrate that accumulates as a result. The most common porphyria is acute intermittent porphyria with an estimated incidence of 5 to 10 per 100,000. It is caused by a deficiency in porphobilinogen deaminase, which catalyzes the conversion of porphobilinogen to hydroxymethylbilane. Patients typically have adequate levels of the enzyme for heme homeostasis; however, in response to endogenous or exogenous triggers that induce the Shemin pathway, the capacity of the system is exceeded and they accumulate precursors leading to symptoms. Common triggers include erythromycin, trimethoprim, rifampicin, phenytoin, and barbiturates. Clinical symptoms of an attack include severe, poorly localized abdominal pain (in >90% of cases), nausea, vomiting, agitation, and confusion. Hyponatremia occurs in 40% of attacks. Change in urine color to dark red (especially on exposure to light) is a common finding. Treatment consists of discontinuing the triggering agent, administering pain medication, carbohydrates, and hematin.³⁰

Bilirubin is a product of heme catabolism. The primary source is senescent erythrocytes that are phagocytosed by macrophages in the spleen, liver, and bone marrow. The released heme is metabolized by heme oxygenase into bilirubin, yielding carbon monoxide and iron in the process. Unconjugated bilirubin is water insoluble and thus tightly bound to albumin in the circulation. Hepatocytes convert bilirubin into a water-soluble form by conjugating it to glucuronic acid via the enzyme glucuronyl transferase. Conjugated bilirubin is then transported across bile canaliculi and excreted in the bile. In the colon, bilirubin is deconjugated, metabolized by bacteria, and converted into urobilinogen. Urobilinogens are either reabsorbed through the EHC or excreted in the urine and stool, giving urine and stool their characteristic colors.³¹

HEPATIC REGULATION OF HORMONES

The liver can participate in endocrine functions through hormone synthesis or hormone degradation. Hepatocytes synthesize hormones or prohormones such as hepcidin, insulin-like growth factor, and angiotensinogen, respectively. In addition to these hormones, thrombopoietin is also synthesized by hepatocytes and LSECs. These hormones and prohormones have specialized roles in the human body. Thus hepcidin is responsible for iron homeostasis and regulates intestinal iron absorption, plasma iron concentrations, and tissue iron distribution by inducing degradation of the hepcidin receptor, ferroportin.³² Insulin-like growth factor promotes systemic growth, especially bone growth in children.³³ Angiotensinogen, the precursor of all angiotensin proteins, regulates the systemic blood pressure as well as the water and sodium composition of the body.³⁴ Thrombopoietin regulates platelet production by stimulating production and differentiation of megakaryocytes.³⁵ In addition to hormone synthesis, the liver participates in endocrine function by inactivating many hormones, including thyroxine, aldosterone, antidiuretic hormone, estrogens, androgens, and insulin.

TABLE 16.2 Liver Blood Tests and the Differential Diagnosis of Hepatobiliary Disorders

Blood Test	PREDOMINANT ABNORMALITY		
	Bilirubin Overload (Hemolysis)	Hepatocellular Injury	Cholestasis
Aminotransferases	Normal	Increased: May be normal or decreased in advanced stages	Normal: May be increased in advanced stages
Serum albumin	Normal	Decreased: May be normal in acute fulminant hepatic failure	Normal: May be decreased in advanced stages
Prothrombin time*	Normal	Prolonged	Normal: May be prolonged in advanced stages
Bilirubin (main form present)	Unconjugated (also mild increase in conjugates)	Conjugated	Conjugated
Alkaline phosphatase	Normal	Normal: May be increased by hepatic infiltrative disease	Increased
γ -Glutamyl transpeptidase 5'-nucleotidase	Normal	Normal	Increased
Blood urea nitrogen	Normal: May be increased by renal dysfunction	Normal: May be decreased by severe liver disease and normal kidney function	Normal
BSP/ICG (dye)	Normal	Retention of dye	Normal or retention of dye

*Used interchangeably with the international normalized ratio.
BSP/ICG, Bromsulphalein and indocyanine green.

Evaluation of the Liver

CLINICAL ASSESSMENT

There are often no signs or symptoms of liver disease until it is quite advanced. Even then, the only clues may be mild or nonspecific symptoms such as loss of appetite, fatigability, malaise, disrupted sleep patterns, or subtle cognitive changes. Major risk factors for liver disease include: alcohol use; illicit drug use; sexual promiscuity; blood transfusions; exposure to hepatotoxins; prior bouts of jaundice; and a family history of genetic diseases such as hemochromatosis, α_1 -antitrypsin deficiency, and Wilson disease. Patients with advanced liver disease may have these nonspecific symptoms, as well as pruritus, easy bruising, and changes in urine or stool color. In advanced liver disease physical examination findings include jaundice, scleral icterus, ascites, spider angiomas, xanthelasma, asterixis, and palmar erythema.

STANDARD LABORATORY TESTS

Standard panels used to evaluate the hepatobiliary system are often called “liver function tests” (Table 16.2).³⁶ In fact, these tests do not measure specific liver functions. Instead, they help define broad categories of hepatobiliary pathology: hepatitis, hepatobiliary dysfunction, or insufficient protein synthesis.

DETECTION OF HEPATOCELLULAR INJURY

Aminotransferases

Serum alanine aminotransferase (ALT) and aspartate aminotransferase (AST), formerly named serum glutamic-pyruvic transaminase and serum glutamic-oxaloacetic transaminase, respectively, are most commonly elevated because of hepatocellular injury. Both are aminotransferases, enzymes

involved in gluconeogenesis. ALT is mainly a cytoplasmic liver enzyme. In contrast, cytoplasmic and mitochondrial isozymes of AST are found in many extrahepatic tissues, including the heart, skeletal muscle, brain, kidney, pancreas, adipose, and blood. Therefore isolated elevations of AST likely represent non-liver sources, but concomitant elevations in AST and ALT usually represent liver injury. Rarely, elevations in AST and ALT levels may result from muscle injury.³⁷

Practice guidelines provide recommendations for the evaluation of abnormal liver enzymes, based on the combination of clinical picture and degree of elevation of AST and ALT. Establishing normal reference ranges for AST and ALT have been complicated by studies with heterogeneous populations, since normal ranges differ with gender and body mass index (BMI). Nevertheless, multiple studies show that even mild elevations of AST and ALT above the upper limit of normal are associated with increased mortality. Some clinicians therefore argue that the normal limits should be lowered.³⁸

Elevated ALT and AST levels are sometimes described in qualitative terms, ranging from mild (>100 IU/L), to extreme (>2000 IU/L). The extent of aminotransferase elevation can sometimes aid in the differential diagnosis. Mild elevations in AST and ALT can arise from any hepatocyte injury. Large elevations often reflect acute hepatocyte ischemia. Extreme elevations signify massive hepatic necrosis, such as from fulminant viral hepatitis, severe drug-induced liver injury, or shock liver.⁵¹ However, aminotransferase levels do not reliably represent the extent of liver damage. Patients with so called “burnt out” livers, such as from chronic hepatitis, have insufficient functioning hepatocytes to bring about a transaminase increase.

The ratio of AST to ALT may help identify the cause of liver disease. Most causes of hepatic injury are associated with higher ALT than AST levels. However, Wilson disease and alcoholic liver disease are classically associated with an

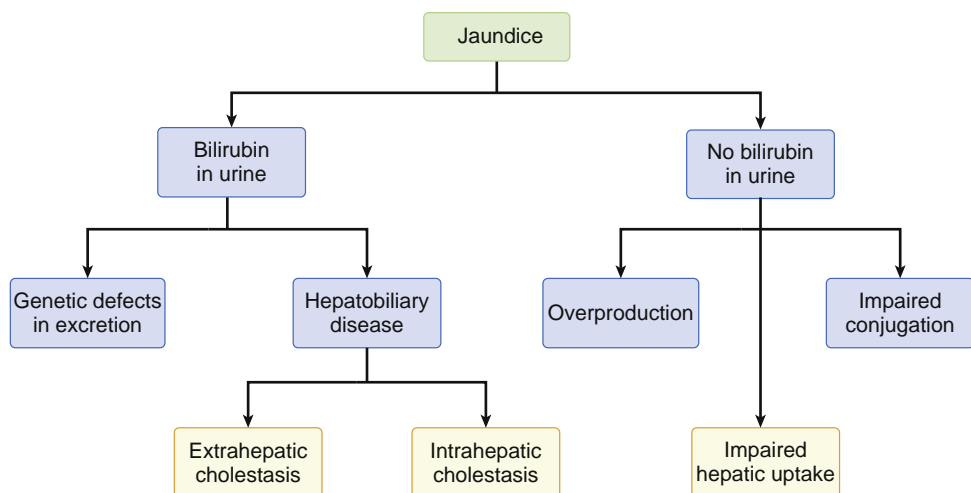


Fig. 16.4 Differential diagnosis of jaundice depending on whether bilirubin is or is not present in the urine.

AST-ALT ratio greater than 1; in some cases, a ratio of 4 has been documented. Chronic hepatitis with minimal fibrosis has a low AST-ALT ratio; however when cirrhosis develops the ratio is greater than 1. Although the AST-ALT ratio may have insufficient predictive value as a sole marker, it can be used in combination with other noninvasive tests to predict the degree of fibrosis in patients with chronic hepatitis.³⁹

Lactate Dehydrogenase

Lactate dehydrogenase (LDH) is a nonspecific marker of hepatocellular injury. Extremely elevated LDH signifies massive hepatocyte damage, usually from ischemia or drug-induced hepatotoxicity (such as acetaminophen overdose). These patients will also have extreme elevations in AST and ALT. Elevated LDH concomitant with elevated alkaline phosphatase (AP) suggests malignant infiltration of the liver. Extrahepatic disorders that cause LDH elevation include hemolysis, rhabdomyolysis, tumor necrosis, renal infarction, acute stroke, and myocardial infarction.³⁷

Glutathione-S-Transferase

GST is a sensitive test for liver injury, with a half-life (60-90 minutes) much shorter than AST or ALT. Following hepatocyte damage, serum GST rises quickly and serial GST measurements can help monitor for disease recovery.⁴⁰ The enzymes AST and ALT are found primarily in periportal hepatocytes (acinar zone 1), whereas GST is present in hepatocytes throughout the acinar zones.⁴¹ Since centrilobular/perivenous hepatocytes are most susceptible to hypoxic injury and acetaminophen toxicity, GST is a useful marker particularly in early stages of injury.

DETECTION OF CHOLESTATIC DISORDERS

Alkaline Phosphatase

AP isoenzymes are present in many tissues, including liver, bone, intestine, and placenta. In the liver, AP is present in the canalicular membranes of the hepatocytes. Mild elevations in AP may be normal, as AP varies with gender, age, blood type, and smoking status.⁴² Nonhepatic causes of AP elevation include bone disorders such as Paget disease, osteomalacia, and tumors of the bone; normal growth

spurts in children; the third trimester of pregnancy; sepsis; renal failure; and some medications. Elevated AP from a hepatobiliary source is most commonly due to cholestatic disease and typically manifests as an increase to 2 to 4 times the upper limit of normal. Rarely, patients with cholestasis can have extreme elevations in AP (10 times the upper limit of normal).⁵¹ AP will also be elevated to a lesser extent in hepatocellular disease such as hepatitis. The ALT to AP ratio helps differentiate hepatocellular injury (ALT:AP > 5) from cholestatic disease (ALT:AP < 2) from a mixed picture.³⁸

AP elevation from cholestasis could be a result of either intrahepatic or extrahepatic biliary obstruction. Common causes include primary biliary cirrhosis, choledocholithiasis, and hepatic malignancy compressing small intrahepatic bile ducts. With a half-life of about 1 week, AP will be normal immediately after the onset of biliary obstruction, and it will remain elevated for days after resolution of obstruction.³⁷

The source of AP isoenzyme elevation can be determined by electrophoresis, but this test is expensive and not routinely available. More commonly clinicians confirm the hepatic origin of the AP elevation with other tests that indicate cholestatic disease. The enzymes 5'-nucleotidase and gamma-glutamyl transpeptidase are also elevated in cholestatic disorders, coincident with AP. Simultaneous elevation of these enzymes help identify liver as the source of AP elevation.

Serum Bilirubin

Serum bilirubin is the most commonly used test to monitor for excretory dysfunction of the liver. Bilirubin is measured in serum assays as either direct or indirect bilirubin. Direct bilirubin measures the water-soluble form, which interacts directly with the assay's reagents. While direct bilirubin correlates with conjugated bilirubin levels, and indirect with unconjugated levels, the two terms are not synonymous. The level of unconjugated bilirubin is typically underestimated by the indirect bilirubin test. Distinguishing conjugated from unconjugated bilirubin is key to the differential diagnosis. The presence of bilirubin in the urine can also help differentiate the clinical cause. Bilirubinuria usually reflects conjugated hyperbilirubinemia, since only the water-soluble conjugated form is excreted by the kidney (Fig. 16.4).³⁷

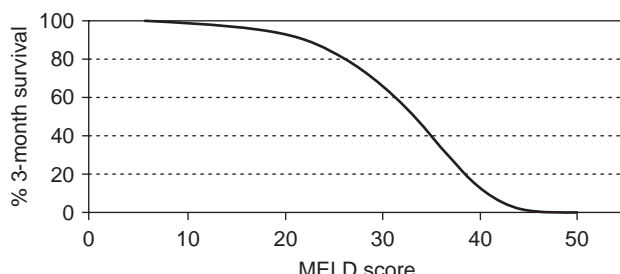


Fig. 16.5 Estimated 3-month survival as a function of the Model for End-Stage Liver Disease (MELD) score.

Elevation in the concentration of unconjugated bilirubin is either due to excessive heme breakdown, or the inability of the liver to conjugate bilirubin. One major cause is hemolysis, in which increased erythrocyte breakdown creates more unconjugated bilirubin than the liver is able to conjugate. Massive hemolysis will cause elevations in both forms of bilirubin, but with unconjugated predominance. Gilbert syndrome is a benign condition with genetically low levels of the hepatic enzyme glucuronyl transferase, associated with mild or intermittent elevation in unconjugated bilirubin. Various drugs may also produce unconjugated hyperbilirubinemia. High levels of unconjugated bilirubin are neurotoxic, particularly in infants.

Conjugated hyperbilirubinemia occurs due to either problems with the secretion of conjugated bilirubin from hepatocytes into canalicular bile or to the blockage of bile flow within the hepatobiliary tree. This can be due to a genetic defect in the excretion of bilirubin, or cholestasis (either intrahepatic or extrahepatic). Intrahepatic cholestasis is caused by an inflammatory or infiltrative process compressing small intrahepatic bile ducts, while extrahepatic cholestasis is due to biliary obstruction such as from stones or a pancreatic mass. Primary sclerosing cholangitis (PSC) can involve both intra- and extrahepatic bile ducts.⁴³

ASSESSMENT OF HEPATIC PROTEIN SYNTHESIS

Serum Albumin

The serum albumin concentration is used to evaluate chronic liver disease and hepatocellular function (protein synthesis). However, it has poor specificity. Hypoalbuminemia has many other causes besides decreased protein synthesis, including increased catabolism, expansion of the plasma volume, renal losses, and maldistribution of total body albumin. The half-life of albumin in the serum is 20 days. As a result, changes in the synthetic function of the liver are not acutely reflected by the serum albumin concentration. Prealbumin is another protein synthesized in the liver that is also involved in transport and binding. It has a much shorter half-life than albumin. However, the level of prealbumin reflects the status of protein nutrition to a greater degree than liver synthetic function given its high percentage of essential amino acids.³⁷

Prothrombin Time

Hepatic synthetic function can also be assessed by measuring the levels of liver-derived coagulation factors. The liver synthesizes coagulation factors in great excess, thus

TABLE 16.3 Interpretation of Hepatitis B Viral Serologies

Hepatitis B Virus Serologies	Interpretation
Hepatitis B surface antigen (HBsAg)	Acute or chronic infection
Antibody to hepatitis B surface antigen (Anti-HBs)	Immunity due to recovery from infection or vaccination
IgM antibody to hepatitis B core antigen (Anti-HBc IgM)	Previous or ongoing infection
IgG antibody to hepatitis B core antigen (Anti-HBc IgG)	Acute infection

INTERPRETATION OF CONSTELLATION OF RESULTS	
HBsAg NEG	Immune due to recovery
Anti-HBs POS	
Anti-HBc IgG POS	
HBsAg NEG	Immune by vaccination
Anti-HBs POS	
Anti-HBc IgG NEG	
HBsAg POS	Acute hepatitis B infection
Anti-HBs NEG	
Anti-HBc IgM POS	
HBsAg POS	Chronic hepatitis B infection
Anti-HBs NEG	
Anti-HBc IgG POS	
Anti-HBc IgM NEG	
HBsAg NEG	Not immune, potentially susceptible
Anti-HBs NEG	
Anti-HBc IgG NEG	

the prothrombin time (PT) will remain normal until significant hepatic impairment occurs. Coagulation factors have shorter half-lives than albumin, ranging from 4 hours for factor VII to 4 days for fibrinogen. Thus when severe liver dysfunction occurs, PT (or the international normalized ratio [INR]) can reflect acute liver failure more quickly than can albumin. It is also used to monitor for restoration of hepatic function, often improving before other clinical signs of improvement occur. However, prolonged PT/INR is not specific for liver disease. It may also represent vitamin K deficiency, warfarin effect, or a genetic factor deficiency.³⁷

TESTING FOR DIAGNOSIS OF SPECIFIC DISEASES

In addition to the above standard laboratory tests, targeted testing can aid in the diagnosis of specific hepatobiliary diseases. Such testing includes serologic testing for viral and autoimmune diseases, genetic testing, and tumor marker assays. Viral markers, including antibodies, antigens, and genetic material, are used to diagnose hepatitis from hepatotropic viruses (A, B, C, D, and E) and herpesviruses such as cytomegalovirus and Epstein-Barr virus. Patients with acute or chronic hepatitis B infection and those with immunity due to resolved infection or vaccination can be distinguished based on measurements of hepatitis B surface antigens and surface and core antibodies (Table 16.3). HBV DNA testing has also emerged to monitor treatment effect and the development of chronic hepatitis B after resolution of acute hepatitis.⁴⁴

Testing for hepatitis C is recommended for those with various risk behaviors and exposures (such as history of intravenous drug use, long term hemodialysis, or HIV

infection) and as part of an evaluation for unexplained liver disease. American guidelines also recommend one-time screening for hepatitis C in all persons in the United States born between 1945 and 1965, as this birth cohort has the highest prevalence of hepatitis C. Screening entails testing for antibodies to HCV; a positive screen indicates exposure to the virus. Active infection can then be confirmed with nucleic acid testing for HCV RNA. Sustained viral response to treatment is defined as the absence of HCV RNA detected at least 12 weeks after the completion of therapy.⁴⁵ Currently, patients also receive HCV genotype testing prior to the initiation of treatment. New direct antiviral agents are highly effective in achieving sustained viral response for most genotypes and most clinical conditions. Therefore genotype testing may soon no longer be routinely required.⁴⁶

Rapid HCV antibody testing and point of care RNA tests are useful in community-based settings serving high-risk populations and remote settings without access to centralized laboratories. The measurement of HCV core antigen (HCVcAg) can diagnose active hepatitis C infection with high sensitivity and specificity as a single test, although it is currently not the standard of care. HCVcAg measurement is particularly useful as a rapid, single test for diagnosis in populations who are at high risk of loss to follow-up. However, it is not yet available as a point of care test.⁴⁷

Markers of hepatic malignancy include alpha fetoprotein (AFP) and protein induced by vitamin K absence or antagonist-II (PIVKA-II).⁴⁸⁻⁵⁰ AFP is a glycoprotein synthesized in the liver, fetal yolk sac, and GI tract. The normal value of AFP is less than 20 ng/mL. A significantly elevated concentration of AFP, often greater than 1000 ng/mL, is common in patients with hepatocellular carcinoma (HCC). AFP is also elevated in testicular germ cell tumors, and less frequently in prostate and other gastrointestinal cancers. The concentration of AFP is used to monitor HCC disease progression and response to treatment. It is also widely used to screen for HCC in high-risk patients, along with ultrasound. However, AFP's role in HCC surveillance has recently been debated, as studies suggest that AFP has insufficient sensitivity as a screening tool for HCC, particularly for small and solitary tumors. AFP may be normal in 40% of HCC patients.^{51,52} PIVKA-II, also known as des- γ -carboxylated prothrombin, is a biomarker for HCC with high specificity.^{48,50} With a shorter half-life than AFP, PIVKA-II is useful in monitoring for treatment response and recurrence. PIVKA-II is also associated with worse survival. AFP and PIVKA-II combined can diagnose HCC with further increased sensitivity and specificity.⁵³

TESTING IN MANAGEMENT AND PROGNOSIS OF LIVER DISEASE

Laboratory tests can help define the type of liver dysfunction, and even identify specific causes. In addition, some of these markers are used to assess disease severity, monitor disease progression and treatment, and predict mortality. Taken alone, thrombocytopenia is the earliest sign of cirrhosis among the routine serum tests, indicating both decreased hepatic function and splenic sequestration from portal hypertension.⁵⁴ Some markers are combined to create scoring systems, thereby improving the sensitivity and specificity of single tests. For example, the Model for End-Stage

Liver Disease (MELD) score (a calculation that combines INR, bilirubin, and creatinine) was created to assess risk of mortality in cirrhotic patients undergoing transjugular intrahepatic portosystemic shunt (TIPS) procedures. The MELD score now is used for liver transplant listing, as it correlates with wait-list mortality. Standard tests such as INR, lactate and platelet count, as well as novel quantitative tests have been used to predict short-term outcome after liver transplantation.⁵⁵ The HCC-MELD score, which combines AFP, MELD, and tumor size, can predict survival after liver transplantation in HCC patients.⁵⁶ Elevated bilirubin predicts poor prognosis in acute or chronic liver disease, and AP and bilirubin together predict poor outcome in primary biliary cirrhosis.

Noninvasive Serum Testing for Fibrosis

Multiple models combining noninvasive measurements have been used to assess the severity of fibrosis. The goal of these models is to allow for disease staging (from mild fibrosis to cirrhosis) without requiring liver biopsy. Although liver biopsy remains the diagnostic gold standard, limitations include sampling error, subjectivity in interpretation, pain, bleeding, and cost.⁵⁴ These models include various combinations of standard tests such as aminotransferases, platelet count, and INR; as well serum markers of extracellular matrix turnover such as alpha-2-macroglobulin, apolipoprotein A1, and hyaluronic acid. New commercial panels test an array of direct markers of collagen turnover, which correlate with fibrosis.^{39,57,58}

Quantitative Liver Tests

Quantitative liver function tests can estimate hepatocellular function by measuring the clearance of various substances metabolized by the liver. Two such substances are indocyanine green (ICG) and bromsulphalein. However, clearance techniques are imperfect tests, potentially influenced by extrahepatic uptake or clearance of the substance, changes in blood flow including portosystemic shunting, and other unknown factors. ICG is avidly extracted by the liver and undergoes minimal extrahepatic uptake and metabolism. Its elimination kinetics are expressed in the ICG plasma disappearance rate (PDR). It can be measured noninvasively by a transcutaneous method. The test is even sensitive to early changes in liver function, and it may be used to guide clinical management. By estimating functional hepatocellular mass, it may help predict outcomes after partial liver resections. It is also used as an early test of graft function following liver transplantation. However, like other highly extracted substances, ICG clearance is dependent on hepatic blood flow, and therefore reflects changes in both hepatic blood flow and hepatocyte function. In fact, ICG is also used specifically to test hepatic blood flow as discussed below. A drop in the ICG PDR may represent a reduction in hepatocellular function, a decrease in hepatic blood flow, or both. Bromsulphalein is another highly extracted substance that can be used to measure hepatic clearance. Bromsulphalein has been associated with severe systemic reactions, and therefore is largely no longer used.⁵⁹

The capacity of the liver to metabolize drugs can also be measured by caffeine clearance, galactose elimination, aminopyrine breath test, and monoethylglycinexylidide (MEGX).^{37,60-62} Caffeine clearance can be measured

noninvasively through metabolites present in the saliva up to 24 hours after oral caffeine intake. MEGX is the primary metabolite of lidocaine and is measured in the serum after intravenous injection of lidocaine. MEGX concentration may be used to estimate liver function after partial hepatectomy and may have prognostic value in intensive care unit patients with liver dysfunction. MEGX was found to independently predict poor outcomes in patients with chronic hepatitis C, and it was more sensitive than standard liver tests in identifying these patients.⁶³ Expensive and time consuming, quantitative tests currently remain primarily research tools and require further validation.

MEASUREMENT OF HEPATIC BLOOD FLOW

Blood flow to the liver can be measured using clearance techniques, indicator dilution techniques, and direct measurements.

Clearance Techniques

Based upon the Fick principle, clearance techniques estimate the hepatic blood flow by measuring the rate of disappearance of substances that are exclusively and avidly cleared by the liver. Such substances with high extraction ratios include ICG, propranolol, lidocaine, and radiolabeled colloid particles. The primary limitation of clearance techniques is they assume normal hepatocyte function. Hepatic capacity to eliminate these substances can be variably or significantly diminished in liver disease. This is particularly problematic since liver dysfunction and altered hepatic flow are so often linked.⁶⁴

The dual cholate test measures the clearance of cholate, a bile salt, given in both oral and intravenous form. The oral cholate undergoes a high first-pass extraction and allows for a calculation of portal circulation. Clearance from the systemic circulation is measured using the intravenous cholate. One can quantify the degree of portal-systemic shunting and calculate a disease severity index. This index correlates with degree of fibrosis on liver biopsy and can predict risk of cirrhosis and poor clinical outcomes.^{63,65}

Indicator Dilution Techniques

Unlike clearance methods, indicator dilution techniques can measure hepatic blood flow even in the setting of liver dysfunction. A known quantity of a radiolabeled indicator (e.g., iodinated albumin) is injected into the portal system and hepatic artery. The concentration of that substance is then measured continuously from a hepatic vein. Hepatic blood flow can then be calculated by creating indicator dilution curves. The substance used should be resistant to hepatic clearance.⁴ Indicator dilution techniques also presume uniform liver perfusion, and therefore results could be altered in patients with shunting. These techniques are invasive and are still primarily research tools as well.⁶⁴

Direct Measurements

Blood flow through the portal vein or hepatic artery can be measured directly using electromagnetic or ultrasonic probes. These techniques are invasive and subject to significant error. The surgical procedures required to implant the probes can themselves alter hepatic blood flow. Once implanted, the probes are often left in place, and blood flow

is then measured via telemetry. Implantable Doppler probes are sometimes used in patients immediately post-liver transplantation, and in patients who are at high risk for hepatic artery or portal vein thromboses.⁶⁴

RADIOLOGIC METHODS

Radiologic techniques play important roles in diagnosing liver disease. Splenoportography evaluates the splenic and portal veins; it is useful in identifying varices and thromboses. Portal venography uses three-dimensional CT to create vascular maps of portosystemic collateral vessels. These noninvasive imaging techniques are particularly useful in surgical planning, such as before liver transplantation.⁶⁶

Inexpensive and routinely available, ultrasound can help diagnose cirrhosis with high sensitivity and specificity. Ultrasonic signs of cirrhosis include surface nodularity, hepatomegaly, and hypertrophy of the caudate lobe, as well as signs of portal hypertension, such as ascites, splenomegaly, and increased portal vein diameter. Doppler ultrasonography can show diminished portal flow and portal venous flow reversal.^{54,67,68} Fibrosis can also be estimated using elastography, a noninvasive measure of liver stiffness (LS). A shear wave is delivered across the liver via an ultrasound probe, and the wave propagation is then measured. Transient elastography is reproducible and easily performed in the office. Magnetic resonance elastography is especially useful in obese patients and those with ascites, where transient elastography is less accurate. Stiffness is a continuous measure which correlates with the histological stage of fibrosis, with high sensitivity and specificity.^{67,69,70} The combination of serum tests along with elastography offers much improved accuracy in diagnosing fibrosis. These tests are now widely used in practice, although they have not yet supplanted the role of liver biopsy.

Patients with chronic liver disease and chronic hepatitis B virus carriers are at increased risk for developing HCC and require regular screening for the cancer. Ultrasound is the most widely used screening tool for HCC worldwide. Multi-phasic, contrast-enhanced CT and MRI are used to evaluate focal liver lesions suspicious for HCC with high sensitivity and specificity. While normal liver parenchyma receives only 25% blood flow from the hepatic artery (the rest via the portal vein), HCC cells receive their blood supply primarily from the hepatic artery. Contrast-enhanced imaging reflects this fact with HCCs showing hyperintensity in the arterial phase and washout during the portal venous phase. The Liver Imaging Reporting and Data System (LI-RADS) is a standardized tool for the radiologic classification of liver lesions in patients with chronic liver disease. Use of the LI-RADS has improved radiologic diagnostic accuracy and reduced the need for biopsy in these patients. In fact, confirmatory biopsy is rarely used, even prior to liver transplantation for HCC.^{54,71,72}

Hepatic Pathophysiology

CHOLESTATIC DISEASE

Cholestasis is the impairment of bile production or flow. Cholestatic disorders are characterized primarily by elevations of serum AP and gamma-glutamyl transferase (GGT),